# Assessment and Reduction of the Impacts of Large Freight Vehicles on Urban Traffic Corridor Performance

Euan Douglas Ramsay
B.E. (*Mech.*) (*Hons*)

A thesis submitted for the degree of
Doctor of Philosophy

Centre for Built Environment and Engineering Research
Queensland University of Technology

9 February 2007

# Abstract

Increasing demand for road freight has lead to a widespread adoption of more-productive large freight vehicles (LFVs), such as B-Doubles, by Australia's road freight industry. Individual LFVs have a greater potential to impact traffic efficiency through their greater length and poorer longitudinal performance. However, this is offset to an extent as fewer vehicles are required to perform a given freight task on a tonne-km basis.

This research has developed a means of characterising the effects that large freight vehicles have on the performance of an urban arterial corridor managed by signalised intersections. A corridor-level microsimulation model was developed from first principles, which modelled the longitudinal performance of individual vehicles to a greater accuracy than most existing traffic simulation software does. The model was calibrated from traffic counts and GPS-equipped chase car surveys conducted on an urban arterial corridor in Brisbane's southern suburbs.

The model was applied to various freight policy and traffic management scenarios, including freight vehicle mode choice, lane utilisation and traffic signal settings; as well as the effectiveness of green time extension for approaching heavy vehicles. Benefits were able to be quantified in terms of reduced travel times and stop rates for both heavy and light vehicles in urban arterial corridors.

# Keywords

Traffic management; Traffic analysis; Signalised intersection; Microsimulation; Passenger car equivalence; Delay; Truck; Heavy vehicle; B-double

# Contents

# Figures

# Tables

# Symbols

| | |
|---|---|
| $t$ | Time |
| $x$ | Distance |
| $v$ | Speed |
| $a$ | Acceleration |
| $g$ | Gradient = tan(θ) |
| $v_{max}$ | Maximum velocity, occurring when $a = 0$ |
| $\alpha$ | Initial acceleration, occurring when $v = 0$ |
| $\beta$ | Rate of decrease of acceleration with increasing speed, $\beta = \alpha / v_{max}$ |
| $\gamma$ | Rate of decrease of initial acceleration with increasing grade |
| $\alpha_0$ | Initial acceleration on level ground, occurring when $v = 0$ and $g = 0$ |
| $\mathbf{g}$ | Acceleration due to gravity, ≈ 9.807 m/s$^2$ |
| $C$ | Cycle time |
| $G$ | Displayed green time |
| $I$ | Start loss (start-up lost time) |
| $R$ | Displayed red time |
| $Y$ | Displayed yellow time |
| g | Effective green time |
| $q$ | Flow (vehicles per unit time) |
| $k$ | Density (vehicles per unit distance) |
| Δ | Minimum headway in Cowan's M3 model |
| α | Proportion of free vehicles in Cowan's M3 model |
| λ | Flow-related parameter in Cowan's M3 model |

# Abbreviations

| | |
|---|---|
| AADT | Annual Average Daily Traffic |
| ABS | Australian Bureau of Statistics |
| ARRB | Australian Road Research Board (later ARRB Transport Research) |
| BUC | Brisbane Urban Corridor (an arterial road link through suburban Brisbane between Ipswich Motorway and South Eastern Motorway) |
| BTRE | Bureau of Transport and Regional Economics |
| GPS | Global Positioning System |
| GVM | Gross Vehicle Mass |
| LCV | Light Commercial Vehicle |
| LFV | Large Freight Vehicle |
| LV | Light Vehicle |
| HV | Heavy Vehicle |
| NRTC | National Road Transport Commission (later NTC – National Transport Commission) |
| ODE | Ordinary Differential Equation |
| p.a. | Per Annum |
| PCE | Passenger Car Equivalence |
| pcu | Passenger Car Unit |
| pcphgpl | Passenger Car Per Hour Green Per Lane |
| PDS | Progression Design Speed |
| QUT | Queensland University of Technology |
| QDMR | Queensland Department of Main Roads |
| QT | Queensland Transport |
| SMVU | Survey of Motor Vehicle Use |
| TCE | Through-Car Equivalence |
| TLA | Three Letter Acronym |
| TRB | Transportation Research Board |
| UTM | Universal Transverse Mercator (cartographic projection) |

# Publications

Ramsay, E. D and Bunker, J. M (2007) Management of competing demands on urban freight corridors. *Road & Transport Research* (submitted)

Ramsay, E. D., Bunker, J. M. and Bruzsa, L. (2006) Management of traffic-related effects of heavy vehicles on urban freight corridors. In *Proceedings 9th International Symposium on Heavy Vehicle Weights and Dimensions*, Pennsylvania State University, Pennsylvania, United States

Ramsay, E. D. and Bunker, J. M. (2005) Management of competing demands on urban freight corridors. In Bunker, J. M. and Dia, H., Eds. *Proceedings 27th Conference of Australian Institutes of Transport Research*, Queensland University of Technology, Brisbane

Ramsay, E. D. and Bunker, J. M. (2005) Coordinating for priority on urban arterial freight routes. In *Proceedings Australian Institute of Traffic Planning and Management National Conference*, 117-129, Brisbane

Ramsay, E. D. and Bunker, J. M. (2004) Progression of different vehicle types in a signalised urban arterial corridor - Model development and calibration. In *Proceedings 26th Conference of Australian Institutes of Transport Research*, Melbourne

Ramsay, E. D., Bunker, J. M. and Troutbeck, R. J. (2004) Signalised intersection capacity reduction of trucks. In Mao, B., Tian, Z. and Sun, Q., Eds. *Proceedings Fourth International Conference on Traffic and Transportation Studies*, 793-802, Dalian, China

Ramsay, E. D and Bunker, J. M. (2003) Acceleration of multi-combination vehicles in urban arterial traffic corridors. In Mathams, J., Ed. *Proceedings Main Roads Road System and Engineering Technology Forum*, Brisbane

# Statement of Original Authorship

The work contained in this thesis has not been previously submitted for a degree or diploma at any higher education institution. To the best of my knowledge and belief, the thesis contains no material previously published or written by another person except where due reference is made.

Signature

Date

# Acknowledgements

I would like to thank my principal supervisor, Dr Jon Bunker for his support, guidance and advice during the course of this project. My associate supervisor, Prof. Rod Troutbeck has been an eternal inspiration and of great use in maintaining the focus of the project. The advice and assistance of the staff of the School of Urban Development at QUT is also gratefully acknowledged.

This project was funded by an Australian Postgraduate Industry Award provided by the Australian Research Council, which was supplemented by direct and in-kind support from Queensland Department of Main Roads. A project reference group, chaired by Mr Greg Hollingworth, monitored and advised the project.

Australasian Traffic Surveys loaned a Vehdat automatic traffic counter for use in the project, and Toll Holdings supplied a B-double test vehicle and driver for testing of in-service vehicle performance. Queensland Department of Main Roads staff deserve particular mention for their enthusiastic professional approach in providing in-kind assistance to the project.

I would finally like to express my appreciation to my family, friends, fellow students and professional colleagues for their moral support and encouragement through these challenging years; and in particular to my mother for her strength and generosity in helping me achieve my goals.

# CHAPTER 1 INTRODUCTION

## 1.1 Background to this Study

Increasing demand for road freight has lead to a widespread adoption of more-productive large freight vehicles (LFVs) by Australia's road freight operators. The accessibility of these large freight vehicles to urban road networks reflects concerns about their effects on urban arterial traffic corridor performance.

These larger vehicles are more productive, some being capable of carrying up to twice the payload of standard semi-trailers, and have potential to reduce crash rates and environmental degradation through reduced exposure. These benefits need to be considered in the context of individual vehicles having greater impacts on traffic within urban arterial environments.

A comparative evaluation of impacts of different vehicle types on urban arterial traffic corridor performance requires that an appropriate methodology exists to give valid and objective results.

Current design procedures for urban arterial environments and signalised intersections in particular cater for the presence of vehicles other than passenger cars through use of passenger-car equivalence (PCE) values. Both the Highway Capacity Manual (HCM, Transportation Research Board 2000) and the basis for Australia's signalised intersection design practice (ARR123, Akçelik 1995) recommend a PCE value for a given movement that is independent of the *range* of sizes of heavy vehicles in the stream. Derivation of this value can be traced back forty years (Miller 1963), to a time when heavy vehicles were considerably smaller than the LFVs that are found on today's urban arterial roads. Additionally, the lower platoon acceleration rates associated with the presence of LFVs and other slowly-accelerating vehicles are currently not accounted for when estimating start-up lost time and the associated acceleration delay at signalised intersections.

## 1.2 Research Aims

Hypothesis:

> *"The representation of the impacts of large freight vehicles upon urban arterial traffic corridor performance can be improved."*

This research aims to test this hypothesis by developing an improvement to the current methodology for representing heavy vehicles in an urban arterial traffic corridor. This improved methodology shall be suitable for consideration for use in current design procedures.

The second aim of this research project is to address two basic questions, which will require application of this improved methodology:

> *For a given freight task, does a lesser number of large freight vehicles have a greater or a lesser impact on traffic within an urban corridor than a greater number of relatively smaller freight vehicles?*

and

> *Is there a viable means of giving an optimal level of priority to a large freight vehicle in an urban corridor to minimise delay to the large freight vehicle; and what is the impact on traffic delay and corridor capacity?*

## 1.3 Objectives

These aims are addressed by meeting the following four objectives.

1) Improve the understanding of the interaction of large freight vehicles within urban arterial traffic corridors.
2) Define a methodology to quantify the traffic-related effects of large freight vehicles upon urban arterial traffic corridor performance.

3) Implement the methodology outlined in Objective 2 as a practical application.

4) Evaluate the effectiveness of existing and alternative scenarios in minimising the traffic-related impacts of large freight vehicles.

The work presented in this thesis is directed towards the meeting of these four project objectives, and a summary of how each had been addressed is presented in the concluding chapter.

In doing so, the thesis intends to further the research base in this area by providing a summary of the existing literature and a traffic corridor model that can serve as a useful basis for future work.

## 1.4 Scope and Limitations of the Study

To clarify the scope of the project in addressing these aims, the following definitions have been used in this thesis.

### 1.4.1 Definitions

**Large Freight Vehicle** – a freight vehicle which is longer and/or heavier than those permitted general access to the entire road network, particularly including examples present in the current Australian vehicle population such as B-doubles and Road Trains. General-access freight vehicles would be indirectly covered by ensuring that the methodology is equally as applicable to them as to large freight vehicles.

**Urban Arterial Traffic Corridor** – an individual identifiable route through an urban road network, which carries a high traffic volume across multiple lanes. These corridors also generally act as major identifiable freight routes, and are designated as accessible to B-doubles by the relevant state road authority. Depending upon existing traffic volumes and road widths, these may or may not feature divided carriageways, side property access and on street parking. Speed environments on the urban arterial traffic corridors will generally range from 60 to 80 km/h.

The term "corridor" is often used in a transport planning context to refer to an area where there may be multiple routes and possibly multiple modes available (e.g. alternative roads and public transport services). In the context of this thesis, the term refers to a single route within a larger urban traffic network.

Limited access, grade separated roads in urban areas, such as freeways, motorways or tollways, will not be considered.

Many intersections along the type of corridor to be studied are controlled by traffic signals. These often operate on a common coordinated signal plan. With much of the delay and capacity restraint along a traffic corridor occurring at signalised intersections, much of the focus of the project will be upon the performance of individual signalised intersections. Traffic at unsignalised intersections will not be covered, since route selection guidelines for major urban freight routes generally require full signalisation at major intersections.

Network-level analyses will not be conducted. Where the corridor is considered part of a larger network in which alternative routes may exist between origin and destination pairs, a full traffic-assignment analysis based on minimising user costs is considered to be beyond the scope of the project. Scenarios examined in this thesis may predict travel time changes along the corridor, which in turn may attract or deter users from using the corridor. The degree to which this occurs can only be estimated by accurate modelling of traffic volumes and travel times through the entire urban network, which is considered to be beyond an investigation of traffic around individual large freight vehicles.

Traffic on the arterial corridor will be considered during peak and off-peak periods, in order to determine impacts at various levels of service. Low-flow (night time) periods would be used to obtain travel times in the absence of other traffic, which is used in estimating the expected delay.

**Traffic-Related Impact** – a direct contribution to a change in the measurable performance of the traffic corridor in providing for the flow of traffic. A direct

contribution is defined as that due to the physical presence of the individual large freight vehicle moving through the urban arterial traffic corridor.

It is acknowledged that additional contributions to arterial corridor performance have been attributed to heavy vehicles. These include on-street parking, vehicle breakdowns and accidents, turning, obscuring of other traffic, and lateral behaviour. These are considered to be indirect factors, since they are not attributable to the heavy vehicle attempting to progress along the corridor with the other traffic, and are considered to be beyond the scope of this current project.

Many non traffic-related or external impacts of heavy vehicles operating on an arterial corridor have been identified earlier. These include noise, emissions and fuel consumption of heavy vehicles, crashworthiness and crash-compatibility, accident rates and severity, movement of hazardous materials, perceived threats to road users, urban amenity, quality of life and adjoining property value. These are also considered to be beyond the scope of the current project; however, it is considered that improvements in many of these external impacts would be achieved by seeking to improve the overall performance of the traffic corridor.

The focus of the thesis is to investigate the difference in longitudinal kinematic effect of large freight vehicles compared to general traffic upon the delay and capacity of urban arterial traffic corridors as defined above. This clarifies the aims of the project by defining the specific effects to be considered and the objective measures used to quantify traffic performance.

Scenarios to minimise the traffic-related impacts will be limited to those using technologies that are available currently or in the near future. Effects of major infrastructure works will not be examined. Low-cost options that are intended to make the most of the existing infrastructure will form the basis of scenarios to be examined. Typically these may include (Ogden 1991): varying signal timing plans and offsets between adjacent signals, and heavy vehicle detection with associated green time extension.

### 1.4.2 Coverage

Table 1.1 presents the areas of investigation that are included and excluded from this thesis. Many of the topics excluded will be indirectly covered by association, or would be able to be addressed in latter studies.

**Table 1.1 – Topics included in and excluded from this thesis**

| *Included* | *Excluded* |
|---|---|
| **Road-Related** | |
| Urban arterial traffic corridors,<br>Designated multi-combination vehicle routes | Rural / Remote area roads<br>Freeways, Motorways, Tollways<br>Local roads, Collector streets |
| Signalised intersections | Grade-separate intersections,<br>Unsignalised intersections,<br>Roundabouts |
| Vertical alignment<br>(grade) | Horizontal alignment<br>(curvature, crossfall)<br>Road roughness and unevenness |
| **Vehicle-Related** | |
| General access freight vehicles<br>(Rigid Truck, Articulated Vehicle)<br>Urban Large Freight Vehicles (B-doubles) | Non-urban Large Freight Vehicles<br>(Road trains) |
| Longitudinal performance<br>(acceleration, braking,<br>speed capability) | Lateral performance<br>(offtracking, swept path,<br>tracking ability) |
| Vehicle length and mass | Vehicle width and height |
| **Impacts / Effects** | |
| Traffic-related<br>(capacity, delay) | Infrastructure-related<br>(road wear, bridge loading)<br>Safety-related (rollover, crash compatibility, crashworthiness) |
| Lane selection | Overtaking / passing / merging |
| Direct impacts<br>Attributable to physical presence of moving heavy vehicle | Indirect impacts<br>(emissions, fuel consumption,<br>urban amenity, 'quality of life' etc) |
| **Analysis** | |
| Corridor level<br>(fixed traffic volumes by itinerary) | Network level<br>(traffic assignment to alternate routes) |
| Peak and inter-peak periods | Low-flow periods |

## 1.5 Outline of the Research Methodology

The research methodology employed in this study can be summarised as follows:

1) Establish a clear set of project aims and objectives, and the scope of the study.
2) Undertake a review of existing literature on the traffic impacts of LFVs in urban areas, establishing deficiencies and opportunities in the existing literature.
3) Undertake a review of existing traffic models having the potential to be used or adapted for this current application, identifying their strengths and limitations.
4) Specify and develop or adapt a model suitable for investigating the urban traffic-related effects of LFVs.
5) Collect and analyse vehicle and traffic data, using it to calibrate the model that had been developed.
6) Validate the operation of the calibrated model by investigating its sensitivity to key parameters.
7) Use the model to investigate the effectiveness of several traffic, policy and vehicle-related strategies having the potential to reduce traffic-related impacts of LFVs.

Further details on the data collection and analysis methodology are presented at the start of Chapter 6, which describes the collection of traffic and vehicle data used to calibrate the parameters of the model developed in this project.

## 1.6 Structure of this Thesis

The structure of this thesis closely follows the research methodology outlined above. Figure 1.1 shows the relationships between the 11 chapters in this thesis.

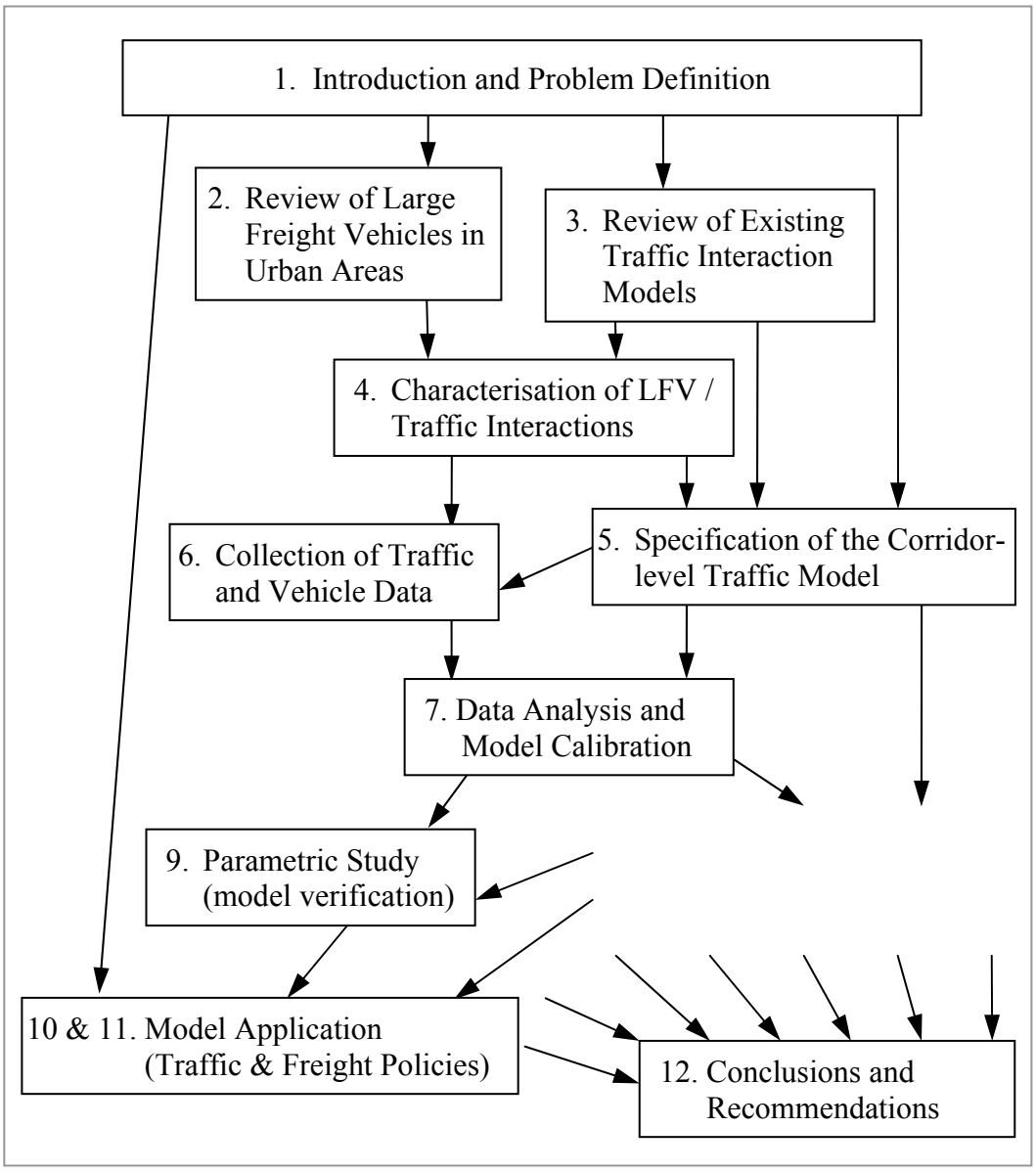


**Figure 1.1 – Structure of this thesis**

Chapter 1 (this chapter) is an introduction to the thesis. It describes the aims and objectives of the study, the scope and limitations of the investigations, and provides this outline of the thesis.

Chapter 2 reviews existing literature on the operation of LFVs, concentrating on the traffic related effects of their use in urban areas.

Chapter 3 reviews existing traffic models, describing their advantages and disadvantages for use in the current application.

Chapter 4 characterises the performance of individual vehicles in urban traffic, with particular emphasis on LFVs and their effects on surrounding vehicles and the traffic corridor performance.

Chapter 5 provides a specification for a corridor-level traffic model that can be used to investigate the effectiveness of various strategic policies. The data requirements for calibrating the model are also specified.

Chapter 6 describes the collection of the traffic and vehicle data that are used in the calibration of the model.

Chapter 7 describes the analysis of the traffic data, providing a set of model parameters used to calibrate the model.

Chapter 8 describes the development of the corridor-level traffic simulation model.

Chapter 9 describes the parametric study undertaken using the traffic corridor simulation model, showing the sensitivity of the model to various input parameters.

Chapter 10 describes the application of the model to investigating the effectiveness of various traffic- and vehicle-related policies and strategies and validating its operation.

Chapter 11 applies the model to an existing urban arterial freight corridor, demonstrating the usability of the model in realistic applications.

Chapter 12 concludes the thesis, substantiating the novel and innovative work undertaken, and presenting a set of opportunities for further research.

# CHAPTER 2 REVIEW OF LARGE FREIGHT VEHICLES IN URBAN AREAS

## 2.1 Introduction to this Review

This chapter reviews much of the current literature relating to Large Freight Vehicle (LFV) operations and their impacts on urban traffic networks. It begins by describing what a LFV is, and a brief history of their development. The growth of LFV numbers is documented by referring to published statistics. A section then follows on characterising LFVs, emphasising their longitudinal performance capability in urban traffic. This leads into a section on quantifying the effects of LFVs upon traffic, including the concept of Passenger Car Equivalence (PCE).

From the traffic side, the needs and desires of LFV operators in urban traffic is covered, particularly in terms of signal and network area control strategies. A concluding section brings the various topics together and identifies areas requiring further investigation.

## 2.2 Freight Vehicle Hierarchy

### 2.2.1 Definitions

A **Large Freight Vehicle** is a vehicle combination, comprised of a powered unit towing more than one trailer or semi-trailer, which exceeds the dimension limits imposed upon vehicles that have general access to the road system. Vehicles or combinations exceeding these dimensions have restricted access to parts of the road network declared by the individual state road authorities.

These statutory limits for general access vehicles are (Australia 1999):

- width of 2.5 metres
- height of 4.3 metres
- maximum length of 12.5 metres for a single vehicle and 19 metres for a combination (e.g. prime mover / semi-trailer or truck / trailer combination)
- deck length of 13.7 metres for semi-trailers

An **Articulated Truck** is a vehicle having at least three axle groups, the first two on a common vehicle unit. Figure 2.1 shows a typical 6-axle articulated truck, which conforms to the statutory limits, specified above, and thus has general access to the road network.

This figure is not available online.
Please consult the hardcopy thesis
available from the QUT Library

*www.bunker.com.au*

**Figure 2.1 – Typical 6-axle articulated truck, having general access to the road network**

A **B-double** (Figure 2.2) is an example of a LFV that comprises a prime mover towing two semi-trailers. The combination has a maximum length of 25 metres, specified in the Vehicle Standard Rules. The maximum mass of a B-double is generally taken to be 62.5 tonnes, however in some applications Higher Mass Limit and Concessional (Livestock) loading schemes may apply.

Since the B-double exceeds the dimension limits of a general access vehicle, it is restricted to operating on nominated routes. Each state road and/or transport authority publishes a network of routes that are eligible for use by B-doubles.

Note that a B-double having a length of less than 19 metres conforms to the requirements for general access. These vehicles generally have seven axles, and a gross vehicle mass of 49.5 tonne.

This figure is not available online.
Please consult the hardcopy thesis
available from the QUT Library

*www.bunker.com.au*

**Figure 2.2 – Typical 9-axle B-double, having access to restricted routes through urban areas**

A **B-triple** is a LFV consisting of a prime mover towing three semi-trailers. The rear semi-trailer sits on the back of the second semi-trailer, and the second semi-trailer sits on the back of the first semi-trailer. The combination has a maximum length of 36.5 metres and a maximum gross vehicle mass of 82.5 tonnes.

A **Road train** is LFV, other than a B-double, consisting of a motor vehicle towing at least two trailers (counting a converter dolly supporting a semi-trailer as a single trailer). For route classification purposes, the following two classes of Road trains are commonly specified by state road and/or transport authorities:

- Type 1 Road trains, having a maximum length of 36.5 metres; and
- Type 2 Road trains, having a maximum length of 53.5 metres.

There are various vehicle and trailer combinations within each of these two classes. An A-double refers to a Type 1 Road train consisting of a prime mover and semi-trailer towing a full trailer. A B-triple (as described above) is another example of a Type 1 Road train. An A-triple, shown in Figure 2.3, refers to a Type 2 Road train consisting of a prime mover and a semi-trailer towing two full trailers. An AAB-Quad refers to a Type 2 Road train consisting of four trailers, the rear two of which are connected as a B-double.

Road trains do not have access to capital cities on the Australian east coast. Adelaide, Darwin and Perth permit limited access of Type 1 Road Trains to their ports and some industrial areas.

This figure is not available online. Please consult the hardcopy thesis available from the QUT Library

*www.westernstar.com.au*

**Figure 2.3 – Typical Road train, not permitted to access urban areas**

### 2.2.2 Vehicle specifications

Table 2.1, from Ramsay (1998), shows the typical overall vehicle lengths, gross vehicle masses and engine power ratings for a number of vehicle types found on Australian roads. Note that, despite power increasing with mass, the power-to-mass ratio generally decreases with vehicle size. This leads to the poorer acceleration capabilities of LFVs relative to smaller vehicles.

**Table 2.1 – Lengths, masses and power ratings for various vehicle types**

*Source: Ramsay (1998)*

| *Vehicle Type* | *Overall Vehicle Length (m)* | *Gross Vehicle Mass (tonne)* | *Typical Horsepower (hp)* | *Power / Mass Ratio (hp/tonne)* |
|---|---|---|---|---|
| Semi-Trailer | 19.0 | 42.5 | 350 | 8.2 |
| B-double | 25.0 | 62.5 | 400 | 6.4 |
| A-double | 36.5 | 79.0 | 450 | 5.7 |
| A-triple | 53.5 | 115.5 | 500 | 5.3 |

*Notes : 1 hp = 0.746 kW*

*Gross Vehicle Mass applies to vehicles without Road Friendly Suspension*

For comparison, a typical passenger car has a length of 5 metres, mass of 1.6 tonne, and power of 134 hp (100 kW), giving a power / mass ratio of 84 hp/tonne.

### 2.2.3 Vehicle classification

Because of their specific vehicle types, different countries have developed their own vehicle classification schemes. The Austroads Vehicle Classification Scheme (Peters 1993) is the most widely used scheme in Australia. This classification scheme comprises 13 separate classes ranging from passenger cars through to triple road trains, as shown in Figure 2.4. Classification is based on the number of axles and axle groups on the vehicle. This classification scheme has been included in most of the automatic vehicle counter / classifiers available in Australia, and the algorithm has been coded into the revised detection algorithm for unidirectional traffic described in Appendix A of this thesis.

# VEHICLE CLASSIFICATION SYSTEM

**AUSTROADS**

| CLASS | LIGHT VEHICLES |
|---|---|
| **1** | SHORT<br>Car, Van, Wagon, 4WD,<br>Utility, Bicycle, Motorcycle |
| **2** | SHORT - TOWING<br>Trailer, Caravan, Boat |
| | HEAVY VEHICLES |
| **3** | TWO AXLE TRUCK OR BUS<br>*2 axles |
| **4** | THREE AXLE TRUCK OR BUS<br>*3 axles, 2 axle groups |
| **5** | FOUR (or FIVE) AXLE TRUCK<br>*4 (5) axles, 2 axle groups |
| **6** | THREE AXLE ARTICULATED<br>*3 axles, 3 axle groups |
| **7** | FOUR AXLE ARTICULATED<br>*4 axles, 3 or 4 axle groups |
| **8** | FIVE AXLE ARTICULATED<br>*5 axles, 3+ axle groups |
| **9** | SIX AXLE ARTICULATED<br>*6 axles, 3+ axle groups or 7+ axles, 3 axle groups |
| | LONG VEHICLES AND ROAD TRAINS |
| **10** | B DOUBLE or HEAVY TRUCK and TRAILER<br>*7+ axles, 4 axle groups |
| **11** | DOUBLE ROAD TRAIN<br>*7+ axles, 5 or 6 axle groups |
| **12** | TRIPLE ROAD TRAIN<br>*7+ axles, 7+ axle groups |

*Based on a table by Main Roads Western Australia (www.mrwa.wa.gov.au)*

**Figure 2.4 – Austroads vehicle classification scheme**

## 2.3 Presence of Large Freight Vehicles

Usage of LFVs in Australia has increased rapidly over the past decade. Road trains operate in the more remote areas of Australia. B-doubles have been becoming more frequent in the more populous states, and now carry much of the interstate freight between the capital cities on the eastern seaboard.

The Survey of Motor Vehicle Use (SMVU) is conducted annually by the Australian Bureau of Statistics (ABS 1999-2006), documenting motor vehicle travel characteristics and freight movements in each Australian state. The surveys have indicated a continued growth in commercial vehicle traffic volumes and the amount of freight moved (Table 2.2 and Figure 2.5), both in capital cities (urban areas) as much as in rural and remote locations.

**Table 2.2 – Growth in freight carried by vehicle type, 1998-2005**

*Source : Survey of Motor Vehicle Use (ABS 1999-2006)*

| | *Millions of tonne-kilometres of freight carried in Australia each year* | | | | | | | |
|---|---|---|---|---|---|---|---|---|
| *Vehicle Type* | *1998* | *1999* | *2000* | *2001* | *2002* | *2003* | *2004* | *2005* |
| 2-axle rigid trucks | 8 826 | 9 816 | 9 058 | 9 736 | 10 231 | 10 995 | 11 045 | 9 965 |
| 3-axle rigid trucks | 12 069 | 12 214 | 12 709 | 12 932 | 15 120 | 17 165 | 15 518 | 17 801 |
| 4+ axle rigid trucks | 1 916 | 1 710 | 2 035 | 2 213 | 2 987 | 2 422 | 3 189 | 2 395 |
| Single axle trailers | 216 | 262 | 188 | 218 | 124 | 112 | 168 | 161 |
| Tandem axle trailers | 4 329 | 4 422 | 5 166 | 4 891 | 4 664 | 4 749 | 4 199 | 4 721 |
| Triaxle trailers | 51 518 | 52 463 | 50 421 | 50 865 | 47 852 | 53 113 | 49 102 | 50 611 |
| B-doubles | 15 449 | 19 889 | 22 131 | 26 387 | 29 260 | 35 277 | 38 244 | 46 934 |
| Road trains | 15 645 | 21 584 | 18 269 | 16 865 | 21 843 | 18 773 | 25 594 | 19 398 |
| Other | 1 603 | 2 404 | 3 248 | 2 667 | 3 233 | 3 633 | 3 974 | 5 100 |
| **Total** | **111 571** | **124 764** | **123 225** | **126 774** | **135 314** | **146 239** | **151 033** | **157 086** |

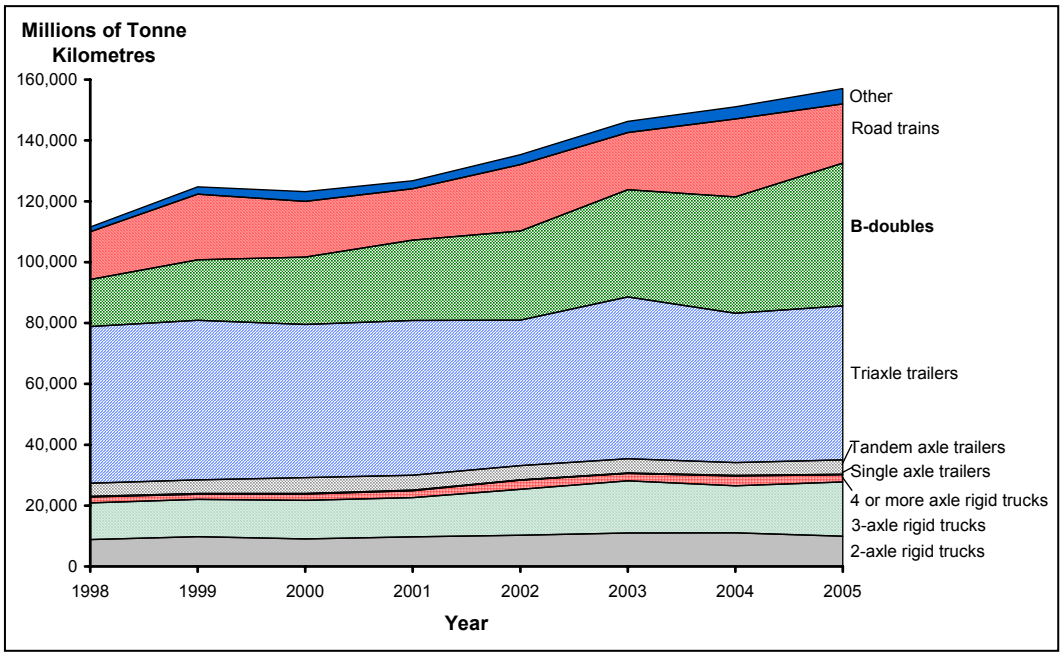


*Survey of Motor Vehicle Use (ABS 1999-2006)*

**Figure 2.5 – Growth in freight volume by vehicle type, 1998-2005**

The survey series has shown that B-double usage has increased over the past seven years from 14% in 1998 to 30% in 2005. This increase has accounted for almost all (69%) of the growth in tonne kilometres carried over that period.

Not all of this growth has occurred in urban areas, but the accessibility of B-doubles to urban areas and their greater productivity are major factors contributing to this growth.

Historical data from the SMVU was extrapolated by BTRE (2002) to predict the greenhouse gas emissions from transport through to the year 2020. Both the number of commercial vehicles and the freight volume carried (Figure 2.5) was forecast to increase continually over this period. The majority of this increased freight volume was predicted to be carried by a greater number of articulated trucks. LFV usage was not considered separately.

Within BTRE's aggregate forecast growth in domestic transport emissions (at about 1.7 per cent per annum), aviation is projected to have the strongest rate of growth (of about 4.4 per cent per annum), followed by commercial road vehicles (2.2 per cent per annum). The passenger car fleet is forecast to exhibit a slower rate of growth (of around 1 per cent per annum).

This figure is not available online.
Please consult the hardcopy thesis
available from the QUT Library

*Source: BTRE(2002)*

**Figure 2.6 – BTRE forecast freight growth in Australia, 1990-2020**

This 'doubling of the freight task' forecast has led to concerns about the capacity of the current road network to cope with the increase. This, in turn, has led to by the state road authorities and the National Transport Commission (NTC) having a more liberal approach of permitting greater innovation in road transport vehicle design.

More recently, the Bureau of Transport and Regional Economics (BTRE 2006) predicted a continuing increase of capital city road freight, growing in Brisbane at 3.7% per annual (p.a.), compared to an average rate of 3.1% p.a. across all 8 capital cities. This represents more than double the 2003 volume of urban road freight being moved by 2020. Placing this in context, this is more modest than the 5.0% p.a. growth rate documented by the SMVU between 1971 and 2003.

## 2.4 A History of the Introduction and Use of LFVs in Australia

### 2.4.1 LFVs in rural and remote areas

Australia has a long history of innovation in road transport. One of the first examples was the "Government Road train", which was imported from Britain in 1934 as an eight-wheel drive rigid truck towing two self-steering trailers. Having an overall length of 22 metres, payload of 15 tonne, and maximum speed of 45 km/h, it served on the rough tracks of the Northern Territory for many years, delivering mail and supplies to remote stations (Maddock 1988).

Following World War II, a number of ex-US army trucks and trailers remained in Northern Australia; these were put to good use in opening up the interior of Australia. Due to the poor roads, low speeds and traffic volumes, there were few safety-related problems with these vehicles. Road improvements led to increasing speeds and traffic volumes, and calls for greater regulation of Road trains. By the 1970's individual states (excluding Victoria, Tasmania and Australian Capital Territory) had developed networks of designated routes for Type 1 and Type 2 Road trains.

The National Association of Australian State Road Authorities conducted the Review of Road Vehicle Limits (RORVL) study in the early 1980's (NAASRA 1985), which recommended a standardisation of masses and dimensions for heavy vehicles across Australia as well as the trial introduction of B-doubles. Originally referred to as B-Trains, but later renamed to avoid confusion with the larger Road trains, these vehicles had been used in Canada for several years. Overall lengths were set at 23 metres, but have since increased to 25 metres.

B-triples, consisting of a prime mover towing three semi-trailers, operate in many remote and rural areas of Queensland and other states, including in urban areas of regional centres. A study by Queensland Transport (Bruzsa and Hurnall 1998) identified significant productivity and safety benefits to the road transport industry and the community. Their impacts on traffic operations were considered, particularly in relation to: extra time required to accelerate to the posted speed limit; increased sight distance requirements; and increased intersection clearance

times (altering signal timing requirements). B-triples also currently operate in outer suburban Melbourne on the Princes Freeway and Western Ring Road between the Ford assembly plants in Geelong and Broadmeadows.

This current decade has seen a move towards a consistent approach to the introduction of innovative vehicles onto the road network. In recognition of the limitations of the current prescriptive standards for regulating vehicles, Austroads and the National Road Transport Commission (NRTC) are leading a number of studies into the introduction of a Performance-Based Standards (PBS) approach to the regulation of heavy vehicles. This will be covered later in this review.

### 2.4.2 LFVs in urban areas

The current practice of designating routes for different vehicle classes, based on route access criteria such as existing road characteristics and traffic levels (Austroads 2000), generally precludes operation of Road trains in urban areas. Road trains carrying freight between urban areas must be assembled from and disaggregated into smaller combination vehicles at the boundaries of designated Road train areas. B-doubles have greater access to major cities within Australia, but are restricted to major designated freight routes that meet the appropriate route access criteria. These higher-standard routes also tend to serve as major commuting routes for travellers within the cities.

A study of the feasibility of permitting Road trains in metropolitan Perth (Pearson *et al.* 1990) was conducted in the early 1990's. As a result of this study, short Double Road trains, with an overall length of up to 27.5 metres are currently permitted to use select routes in the Perth metropolitan area. A recent proposal to allow full-sized Double Road trains (length up to 36.5 m) into Perth was rejected, primarily due to community objections (Peters 2002).

Ramsay (1998) highlighted many of the areas of potential concern to large freight vehicle operations in urban areas, including road-space requirements, acceleration and braking, urban traffic flow interaction, signalised intersections and railway

crossings, infrastructure requirements, and safety and environmental issues. Several options for limiting these impacts were identified, such as better use of vehicle detection technology, optimising of traffic signal and railway level crossing timing for large freight vehicles, and signal coordination to facilitate large freight vehicle movement.

Canada has had a longer history of B-double operation than Australia, but mainly restricted to rural and remote operations. Bruce and Morrall (2000) conducted an investigation on the use in Calgary's urban areas of LFVs operating under permit on Alberta's highways. Investigations were limited to the road space required as an LFV executes a low speed turn, timed acceleration tests, and turning movement clearance times at intersections. Results indicated that LFVs had slower accelerations and longer clearance times than those for which the infrastructure had been designed.

### 2.4.3 Future regulation of LFVs under Performance-Based Standards

In order to meet the forecast increase in freight volumes over the next few decades, it became evident that more freight-efficient vehicles and improved logistics were required. These innovations would need to be fostered by a more flexible and accommodating regulatory process without sacrificing safety and infrastructure-related outcomes.

The introduction of Performance-Based Standards (PBS) was seen as a better means to manage the regulatory process where previously problems had been identified. The prescriptive measures currently regulating vehicles, such as the maximum masses and lengths for different vehicle types mentioned at the start of this review, were seen to be surrogates for the actual impacts that heavy vehicles have on various outcomes, such as vehicle stability, offtracking in low-speed turns, and pavement loading.

Austroads and the National Road Transport Commission managed a number of projects related to PBS for Heavy Vehicles. These projects developed the following list of vehicle-based safety-related performance measures (NRTC 2003a), many of which require detailed computer-based analyses to be conducted.

1) Startability
2) Gradeability
3) Acceleration Capability
4) Overtaking Provision
5) Tracking Ability on a Straight Path
6) Low-Speed Offtracking
7) Frontal Swing
8) Tail Swing
9) Steer Tyre Friction Demand
10) Static Rollover Threshold
11) Rearward Amplification
12) High-Speed Transient Offtracking
13) Yaw Damping Coefficient

In addition to these safety-related measures, three infrastructure-related performance measures are defined in NRTC (2003b):

14) Pavement Vertical Forces
15) Pavement Horizontal Forces
16) Bridge Loading

Levels were set for each performance measure based on the designated area of operation, these being:

| | | |
|---|---|---|
| Level 1: | Unrestricted Access | (currently General Access) |
| Level 2: | Significant Freight Route | (currently B-double routes) |
| Level 3: | Major Freight Route | (currently Type 1 Road train routes) |
| Level 4: | Remote Areas | (currently Type 2 Road train routes) |

As PBS implementation details are being finalised, it is becoming evident that the effects upon traffic capacity and delay, particularly in urban areas, have received less attention than either safety or infrastructure related outcomes.

> *"The main obstacle in implementing performance-based standards is lack of reliable models of the relationships between truck performance characteristics and truck safety and other highway costs"*
>
> *(Kulakowski 2003)*

### 2.4.4 Route access

The selection of routes appropriate for Large Freight Vehicles access is closely related to Performance-Based Standards for Heavy Vehicles. Just as a heavy vehicle is required to meet certain standards to be allowed access to a route, so the route must be of a standard to permit safe operation of vehicles accessing it.

As an example, there may be an intersection clearance time requirement for vehicles in an urban area. Signalised intersections must be set so that times available to clear the intersection always exceed the time allowed to clear it.

A guide to the geometric design of roads specifically for trucks has recently been completed (Austroads 2002). It presents results of a study that was aimed at deriving current truck-based geometric design standards and establishing the traffic volumes and mix at which the adoption of such standards is economically warranted. Parameters are included for a design vehicle, based upon a six-axle articulated truck. These include overall dimensions and masses as well as the power/mass ratio that determines a vehicle's acceleration capability, as will be covered in the next two sections.

## 2.5 Performance of Large Freight Vehicles

### 2.5.1 Length and acceleration capability

Both the greater length and lower power/mass ratio of LFVs contribute to their requiring a greater time to clear an obstacle, such as an intersection or railway level crossing, when starting from rest. Bunker and Haldane (2003) illustrated this by calculating the time taken for a range of LFVs to clear a 17.1-metre width double-track railway level crossing, as shown in Table 2.3. The equivalent average acceleration rate, being the constant acceleration required to travel the crossing distance in the available crossing time when starting from rest, can be seen to decrease with increasing vehicle size.

**Table 2.3 – Times for LFVs to clear a double rail crossing on level grade**

*Source: Bunker and Haldane (2003)*

This table is not available online.
Please consult the hardcopy thesis
available from the QUT Library

McLean (1989) tabulated various truck power/mass ratios used for road design and traffic analyses. These are reproduced in part in Table 2.4, together with the Austroads (2002) power/mass ratio parameter for an articulated truck used for geometric design. References in this table may be found in McLean (1989).

This table shows the increasing power/mass ratio of heavy vehicles with time in the significantly motorised countries. Further, the power / mass ratio of current LFVs (given earlier in Table 2.1) approximate those values of single-articulated vehicles used for design purposes 30 to 40 years ago. However, the lengths of modern LFVs are considerably greater than those of the older design vehicles.

The lower acceleration capability resulting from this lower power/mass ratio has a direct effect upon queue discharge characteristics at intersections, intersection sight distances, acceleration lane lengths and intersection (or railway level crossing) clearance times.

**Table 2.4 – Truck power/mass ratios for road design and traffic analyses**

*Source: McLean (1989), Austroads (2002)*

| *Source* | *Country* | *Basis* | *Power / mass ratio (W/kg)* |
|---|---|---|---|
| 1965 HCM | USA | Typical truck, 2-lane highway | 5.1 |
| AASHO (1965) | USA | Design truck | 4.1 |
| St John and Kobett (1978) | USA | Design truck | 5.5 |
| Gynnerstedt *et al.* (1977) | Sweden | Rigid truck<br>Truck trailer (3/4 axles)<br>Truck trailer (5+ axles) | 9.1<br>6.6<br>4.4 |
| Central Road Res. Inst. (1985) | India | Median value | 3.6 |
| Austroads (2002) | Australia | Design truck | 6.1 |

### 2.5.2 Startup

In addition to having lower acceleration capabilities, the time taken to get a stationary vehicle into a state that it can use its maximum acceleration rate is greater for a heavy vehicle than for a passenger car. Di Cristoforo *et al*. (2004) measured an average start response time for a number of heavy vehicles at 3.25 seconds. This can be compared to an average start response time of 1.15 seconds for passenger cars (Akçelik *et al.* 1999).

This difference is attributed to the greater complexity of starting a heavy vehicle – there is delay in air brake pressure releasing over the length of the vehicle, a greater clutch engagement time, lag in the turbocharger, less than maximum torque being applied at low speeds to prevent driveline damage, and the greater inertia of the rotating engine components at high gear ratios adding to the equivalent mass of the vehicle that must be accelerated (Bosch 2004). All of these factors contribute to a greater time taken to start motion in a heavy vehicle.

Acting against this, the driver of a heavy vehicle is in a much better position to pre-empt the need to start the vehicle into motion, being able to see above passenger cars in front in a queue at an intersection.

### 2.5.3 Braking

Braking capabilities of heavy vehicles are regulated by Australian Design Rules, which prescribe emergency stopping distances that are compatible with those of the surrounding traffic. In-service braking rates may be lower than for cars, due to a greater sight distance offered from a truck cabin. Actions when approaching a changing traffic signal may be different for a heavy vehicle, partly due to the unpleasant prospect of having to regain lost momentum (Ramsay 1998).

The deceleration rate has a lesser effect on the control delay experienced by a vehicle than its acceleration rate. Control delay is the total elapsed time from a vehicle joining the queue until its departure from the stopped position at the head of the queue, including the time required to decelerate to a stop and to accelerate to the free-flow speed (Transportation Research Board 2000, page 7-9).

A faster deceleration rate means that a vehicle approaching the back of a queue at an intersection will need to start braking later; it does not affect the time at which it will start accelerating when the queue discharges, or the time at which it resumes travelling at the free speed after passing through an intersection.

## 2.6 Quantifying the Effects of Large Freight Vehicles in Traffic

The impeding effect of a slow-moving vehicle upon the performance of the general traffic stream has traditionally been expressed in terms of the passenger-car equivalence (PCE) value for the slow-moving vehicle type. The Highway Capacity Manual (HCM, Transportation Research Board 2000) defines PCE as the number of passenger cars displaced by a single heavy vehicle of a particular type under specified roadway, traffic, and control conditions.

PCEs have been applied to various vehicle types, including non-motorised transport in developing countries, and to various traffic scenarios, from rural highways (where the main concern is the reduced speed of heavy vehicles on long grades) through to urban traffic intersections (mainly concerned with reduced saturation flow attributable to heavy vehicles and the associated delays).

### 2.6.1 PCEs in uninterrupted flow

Probably the most widespread application of PCEs is that used in the HCM. PCE values are defined for a number of vehicle types under different levels of service and different terrain. Uninterrupted flow PCE values for trucks range from 1.5 for level terrain to 15.0 for mountainous terrain.

PCEs are used to determine a heavy vehicle adjustment factor using Equation 2.1, which in turn is used to adjust the recorded traffic volume to give the flow rate and ultimately the Level of Service.

$$f_{HV} = 1 \Big/ \left[ \sum_i P_i \left( E_i - 1 \right) \right] \qquad \text{Equation 2.1}$$

where $f_{HV}$ = heavy vehicle adjustment factor

$P_i$ = proportion of vehicles of type $i$ in the traffic stream

$E_i$ = passenger car equivalence of vehicle type $i$.

The 'equivalency' between different vehicle types must be defined in relation to measurable characteristics of the traffic flow. Ideally, these criteria would be related to those used to quantify the performance of the traffic flow; however, this has proven difficult in practice, particularly in empirical studies where there is little control over the composition of the traffic stream.

The most common definition of PCEs is that based upon the ratio of headways of different types of vehicles. The headway in front of a truck or other large vehicle in general is larger than for a passenger car. In accelerating traffic, this is due to

the lower acceleration capability of heavy vehicles (as mentioned in the previous section). In free-flowing urban traffic, this is partially due to the greater braking distance maintained to reduce the likelihood of needing to stop a heavy vehicle. In rural traffic, particularly on grades, larger headways of trucks are more likely due to their being more likely to be platoon leaders, giving a direct link to impedance to traffic and a less direct link to flow performance.

Al-Kaisy *et al*. (2002) suggested that the effect of heavy vehicles on traffic was greater in congested traffic than in uncongested traffic. By considering queue discharge flows at a freeway entrance ramp merge area and at a freeway road works site, it was found that the effect of heavy vehicles was greater during congestion. It was suggested that this was primarily due to the greater number of stops and associated acceleration / deceleration cycles encountered during heavy congestion leading to generally greater headways in front of heavy vehicles.

### 2.6.2 PCEs in interrupted flow

Webster (1958) conducted a controlled experiment that investigated the effects of different proportions of cars, taxis and light commercial vehicles (collectively "light vehicles"), medium and heavy commercial vehicles (collectively "goods vehicles") and some double-decker buses. Percentages of heavy vehicles were increased from 0 to 100 percent, and the times of departures recorded at an intersection stop line.

A linear interpolation of traffic parameters (saturation flow and effective green time) was conducted (Branston and van Zuylen 1978), giving the basis for a methodology which is widely used today for the prediction of these parameters from measured headway data. PCE values, based on headway ratios can also be calculated from this procedure. The differences between synchronous and asynchronous counting methods was highlighted – the former regressing elapsed time onto number of vehicles of given classes, the latter regressing number of passenger cars onto elapsed time and the number of other vehicles.

Different methods of deriving PCEs have been found to give noticeably different results. A study of saturation flows at intersections in the United Kingdom

(Kimber *et al.* 1985) predicted PCE values for heavy goods vehicles ranging from 2.29 for the headway ratio method to 1.6 for asynchronous regression and 2.38 for synchronous regression – all for the same data set. It was also proposed that vehicular delay be considered as an alternative criterion for estimating PCE. An experiment was conducted with a known theoretical traffic distribution, varying the assumed PCEs (based on headway ratio definition) and selecting appropriate signal timings. The PCE value that gave the minimum mean vehicular delay was determined by plotting delay against assumed PCE value. Based on headway measurements, PCE values of 1.5 for medium commercial vehicles, 2.3 for heavy commercial vehicles, and 1.9 for buses and coaches were proposed for examination of saturation flow rates.

Recognising that the position of a large vehicle within a queue has a large effect on its PCE was a major finding (Molina 1987). PCEs of smaller trucks were found to be not significantly affected by their position within the queue. Positioning of large trucks within the queue was found to be significant (Table 2.5), primarily due to the lower acceleration capability of a large truck leading to larger headways when starting from an intersection. Additionally it was found that the number of vehicles affected behind a large truck at an intersection varies with truck type and position in the queue, varying between three and eight vehicles. It was recommended that the heavy vehicle adjustment factor equation in the HCM be modified to include the effects of both light and heavy trucks, in addition to buses and recreational vehicles. PCEs of 3.7 and 1.7 were recommended to be used for heavy and light trucks respectively.

**Table 2.5 – PCE values for various truck types in different queue positions**

*Source: Molina (1987)*

This table is not available online.
Please consult the hardcopy thesis
available from the QUT Library

*Note -n/a-: the sample size was too small to obtain a reliable estimate of PCE*

West and Thurgood (1995) conducted a similar study to that of Molina, introducing a greater range of vehicle types in the traffic mix, including a nine-axle double road train and a rigid truck towing two trailers. Once again, PCE values were found to be greatest for LFVs located at the front of queues at signalised intersections.

**Table 2.6 – PCE values for truck and LFV types in different queue positions**

*Source: West and Thurgood (1995)*

This table is not available online.
Please consult the hardcopy thesis
available from the QUT Library

*Note -n/a-: the sample size was too small to obtain a reliable estimate of PCE*

West and Thurgood (1995) also found differences in PCE values of turning trucks and trucks passing straight through signalised intersections. Higher PCEs were found for large turning vehicles than for straight-through vehicles. A weighted average PCE was calculated based on the proportion of different vehicle types in the traffic stream. Differences in LFVs for turning manoeuvres were attributed to the limited ability of large vehicles to turn sharp corners in addition to their poorer acceleration capability.

### 2.6.3 Through-Car Equivalence

Comparison of different vehicle types in different manoeuvres often extends the PCE concept of relating vehicles to that of through-car equivalence (TCE). The reference vehicle is always a car going straight through the intersection rather than a car conducting the same manoeuvre as the subject vehicle type. Miller (1968a; 1968b) conducted several surveys of headways at signalised intersections in Australia. "Heavy vehicles" were defined as any vehicle having more than two axles, or with dual wheels on the rear axle. Miller's tabulation of TCEs for light and heavy vehicles in different manoeuvres is shown in Table 2.7.

This work was the basis for the TCE value of 2 that is used in a definitive study on traffic signal capacity and timing analysis (ARR-123, Akçelik 1995). The HCM also uses a PCE value of two in the estimation of saturation flow at signalised intersections.

**Table 2.7 – Through-Car Equivalents for different types of vehicle and turn**

*Source: (Miller 1968b)*

This table is not available online.
Please consult the hardcopy thesis
available from the QUT Library

Turning of heavy vehicles was also considered in Brown and Ogden's (1988) study of headways for different movements and vehicle types at several intersection in Melbourne. Headways and hence through-car equivalents were found for both left- and right-turning traffic, finding that both turning manoeuvres and heavy vehicles have higher headways, and that vehicles (cars or heavy vehicles) following heavy vehicles also had a higher headway than for the same vehicle following a car in the same movement. It was suggested that the default heavy vehicle through-car equivalent values used in ARR-123 (Akçelik 1995) were too low, especially for unopposed right turn manoeuvres; and should be increased for sites having a significant proportion of heavy vehicles. Further, it was suggested that a greater range of heavy vehicles should be utilised in current

Australian intersection capacity and timing analyses. The weighted average PCEs were estimated at 1.8 for rigid trucks and 2.5 for articulated trucks.

### 2.6.4 Effect of preceding vehicle type

Cuddon and Ogden (1992) conducted an investigation of the dependence of headways on the preceding vehicle type. This effect is negligible for low proportions of heavy vehicles, but must be accounted for with increasing heavy vehicle proportions. Adjustment of raw headway values resulted in a slight improvement in through-car equivalents compared to Brown and Ogden's study (Table 2.8).

**Table 2.8 – Comparison of Through-Car Equivalents**

*Source: Cuddon and Ogden (1992)*

This table is not available online.
Please consult the hardcopy thesis
available from the QUT Library

Tsao and Chu (1995) found that the average headways for passenger cars and heavy vehicles at signalised intersections were not influenced by the preceding vehicle type. This was a different finding to that of Cuddon and Ogden. Vehicle types, traffic congestion and driver behaviour may have contributed to this difference.

### 2.6.5 PCEs of Large Freight Vehicles in Australia

Queensland University of Technology conducted an examination of the impact of LFVs upon signalised intersection operation (Haldane and Bunker 2002). Through a series of field tests of simulated signalised intersections involving three LFV types on level ground, the study derived PCEs ranging from 4.66 for an unladen B-double to 7.45 for a laden Triple Road train.

As a measure of the efficiency of use of traffic resources by different vehicle types, the ratios of PCE units to freight payload were tabulated (Table 2.9). Larger, heavier vehicles were found to require fewer PCE units to carry the same amount of freight than relatively smaller vehicles. Next, the payload carried per queue length used was tabulated (Table 2.10), once again showing the larger vehicles to be more efficient in transporting freight through urban traffic.

**Table 2.9 – Movements and PCEs for vehicles carrying 1,000 t of freight**

*Source: Haldane and Bunker (2002)*

This table is not available online.
Please consult the hardcopy thesis
available from the QUT Library

**Table 2.10 – Queue length efficiency**

*Source: Haldane and Bunker (2002)*

This table is not available online.
Please consult the hardcopy thesis
available from the QUT Library

### 2.6.6 Modelling and simulation of PCEs

Use of modelling and simulation techniques to predict PCE values has several advantages, most notably the ability to control the traffic levels and composition.

Elefteriadou *et al*. (1997) conducted a study of PCEs on freeways, two-lane highways and arterial roads. The effect that heavy vehicles have on the speed/flow relationship was used as the criterion; for a given constant speed a lower flow in a

mixture of heavy and light vehicle was expected than in a flow comprised solely of light vehicles. Three microsimulation programs (FRESIM, TWOPAS and NETSIM) were used for freeways, two-lane highways and arterial roads, respectively. Vehicles simulated in the study included passenger cars, single unit trucks, semi-trailers, double trailers and triple trailers. Increases in predicted PCEs were noted with decreasing power/mass ratio and with increasing vehicle length.

An alternative methodology for computing PCEs was proposed in a study (Benekohal and Zhao 2000). Delays caused to vehicles behind a heavy vehicle were claimed to be not accurately represented in headway-based PCE formulations. A Delay-based PCE was defined as the delay caused by a heavy vehicle to the delay of a car in an all-passenger car traffic stream. Delay-based PCEs, calculated from measurements at 10 intersections, ranged from 1.07 to 1.47 for single-unit trucks, and from 1.19 to 1.81 for combination trucks. To generalise the results to other conditions, the microsimulation model TRAF-NETSIM was calibrated for the sites and used to predict delay under varying traffic conditions.

It is worth noting that alternative characterisations of PCEs, such as the delay-based PCE mentioned above serve as a useful means of comparing the effects of different vehicles, but they should not be used as surrogates for headway-based PCEs when applied to calculation of saturations flows at signalised intersections.

### 2.6.7 Modelling and simulation of PCEs in congested conditions

Al-Kaisy and Jung (2004) conducted an investigation into the effects of heavy vehicles on traffic flow during congestion. Field data and traffic simulations were conducted into the effects of grade, grade length, percentage of heavy vehicles, restrictions on lane use by heavy vehicles and the location of a bottleneck with respect to an upgrade. Heavy vehicles were represented in the traffic mix within the INTEGRATION microsimulation software by a fixed ratio of 60% smaller heavy vehicles (with a power-to-mass ratio of 16.4 W/kg), and 40% larger heavy vehicles (8.2 W/kg). A PCE factor based on queue discharge flow was used rather than the headway ratio-based definition used in the HCM. PCE effects of heavy vehicles were calculated for the various scenarios, finding that:

1) The effect of heavy vehicles increases with grade

2) Grade length has a greater effect on more severe grades

3) The effect of heavy vehicle percentage on the PCE factor depends on grade. This was not found in uncongested conditions.

4) Lane utilisation strategies have an effect on the PCE factor, with the best case for a three-lane road having all heavy vehicles restricted from using one lane and larger heavy vehicles restricted from using another lane.

5) A bottleneck at the end of an up-grade gives higher PCE factors than if the bottleneck was located at the bottom of the up-grade.

Al-Kaisy *et al*. (2005) took the results of their previous investigations, producing a table of PCE factors for oversaturated traffic conditions on grades of specified lengths. These were intended to supplement those already in the HCM for free-flow traffic conditions.

It should be noted that these investigations applied to heavy vehicle effects on congested traffic in freeway and multi-lane highway conditions <u>without signalised intersections</u>.

## 2.7 Review of Measures to Reduce the Traffic Impacts of LFVs

A review (TTM Consulting 1987) of problems with truck operations under SCRAM, the signal control system operating Melbourne at the time mentioned that:

> *The current method of determining traffic strategies on which to base signal-linking design, rarely addresses the needs other than general traffic flows, public transport priority, and minimal pedestrian requirements. Only one or two examples of providing preferential strategies for heavy movements of large trucks were cited. No specific routes strategies were cited in which truck movements were the prime consideration.*

Several specific problem areas were identified, as were strategies to improve traffic management for freight; these are covered below.

### 2.7.1 Strategic measures

Referring to TTM Consulting's work, Ogden (1999) identified two groups of strategies to handle freight in urban traffic:

1) Strategies that act to disadvantage freight movements on a particular route or location, including route and area bans or geometric constraints. These may move the problem elsewhere, require enforcement, and impose extra costs to operators (and ultimately consumers).

2) Management, rather than elimination, of the problem of trucks in urban areas. By accepting that a range of vehicle types must continue to be catered for, strategies can be developed to reduce overall transport costs without excessively disadvantaging any particular group or vehicle type.

### 2.7.2 Signal settings

Settings at individual signalised intersections may be able to be managed to cater explicitly for the needs of trucks. Ogden (1999) included the following in these measures, based on work done by TTM Consulting (1987):

- Longer clearance times or all-red times (to allow for lower speed and poorer braking)
- Dynamic truck detection and green phase extension so that signals do not turn yellow as a truck is approaching
- Longer minimum phase times (to allow for slower acceleration)
- Adjustment of the gap and waste timers to allow for longer headways between vehicles (caused by slower truck acceleration)
- Turning phase warrants taking particular account of truck turning volumes
- Adjusting PCE values if there is a high proportion of articulated trucks

In the general case of cars and trucks having access to all lanes, these strategies may offer advantages to cars as well as to trucks by removing the bottleneck effect of slow moving trucks at intersections. However, if trucks were restricted to specific lanes, these measures would be likely to disadvantage cars.

### 2.7.3 Linked signals

Ramsay (1998) suggested that signal timings along a corridor optimised for light vehicle may actually lead to a worst case scenario for heavy vehicles. As can be seen in Figure 2.7, a vehicle that is capable of reaching the design speed, but has insufficient acceleration capability to reach the next traffic signal in time to make use of the linking, may actually be subjected to a 'red wave' rather than the 'green wave' that the corridor linking is designed to provide. In the worst case, with a narrow bandwidth and closely-spaced intersections on a significant grade, these slower-accelerating vehicles may arrive at every signal as it turns red. Following vehicles would also be disadvantaged if they had limited passing opportunities.

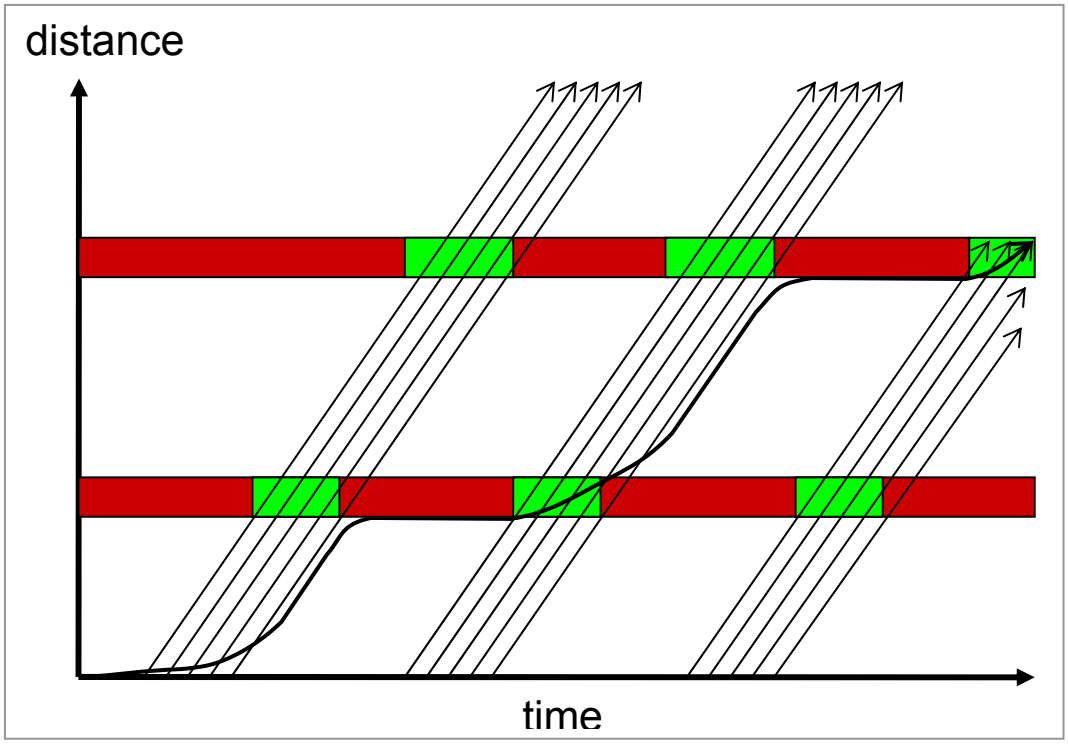


**Figure 2.7 – The "Red Wave" experienced by a slowly-accelerating vehicle**

Lane changing, vehicles entering and leaving the corridor, and more representative bandwidth and signal offset settings ensure that this is extreme instance would rarely be encountered in normal traffic operating conditions.

Signal linking strategies which are mentioned by Ogden (1999) include:

- Linking based on truck speeds
- Link high volume truck turning movements
- Link on the basis of counter-peak travel times when congestion in the peak direction precludes linking
- Minimise the density of signals (signals per kilometre)
- Reduce cycle times as far as possible
- Vehicle detection for priority vehicles

Although many of the measures mentioned above offer advantages to all road users, others seek overall gains in traffic efficiency at the expense of particular user groups. These disadvantages could be reduced if priority measures were implemented only when they were required.

### 2.7.4 Vehicle detection for LFVs

Detection of priority vehicles, and implementation of associated favourable traffic strategies, is already widely in use in Australia and elsewhere in the world. A review of available schemes (Fox *et al.* 1998) identified Brisbane's RAPID bus priority system and SCATS' ability to prioritise trams in Melbourne amongst numerous successful public transport priority systems. Some schemes can provide for emergency vehicle priority, relying on vehicle-mounted transponders.

Fox noted that BLISS (Brisbane Linked Intersection Signal System) has two further 'selective vehicle priority' applications: the ability to handle long, slow-moving vehicles which require longer than the normally-available green time to cross an intersection; and the express handling of convoys of vehicles (for

example for international dignitaries). The former requires vehicle identification tags and the latter involves special signal timing plans.

Several strategies were identified for handling individual priority vehicles once detected:

- **Extension**, where a green is extended to allow the priority vehicle through the junction
- **Recall**, where a movement giving green to the priority vehicle is brought in early
- **Queue jumping**, where a special movement which gives priority vehicles a chance to start ahead of other traffic is triggered
- **Queue management**, where queues of traffic are cleared to allow the priority vehicle a clear run through a junction
- **Triggering green wave**, where progression through a series of junctions is triggered by the arrival of a priority vehicle.

An analysis of the benefits of the intersection priority system adopted in a Sydney-based Bus Rapid Transit network (Vandebona and Rossi 2006) found significant travel times benefits to passengers as well as fewer buses and drivers required to provide a service. The system comprised advance detectors located upstream of the intersection that are actuated by transponders fitted to the buses.

Research conducted in Texas (Middleton *et al.* 1997; Sunkari *et al.* 2000) recognised the benefits of detecting and assisting the passage of heavy-vehicles at isolated rural intersections. Improvements were promoted in operation of the intersection, reduced crash frequency and severity, and reduced pavement deterioration (particularly on thin flexible pavements typically used in Australia).

Although this research was directed towards isolated traffic signals in rural operations (which are not as commonplace in Australia), it is considered to be equally applicable to urban traffic signals operating in vehicle-actuated mode in off-peak periods. Light vehicles arriving on minor approaches to signalised

intersections have the potential to cause inconvenience to vehicles (particularly heavy vehicles) on the major approach. Appropriate detection linked to the traffic signal could delay the signal change if traffic exists on the major approach.

## 2.8 External Implications of LFV Operations in Urban Areas

This review has concentrated on the traffic related impacts of heavy vehicles in urban areas. It is recognised that there are many other areas of impact that are not directly related to the capacity and delay of vehicles in the traffic stream. This section briefly mentions these impacts, but does not intend to provide a detailed review of research into them.

### 2.8.1 Fuel consumption and emissions

On a per-vehicle basis, the fuel consumption of a heavier vehicle is generally higher than for a light vehicle; however fuel consumption (and emissions) on a per-payload-carried basis is less for large freight vehicles than for smaller freight vehicles. As mentioned earlier in this chapter, a forecast increase in greenhouse gas emissions from transport through to the year 2020 was attributed to the increase in light commercial vehicle numbers which were less efficient than larger freight vehicles for the same transport task (BTRE 2002).

This finding was also suggested in responding to a proposal to impose large truck restrictions in Los Angeles (Campbell 1995). The resultant mode shift to a greater number of small trucks was predicted to have negative impacts on overall fuel consumption and atmospheric pollution.

Despite this, the increased congestion and delay that is frequently attributed to heavy trucks would have a negative impact on fuel consumption and emissions.

Rakha and Ding (2003) demonstrated that macroscopic models for prediction of vehicular emissions are deficient in using average speed as the sole traffic-related explanatory variable. The impact of stops on fuel consumptions and hydrocarbon

emissions was quantified, and it was concluded that the number and aggressiveness of vehicle stops (deceleration/acceleration cycles) has a significant impact on vehicle emission rates, particularly hydrocarbons and carbon monoxide.

Noise emitted by heavy vehicles is a primary concern, particularly to residents living near urban freight routes (Jan Taylor and Associates 2003). Noise is greatest during acceleration and braking (particularly engine braking), so any efforts to minimise the number of number of stops that heavy vehicles are required to make would be expected to reduce the noise levels on the corridor. Heavy vehicle detection, as covered in the previous section, was found to be more effective in reducing the number of stops of heavy vehicles in off-peak conditions than in peak conditions. It thus has potential for decreasing the occurrences of acceleration and braking noise of heavy vehicles at night.

### 2.8.2 Infrastructure damage

On a per-vehicle basis, large trucks are generally acknowledged to have a greater potential than small trucks to damage road and bridge infrastructure. Having a greater mass on a greater number of axles, vertical loadings on pavements and stresses imposed on road bridges would be higher. Once again, on a payload-carried basis this loading would be less.

Offtracking of the rear of large vehicles often results in damage to roadside objects and to property damage. It would be expected that smaller vehicles (with an associated smaller offtracking) would be less likely to incur such problems, even if a greater number were present. It should be recognised that routes for large freight vehicles are usually assessed based on having sufficient road-space available to accommodate the vehicle.

Specification of Performance-Based Standards for the Australian road freight vehicles will go well towards improving productivity of the road freight industry whilst maintaining current levels of safety (NRTC 2003a) and infrastructure protection (NRTC 2003b).

Increased traffic congestion is usually associated with an increased number of stops for vehicles in travelling through an urban traffic network. The horizontal stresses imposed on pavements due to the acceleration and braking of heavy vehicles would increase accordingly. Minimising the occurrence of unnecessary stops by heavy vehicles at intersections, as mentioned in the previous section on vehicle detection, would have benefits to the infrastructure as well as traffic operations.

### 2.8.3 Crashes

Heavy vehicle crashes in urban areas of Sydney and Melbourne from 1988 to 1993 were reviewed by Sweatman and Ogden (1995), finding that a majority of rigid truck crashes occurred in urban areas, as did a significant proportion of articulated truck crashes. Most of the crashes at intersections involved turning movements by the heavy vehicle across the path of the other vehicle; however the other vehicle was found to be 'solely responsible' in a majority of cases. Most common factors contributing to the crashes investigated were found to be: inappropriate behaviour by pedestrians or cyclists; excess speed by car / motorcycle drivers; disregard of traffic control by heavy vehicle drivers; disregard of traffic control by car / motorcycle drivers; and alcohol or drug use by car drivers.

With significant urban growth since the original survey period, a subsequent review was undertaken (Hassall 2002). A minority of fatal truck accidents were found to have occurred in urban areas, the majority being on rural highways. For accidents that led to major injuries, 33% of rigid truck and 23% of articulated truck-related accidents occurred in urban areas. The truck or its driver was found to be solely or partially responsible for the accident in 34% of incidents. It was indicated that car and pedestrian behaviour around heavy vehicles still needed considerable modification. Since the 1995 study the numbers of, and distance travelled by, urban articulated truck combinations had increased by 23% and 37% respectively. This had not been reflected in urban articulated fatalities, which were found to have decreased significantly over the same period.

A study of fatal crash rates of multiple trailer trucks in comparison to single trailer trucks in the United States (Forkenbrock and Hanley 2003) found that multiple trailer trucks were more likely to be involved in fatal crashes in conditions of darkness, poor weather, involvement of three or more vehicles, moderate traffic volume, and on roads having higher speed limits. Neither location (urban/rural), nor proximity to an intersection were found to be indicators of increased fatal accident involvement for multiple trailer trucks, primarily due to the relative scarcity of multiple trailer trucks in urban areas and hence near intersections.

## 2.9 Conclusions of this Review

This review has identified many areas of research into heavy vehicle performance in, and upon traffic. It was generally found that a proportionally greater amount of research had been conducted into rural and remote operations than into urban operations for heavy vehicles. Additionally, a majority of traffic-related studies of heavy vehicles were found to have been conducted either prior to the growth of large freight vehicles operations in urban areas, or in countries where large freight vehicles are not as prevalent or are non-existent.

General findings of the review include:

- The majority of the freight growth on Australia's road network over the past 7 years had been carried by B-doubles.
- Major urban freight routes through Australian cities also tended to be major arterial routes for non-freight traffic. Exclusive use of road infrastructure by freight vehicles was a relative rarity.
- Performance-Based Standards had been proposed to ensure that non-standard freight vehicles met certain safety and infrastructure performance criteria. Relatively little emphasis had been placed on the traffic-related impacts of heavy vehicles.

- Early definitions of Passenger-Car Equivalents (PCEs) used different criteria for determining equivalency. With the increasing adoption of the Highway Capacity Manual (HCM), use of average headway as the criterion had become the standard.
- PCE values used in the HCM and ARR123 in determining saturation flow rates at signalised intersections did not reflect the impacts of the range of current heavy vehicles. Use of different PCE values for different classes of heavy vehicles was widely recommended.
- At signalised intersections, PCE values were found to vary with traffic volume and position of the heavy vehicle in the queue. A delay-based PCE had been used as an alternative measure of a heavy vehicle's equivalence.
- Modelling of the effects of heavy vehicles on congested traffic flow and on isolated traffic signal operation had been undertaken in separate studies, producing PCE values for various conditions. This had not yet been taken the additional step of considering their effects on congested traffic along a corridor of signalised intersections.
- Adjustment of signal parameters, such as increased all-red and minimum phase times, were suggested as benefiting heavy vehicles at signalised intersections.
- Detection and appropriate control of heavy vehicles approaching intersections was suggested as having the potential to achieve benefits for the heavy vehicle, other traffic, and the road infrastructure.
- Appropriate linking of traffic signals was suggested as a means of facilitating heavy vehicle progression. Linking based on assumed car travel speed profiles may adversely affect truck progression.

This review has identified specific areas that require further investigation in this current project:

- There was a need for a more accurate representation of heavy vehicles in urban traffic, particularly at signalised intersections. One of the aims of this project is to develop such a representation.

- The relationship of heavy vehicles to start loss and saturation flow at signalised intersections was seen as a key component of this research. A model was required that is capable of determining an appropriate relationship.
- Further investigations of signal coordination along an urban arterial traffic corridor were warranted. These investigation should include coordination of signals based on truck travel time, heavy vehicle detection, and other scenarios identified by Ogden (1991).

These specific areas of investigation warrant an indepth understanding of the operational design and analysis of signalised intersections. The next chapter reviews the current practices and models used to determine the performance of signalised intersections, with particular emphasis placed on their representation of heavy vehicles.

# CHAPTER 3 REVIEW OF SIGNALISED INTERSECTION TRAFFIC MODELS

## 3.1 Introduction to this Review

The operational design of signalised intersections has a strong influence on the traffic flow, delay and efficiency of urban arterial road networks. By direct regulation of the various traffic streams at an intersection, signalisation of an intersection leads to a more-orderly flow of traffic and a reduction in the potential for accidents. With this regulation of traffic by timesharing of priority, there is an increased delay to vehicles at the intersection, this delay being dependent upon the capacity of the intersection to serve the competing phases.

This chapter reviews current Australian and overseas practices to determine the capacity of intersections and delay at intersections. This study is an investigation of the effects of heavy vehicles on signalised intersection performance (as a major component of urban arterial traffic performance), and as such needs to examine the alternative models and evaluate how they manage, or can be modified to manage, the effects of heavy vehicles.

### 3.1.1 Scope of this review

Many of the principles covered in this chapter are equally relevant to coordinated or linked signalised intersections along an arterial corridor or to vehicle-actuation based on minor stream traffic.

It is not intended to cover either the geometric design of signalised intersections or the physical installation of traffic signals at intersections. For these aspects, the reader is referred to the Guide to Traffic Engineering Practice (Austroads 2003), Australian Standard AS 1742.14 (Standards Australia 1996) or to an appropriate road design manual (for example, Main Roads 2006).

Additionally, opposed movements operating under gap acceptance rules will not be covered; nor will actuated operation of signals by traffic on minor approaches.

### 3.1.2 Background

The basic function of a signalised intersection is to assign priority sequentially to conflicting movements by displaying a green light to vehicles when they are permitted to proceed through the intersection. Conflicts are prevented by ensuring that green signals are not indicated at the same time to vehicles on conflicting movements, except for manoeuvres having lower priority which are permitted to proceed under a gap acceptance process.

In this section, we will mainly be considering a fixed-time signal plan of an isolated traffic signal. This is characterised by predetermining the times allocated for the conflicting phases, and the signal controller running each phase sequentially with no feedback to indicate whether greater or lesser times are required to handle each of the traffic movements. Actuated traffic control is an alternative strategy that is often used to handle traffic only when present, such as allocating green time to a minor approach only when vehicles are waiting.

Considerable gains can be obtained in the coordination of signalised intersections to enable platoons of traffic to pass through multiple intersections on a 'green wave'. This is particularly applicable along identifiable urban arterial traffic corridors having a high density of signalised intersections. Strategies for signal coordination will not be covered in this review of isolated intersections; however, the effect of coordination on control delay will be covered when discussing 'progression factors' in the chapter on delay.

### 3.1.3 Model types

Models of traffic at signalised intersections exist for different purposes, including the calculation of appropriate timing plans, prediction of delay and capacity, estimation of emissions and fuel consumption, accident rates, road space requirements and effects of individual vehicles. Different levels of detail within models are required in each case, with models usually optimised for their intended purposes and hence being sub-optimal for other purposes.

Generally speaking, there are two classes of models commonly used for analysis of traffic at signalised intersections – microscopic, which are those that consider the paths (trajectories) of individual vehicles; and macroscopic, which consider the coarser level of traffic flow as a continuum through time and space.

Microscopic level traffic models consider the paths of individual vehicles passing through a network. With the continuing increase in computing power and developments in user interfaces, commercial software for the simulation of traffic at a microscopic level is becoming more frequent, as evidenced by commercial products such as PARAMICS, AIMSUN2 and INTEGRATION. They offer a far greater level of detail than other models, but with an associated loss of generality and an increase in model complexity. Often this complexity is not appreciated by users, and calibration and validation of models continues to be a concern.

Microscopic models often handle non-standard vehicles, such as long and slowly-accelerating LFVs, by the specification of different vehicle classes and parameters. As well as their vehicles, drivers are often assumed heterogeneous, not having the same characteristics for headways, desired speeds, car-following, lane-changing, or gap acceptance criteria. Random numbers are often used to assign vehicle and driver characteristics to vehicles.

This random component leads to a probabilistic model, in that the stochastic nature of traffic is accounted for, but at the expense of not being able to obtain an 'exact' solution, and results generally not being repeatable (unless the same random number sequence is used).

The high complexity of many microscopic traffic models, combined with the need to conduct multiple analyses to account for the probabilistic nature of a randomly heterogeneous model, often leads to a computational requirement far in excess of simpler models.

Macroscopic level traffic models do not consider the individual vehicles that constitute a traffic stream. Rather, traffic is considered to consist of homogeneous flows that may vary with time and space, but always obeying laws of continuity.

Analogies to fluid or compressible gas flows are common (for example Lighthill and Whitham 1955; Richards 1956).

Software packages such as SIDRA Intersection (Akcelik and Associates 2006) and TRANSYT (Robertson 1969; McTrans 1990-2002) are examples of macroscopic models for analysis of signalised intersections and corridors thereof, respectively. Compared to many microscopic packages, they offer a reduced parameter set, fewer computational resources and repeatability of results.

Homogeneity of vehicle and driver characteristics is a feature of macroscopic models. The presence of heterogeneous vehicles, such as trucks, buses and recreational vehicles, is regularly covered using Passenger Car Equivalence (PCE) factors that are used to scale the base flow rates. As mentioned in the previous chapter, this assumption of using a single number to account for a range of different vehicle characteristics has been questioned on several occasions (for example Molina 1987; Cuddon and Ogden 1992; Benekohal and Zhao 2000). Many similar simplifying assumptions need to be made in handling the diversity of vehicles and drivers that exist in reality.

The stochastic nature of traffic is handled through analysis of the probability distributions directly, without having to generate sequences of numbers matching the distributions from random numbers. Thus, a deterministic and repeatable result can be achieved using a macroscopic traffic model.

Both the Highway Capacity Manual (Transportation Research Board 2000) and ARR 123 (Akçelik 1995) model signalised intersections at a macroscopic level. Managing traffic stochasticity whilst still providing a deterministic result is expected of models formulated at this level. The ability of handling different vehicle types must also be considered.

Hybrid models combine elements of both micro- and macroscopic level traffic models. They offer advantages in being able exercise a greater control on the level of detail required, accurately modelling specific features without incurring the overhead of excessive detail.

Examples include application of the LWR kinematic wave model (Lighthill and Whitham 1955; Richards 1956) to signalised intersections and/or to moving bottlenecks. Two recent studies (Laval and Daganzo 2003; Bourrel and Lesort 2003) modelled the trajectory of a moving obstacle in detail, as in a microscopic model, however its effect on the surrounding traffic was modelled as a shock wave, or moving bottleneck, located at an instantaneous position given by the trajectory of the obstacle. Laval and Daganzo's study predicted the capacity of uphill grades in uninterrupted conditions subjected to heavy vehicles. The results were found to "disagree significantly" with results from microscopic models that appear in the latest Highway Capacity Manual (Transportation Research Board 2000), prompting a recommendation of further investigation.

An alternative formulation of a hybrid model is that of a cell-transmission model (Daganzo 1994). The road is subdivided into separate cells, which are observed at regular intervals. Occupancies of the cells vary according to conservation laws in which the net flow across the cell boundaries results in a change of density of traffic within the cell. Heterogeneity of the road with time or with space can be introduced into this type of model (once again using the examples of time-dependent signalised intersections and moving bottlenecks).

## 3.2 Basic Concepts

The models of signalised intersection performance that are used in many current guides and manuals (as covered in the next section) are based upon a model that is generally attributed to Webster (1958).

Webster's model assumes that flow from an intersection approach can only occur during an effective green time, which commences shortly after the start of the displayed green time (given by the start-up lost time) and continues until shortly after the end of the displayed green time (given by the end gain). During this period, flow is assumed to be at a constant rate so long as vehicles remain in the queue.

### 3.2.1 Vehicle trajectories

Figure 3.1 shows the fundamental attributes of flow at a signalised intersection that is assumed by the model used in the Highway Capacity Manual (Transportation Research Board 2000). The upper part of the diagram shows the displayed signal state and the trajectories of seven vehicles passing through the signalised intersection approach. Vehicles #0 and #7 pass freely through the intersection, vehicle #1 stops at the stop line, with vehicles #2 to #6 forming a queue behind it. The middle part of the diagram shows the displayed and effective signal states, and the lower part of the diagram shows the assumed flow profile at the stop line.

This figure is not available online.
Please consult the hardcopy thesis
available from the QUT Library

*Source: (Transportation Research Board 2000, Exhibit 10-8)*

**Figure 3.1 – Fundamental attributes of flow at signalised intersections**

The similarity of the trajectories is evident from this diagram. All vehicles and their drivers have been assumed to have the same deceleration and acceleration, the same reaction times and the same spacing when waiting in the queue (the jam spacing). Arrivals are at uniform headways and speeds, as are departures.

The control delay is shown for one of the vehicles (#2). This is defined as the difference in time taken for the vehicle to pass through the intersection compared to passing through at the free-flow speed if it were unimpeded by the signal.

### 3.2.2 Timing

The middle part of Figure 3.1 defines various times that occur through the cycle. The amount of green time displayed to a particular movement is referred to as **Displayed Green Time** ($G_i$). Similarly, displayed red and yellow times are referred to as $R_i$ and $Y_i$ respectively. Upon receiving a green light, traffic starts to flow on the approach. Depending upon the driver's reaction time, vehicles at the front of the queue will start to accelerate past the stop line and through the intersection. The time taken for all movements in the $i^{th}$ cycle to receive their green time is referred to as the **Cycle Time** ($C_i$).

### 3.2.3 Speeds

Vehicles further upstream in the queue take a longer time to reach the stop line (or any reference line) because they are starting from a position further away from the stop line and they have to wait for the accumulated reaction times of the drivers in front of them. In taking a longer time (and distance), they will be travelling at a higher speed than those vehicles in front of them when crossing the stop line. As speeds of vehicles crossing the stop line increase, their headways decrease asymptotically towards a constant value, known as the saturation headway.

This time taken for the lead vehicles to attain free-flow speed (at some position downstream of the intersection) is greater than if they were to reach the same position when already travelling at the free-flow speed, crossing the stop-line just as the lights changed to green. This excess time is referred to as the **Start Loss** ($I_1$), referred to in the Highway Capacity Manual as the **Start-Up Lost Time**.

### 3.2.4 Flow

The lower part of Figure 3.1 shows the development of flow across the stop line after the signal changes to green. Just as flow through the intersection does not commence as soon as the displayed green period starts, it does not stop as soon as the displayed green period ends. The yellow period prior to the red is intended to account for the driver's reaction time, plus the time taken for vehicles to safely decelerate to a stop at the stop line (or behind the vehicle in front). This additional period of flow after the end of the displayed green time is referred to as the **End Gain** ($e$).

The time available for flow to occur from the approach is referred to as the **Effective Green Time** ($g_i$), and is given by the displayed green time, less the start loss, added to the end gain ($g_i = G_i - I_1 + e$).

An all-red period is used before the next phase is permitted to move. This next phase is handled in the same way as described above, as are any other phases in the timing plan.

### 3.2.5 Capacity

During the effective green period, vehicles are able to pass through the intersection at a constant flow rate that is known as **Saturation Flow**. Flow from the approach is assumed to continue at this rate until the queue of vehicles is depleted or the traffic light changes from green to yellow (and then to red).

The **Capacity** of the approach is defined as the maximum number of vehicles that can be discharged from the queue in the available green time. That is, capacity is the saturation flow multiplied by the effective green period.

Over the cycle time, there may be fewer or greater vehicles arriving at the approach than the capacity of the approach. For the case of fewer arrivals, the queue can be discharged before the green period finishes, and the approach is said to be **Undersaturated**. Alternatively, if the arrival demand exceeds capacity, then

there are vehicles remaining that must wait until the next green period. This is referred to as an Oversaturated condition.

The **Degree of Saturation** is used in ARR 123 as the measure of effectiveness of the intersection. It is defined as the ratio of demand to capacity. Given that the arrival volumes are a random process (and vary throughout the day), occasional over– or undersaturated cycles would not be unexpected. The estimation of an appropriate value for the saturation flow rate is important since it has a direct bearing on the measure of effectiveness of the intersection.

### 3.2.6 Delay

The delay experienced by vehicles at the intersection is also commonly used as a measure of effectiveness. A vehicle travelling unimpeded through the intersection under a green light at the free-flow speed is considered to have no delay. If it is required to stop (or slow) due to the traffic signal or due to stopped or slow traffic at the intersection, there is an associated **Control Delay** that is the additional time taken for the vehicle to pass through the intersection and to regain its original free-flow speed, compared to passing unimpeded through the intersection.

At a microscopic level, referring to Figure 3.2 (Dion *et al.* 2004), this control delay is considered to consist of the following three components:

**Deceleration Delay**, which is the time taken for a vehicle to slow from free-flow speed to stop at the rear of the queue subtracted from the time taken to travel the same distance when travelling at the free-flow speed

**Stopped Delay**, which is the time spent stationary in the queue, or moving up in the queue before finally leaving it

**Acceleration Delay**, which is the time taken to accelerate from rest at the head of the queue up to free-flow speed subtracted from the time taken to travel the same distance when travelling at the free-flow speed.

This figure is not available online.
Please consult the hardcopy thesis
available from the QUT Library

*Source: (Dion et al. 2004)*

**Figure 3.2 – Definition of total, stopped, deceleration and acceleration delays**

Especially at the rear of the queue in undersaturated conditions, vehicles will not need to come to a complete stop. In this case, the stopped delay will be zero, and the control delay will be less than the sum of the deceleration delay and the acceleration delay that would apply if the vehicle had come to rest.

**Average Delay** is generally defined as the sum of the control delay for all vehicles impeded by the signal in a particular cycle divided by the number of vehicles that arrive in that cycle.

**Level-of-Service** is a common means of grading the performance of an intersection or any highway facility. It is widely used in the HCM for various applications. In regards to signalised intersections, threshold values are placed on the average delay in order to determine the level-of-service of the approach or the intersection, on a scale ranging from "A" through to "F".

The derivation of appropriate delay formulae has been the topic of considerable research over the past few decades. The more-widely used models have a fixed component, based on mean arrival and departure rates; a random component for variations in arrivals and departures; a component to account for different arrival rates for red and green periods; and an oversaturation component, in which vehicles may be delayed for multiple cycles.

## 3.3 Common Model Implementations

Webster's intersection model, as described in the previous section, has been implemented in various countries' guides and manuals., including the United States' Highway Capacity Manual (HCM, Transportation Research Board 2000), the Australian Road Research Board's Research Report 123 (ARR123, Akçelik 1995), and Canadian Capacity Guide for Signalized Intersections (CCG, Teply *et al.* 1995). These three bear strong similarities in methodology and application, acknowledging the close working relationship between their authors and their common foundation on Webster's (1958) model.

This section contains a brief history of the development of and differences between these three models.

### 3.3.1 Highway Capacity Manual

The United States' Transportation Research Board (TRB) has undertaken or sponsored considerable research into the performance of transportation systems, including signalised intersections. Much of this research has been directed towards improving the standard manual used throughout the United States (and many other countries) for evaluation of highway facilities.

A major revision of the HCM was undertaken before the fourth edition was released in 2000. This edition, known as HCM2000 (Transportation Research Board 2000) is the current manual used in the United States and many other countries. Coverage of signalised intersections has been split into several chapters: Chapter 10 covers urban street concepts and chapter 16 covers signalised intersection methodologies. Several changes in the way that signalised intersections are handled are evident in comparing this edition to earlier editions.

The methodology for calculation of saturation flow uses a base saturation flow of 1900 passenger cars per hour green per lane, but includes additional adjustment factors for the effects of bicycles, pedestrians and turns from shared lanes.

Headways are based on the times at which the front axle of a vehicle passes the stop line, rather than the rear axle, which was used in previous versions of the HCM. As suggested by Teply and Jones (1991), this would have major effects on the calculation of both start-up lost time and saturation flow. Headways that are measured using the rear bumpers of vehicles, or at a downstream location such as the intersection far side curb line, would be expected to be lower as the accelerating vehicles would be travelling faster when their passages were recorded. For longer vehicles, the greater differences between times at which the front and rear of the vehicle passes a reference line would be expected to lead to a greater difference in consecutive headways than for shorter vehicles.

### 3.3.2 ARR 123

The basis of the current design method used in Australia and several other countries is presented in the Australian Road Research Board's Research Report 123 (Akçelik 1995). This research report presents in detail the methodology for signalised intersection timing and capacity analysis, includes several worked examples, and presents formulae for predicting delay and other measures of effectiveness.

Much of the work behind ARR 123 was conducted in the late 1960's (Miller 1968a; b). One of the improvements included in ARR 123 was the basing of timings on movements, rather than on phases. This is more appropriate for situations where some movements span multiple phases.

The analysis method was implemented as a software program shortly after its initial publication. This software product is known as SIDRA (Signalised Intersection Design and Research Aid) and is widely used in over 2160 sites in 86 countries (as of October 2006). The methods used in SIDRA have developed beyond those originally proposed in ARR 123, now being able to handle roundabouts and other unsignalised intersections, as well as several intersection-specific problems such as short lanes and lane blockages in shared lanes.

ARR 123 does not give a level-of service indication similar to that use in the HCM. The primary measure of effectiveness is the degree of saturation, although formulae are presented for other measures such as delay and queue length.

### 3.3.3 Canadian Capacity Guide

The Canadian Capacity Guide (Teply *et al.* 1995) was developed out of a recognition of a need for a Canadian-specific document to cater for the different analytical and design methods used for signalised intersections in that country compared to those available in the United States' HCM.

Major differences between the CCG and HCM include calculation of saturation flow on a lane-by-lane basis. Saturation flow is expressed in terms of passenger-car units per hour (pcu/h), rather than vehicles per hour as used in the HCM and ARR 123. Hence, adjustments are required when converting saturation flows between the CCG and other manuals/guides.

The CCG assumes the effective green time is one second more than the displayed green time. This leads to the end gain being one second greater than the start loss.

## 3.4 Queue Arrival Models

The rate at which vehicles arrive at the tail of a queue at a signalised intersection has a large impact upon the performance of the intersection, in terms of its capacity and delay to the vehicles passing through it.

The simplest queue arrival profile model assumes that vehicles arrive at a uniform rate, in which case the expected delay can be predicted from a queue arrival polygon, as will be demonstrated later in this chapter.

Webster's (1958) model assumed a random arrival process that accounted for the stochastic variation in arrivals. Occasional oversaturation of the intersection occurred even when the mean arrival rate was below capacity, and this effect was included in the predicted delay.

Explicitly accounting for platooning of vehicles is commonly achieved through having different arrival rates during red and green periods. This leads to the concept of a progression factor for an approach. Progression is said to be favourable if a greater arrival rate occurs during the green period than during the red period; and unfavourable progression if otherwise. The capacity of an intersection is greater under favourable progression conditions, with a greater number of vehicles being able to pass through for a given green period than if arrivals were uniform or under unfavourable progression conditions.

By assuming that the peak period only occurs for a short space of time (15 minutes is often used), a manageable amount of oversupply can be introduced into a model. A 'Peak Hour Factor' is often used to convert the peak 15 minute volume to an equivalent hourly flow rate.

Detailed models of intersection delay, such as the model presented in the HCM include various factors that account for random arrivals, progression factors and peaking. This will be covered in detail in a later section of this chapter.

## 3.5 Queue Discharge Models

### 3.5.1 General queue discharge characteristics

Queue discharge flow develops as vehicles accelerate from rest at their respective positions within the traffic queue. Figure 3.3, from Akçelik and Besley (2002), shows trajectories of individual vehicles as they are discharged from the queue. The first vehicle commences motion at the perception/reaction time of its driver ($t_r$). Subsequent vehicles start moving at a (generally lesser) time between vehicles ($t_x$). Vehicles are initially at the jam spacing distance ($L_{hj}$) apart, so the queue clearance progresses at a wave speed of $v_x = L_{hj} / t_x$. Vehicles continue to accelerate up to the saturation speed ($v_s$), which is reached in distance $L_a$ and time $t_a$. Acceleration delay ($d_a$) is given by the acceleration time less the time taken to reach $L_a$ if the vehicle was travelling at the saturation speed, $d_a = t_a - L_a / v_s$.

This figure is not available online.
Please consult the hardcopy thesis
available from the QUT Library

*Akçelik and Besley (2002)*

**Figure 3.3 – Arrival and departure wave speed relationships**

A similar mechanism is used to model arrivals at the tail of the queue. Vehicle arrivals are shown in Figure 3.3 as being at a constant rate (although a more general arrival profile could equally have been applied). Vehicles are shown as stopping instantaneously, which is not realistic but is sufficient for its intended purpose of showing the arrival and departure waves.

The rate at which a vehicle decelerates to stop at the tail of a queue does not affect the control delay, only the time at which it stops at the tail of the queue and hence the ratio of deceleration delay to stopped delay. Conversely, the rate of acceleration affects acceleration delay and control delay, but not stopped delay. Slowly decelerating vehicles are not delayed any more so than other vehicles; however, slowly accelerating vehicles take a longer time to reach the free speed and hence are delayed more than other vehicles.

### 3.5.2 Headways

Several authors (for example Briggs 1977; Bonneson 1992; Akçelik *et al.* 1999) have characterised vehicles leaving a queue, noting that increasing speeds as vehicles cross the stop line result in decreasing headways and increasing flows. Bonneson presented the results of several previous studies (Figure 3.4), showing the headways reducing asymptotically towards a constant value, taken to be the reciprocal of the saturation flow rate.

Bonneson did not specifically account for the differences between the four studies presented in this figure, although it can be seen that saturation flows are higher (indicated by lower headways for the latter queue positions) for the more recent studies. This may be a reflection of a general increase in base saturation flows over time (for example the HCM base saturation flow increased from 1800 to 1950 pcphgpl with the introduction of the 2000 edition).

This figure is not available online.
Please consult the hardcopy thesis
available from the QUT Library

*Source: (Bonneson 1992, Figure 1)*

**Figure 3.4 – Comparison of past studies of queue discharge headway**

Bonneson noted the difficulties encountered in fitting the Briggs (1977) model to this data, as shown by the dotted line in this figure. Briggs had utilised a simple constant acceleration model. Bonneson replaced this with an acceleration that

decreased linearly with increasing speed. The revised model was calibrated against stop line speed data collected from five study sites, resulting in the following negative-exponential stop line speed model (Equation 3.1).

$$V_{sl(n)} = V_{\max}\left(1 - e^{-nk}\right) \qquad \text{Equation 3.1}$$

where $V_{sl}(n)$ = stop line speed of the $n^{th}$ queued vehicle

$V_{\max}$ = common desired speed of queued traffic

$k$ = a calibration parameter, which was found to depend upon $V_{\max}$.

A comparison of queue discharge headways (Niittymäki and Pursula 1997) showed variations in queue discharge headway amongst the first few vehicles of a discharging queue (Figure 3.5). Variations were attributed to different observation points and a shorter initial reaction time due to the use of a red / yellow display before the green display in Finnish traffic signals.

This figure is not available online. Please consult the hardcopy thesis available from the QUT Library

*Source: (Niittymäki and Pursula 1997, Figure 2)*

**Figure 3.5 – Queue discharge headways**

Teply and Jones (1991) attributed much of the variations in headways to the different criteria used to measure headway. As shown in Figure 3.6, large differences were predicted between using different locations on consecutive

vehicles, such as using the front or rear axle, or the front or rear bumper. Recording of headways at different locations (at the stop-line and nearside or farside kerb lane) resulted in similar differences.

These differences were seen as leading to difficulties in applying a method from one document to convert to values needed in the calculation procedures used by another document.

Although not specifically covered by Teply and Jones, the presence of alternative headway definitions is particularly relevant in cases of long vehicles in the traffic stream.

This figure is not available online.
Please consult the hardcopy thesis
available from the QUT Library

*Source: (Teply and Jones 1991, Figure 3)*

**Figure 3.6 – Variations in time difference between consecutive vehicles**

Early versions of the HCM (1997 and earlier) measured headways between consecutive rear axles of vehicles, whereas HCM2000 (Transportation Research Board 2000, page 7-8) measures headways between consecutive front axles of vehicles. The difference is particularly important in the queue discharge characteristics of long, slowly accelerating vehicles; in the case of a single truck in a stream of cars, the former would have a single large headway between the rear axles of the truck and the car in front of it, whilst the latter would have two large headways between the front axle of the truck and the cars in front of and behind it.

This project uses the current HCM definition of headway being the time between the passage of a vehicle's front axle and the front axle of the vehicle following it.

### 3.5.3 The effective flow diagram

The flow of vehicles from an intersection approach is best shown by the effective flow diagram, Figure 3.1 (Transportation Research Board 2000) or Figure 3.7 (Akçelik 1981):

This figure is not available online.
Please consult the hardcopy thesis
available from the QUT Library

*Source: (Akçelik 1981, Figure 2.3)*

**Figure 3.7 – Basic saturation flow model**

In both cases, the flow rate is assumed to increase to the saturation flow rate some time after priority is given to the movement. Similarly, if the queue is not fully discharged in the available green time, flow will decrease after the green signal is terminated. The area under the flow curve is taken to be equal to the area of a rectangle of the same height (the saturation flow), and a base length of the effective green time, as shown in Equation 3.2.

$$g = G + \mathrm{I} - \ell \qquad \text{Equation 3.2}$$

where $g$ is the effective green time

$G$ is the displayed green time

I is the inter-green time, including yellow and all-red times

$\ell$ is the lost time, $\ell = a - b$, where $a$ is the start lag, and $b$ is the end gain.

This model is conceptually the same as that used in HCM2000, utilising the same concepts of displayed and effective green times, and an assumed period of saturation flow that is constant over the effective green period. Equation 3.5 shows a similar saturation flow curve from the HCM, with displayed and effective signal timing, and relating it to the space-time diagram.

### 3.5.4 Start loss

HCM2000 defines the start-up lost time as the additional time consumed by the first few vehicles in a queue at a signalised intersection beyond the saturation headway, because of the need to react to the initiation of the green phase and to accelerate.

This thesis uses the term start loss, as used in ARR123, in place of the more-cumbersome term start-up lost time.

Start loss is a function of the acceleration of the vehicles in the queue – the faster they can reach the free speed, the shorter the start loss and the longer the effective green time. For this reason, it is an important consideration when slowly-accelerating heavy vehicles are present in the queue.

Start loss can be estimated from the headways of vehicles crossing the stop line. The difference between headways of the first few vehicles and that of the last vehicles (travelling in saturated conditions) is an estimate of the start loss.

Bonneson and Messer (1998) considered the first four vehicles in the queue to be contributing to the start loss, with the remainder assumed to be travelling at the saturated headway. As shown in Figure 3.8, taken from the HCM, the start loss is the sum over the first four vehicles of their measured headway less the average minimum discharge headway.

The saturation flow rate is the reciprocal of the average minimum discharge headway, which is measured for vehicles after the fourth vehicle through to the end of the saturated period. This procedure for measurement of saturation flow is recommended by the HCM, but the procedure does not extend to the measurement of start loss.

Previous versions of the HCM (1997 and earlier) used the fourth vehicle following the start of the green period as the starting vehicle for saturation flow measurements, and based the headways on the rear axles of consecutive vehicles (not the front axles as used in the 2000 edition of the HCM).

ARR123 recommends that the first 10 seconds of queue discharge is disregarded in the measurement of saturation flow, which be expected to give different results to those obtained using the HCM method. Teply and Jones (1991) showed that the criterion used in ARR123 consistently overestimated saturation flow (by 5 to 23 per cent) when compared to that of the 1985 edition of the HCM. This was primarily attributed to the fact that the ARR123 method excludes the first 10 seconds of the green interval, calculating saturation flow only based upon the more-stable latter flow period. The apparently greater capacity that is calculated using the ARR123 method is offset by a larger lost time.

This figure is not available online.
Please consult the hardcopy thesis
available from the QUT Library

*Source: (Transportation Research Board 2000)*

**Figure 3.8 – Discharge headway by queue position**

In the absence of field data, the 1994 HCM recommend a default value of 3 seconds per phase for lost time (start-up lost time minus end gain), and an example in HCM2000 uses this same value. HCM2000 (page 16-109) recommends (based on Webster and Cobbe 1966) that 1 second of the lost time be allocated to the clearance lost time, leaving 2 seconds for start-up lost time. This is also the value suggested by Messer and Bonneson (1998). ARR123 includes some examples using start loss values ranging from one to six seconds, corresponding to a through movement and a left turn movement at a T-intersection respectively.

Bonneson (1992) suggested that start loss may be longer than the 2 seconds recommended in the 1985 HCM. A discharge headway model was used to relate start-up lost time to parameters of the acceleration model (Equation 3.3). Parameters calibrated to experimental data gave a start-up lost time of 3.67 seconds. This model appears promising in accounting for the effects of different acceleration capabilities upon start loss.

$$K_s = \tau + \frac{V_{\max}}{A_{\max}} \qquad \text{Equation 3.3}$$

where $K_s$ is the start-up lost time (start loss)

$\tau$ is the reaction time

$V_{max}$ is the maximum velocity

$A_{max}$ is the maximum acceleration.

Messer and Bonneson (1998) suggested that higher saturation flows are generally associated with higher speeds, which in turn requires a greater time for vehicles to accelerate. A linear regression of start-up lost time data against saturation flow data obtaining the following relationship (Equation 3.4).

$$l_s = -4.64 + 0.00373\, s_l \qquad \text{Equation 3.4}$$

where $l_s$ is the start-up lost time (start loss)

$s_l$ is the saturation flow.

This empirically-based equation ($r^2$ = 0.41) has little theoretical basis apart from the previously-mentioned association between start loss, saturation flow and free-flow speed. In fact, for low saturation flows (below 1,200 vehicles per hour) it predicts negative start loss values. It was noted that this model predicted greater start loss values of 2.0 and 2.5 seconds (for saturation flow rates of 1800 and 1900 pcphgpl), compared to the 1.0 and 2.0 seconds recommended in Chapter 2 of the 1994 version of the HCM.

Although this relationship is intended for use with homogeneous traffic, it is interesting to see the effect of introducing heavy vehicles. Heavy vehicle adjustment factors for saturation flow would result in a lower predicted saturation flow, and this relationship would predict a shorter start-up lost time.

No relationships were found relating start-up lost time directly to heavy vehicles or road geometric features such as approach grade. Powell (1998) highlighted the lack of an explicit heavy-vehicle adjustment in the intersection delay measurement appendix to Chapter 9 of the 1997 edition of the HCM.

## 3.6 Queue Formation and Discharge Model Parameters

### 3.6.1 Jam spacing

Jam Spacing refers to the spacing of vehicles when they are stopped, as in a queue at an intersection. It is important in signalised intersection analysis because it is one of the two parameters determining the rate at which the departure wave propagates along the queue.

Akçelik *et al*. (1999) reported jam spacings of passenger cars ranging from 5.9 to 7.3 metres from studies of various signalised intersections in Melbourne and Sydney, Australia. An average value of 7.0 metres was suggested for passenger cars, and 11.3 metres for heavy vehicles.

The intersection analysis software package SIDRA Intersection (Akcelik and Associates 2006) uses jam spacings of 7.0 metres for light vehicles and 13.0 metres for heavy vehicles as default parameters, or 7.6 and 14.0 metres respectively if using the HCM parameters.

The CCG (Teply *et al.* 1995) uses a default jam spacing of 6.0 metres for passenger cars. It did not document jam spacings for heavy vehicles.

Austroads (1995) published a number of design vehicles and turning path templates for geometric intersection design purposes. The design car is 5.0 metres long, the design rigid truck is 8.8 metres long, the design articulated vehicle is 19metres long and the design B-double is 25 metres long. Being used for design purposes, these dimensions were intended to represent 98$^{th}$ percentile vehicles; mean vehicle lengths would be slightly less. It should be noted that the empty space between queued vehicles needs to be added to the vehicle lengths to give jam spacings.

Herman *et al*. (1971) reported jam spacings for passenger vehicles of 7.9 metres (25.9 ft), although this was based on the length of the specific car used in their experiments. Messer and Fambro (1977) reported a value of 7.6 metres (25 ft).

Cohen's (2002b) model of car-following includes several example scenarios which used a jam spacing of 20 foot (6.1 metres) between passenger cars and 50 foot (15.24 metres) for the queue positions that are occupied by trucks.

A study in Florida (Long 2002) produced the formula given in Equation 3.5 for the expected queue length based on number of cars, trucks & combination trucks. Also reported were the inter-vehicle spacings between leading and trailing vehicles of different classes.

$$EQL = 0.305 * (12 + 15PPV + 65PTT + 30PO) * EN \qquad \text{Equation 3.5}$$

where $EQL$ = Equivalent Queue Length (in metres)

$PPV$ = proportion of passenger vehicles in queue

$PTT$ = proportion of tractor-trailers in queue

$PO$ = proportion of other trucks in queue

$EN$ = total number of vehicles in queue.

These jam spacing values are tabulated in Table 3.1. Generally evident is the smaller jam spacing of passenger cars in Australia compared to the United States, and the decrease in jam spacing of passenger cars with time. Both of these are most likely associated with differences in average overall vehicle lengths.

**Table 3.1 – Jam spacing parameters from various sources**

| *Vehicle Type* | *Jam spacing (m)* | *Source (Year)* | *Country* |
|---|---|---|---|
| Passenger Car | 7.0 | Akçelik (1999) | Australia |
| " | 7.0 | SIDRA (default) (Akçelik *et al*. 2006) | Australia |
| " | 7.6 | SIDRA (HCM values) (Akçelik *et al*. 2006) | Australia / United States |
| " | 6.0 | CCG (Teply *et al.* 1995) | Canada |
| " | 5.0* | Austroads (1995) | Australia |
| " | 7.9 | Herman *et al*. (1971) | United States |
| " | 7.6 | Messer and Fambro (1977) | United States |
| " | 6.1 | Cohen (2002b) | United States |
| " | 8.2 | Long (2002) | United States |
| Heavy Vehicle | 11.3 | (Akçelik *et al.* 1999) | Australia |
| " | 13.0 | SIDRA (default) (Akçelik *et al*. 2006) | Australia |
| " | 14.0 | SIDRA (HCM values) (Akçelik *et al*. 2006) | Australia / United States |
| " | 15.24 | Cohen (2002b) | United States |
| Prime mover & semi-trailer | 19.0* | Austroads (1995) | Australia |
| Prime mover & semi-trailer | 23.4 | Long (2002) | United States |

* *Vehicle length only, not jam spacing*

### 3.6.2 Reaction times and queue departure response time

The reaction time, or departure response time, between consecutive drivers commencing acceleration is important in establishing saturation flow rate and the speed of the queue departure wave. Figure 3.3 on page 61, taken from Akçelik and Besley (2002), shows the relationships between departure response time and jam spacing, and the queue clearance wave speed and saturation headway.

The queue clearance wave speed, $v_x$ is given by $v_x = L_{hj} / t_x$, where $L_{hj}$ is the jam spacing and $t_x$ is the departure response time. Saturation headway, $h_n$ is then given by $h_n = t_x + 3.6\ L_{hj} / v_n$, where $v_n$ is the maximum queue discharge speed.

It should be noted that Figure 3.3 shows a different response time for the first driver's reaction to the display of the green signal compared to subsequent drivers' reactions to the vehicle in front commencing movement.

Bonneson (1992) reported departure response times in the range 0.8 to 1.4 s. Niittymäki and Pursula (1997) found response times in Finland to be in the range 0.9 to 1.0 seconds. Akçelik *et al*. (1999) reported an average queue departure response time of 1.15 seconds for through movements, and 0.84 seconds for right turn movements.

The lower response times in the Finnish study were attributed to the use of a red / yellow signal display prior to the green display, which was suggested as being a prompt to increase the drivers' alertness. Similarly, increased driver alertness may have contributed to the lower response times measured for right turning movements in the Akçelik *et al*. (1999) study.

Anecdotally, heavy vehicle drivers have been known to predict the onset of the green phase, so it may be appropriate to use lower value of reaction time in comparison to passenger cars.

## 3.7 Saturation Flow Estimation

ARR123, the HCM and the CCG all contain procedures for estimating saturation flow that may be used in the absence of experimental data. In each case, adjustment factors are applied to the base saturation flow in order to obtain a value that is more appropriate for the particular intersection being investigated.

### 3.7.1 ARR 123

ARR 123 uses Equation 3.6 to adjust the base saturation flow to account for lane width, gradient and traffic composition. Heavy vehicles are accounted for using the traffic composition factor. Interactions between heavy vehicles and other factors, such as the gradient of the approach are not taken into account.

$$s = \frac{f_w f_g}{f_c} s_b \qquad \text{Equation 3.6}$$

where $s$ = saturation flow estimate in vehicles/hour

$s_b$ = base saturation flow in through car units per hour

$f_w$ = lane width factor

$f_g$ = gradient factor

$f_c$ = traffic composition factor.

The base saturation flow is determined from the environment class and lane type, as given in Table 3.2, from Miller (1968a).

**Table 3.2 – Base saturation flow (vehicles/hour) for environment class and lane type**

*Source: (Miller 1968a)*

| *Environment Class* | *Lane Type* | | |
|---|---|---|---|
| | *1* | *2* | *3* |
| A | 1850 | 1810 | 1700 |
| B | 1700 | 1670 | 1570 |
| C | 1580 | 1550 | 1270 |

### 3.7.2 Highway Capacity Manual

The HCM recommends that a saturation flow survey is conducted as part of any analysis, and includes a recommended practice for conducting such a survey. In the absence of definitive saturation flow results, the 1984 version the HCM recommended that Equation 3.7 should be used to estimate saturation flow.

$$s = s_o N f_w f_{HV} f_g f_p f_{bb} f_a f_{RT} f_{LT} \qquad \text{Equation 3.7}$$

*Source: HCM 1994, Eqn 9-12*

where $s_o$ = base saturation flow per lane

$N$ = number of lanes

$f_w$ = adjustment factor for lane width

$f_{HV}$ = adjustment factor for heavy vehicles = $100/(100+\%HV(E_T-1)$

where $\%HV$ is the percentage of heavy vehicles, $E_T = 2$ pcphv

$f_g$ = adjustment factor for approach grade

$f_p$ = adjustment factor for parking

$f_{bb}$ = adjustment factor for blocking effect of local buses stopping

$f_a$ = adjustment factor for area, = 0.9 for CBD, 1.0 otherwise

$f_{LT}$ = factor to account for left-turning traffic

$f_{RT}$ = factor to account for right-turning traffic.

A base saturation flow ($s_o$) of 1800 passenger cars per hour green per lane (pcphgpl) was used in the 1984 edition HCM; for the 1994 and 2000 editions of the HCM this was increased to 1900 pcphgpl.

The 2000 edition of the HCM uses a similar equation to Equation 3.7, with the inclusion of additional factors for lane utilisation ($f_{LU}$) and pedestrian adjustment factors for left and right turning traffic ($f_{Lpb}$ and $f_{Rpb}$).

Heavy vehicles are accounted for with $f_{HV}$, which assumes a default PCE value of $E_T = 2$. Using the default percentage of heavy vehicles of 2% (HCM 2000, Exhibit 10-12), $f_{HV}$ can be calculated to be 0.98.

### 3.7.3 Canadian Capacity Guide

The major difference in the way that the CCG estimates saturation flow compared to the HCM or ARR123 is that all flows are defined in terms of PCUs, rather than individual vehicles.

Adjustment factors are present to account for the effects of lane width, grade, turning radius, transit stops, parking, pedestrians, duration of green, protected left turns, permissive left turns (with and without pedestrians), right turns with pedestrians, and shared lanes.

The presence of heavy vehicles is handled in the grade adjustment factor (Equation 3.8), as well as by defining saturation flow in PCUs/hour.

$$F_{grade} = 1 - (G + HV) \qquad \text{Equation 3.8}$$

where $F_{grade}$ = saturation flow rate adjustment factor for the effect of grade

$G$ = average approach grade within 50 m upstream of the intersection

$HV$ = proportion of heavy vehicles, such as buses, trucks or recreational vehicles in the vehicular arrival flow. The arrival flow is not converted to passenger car units (% / 100).

## 3.8 Delay Models

Vehicles are subject to delays at signalised intersections as they slow down, come to a stop, and then speed up again. Quantification of this delay is an important factor in determining the impacts of a signalised intersection, and provides one of several measures of effectiveness by which different options may be examined. The HCM uses delay as the measure by which the Level of Service of an intersection is based, because it is experienced by the motorist – highlighting the importance of this topic.

The presence of heavy vehicles at signalised intersections is generally accepted as contributing to increased delay at intersections, and hence to delay along an entire urban arterial traffic corridor. This increased intersection delay would primarily be

attributable to the lower acceleration capability of heavy vehicles compared to passenger cars. It would not be expected to influence stopped delay to a significant amount:

> *"The presence of commercial vehicles in a platoon of vehicles approaching a signalised intersection does not significantly increase or decrease the average vehicle stop time at the signalised intersection".*
>
> *(Yurysta and Michael 1976)*

With the earlier editions of the HCM basing level of service on stopped delay, the effects of heavy vehicles on level of service would have been through a reduction in queue discharge rate associated with the use of a heavy vehicle factor that would lower the saturation flow rate.

Both the 2000 edition of the HCM and ARR123 use control delay as a measure of effectiveness. The reduction in acceleration rate associated with heavy vehicles leads to increased acceleration delay, and thus to increased start loss and reduced effective green time. Increases in control delay due to heavy vehicles would be expected to be more significant than increases in stopped delay.

The proportional change in control delay due to heavy vehicles would be expected to be higher as displayed green time decreases, this is particularly relevant to low volume movements, where only short periods of green time are required (by allocating time based on equating degrees of saturation). This increased delay would be particularly evident if the presence of heavy vehicles forces an otherwise undersaturated movement into oversaturation.

## 3.9 Conclusions of this Review

Modelling of the capacity and delay at signalised intersections has been the topic of considerable research over the past few decades. The Highway Capacity Manual, ARR 123 and the CCG all use macroscopic-level methods for estimating capacity and delay at intersections subject to homogeneous traffic.

In dealing with large freight vehicles in urban traffic corridors, this project must consider the heterogeneity of vehicles that constitute the traffic. In aggregating vehicles into homogeneous traffic streams, macroscopic level models generally are less able to account for the differences between vehicles and vehicle-types that the project is investigating. As such, a microscopic level model is considered more appropriate for use in this project.

This comparison has identified a number of alternatives for modelling particular elements that lead to the calculation of capacity and delay at signalised intersections. The models that are considered most appropriate for each of these elements are outlined below.

- **Model level:** A microscopic level model is considered more appropriate than a macroscopic level model in accounting for the effects of a heterogeneous traffic mix.
- **Queue departure:** This shall be examined at a microscopic level, calculating saturation flow, start loss and end gain from the trajectories of the simulated vehicles.
- **Saturation flow:** In adopting a microscopic-level model for the simulation of traffic in this project, saturation flow can be calculated from first principles for the queue departure headways at the stop line.
- **Delay:** At a microscopic level, the various components of delay (deceleration delay, stopped delay and acceleration delay) need to be evaluated for each vehicle.

This chapter has presented many of the more common models used to predict the capacity and delay at signalised intersections. In comparing these existing models, it has become evident that heterogeneity in the traffic composition is rarely accounted for beyond the use of passenger car equivalence factors. As such, a need was identified for a model that specifically incorporates the effects of traffic composition heterogeneity – particularly those related to larger heavy vehicles such as multi-combination vehicles and road trains. Subsequent chapters present details of the development and use of that model.

# CHAPTER 4 CHARACTERISATION OF LARGE FREIGHT VEHICLE PERFORMANCE IN URBAN TRAFFIC

## 4.1 Introduction

The inputs, parameters and assumptions used in any traffic model are important in formulating an accurate representation that captures the detail required. This chapter presents a comparison of models of important vehicle and driver factors that contribute to the modelling of signalised intersection performance.

## 4.2 Vehicle Acceleration Models

The performance of heavy vehicles starting from rest represents one of the most important contributors to the impact of large freight vehicles on urban traffic. Trucks generally possess the lowest levels of acceleration performance, which, in combination with their length, makes them the vehicle classes most likely to impede traffic.

This lower acceleration capability has a direct effect upon queue discharge characteristics at intersections, intersection sight distance requirements, acceleration lane lengths and intersection (or railway level crossing) clearance times. Further, low acceleration rates can lead to large headways in front of a LFV, which in turn may influence the effectiveness of detectors for vehicle-actuated signals.

### 4.2.1 Mechanistic relationships

Mechanistic relationships for the longitudinal performance of heavy vehicles have been developed by several authors (for example Smith 1970; Fitch 1993). By subtracting the longitudinal aerodynamic, rolling and grade resistance from the force available at the drive wheels, as shown in Figure 4.1, the net force is available to provide acceleration to the mass of the vehicle.

This figure is not available online.
Please consult the hardcopy thesis
available from the QUT Library

*Source: McLean (1992)*

**Figure 4.1 – Longitudinal forces acting on a heavy vehicle**

A second order differential equation (Equation 4.1) can be solved numerically to predict the vehicle's longitudinal performance.

$$a(t) = \left(F_t - F_a - F_r - F_g\right) / M_e \qquad \text{Equation 4.1}$$

where $a(t)$ = instantaneous acceleration of vehicle at time t

$F_t$ = tractive force available at driving wheels

$F_a$ = aerodynamic drag force

$F_r$ = rolling resistance force

$F_g$ = grade force = $M\mathbf{g} \sin \theta$

$M_e$ = effective vehicle mass, including inertia of the rotating driveline.

Gillespie (1986) considered the mechanics of truck acceleration on grade, concluding that the time required for a large freight vehicle to clear a hazard zone (such as an intersection or railway level crossing) often greatly exceeded that allowed for by design standards. The presence of an adverse grade further increased the required clearance time.

In order to standardise vehicle performance prediction information, the Society of Automotive Engineers (1996) produced a standard (J2188) for the presentation of technical information relating to commercial vehicle gradeability. This has been found to be an excellent reference for vehicle driveline parameters and, although not directly relevant to acceleration capability, with the addition of an appropriate numerical integration algorithm it can be used as the basis for a detailed model.

### 4.2.2 Variable power

Rakha and Lucic (2002) recognised that not all tractive force is available at low speed, applied a scaling factor β that reduces the available force at lower speeds, as shown in Equation 4.2:

$$F_t = 3,600\beta\eta\frac{P}{v} \qquad \text{Equation 4.2}$$

where β is a speed-dependent term given by $\beta = 1/v_0\ [1 + \min(v,v_0)(1 - v/v_0)]$

$v_0 = 1164\ w^{-0.75}$, $w$ being the mass-to-power ratio (kg/kW).

Figure 4.2, reproduced from Rakha and Lucic (2002) shows the observed and modelled vehicle acceleration plotted against speed for a truck accelerating from rest. The discontinuous nature of the measured acceleration curve is evident, with acceleration becoming negative during gear changes. The modelled acceleration smooths out those discontinuities whilst maintaining a good representation of the speed and distance travelled.

This figure is not available online.
Please consult the hardcopy thesis
available from the QUT Library

*Source: Rakha and Lucic (2002)*

**Figure 4.2 – Observed and modelled acceleration versus speed**

### 4.2.3 Inertia effects

An often overlooked factor in considering a vehicle's performance is that the rotating components of the engine and driveline must also be accelerated. The inertia due to rotating and reciprocating masses is proportional to square of gear ratio; hence, the vehicle has a greater effective mass when it is in its lowest gears. Lechner and Naunheimer (1999) suggested that rotational inertia coefficient, λ (the ratio of the effective mass which mass which has to be accelerated to the

actual mass of the vehicle), for trucks ranges from $\lambda \approx 10$ when in the lowest gear, $\lambda \approx 3$ for the first gear usually used for starting the vehicle, and $\lambda \approx 1.1$ for the top (fastest) gear.

## 4.3 Empirical Vehicle Acceleration Models

A vehicle's acceleration capability is dependent upon its power-to-mass ratio, and as a rough approximation, for a constant power output, acceleration will decrease with increasing speed. However, the actual acceleration rate used is under the control of the driver of the vehicle, and will always be less than the maximum possible acceleration that can be calculated by a mechanistic model.

The rate at which vehicles move away from their stationary position in a traffic queue has an important effect in determining the time taken to reach the free-flow speed, and therefore the start-up lost time for the movement. Various models have been proposed, ranging from a simple constant acceleration model through to polynomial functions of time or speed.

### 4.3.1 Constant acceleration

The simplest possible model of vehicle acceleration from a traffic queue assumes that acceleration is constant over the entire time from rest through to reaching the free-flow speed. This is sufficient for many microscopic level software products (such as Paramics, AIMSUN2, INTEGRATION and HUTSIM) that use this assumption. However, it does not recognise that a vehicle's maximum acceleration capability decreases with increasing speed, due to changing gear ratios and resistance forces.

Using a constant acceleration model for acceleration from rest to a final velocity $v$ in time $t$, the acceleration is given by $a = v / t$. The distance travelled in this time is given by $s = ½ at^2 = v / 2t$. Having the distance dependent solely upon the final speed and time taken to reach it, a problem arises in attempting to calibrate the model with data in which distance, speed and time are known. With only one parameter (the acceleration rate) to adjust, the model cannot adequately fit both speed and distance data.

### 4.3.2 Acceleration decreasing linearly with increasing speed

A common formulation is to have acceleration decrease linearly with increasing speed, as shown in Equation 4.3. Having two parameters (maximum acceleration and terminal speed) in the acceleration formulation ensures that a match can be made of both the distance and time taken to reach the free-flow speed.

$$a(t) = \alpha\left(1 - v(t)/v_{\max}\right) \qquad \text{Equation 4.3}$$

where $a(t)$ is the acceleration at time $t$

$v(t)$ is the speed at time $t$

$\alpha$ is the maximum acceleration, which occurs at $t = 0$

$v_{\max}$ is the terminal speed, at which there is no acceleration.

Equations for acceleration, speed and distance $x(t)$ in terms of time can be derived using integral calculus:

$$a(t) = \alpha \exp(-\beta t) \qquad \text{Equation 4.4}$$

$$v(t) = v_{\max}\left[1 - \exp(-\beta t)\right] + v_0 \exp(-\beta t) \qquad \text{Equation 4.5}$$

$$x(t) = v_{\max}\, t - \frac{v_{\max}}{\beta}\left[1 - \exp(-\beta t)\right] + \frac{v_0}{\beta}\left[1 - \exp(-\beta t)\right] \qquad \text{Equation 4.6}$$

where $v_0$ is the initial speed of the vehicle

$\beta = \alpha / v_{\max}$.

The time taken to accelerate to a specified speed $v$, starting from rest ($v_0 = 0$) can be determined by re-expressing Equation 4.5 as Equation 4.7.

$$t = -\frac{1}{\beta}\ln\left(1 - \frac{v}{v_{\max}}\right) \qquad \text{Equation 4.7}$$

The time taken to reach a specified distance cannot be explicitly determined. It can be determined numerically by repeatedly substituting values of $t$ into Equation 4.6 until the required value of $x$ is obtained to sufficient accuracy.

Many authors have used this relationship to study queue discharge. Bonneson (1992) used this relationship in his examination of queued driver behaviour at signalised intersections to predict both headways and the exponential development of discharge flow. Evans and Rothery (1981) showed that this form of relationship gives a very good fit to the measured data (Figure 4.3).

This figure is not available online. Please consult the hardcopy thesis available from the QUT Library

*Source: (Evans and Rothery 1981)*

**Figure 4.3 – Acceleration versus speed of queued vehicles at the stop line**

Long (2000) also assumed an acceleration model that decreases linearly with speed. A review of data collected from 1937 to 1992 (including Bonneson's study), showed that a linearly decreasing acceleration model provided good correlation with data from a wide range of methods and vehicle types.

Bester (2000) proposed a method for calculating truck speed profiles in mountainous terrain by starting with the equations of motion of the vehicle and deriving the coefficients of the above linearly-decreasing acceleration model. This is extremely useful in obtaining appropriate coefficients for situations where collected data is not available.

### 4.3.3 Acceleration decreasing linearly with increasing time

An alternative formulation (Equation 4.8) was used by Bunker and Haldane (2003), assuming that acceleration decreases linearly with time. Such a relationship, having two parameters, would be able to match both the distance an time taken for an acceleration from rest to speed, and has the correct monotonically decreasing acceleration with time (or with speed). It was emphasised that the relationship is only be valid for a limited range of input times, and would give erroneous results if extrapolated beyond that range.

$$a(t) = C\,t + a_0 \qquad \text{Equation 4.8}$$

where $C$ is the rate at which acceleration decreases with time ($C < 0$)

$a_0$ is the initial acceleration of the vehicle at rest at time $t = 0$.

By integrating the above equation, expressions may be obtained for speed and distance ($v_0 = 0$ for vehicles starting from rest).

$$v(t) = \tfrac{1}{2} C\,t^2 + a_0\,t + v_0$$
$$x(t) = \tfrac{1}{6} C\,t^3 + \tfrac{1}{2} a_0\,t^2 + v_0\,t$$

This empirical relationship was found to give an excellent fit ($r^2 > 0.99$) to data collected from acceleration tests of a range of LFVs and grades.

It should be noted that a vehicle's decreasing acceleration capability occurs through a combination of having to use numerically lower gear ratios and being subjected to increasing resistance forces as speed increases. Thus, it is more intuitive to relate acceleration to speed rather than to elapsed time.

### 4.3.4 Acceleration as a polynomial function of time

In a study of fuel consumption and vehicle emissions, Akçelik and Biggs (1987) compared several acceleration models, including two- and three-term sinusoidal models, constant acceleration, and linearly decreasing with speed. They found that the polynomial model presented in Equation 4.9 was the best overall in predicting acceleration distance and fuel consumption.

$$a(t) = r\, a_m \theta \left(1 - \theta^m\right)^2 \qquad \text{Equation 4.9}$$

where $a_m$ = maximum acceleration

$\theta$ = time ratio = $t / t_a$

$t_a$ = duration of acceleration, acceleration equals zero for $t > t_a$

$m$ = a model parameter determining the shape of the function, $m > -0.5$

$r$ = a parameter given by $r = \left[\left(1+2m\right)^{2+1/m}\right] \Big/ 4m^2$ .

This is an empirical model that is valid for a limited time range (until $t = t_a$), that has parameters $a_m$ and $m$ to adjust the amplitude and shape of the acceleration function. It has the advantage of being a continuous function, with zero initial acceleration, and zero jerk at the completion of acceleration.

Expressions for speed and distance for acceleration from rest can be obtained by integrating the above expression. They have been found to be more complex than equivalent expressions for speed and distance for the other models.

In the current study, we are concerned primarily with the distance and time taken to reach a free-flow speed. A model such as this is more representative of the true acceleration profile, but is more complex that other models that meet our requirements.

### 4.3.5 Acceleration as a gamma function of time

Bham and Benekohal (2002) reviewed 12 empirical acceleration models, finding that a model based on the shape of the mathematical Gamma probability density function gave the best fit to acceleration / time data they had collected. The format (Equation 4.10) and parameters of this model are less intuitive than other, simpler models that give similar results for speed and distance.

$$a(t) = \frac{\beta^{-\alpha} t^{\alpha-1} e^{-t/\beta}}{\Gamma(\alpha)} * \eta, \alpha > 0, \beta > 0 \qquad \text{Equation 4.10}$$

where $\Gamma$ is the mathematical Gamma function

$\alpha$ and $\beta$ are shape and scale parameters, respectively

$\eta$ is a size parameter, equal to the final speed after the acceleration.

### 4.3.6 Comparison of acceleration profiles

Given that, in this current study, we are using acceleration profiles as a means to construct the trajectory diagrams of vehicles discharging from a traffic queue, it is useful to know what differences exist between the trajectory diagrams of the different acceleration profiles. The five acceleration profile models described above were compared, using the first 30 seconds of distance data from Bunker and Haldane's (2003) study for a B-double accelerating on level ground. Parameters in the models were selected to minimise the sum of squared errors in distance between the model and the data. With the exception of the constant acceleration model, constraints were imposed to ensure that the final speed and displacement were the same as for the Bunker-Haldane model. Two cases of the constant acceleration model were used, matching either the final speed or final distance.

Results are shown in Figure 4.4. The constant acceleration models are not able to match both final speed and distance, and large differences are evident between these models and the other four models. Differences are evident between the acceleration profiles (particularly the non-monotonic nature of the polynomial time model); however, these are less noticeable when looking at the speed profile, and almost imperceptible when looking at the trajectory diagram.

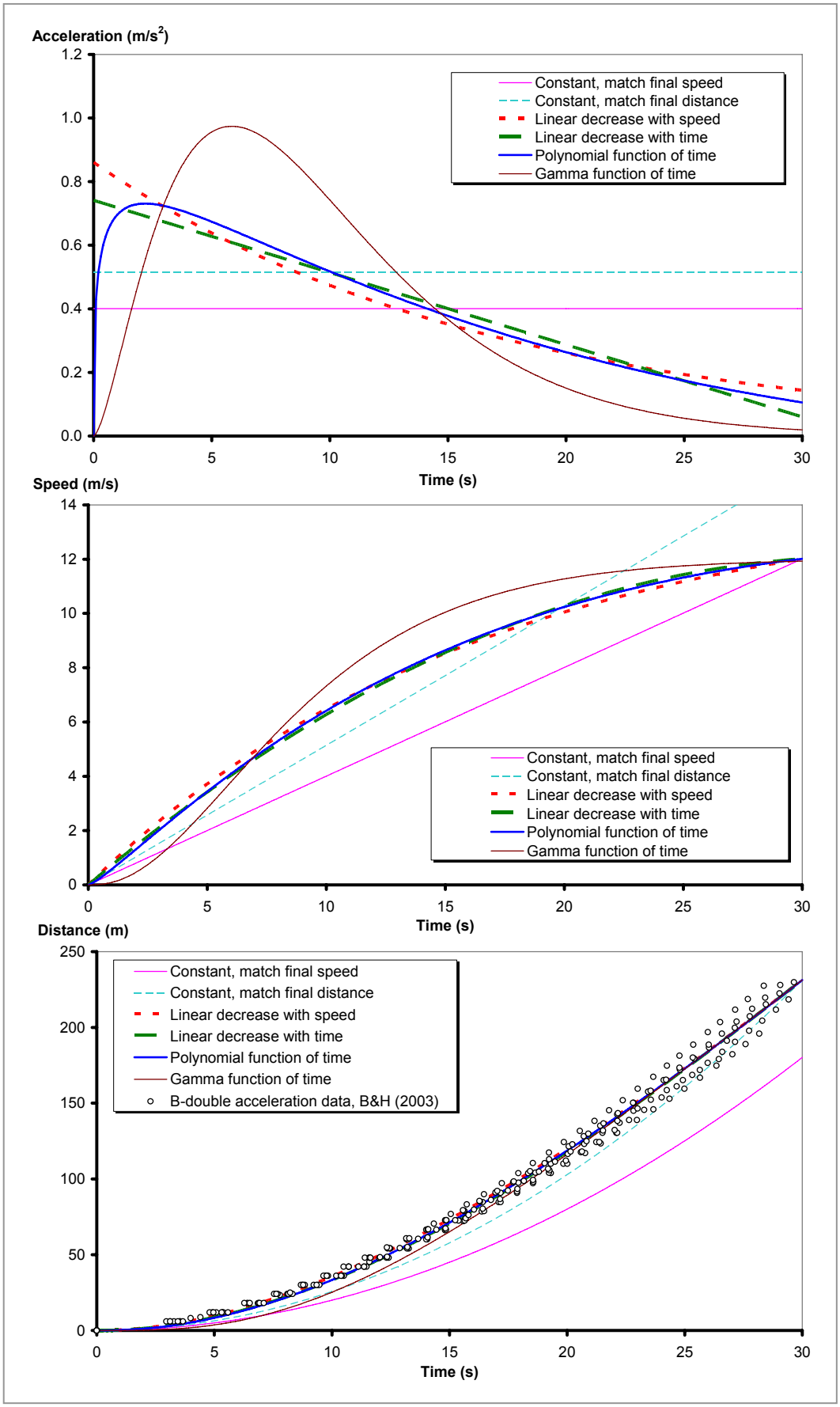


**Figure 4.4 – The result of integrating different acceleration profiles**

Parameters used in these five models are presented in Table 4.1, together with the standard error distance for each model compared to the data. Standard errors of the constant acceleration models are much higher than for those of the other models since; having only one adjustable parameter they cannot match both the final distance and final speed.

**Table 4.1 – Parameters and characteristics of different acceleration profiles**

| *Acceleration Model* | *Parameters* | *Can Match Final* | | *Standard Error Distance (m)* |
|---|---|---|---|---|
| | | *Speed* | *Distance* | |
| Constant, match final speed | $A = 0.40$ m/s$^2$ | Yes | No | 32.9 m |
| Constant, match final distance | $A = 0.51$ m/s$^2$ | No | Yes | 12.3 m |
| Linear decrease with speed | $\alpha = 0.86$ m/s$^2$<br>$V_{max} = 14.43$ m/s | Yes | Yes | 5.5 m |
| Linear decrease with time | C = -0.0227 m/s$^3$<br>$a_0 = 0.741$ m/s$^2$<br>$t_{max} = 30$ s | Yes | Yes | 5.3 m |
| Polynomial function of time | $t_a = 49.4$ s<br>$a_m = 0.73$ m/s$^2$<br>$m = -0.31$ | Yes | Yes | 5.4 m |
| Gamma function of time | $\alpha = 2.57$<br>$\beta = 3.72$<br>$\eta = 12.0$ m/s | Yes | Yes | 7.7 m |

As seen in Figure 4.4, the relatively small differences between the four acceleration models that can match both the final speed and the final distance indicated that selection of an appropriate acceleration model was not as crucial as was expected.

The model having acceleration linearly decreasing with time was mathematically the simplest to implement, but it is not as widely used as that which had acceleration decreasing linearly with speed. Both the polynomial function of time and Gamma function of time better represent the true acceleration profile that starts from zero acceleration; however, their added complexity gave few benefits when used for this current application.

### 4.3.7 Selected acceleration profile model

The acceleration decreasing linearly with increasing speed model was seen as the most appropriate to use in the current project. It had already been widely used, with a wide range of calibrated parameters for a range of vehicle types, and provided sufficient accuracy for the modelling of intersection queue discharge with heterogeneous vehicle types.

This model offered sufficient parameters to adequately match both the final distance and speed data, was independent of the elapsed time (which is useful in the general traffic flow case), and has readily interpretable parameters.

## 4.4 Headways and Car-Following

The headways between successive vehicles as they leave a queue and accelerate though the intersection are typically assumed to fall asymptotically to a constant value, given by the reciprocal of the saturation flow. There is an overriding concern whether drivers are comfortable in following the car in front under these conditions. Difference in driver behaviour and vehicle capability (especially in dealing with heavy vehicles) need to be accounted for using car-following theory.

Several reviews of car-following models have been conducted recently, for example Brackstone and McDonald (1999) and Rothery (1997). Models commonly rely on a fundamental relationship of producing a response to a given stimulus. The response typically is the vehicle's acceleration, stimulated by the velocity and displacement relative to the leading vehicle. The ratio of response to stimulus is not constant in many models, this gain often being considered as a function of speed and/or headway.

### 4.4.1 The GHR model and its derivatives

The Gazis, Herman and Rothery (GHR) (1961) model is generally expressed in the form of Equation 4.11, relating the current acceleration to the relative velocity and spacing when perceived by the driver, incorporating a lag of $T_R$.

$$a_n(t) = cv_n^m(t)\frac{\Delta v(t-T_R)}{\Delta x^l(t-T_R)} \qquad \text{Equation 4.11}$$

where $a_n$ is the acceleration of the $n^{th}$ vehicle

$t$ is the current simulation time

$T_R$ is the lag accounting for the driver's perception and reaction time

$v_n$ is the velocity of the $n^{th}$ vehicle

$c$, $m$ and $l$ are model calibration parameters

$\Delta v = v_{n-1} - v_n$ is the relative velocity

$\Delta x = x_{n-1} - x_n$ is the headway to the lead vehicle.

Values for parameters, $c$, $m$ and $l$ have been proposed by several authors, as reported in Brackstone and McDonald (1999). Chandler *et al.* (1958) used parameters $m = 0$ and $l = 0$ in an early version of this model. Using these parameters, the model simplifies to Equation 4.12.

$$a_n(t) = c\Delta v(t-T_R) \qquad \text{Equation 4.12}$$

Stability requires that response to perturbations in the lead vehicle's velocity is either non oscillatory, or oscillatory and damped. It can be shown (Rothery 1997) that a mathematical requirement for stability is that $c < \pi / 2$. One of the tests required to verify the correct operation of the model is to ensure that the car following behaviour is responsive, stable and non-oscillatory.

As mentioned before, the sensitivity, $c$ would vary between drivers, and a driver aggressiveness parameter may be used to select an appropriate sensitivity from a range of values.

Note that the general GHR model varies the gain with the spatial headway between consecutive vehicles; it does not consider the length of the leading vehicle. Further, Chandler's model (Equation 4.12) does not consider the separation (headway) between vehicles whatsoever. Particularly for heterogeneous vehicles in non-steady-state flow conditions, the model must respond to the spacing between the front bumper of a vehicle and the rear bumper of the vehicle in front of it, as indicated in Figure 4.5.

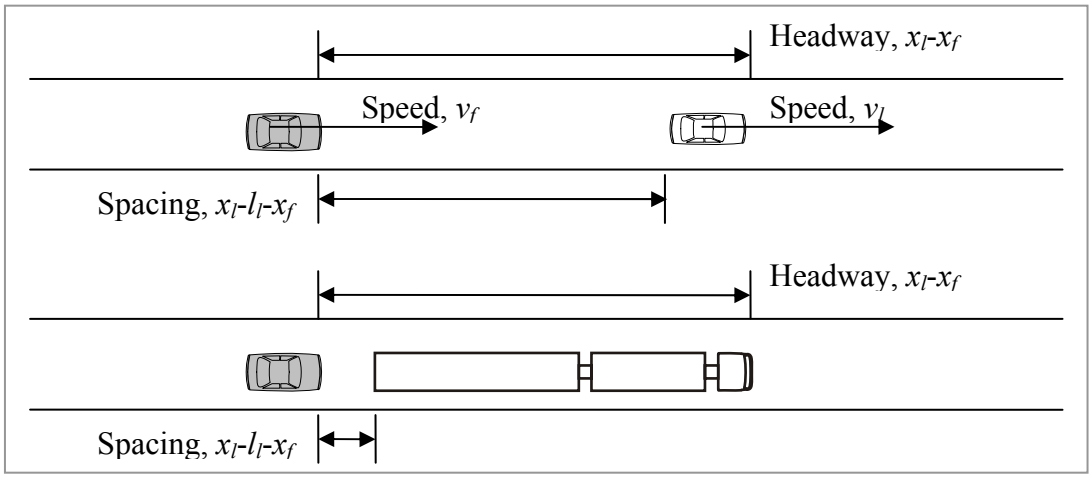


**Figure 4.5 – Car-following with homogeneous and heterogeneous vehicles**

Thus, a modified GHR model, Equation 4.13, would be more appropriate when investigating vehicles of markedly different lengths. This depends on the spacing between vehicles, rather than their headway. The length of the lead vehicle, $L_l$, is a characteristic of the vehicle class.

$$a_n(t) = c v_n^m(t) \frac{\Delta v(t - T_R)}{\left(\Delta x(t - T_R) - L_l\right)^l} \qquad \text{Equation 4.13}$$

where $L_l$ is the length of the lead vehicle

$\Delta x = x_{n\text{-}1} - x_n$ is the headway between lead and following vehicles.

### 4.4.2 Gipps' model

An alternative family of car-following models is based upon a collision avoidance criterion rather than relative velocity. Vehicles maintain headways to be able to stop safely without colliding with the lead vehicle if it (the lead vehicle) stops at its maximum deceleration rate. Gipps (1981) proposed the following car following model (Equation 4.14) based on this principle.

$$v_n(t+T) = b_n T + \left[ b_n^2 T - b_n \left( 2\left\{ x_{n-1}(t) - s_{n-1} - x_n(t) \right\} - v_n(t)T - v_{n-1}(t)^2 / \hat{b} \right) \right]^{1/2}$$

Equation 4.14

where $v_n(t + T)$ is the maximum safe velocity for vehicle $n$ with respect to the preceding vehicle at time $(t + T)$

$b_n$ (<0) is the most severe braking the driver is prepared to undertake

$T$ is the time between consecutive calculations of velocity and displacement

$x_n(t)$ is the location of the front of vehicle $n - 1$ at time $t$

$s_{n\text{-}1}$ is the effective length of vehicle $n - 1$

$\hat{b}$ is an estimate of $b_{n\text{-}1}$ employed by the driver of vehicle $n$.

Unlike the GHR model and others covered later in this section, Gipps' model does not predict the acceleration required to maintain a safe speed. It would be difficult to use accurately when acceleration capability varies markedly with vehicle type.

### 4.4.3 Cohen's model

Cohen (2002a; 2002b) combined elements of both the GHR relative velocity and a collision avoidance model in applying a car-following model to the simulation of queue discharge at a signalised intersection. The following expression for acceleration was used (Equation 4.15):

$$a_f(t+T) = \frac{K\left\{\begin{array}{l} s_l(t+R) - s_f(t+R) - L_l - hv_f(t+R) \\ +\left[v_f(t+R) - v_l(t+R)\right]T - \frac{1}{2}a_l(t+T)T^2 \end{array}\right\}}{T\left(h + \frac{1}{2}T\right)} \qquad \text{Equation 4.15}$$

where $a_f$ is the acceleration of the following vehicle

$t$ is the current simulation time

$T$ is the time step

$K$ is a sensitivity parameter

$s_l$ and $s_f$ are the displacements of the lead and following vehicles

$R$ is the reaction time of the following vehicle

$L_l$ is the length of the lead vehicle

$h$ is a time headway parameter

$v_f$ and $v_l$ are the velocities of the lead and following vehicles

$a_l(t + T)$ is the acceleration of the lead vehicle at time $t + T$.

Cohen added three additional constraints on the following vehicle's motion:

- The acceleration must not exceed the vehicle's maximum acceleration and minimum acceleration (i.e. the maximum deceleration) capabilities;
- The velocity must not exceed the maximum desired velocity; and
- The spacing is such that the vehicle can stop safely if the lead vehicle does so (collision avoidance).

A detailed car-following system based on the above model was applied to microscopic simulation models (Cohen 2002a), and as a case study to queue discharge from a signalised intersection (Cohen 2002b). The model predicted the

acceleration of the following vehicle, limiting it to the acceleration capability (as a function of vehicle speed), and ensuring that sufficient spacing is maintained for an emergency stop if required. The car-following model was implemented as a spreadsheet and applied to a queue discharge problem. It was noted that significantly different car-following parameters were required when applied to queue discharge than when applied to uninterrupted flow. The gain of the model (parameter $K$ in Equation 4.15) was higher for a tightly coupled system corresponding to intersection queue discharge than for a loosely coupled system corresponding to individual vehicle behaviour in free-flowing traffic.

The queue discharge headways predicted by Cohen's model with a truck in queue position 7 are shown in Figure 4.6. The HCM definition of headways being between the front axles of consecutive vehicles is used. Headways of vehicles in front of the truck can decrease asymptotically towards the saturation headway as their speeds increase; however the slowly accelerating truck has a large headway due to the gap in front of it, a large headway due to the greater length of the truck, and also larger headways (due to their lower speeds) of vehicles behind it.

This figure is not available online.
Please consult the hardcopy thesis
available from the QUT Library

*Source: (Cohen 2002b)*

**Figure 4.6 – Discharge headways with an articulated vehicle in the queue**

The physical requirements raised by Cohen of the following vehicle not exceeding its acceleration capability and being able to safely stop if the lead vehicle does so must also be considered with any alternative car-following model. The maximum acceleration capability of the vehicle is often the limiting factor in any such simulation, particularly in dealing with heavy vehicles in a traffic queue.

### 4.4.4 Newell's model

Newell (2002) proposed a simpler car-following model that was intended for homogenous vehicles travelling on a homogeneous highway. The model assumed that the time-space diagram of the following vehicle is the same as that of the leading vehicle apart from a translation in time and in space. This may be thought of as a wave propagating through the traffic at a rate dependent on $\Delta d$ and $\Delta t$, the translations in space and time.

This model is easier to implement than other models (such as Cohen's), and was claimed by Newell to be *"at least as accurate as any of the more elaborate rules of car-following that have been proposed over the last 50 years or so"*.

Newell's simplified model does not account for vehicles having different acceleration capabilities or different lengths. Thus, it would be inappropriate for use in the current project, in which traffic heterogeneity is of primary importance.

### 4.4.5 Selected car-following model

A car-following model based on that used by Cohen (2002a; 2002b) was considered to be the most appropriate for use in the current project. Based on the motion of individual vehicles and their leaders, this model can be implemented as a differential equation in which accelerations are used to predict future speeds. These accelerations predicted by the model must be limited by the each vehicle's maximum acceleration capability and the current speed limit.

## 4.5 Testing the Effect of Heavy Vehicles on Surrounding Traffic and Queue Discharge Characteristics

In order to test the effect of queue composition on queue discharge characteristics, a spreadsheet-based model of the queue discharge process at a signalised intersection was developed. **MCVCorps** (Multi Class Vehicle Corridor Progression Simulation) is a macro-based spreadsheet implementation of a fixed time step numerical integration simulation of a vehicles moving along a corridor.

Figure 4.7 shows the Microsoft Excel spreadsheet main page for MCVCorps. The input parameters for the initial conditions, corridor timing and integrator parameters are entered on the left of the screen, other pages in the spreadsheet are used to enter the types of vehicle at each queue position (up to 20 vehicles), and the characteristics of each vehicle type (such as its jam spacing and maximum acceleration rate). The macro-based program is run by clicking the mouse on the "Run Model" button or pressing the Control+R key combination. After the macro has run, the instantaneous positions and speeds of each vehicle are stored in another spreadsheet page, providing the data for the three graphs shown on the main spreadsheet page and the trajectory diagram as shown in Figure 4.9.

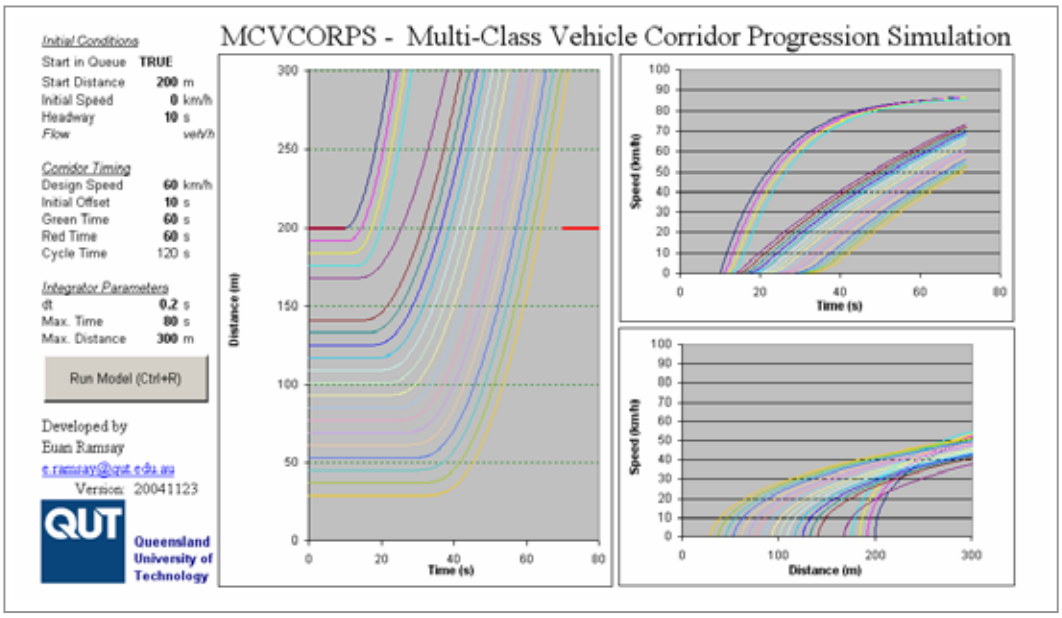


**Figure 4.7 – MCVCorps spreadsheet interface screen**

Figure 4.8 shows the program flowchart for the MCVCorps spreadsheet macro. Essentially, it consists of two nested loops – the inner loop handles updating the position and speed of each vehicle at each time step, whilst the outer loop increments the time and updates the status of the intersection(s). Whenever a vehicle crosses an intersection stop line, the exact time of the crossing within the time step is calculated.

Figure 4.9 shows the trajectories of a platoon of vehicles departing from the front of a queue at a signalised intersection. The fifth vehicle in the queue (shown as a thick line) is a B-double; the remaining vehicles (shown as thin lines) are cars. The B-double occupies a greater queue length than a car, and also accelerates at a lower rate than cars normally would. The cars behind the B-double are unable to accelerate at their normal rate, since they cannot overtake the B-double in this single-lane simulation.

The acceleration characteristics of the different vehicle types were initially calibrated using published vehicle acceleration data (Long 2000). Following the data collection and analysis stages of this project (reported in later chapters), a parameter set was developed that was more representative of Australian urban arterial freight corridors. The figures shown here are from simulations using this latter parameter set, however the same trends and findings were evident using Long's data set.

The headways of the vehicles as they pass the stop line at the intersection are shown in Figure 4.10, defining headways as being between front axles of consecutive vehicles. Headways of vehicles #5 and #6 are considerably greater than for the case when only cars are present. Vehicle #5 is the slowly-accelerating vehicle that takes a greater time to reach the stop line than a car would from the same starting position, and vehicle #6 is starting from a greater distance from the stop line than if the fifth vehicle was a car. All vehicles following the B-double have greater headways due to their lower acceleration rates.

The same discharge headway characteristics with a truck in the queue were found by Cohen (2002b), shown earlier in Figure 4.6.

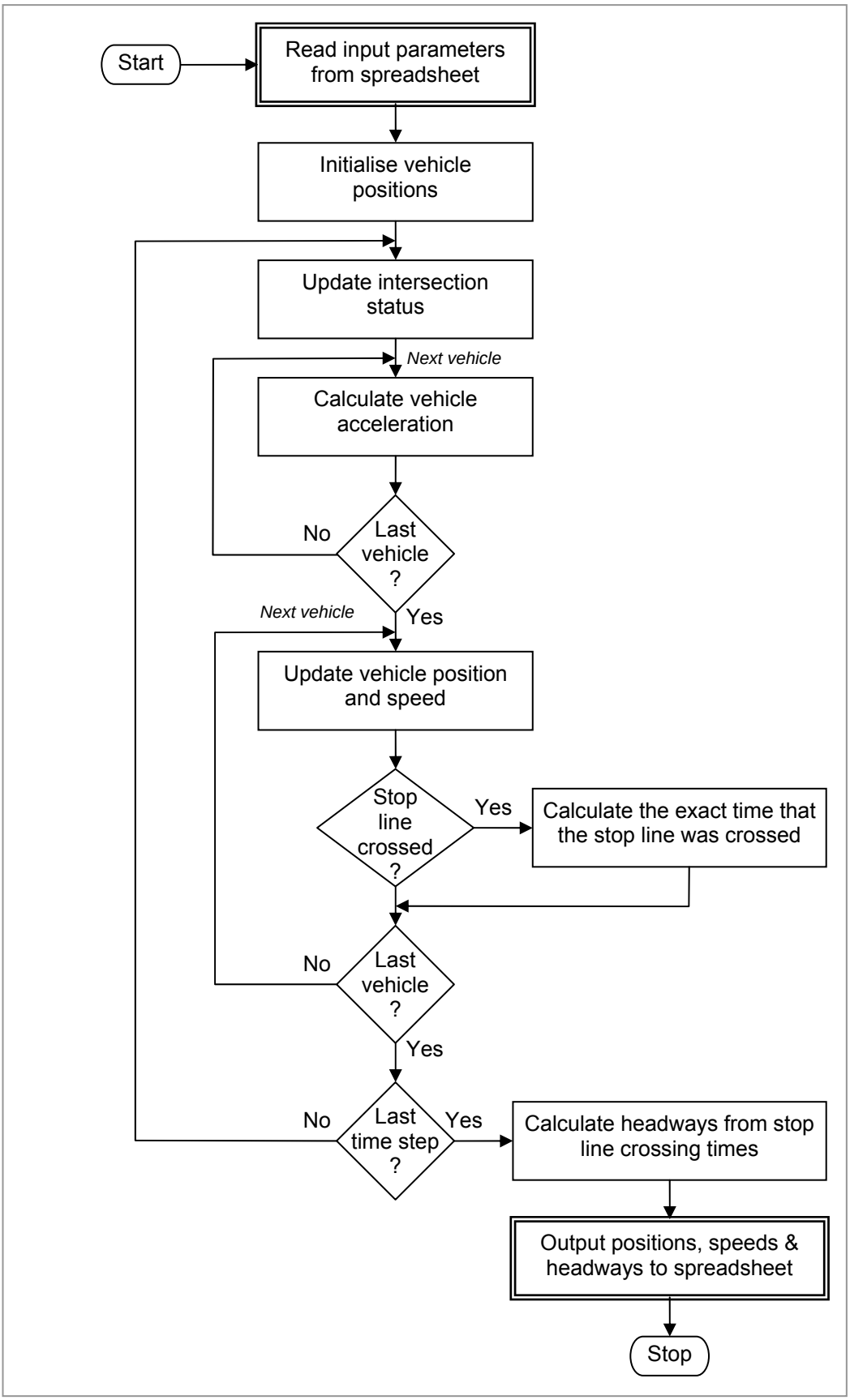


**Figure 4.8 – MCVCorps spreadsheet macro flowchart**

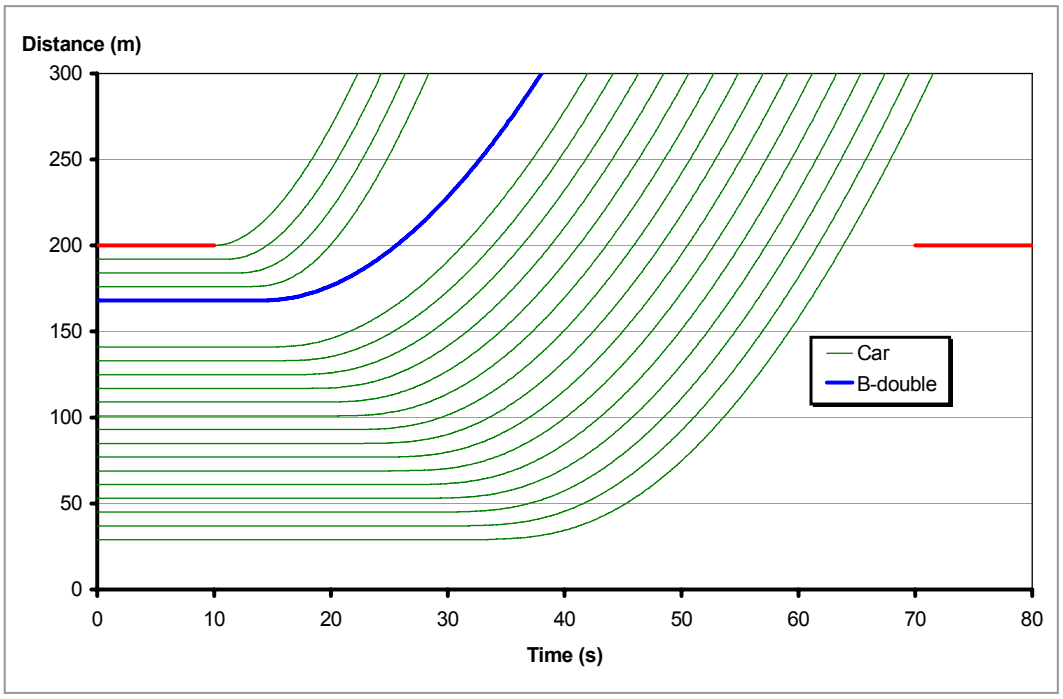


**Figure 4.9 – Queue discharge characteristics with a heavy vehicle present**

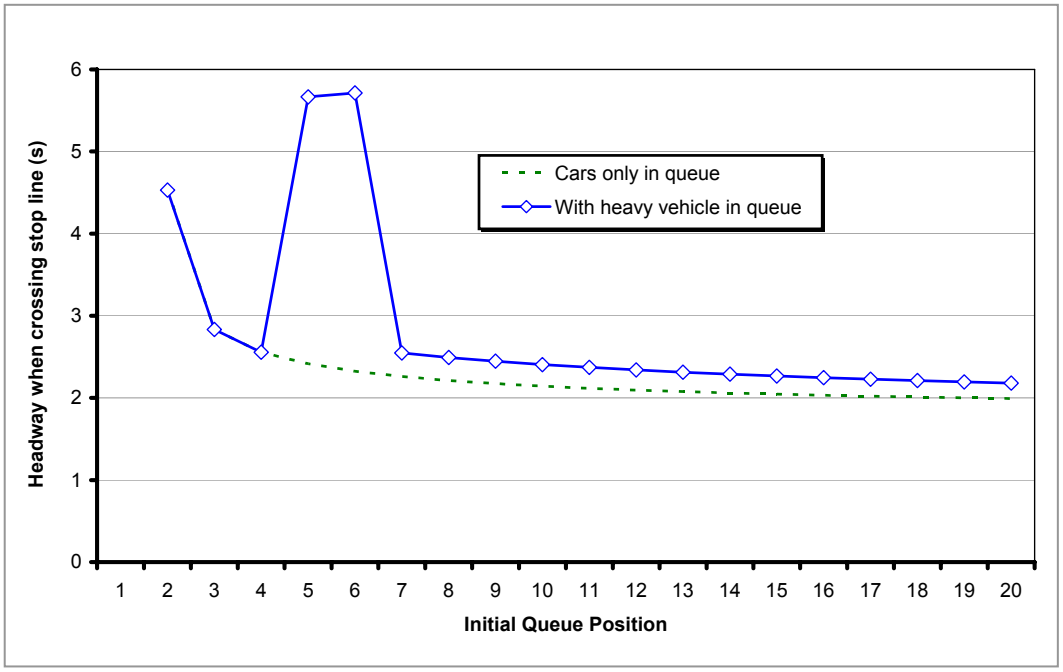


**Figure 4.10 – Stop-line headways of vehicles around a heavy vehicle**

**MCVCorps** proved to be very slow to execute, taking approximately 5 seconds to simulate a single cycle of a single intersection with 20 vehicles. This macro-driven spreadsheet would not be feasible for a study of multiple vehicles passing through a corridor comprising several lanes and several intersections. Despite this, it proved to be a useful tool for examining queue discharge characteristics and became the basis for the Windows-based object-oriented microsimulation program described later in this thesis.

## 4.6 Summary of this Chapter

This chapter reviews the performance capabilities of large freight vehicles as they move through traffic in an urban traffic corridor. The purpose of this is to determine the most appropriate vehicle performance model for use later in this project. The review concentrates on the acceleration capabilities since, generally speaking, other performance measures affecting the longitudinal performance of the corridor are similar to those of other vehicles. For example, braking requirements are regulated by Australian Design Rules to ensure compatibility with other traffic.

Mechanistic models have been widely used for predicting the performance of specific vehicles. They require detailed vehicle and, in particular, driveline specifications; and are seen as not being general enough for the current traffic interaction model.

Many empirical models have been used, ranging from simple constant acceleration assumptions through to more-complicated polynomial formulations. Many of these were only applicable to uninterrupted acceleration cases, which cannot handle the general case of traffic flow in the presence of other vehicles. That is, we require a model that can predict the maximum acceleration of a vehicle given its current state (i.e. current speed on current grade), rather than the time since it was in a past state (i.e. time since acceleration started).

The simplest acceleration model formulations cannot match both the time and the distance required to accelerate to the cruise speed. Thus, they cannot accurately predict the delay experienced by the vehicle; and to others around it.

The model most suitable to this application was having acceleration decrease linearly with increasing speed. It has been widely used elsewhere in studies of urban traffic performance, is relatively easy to calculate and interpret, has meaningful parameters, relies on the current vehicle state, and can simultaneously match both the distance and time to reach cruise speed.

Various car-following models were reviewed. For accurate representation of interrupted flow traffic, a safe stopping distance must be maintained; and in dealing with heterogeneous vehicles, the differences in acceleration capability must be considered. A model that predicted a desired acceleration that would be limited by the vehicles capabilities and whether or not the current speed limit had been reached would be most appropriate in the current project. Of those reviewed, the only one car-following model that both ensured a safe stopping distance was maintained and was formulated in terms of the acceleration of the following vehicle was Cohen's model.

The characteristics of large freight vehicle performance in urban traffic described in this chapter form the basis of the modelling framework presented in the next chapter.

# CHAPTER 5 SPECIFICATION OF A CORRIDOR-LEVEL TRAFFIC MODEL

## 5.1 Introduction

The literature review presented in the preceding chapters identified several areas of LFV interactions with urban traffic that required further investigation. This chapter specifies the requirements of a modelling framework to be used to undertake some of those investigations.

Obtaining an accurate representation of the behaviour of heterogeneous vehicles (and their drivers) in urban traffic is a key component of this project. The different characteristics of heavy and light vehicles require that a detailed analysis at a microscopic (or vehicle-by-vehicle) level be conducted to examine the interactions between individual vehicles.

### 5.1.1 Consideration of existing traffic microsimulation software

Most commercial traffic microsimulation software packages are capable of simulating the effects of LFVs on urban traffic corridor performance. Considerable effort has been invested by their developers, resulting in mature, well-tested and reliable products. Despite this, several advantages were identified in developing a specific-purpose corridor-level microsimulation tool for this project:

1) Existing microsimulation software did not model the kinematical behaviour of vehicles to sufficient accuracy. Generally, they used a constant acceleration model, and effects of grade on vehicle performance were often ignored.
2) A custom model would be expected to be faster to execute simulation runs than a general-purpose microsimulation package. It would have fewer overheads, such as not needing to animate a graphical interface.
3) The model would be completely customisable to the projects' specific requirements. This would be more difficult to do with a commercial

microsimulation package, possibly requiring additional commercial software development resources.

4) In order to limit the random variations due to a stochastic simulation method, the model needed to be able to conduct a large number of similar runs, with different random numbers seeds. Few commercial software packages offered this facility.

5) Management of problems found in a simulation would be more efficient, without having to contact the software developers and wait for them to replicate, analyse and remedy any problems that were identified.

6) It was considered a logical step forward from the spreadsheet-level tools (such as **MCVCorps** in the previous chapter) that had been developed earlier in the project.

7) Most importantly, it enabled development of an in-depth understanding and appreciation of how traffic microsimulation software works. Rather than considering the software to be a 'black box' that produces outputs as a result of different input parameters, the innermost workings of the model would be well understood and optimised for the specific application.

8) It required a significantly greater degree of initiative and problem-solving ability than a simple application of existing software would; and provided an ideal framework for implementation, testing and application of innovative modelling concepts and constructs.

There were disadvantages in not using a commercial software package as well:

1) Considerable time and effort would be invested into the software. This was particularly so considering the resources and budget available compared to commercial software developers.

2) Testing of the model would be limited by the smaller development team and lack of opportunities to call upon external testers.

3) Calibration would be more difficult, lacking a set of default parameters.

### 5.1.2 Modelling scope

The urban arterial traffic corridor model consists of a microsimulation traffic model, considering the motion of individual vehicles and their interactions. The alternative approach, namely a macrosimulation model considering traffic as homogeneous flow, was considered inappropriate since the primary focus is on the effects of the heterogeneity of the traffic.

The model considers the interactions of vehicles with each other and with traffic control devices. These interactions include car-following and lane-changing behaviour, and reactions to grade, speed limits, and traffic signals. Output of the model would consist of a set of vehicle trajectories (displacement / time plots), which may be used to determine traffic facility performance characteristics including travel times, delay, and capacity.

The model represents traffic moving along an urban arterial traffic corridor, comprised of a single-direction, multi-lane carriageway. A number of signalised intersections located along the corridor operate in either fixed-time or vehicle-actuated mode – in the latter case being able to respond to the presence of traffic on the corridor.

By imposing these limitations, the model remains focussed on its primary objective of determining the impact of heavy vehicles on corridor traffic. Additionally, it permits further development of the model at a latter stage as required. Figure 5.1 presents the requirements of the model as a simple process map, showing the distinction between inputs, the process itself, and outputs.

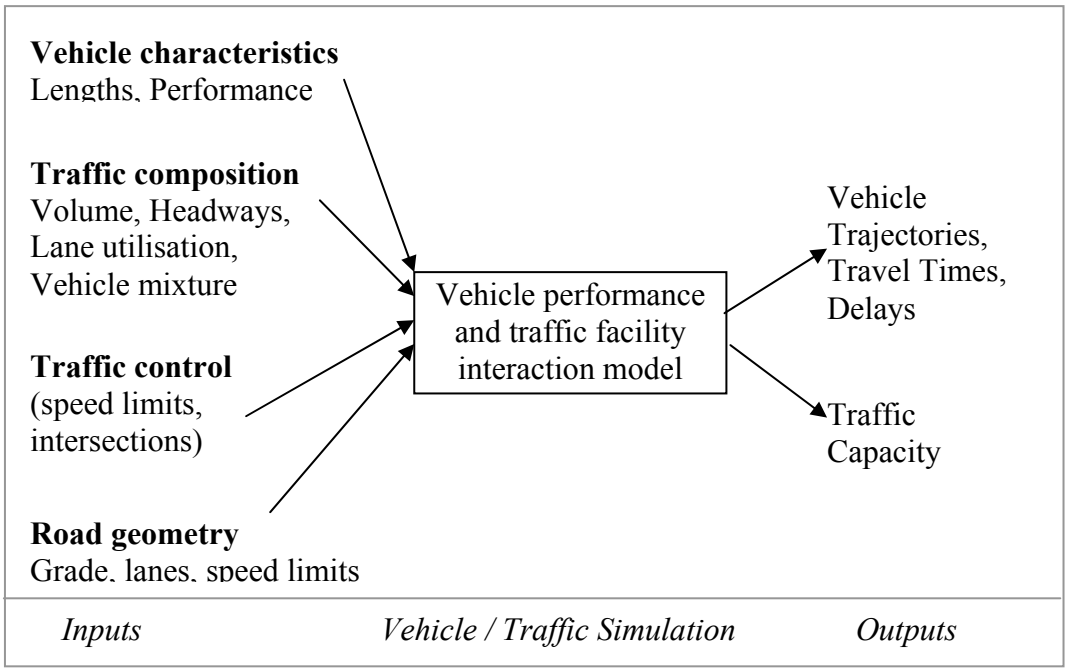


**Figure 5.1 – Queue discharge characteristics with a heavy vehicle present**

### 5.1.3 Kinematic system representation

A traffic microsimulation model may be considered as a system of $N$ vehicles moving in one-dimensional space that requires $2N$ variables to describe its state – corresponding to the displacements and velocities of the individual vehicles. That is, the state of the system may be represented as a vector $\underset{\sim}{\mathbf{y}}$, as shown in Equation 5.1:

$$\underset{\sim}{\mathbf{y}} = \begin{bmatrix} x_1 & v_1 & x_2 & v_2 & \dots & x_i & v_i & \dots & x_N & v_N \end{bmatrix}^{\mathrm{T}} \qquad \text{Equation 5.1}$$

where $x_i$ and $v_i$ represent the displacement and velocity of the $i^{\text{th}}$ vehicle

$^{\mathrm{T}}$ indicates the transpose of the matrix.

If the status of traffic signals and the lane that each vehicle occupies are introduced, the number of variables required to define fully the state of the system will increase.

The rate at which this state vector changes with the current simulation time, $t$, is given by the velocities and accelerations of the vehicles, as shown in Equation 5.2:

$$\frac{d\underset{\sim}{\mathbf{y}}(t)}{dt} = \begin{bmatrix} v_1 & a_1 & v_2 & a_2 & \dots & v_i & a_i & \dots & v_N & a_N \end{bmatrix}^{\mathrm{T}} \qquad \text{Equation 5.2}$$

where $a_i$ represents the acceleration of the $i^{\text{th}}$ vehicle.

The system can then be represented as the ordinary differential equation (ODE) presented in Equation 5.3.

$$\frac{d\underset{\sim}{\mathbf{y}}(t)}{dt} = f\left(t, \underset{\sim}{\mathbf{y}}(t)\right) \qquad \text{Equation 5.3}$$

That is, the velocities and accelerations of individual vehicles are given by the displacements and velocities of the vehicles themselves and of the surrounding vehicles. The accelerations are determined by car-following theory, generally dependent upon the relative velocities and displacements between leading and following vehicles.

As an example, consider two vehicles – the lead vehicle accelerates with $a_1 = A - bv_1$ and the following vehicle accelerates with a simple car-following rule given by $a_2 = c(v_1 - v_{12})$. The rate of change of the system, Equation 5.3, can then be expressed as Equation 5.4.

$$\frac{d\underset{\sim}{\mathbf{y}}(t)}{dt} = \begin{Bmatrix} v_1 \\ a_1 \\ v_2 \\ a_2 \end{Bmatrix} = \begin{Bmatrix} 0 \\ A \\ 0 \\ 0 \end{Bmatrix} + \begin{bmatrix} 0 & 1 & 0 & 0 \\ 0 & -b & 0 & 0 \\ 0 & 0 & 0 & 1 \\ 0 & c & 0 & -c \end{bmatrix} \begin{Bmatrix} x_1 \\ v_1 \\ x_2 \\ v_2 \end{Bmatrix} = \mathbf{A} + \mathbf{B}\,\underset{\sim}{\mathbf{y}}(t) \qquad \text{Equation 5.4}$$

This ODE may be solved numerically to evaluate the state matrix at the next time interval, $t + \Delta t$. A simple Euler integrator may be used (Equation 5.5) or a more precise integrator, such as a Runke-Kutta fourth order integrator may be used to give greater accuracy.

$$\underset{\sim}{\mathbf{y}}_{t+\Delta t} = \underset{\sim}{\mathbf{y}}_{t} + \Delta t\, f\left(t, \underset{\sim}{\mathbf{y}}_{t}\right) \qquad \text{Equation 5.5}$$

Most commercial microsimulation software programs us a simple integrator such as this, which assumes that the vehicle accelerations are constant over each time step. This gives sufficient accuracy if the time step is small enough. Typically, a time step of 0.1 seconds is used.

The state change matrix becomes considerably more complex as the number of vehicles increases, and with the use of more comprehensive car-following, lane-changing and traffic-control models. Nevertheless, the same basic principles of firstly forming an ODE and then solving it numerically can be applied.

### 5.1.4 Interactions between model components

Figure 5.2 shows a map of the framework to be used in the modelling of vehicle behaviour. As described above, the system is represented as an ODE that is initialised with vehicles according to either a random or a predefined series. Headways between vehicles are similarly generated. The simulation itself consists of repeatedly evaluating the ODE to determine the system state at the next time step. A vehicle's velocity is updated by knowing its acceleration, which in turn depends on car-following theory and the status of the next traffic control device. Similarly, the vehicle's displacement is updated by knowing its velocity.

Outside this fundamental loop, which handles the car-following behaviour of vehicles, are two additional loops for lane changing behaviour and traffic control respectively. If a vehicle executes a lane change, then vehicles used in the car-following model must be updated. Traffic control overrides the acceleration calculated in the car-following model – if a red signal is displayed, a vehicle should decelerate if it is within the safe stopping distance.

The principal outputs of the model include the trajectories of individual vehicles; these are used to provide various measures of performance for particular vehicle types, intersections, or the corridor as a whole.

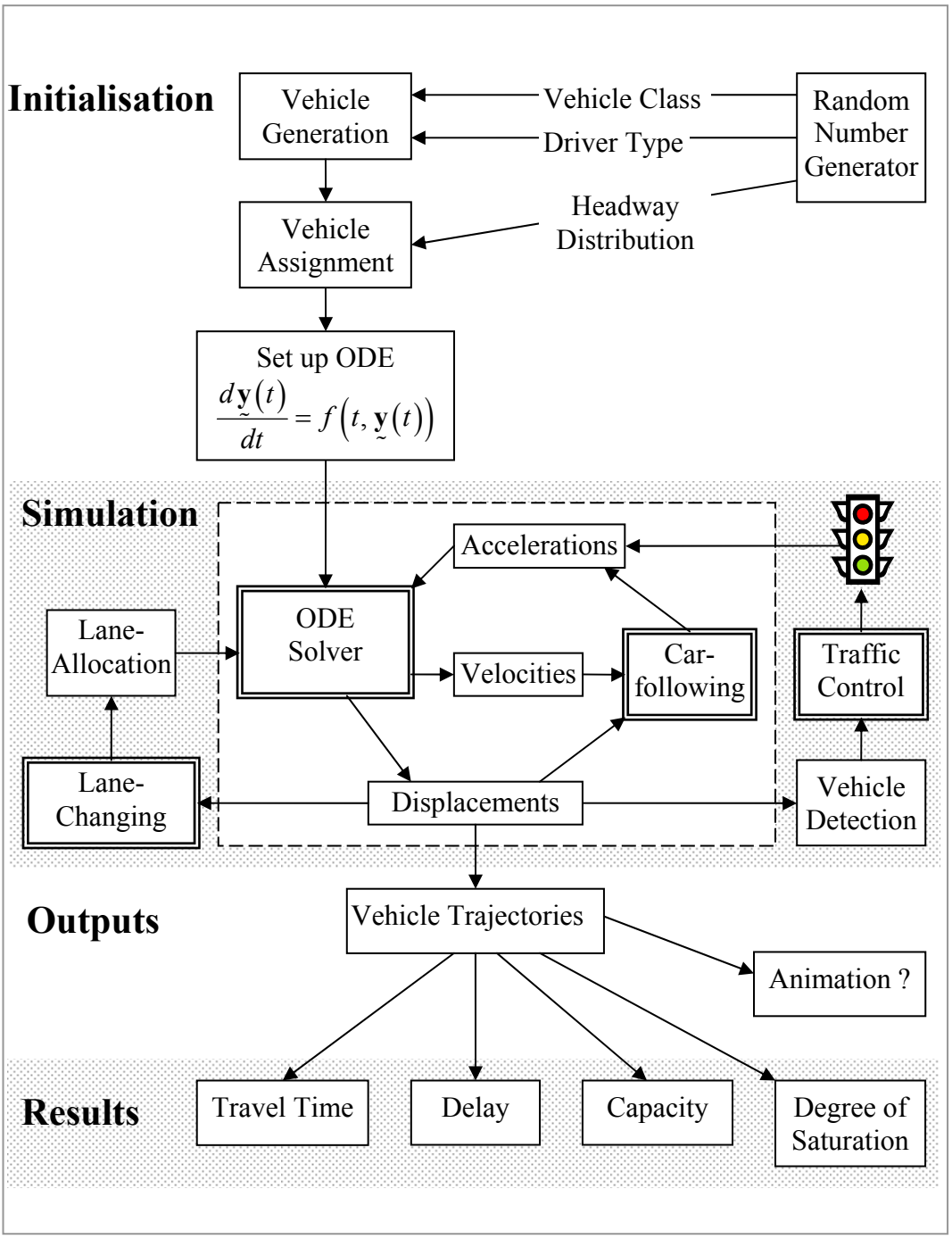


**Figure 5.2 – Model stages and components**

## 5.2 Vehicle Generation

Vehicles are 'generated' at a position upstream of the first signalised intersection, and become active (i.e. they start moving forward at their prescribed initial speed) at a time after the previous vehicle in that lane has done so. Each of the following needs to be specified for each vehicle:

- The **lane** that the vehicle starts in (lane changing is permitted as the simulation proceeds)
- The **vehicle type**, selected randomly within proportionate ranges from a list of classifications, such as the 12 Austroads vehicle classifications
- The **headway** after the previous vehicle, randomly drawn from a specified distribution

Vehicles only become active, and able to move forward through the corridor, when the simulation time exceeds the vehicle's activation time. The vehicle's activation time is calculated by adding the activation time of the vehicle in the same lane in front to its headway.

Vehicles are deactivated when their position exceeds the corridor length. No further calculations are performed for a deactivated vehicle.

### 5.2.1 Lane allocation

Lanes do not need to be explicitly 'allocated'. Rather, a sequence of vehicles is generated in each lane, with the ratio of the average headway between vehicles in each lane determining the proportion of vehicles in each lane.

### 5.2.2 Vehicle types

Individual vehicle characteristics are selected from a random distribution. Vehicles are generated in the appropriate proportions by applying the inverse of the cumulative distribution function to a sequence of random numbers uniformly distributed between zero and one.

For certain applications, it may be appropriate to use a known and repeatable sequence of vehicles with known characteristics. For example, a fixed sequence of vehicle classes may be useful in estimating the effects of heavy vehicles in different queue positions at a signalised intersection approach. For a given random number generating algorithm, specifying a 'seed' for the random numbers, the same sequence of vehicle types and headways will be generated.

### 5.2.3 Headway distribution

A widely used headway distribution for arterial traffic simulation purposes was initially presented in Cowan (1975). This distribution, known as Cowan's M3 distribution, assumes that a fixed proportion of vehicles travel at a fixed short headway, with the remainder following a negative-exponential distribution.

This distribution has been applied to the analysis of unsignalised intersection and roundabout capacity (Troutbeck and Brilon 1997). Sullivan and Troutbeck (1994) used Cowan's M3 distribution for modelling urban traffic flow, finding it accurate and simpler than alternative models to apply to the analysis of intersections within a road network.

The M3 distribution is given as a probability distribution function in Equation 5.6 and as a cumulative distribution function in Equation 5.7.

$$f(\tau) = \begin{cases} 0 & \tau < \Delta \\ 1-\alpha & \tau = \Delta \\ \alpha\lambda e^{-\lambda(\tau-\Delta)} & \tau \geq \Delta \end{cases} \qquad \text{Equation 5.6}$$

$$F(\tau) = \begin{cases} 0 & \tau \leq \Delta \\ 1-\alpha e^{-\lambda(\tau-\Delta)} & \tau > \Delta \end{cases} \qquad \text{Equation 5.7}$$

where $\alpha$ is the proportion of free vehicles

$\Delta$ is the minimum headway
which is used by a proportion of vehicles given by $1 - \alpha$

$\lambda$ is a parameter describing the shape of the distribution.

A sequence of headways, $h$, may be generated using Equation 5.8 that follow this distribution by transforming a sequence of uniform random numbers, Rnd, ranging from 0 to 1.

$$h = \Delta + \max\left[0, \frac{1}{\lambda}\ln\left(\frac{\alpha}{1-\text{Rnd}}\right)\right] \qquad \text{Equation 5.8}$$

Sullivan and Troutbeck (1994) calibrated the Cowan M3 distribution for Australian urban arterial traffic corridors. Although these calibrated coefficients could have been used, calibration of the model for this project was done using headway data from traffic with an appropriate proportion of heavy vehicles, as reported in the next two chapters.

Troutbeck (1997) warned about using Cowan's distribution for other than gap acceptance purposes. It may be suggested that the headway distribution is not a totally random process, and depends to some extent upon the preceding vehicle's headway. Particularly along an arterial corridor with signalised intersections, vehicles tend to travel in platoons – a short headway would be likely to occur immediately after another short headway for vehicles in a platoon, and a long headway would be likely to occur after another long headway for free vehicles.

Different probabilities of generating a free vehicle could be used depending upon whether the previous vehicle was platooned or not. This is expressed as a Markov Chain probability matrix in Table 5.1.

**Table 5.1 – Markov chain probability matrix**

| *Previous vehicle's headway* | *Current vehicle's headway* | |
|---|---|---|
| | $h_i > \Delta$ | $h_i = \Delta$ |
| $h_{i-1} > \Delta$ | $\alpha_{11}$ | $1 - \alpha_{11}$ |
| $h_{i-1} = \Delta$ | $\alpha_{21}$ | $1 - \alpha_{21}$ |

where $\alpha_{11}$ is the probability of the current headway being greater than $\Delta$, given that the previous headway was greater than $\Delta$

$\alpha_{21}$ is the probability of the current headway being greater than $\Delta$, given that the previous headway way equal to $\Delta$.

In Cowan's M3 distribution, a single probability, $\alpha$, of generating a free (unplatooned) vehicle is used, irrespective of the preceding headway. An alternative model allocates different probabilities of generating a free vehicle, depending on the headway of the previous vehicle. The model would be implemented by using either $\alpha_{11}$ or $\alpha_{21}$ in place of $\alpha$ in Equation 5.8, depending

upon the previously generated headway. For traffic consisting of platoons of closely spaced vehicles, it would be expected that $0 < \alpha_{12} < \alpha < \alpha_{11} < 1$.

Since this model focuses on heterogeneous vehicles, the headways between different classes of vehicles may also be found to be different. This is the basis for the formulation of Passenger Car Equivalents (PCEs). A similar strategy of assigning different probability distributions based on the generated and preceding vehicle classes may be used.

The most appropriate distribution model to fit the data would be able to be determined after representative headway data has been collected.

## 5.3 Updating the status of the system

The traffic corridor is represented by a number of vehicles and traffic control devices, all of which require updating as the simulation proceeds.

### 5.3.1 Vehicles

The following method is used to manage the movement of vehicles through the corridor:

- Firstly, calculate the acceleration of each vehicle at the current time step. This acceleration depends on the capabilities of the vehicle as well as the actions of surrounding vehicles and traffic control devices (traffic signals and speed limits).
- Next, update the position and speed of each vehicle assuming that the acceleration is constant over that time step. Speeds are constrained to be non-negative and not in excess of the speed limit at the current position. Positions are constrained to be not less than that in the previous time step.

Note that the accelerations of all vehicles are calculated before their speeds or positions are updated. As outlined in the next section, a vehicle's acceleration depends partly on the distance and relative speed to the leading vehicle – a vehicle's acceleration may be incorrectly calculated if the leading vehicle had been moved forward prematurely.

Vehicles change their speeds in response to vehicles around them and to traffic control devices (particularly speed limits and intersections). The first of these is governed by car-following theory, the latter by an overriding requirement to maintain the speed limit and to stop when required at intersections.

A vehicle cannot exceed its maximum acceleration capability, which depends on current velocity and, for undulating terrain, on the current displacement. Cohen (2002b) represented this by the formula given in Equation 5.9.

$$a_f \leq a_f^{\max}\left(x_f, v_f\right) \qquad \text{Equation 5.9}$$

where $a_f$ is the actual acceleration of the following vehicle

$a_f^{\max}$ is the maximum acceleration of the following vehicle, expressed as a function of its instantaneous displacement, $x_f$, and velocity, $v_f$.

The previous chapter found that a linear relationship of a vehicle's unconstrained acceleration as a function of its velocity was most appropriate for use in this current project. Two parameters would be required to calibrate this model, namely the maximum possible acceleration and maximum possible velocity. These parameters would depend upon the class of the vehicle for which the maximum acceleration is sought.

An additional constraint placed on the motion of each vehicle is required to ensure that the maximum velocity on the current section of the corridor is not exceeded. The maximum velocity itself is considered a function of displacement, to account for situations where the speed limit along the corridor may change. This may be implemented by multiplying the maximum acceleration given in Equation 5.9 by a step function that comes into effect if either the speed limit or the vehicle's free

speed is exceeded. This would have the effect of setting the acceleration to a small negative value so that the vehicle will coast down until the current speed limit is no longer exceeded.

Particularly for a heavy vehicle, the maximum achievable speed on an upgrade and the maximum safe speed on a downgrade are also dependant upon distance for a general undulating terrain. This would require calibration along the entire corridor alignment.

### 5.3.2 Lane changing

Vehicles are able to change lanes if there is an advantage in doing so and an opportunity exists.

An advantage in changing lanes occurs if the vehicle is travelling at less than its desired speed; it is not accelerating at its unconstrained rate; and the vehicles in an adjacent lane are travelling faster. When approaching an intersection queue, this lane-changing advantage is determined by comparing the expected time taken to pass through the intersection in each of the alternative lanes. This expected time depends on the number and type of vehicles in each approach lane at the intersection, effectively replicating the subconscious decision made by a driver approaching an intersection.

In recognition of the multiple tasks a driver performs, lane changing opportunities are not conducted at every time step – instead vehicles consider lane changes at a lower rate, in the order of once every ten seconds. This is to limit the number of lane changing occurrences, and to prevent the possibility of a vehicle toggling between two lanes. This interval between considering lane changes should be readily alterable in the model.

The implementation of a lane changing strategy in this model has two components – firstly, determining when a lane-changing event occurs; and secondly, handling the event within the model. The lane-changing decision and execution process is fairly detailed, and will be discussed in a subsequent chapter once the relevant subcomponents of the model implementation have been defined. Handling the lane changing event is described below.

During the simulation, each vehicle keeps track of the vehicles immediately in front and behind. Within the program, this is done by treating each vehicle as an object, maintaining pointers to the vehicles in front and behind.

These pointers are used primarily to determine the headway and relative velocity for the car-following model. If a vehicle changes lanes into a space between two vehicles in an adjacent lane, then these pointers must be changed for five vehicles: the vehicle that is changing lanes, the vehicles that were previously in front and behind it, and the vehicles in front of and behind the gap into which the lane changing vehicle moved. This is illustrated in Figure 5.3, where the pointers between vehicles are updated following a lane change manoeuvre.

The simulation continues after the lane change, with each vehicle now referring to its new leader when calculating car-following and collision avoidance variables.

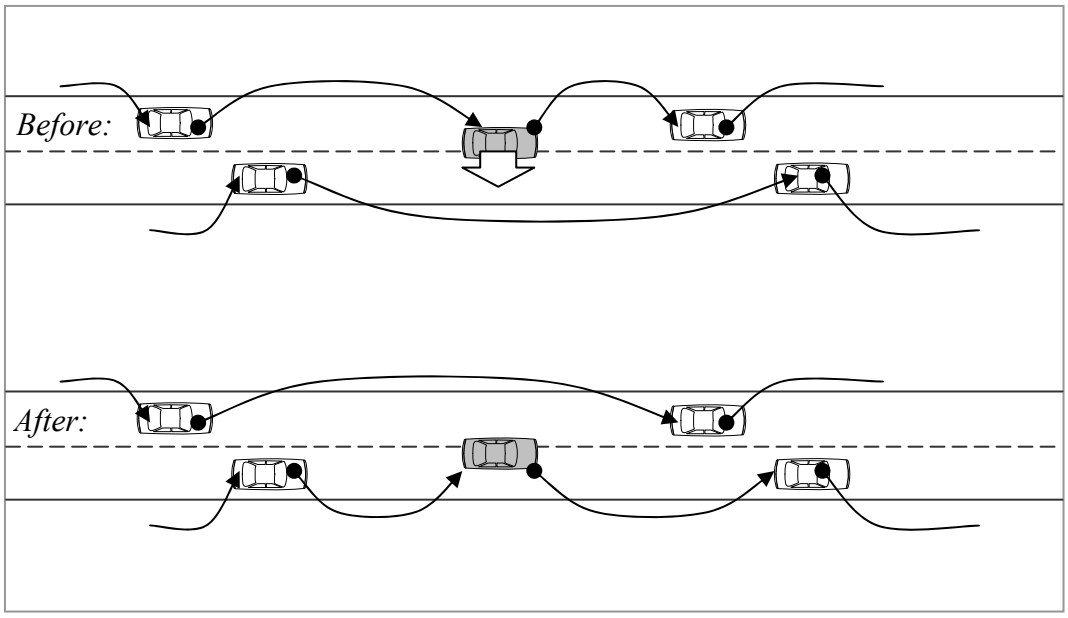


**Figure 5.3 – Changing vehicle pointers during a lane change manoeuvre**

### 5.3.3 Signal displays

Signals operating on fixed time plan can be modelled as having a status given by remainder of the current simulation time divided by the cycle time. This can be modelled by the conditional definition given in Equation 5.10.

$$\begin{aligned} &if\ (t+t_o) \bmod C \le G && \text{then } Status = Green \\ &if\ (t+t_o) \bmod C \le G+Y && \text{then } Status = Yellow \\ &if\ (t+t_o) \bmod C > G+Y && \text{then } Status = Red \end{aligned} \qquad \text{Equation 5.10}$$

where $t$ is the current simulation time

$t_o$ = offset of signal

$G$, $Y$ and $R$ are the displayed green, yellow and red times respectively

$C$ = cycle time = $G + Y + R$.

In calculating the acceleration for each vehicle, if a yellow or red light is displayed at the next traffic signal, and the vehicle is within the safe stopping distance, then the vehicle will commence deceleration so as to come to rest at the stop line. The rate of deceleration can be calculated knowing the current vehicle speed and the distance available in which to stop. Vehicles behind the vehicle that is stopping will also decelerate according to car-following rules.

The duration of the yellow period is required to exceed the safe stopping time at the corridor design speed. This is typically 4 seconds at 60 km/h and 5 seconds at 80 km/h (Austroads 2003, Table C.3).

Upon display of a green signal to the corridor through movement (plus a start-up delay time), the lead vehicle starts accelerating at its typical maximum rate, given by $a_f^{\max}$ in the previous section. This vehicle would be essentially unconstrained by the car-following rules, since its lead vehicle would be too far ahead to influence car-following behaviour.

The vehicles behind this lead vehicle would also accelerate, under car-following conditions.

## 5.4 Model Outputs

The model would produce several output tables to report the results of the simulation. These tables fall into the following categories:

- **Vehicle-type-specific outputs** – including the space mean speed, travel time, stopped time, and number of stops for each vehicle type
- **Intersection-specific outputs** – average cycle time, and green time for each intersection
- **Intersection-lane-specific outputs** – queue length, number of queued vehicles, queue clearance time, saturation flow, start loss, lost time, lane capacity
- **Vehicle type at each intersection** – control delay per cycle, control delay per vehicle, stopped time per cycle, stopped time per vehicle.

Although these measures are specific to traffic engineering applications, further performance measures may be derived or at least estimated from these; including generalised costs, fuel consumption, noise and emissions.

## 5.5 Data Requirements of this Model

Several separate data collection experiments were required to collect the information to calibrate and verify the model. There were considerable advantages in running several of these experiments concurrently in order to ensure that an identical traffic composition was used in the separate experiments. The collection and analysis of this data is described in detail in the next two chapters.

### 5.5.1 Arrival flow characterisation

An automatic traffic counter / classifier provided the information to calibrate the arrival flow characteristics. The counter recorded the time, lane, speed, wheelbase, headway and classification of individual vehicles passing over it; giving data that was used to determine appropriate distributions for vehicle proportions, headways, speeds and lane utilisation.

### 5.5.2 Corridor geometry characterisation

The geometry of the test corridor was characterised to locate significant grades, vertical and horizontal curves and other features that may influence the speeds achievable by heavy vehicles along the route. This was done by obtaining Global Positioning System (GPS) coordinates from a vehicle driven along the corridor. An alternative method would have been done to extract the coordinates from plans of the corridor alignment.

### 5.5.3 Vehicle kinematic characterisation

As well as knowing the proportions of vehicles in each vehicle class, it was essential to know the typical in-service speeds, acceleration and deceleration rates of typical vehicles in those classes.

This information was obtained from a chase car survey; in which an instrumented vehicle was driven over a test route following a particular vehicle. Although the original test method (as outlined in Austroads 2004) did not use it, a Global Positioning System (GPS) recorder was used to simplify the data collection and analysis process. The data would give information on the relationships between acceleration, speed and grade for each vehicle type.

### 5.5.4 Car-following and lane changing characterisation

Reviews of existing car-following and lane-changing models have identified difficulties in conducting experiments in these areas, mainly arising from problems in covertly detecting drivers' responses and the relative scarcity of lane-changing manoeuvres. As such, existing car-following and lane-changing models and parameters were used in this study and their constraints borne in mind.

### 5.5.5 Travel time characterisation

The chase car surveys mentioned earlier in this section also provided information on the travel times and stop rates of the different vehicle types using the test corridor. This assisted in providing information to validate the travel times and stop rates predicted by the model.

## 5.6 Conclusions

This chapter defines some of the specifications for a microsimulation-based model of traffic flowing along an urban arterial corridor.

The simulation was essentially a discrete-time based simulation of the kinematics of several vehicles being driven along a corridor. Interactions between surrounding vehicles and with traffic control devices determined the accelerations of the vehicles, which, in turn, determined the velocities, and displacements of the vehicles.

Parameters required to calibrate the model and to verify its correct operation have been outlined, as were a number of experiments designed to evaluate those parameters.

Details of the experiments conducted to calibrate these parameters for a specific urban arterial traffic corridor are presented in the next chapter.

# CHAPTER 6 COLLECTION OF TRAFFIC AND VEHICLE DATA

## 6.1 Introduction

This chapter describes the surveys undertaken to provide data to calibrate and validate the model specified in the previous chapter. Analysis of that data is covered in the following chapter.

The surveys were undertaken in order to characterise the traffic on a representative urban arterial traffic corridor having a large proportion of large freight vehicles. This was done with the objective of calibrating the input parameters of the corridor-level traffic model described in the previous chapter.

Several experiments were undertaken separately to provide traffic- and vehicle-related data. These were conducted concurrently in September 2004 on the same urban traffic corridor, thus ensuring that traffic conditions were consistent between the experiments.

## 6.2 Data Collection Methodology

The following research methodology was used to collect and analyse the data, giving sufficient data for the project's needs without requiring excessive effort or risk:

1) Identify a suitable corridor
1) Record traffic volumes and headways using an automated traffic counter-classifier
2) Conduct chase car surveys, following a range of vehicles over the corridor
3) Obtain intersection status reports from the traffic management system for the corridor
4) Analyse the traffic volumes to give vehicle type proportions and headways

5) Analyse GPS data recorded during the chase car surveys to give travel times over the corridor

6) Extract acceleration profiles for each vehicle type from the GPS data

Figure 6.1 illustrates the need for and use of each of the data sources. Calibration of the model is done using the arrival flow characterisation from the traffic counter, the corridor timing information from STREAMS (Queensland Main Roads' traffic management system), and the vehicle performance characteristics measured from the in-vehicle GPS data system.

The measured travel times and stop would be able to be compared to those predicted by the model.

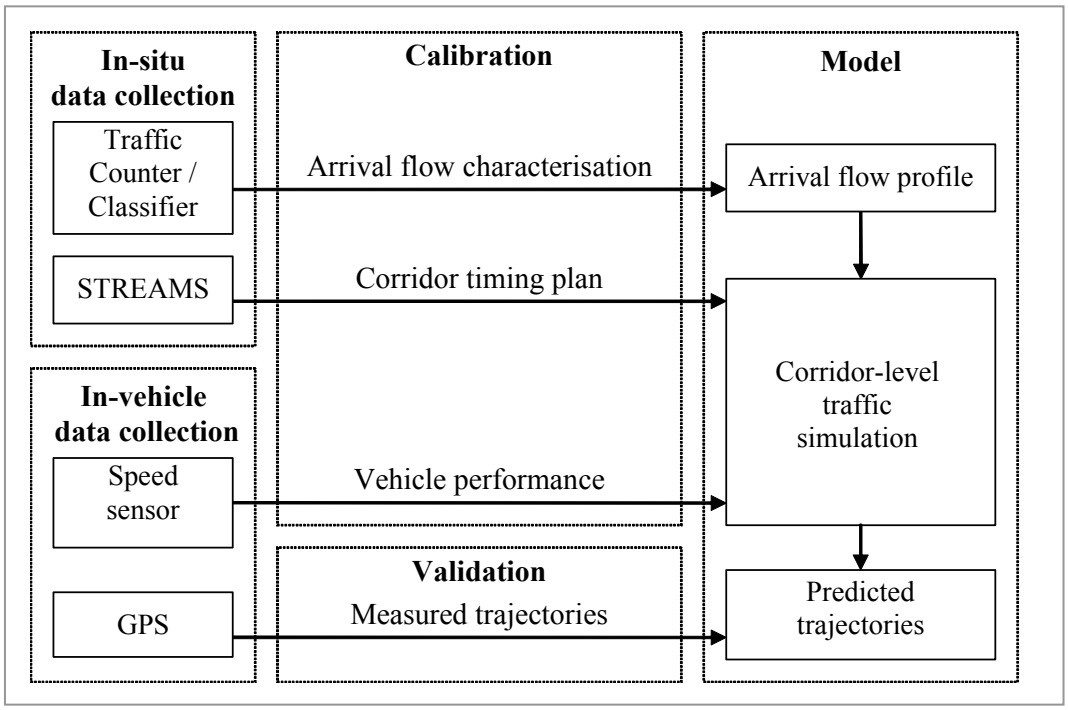


**Figure 6.1 – The data collection and calibration process**

## 6.3 Selection of the Study Corridor

The following were identified as desirable selection criteria for the test corridor:

- **Presence of heavy vehicles:** The site should be on a route that is designated as suitable for B-doubles by the relevant state road authority. A high, but not excessive, volume of heavy vehicles was required to

determine the effects of heavy vehicles on traffic performance (including other vehicle types). A corridor having from 10% to 20% heavy commercial vehicles was considered representative of typical urban arterial freight corridors.

- **Multiple lanes:** A location with multiple lanes in each direction was required in order to account for lane-changing around slower-moving vehicles. However, more lanes required more instrumentation and added model complexity. Thus, a location with two lanes per direction was sought. Note that the model only considers traffic in a single direction.
- **Traffic variation:** Traffic volumes were required to vary through the day, as was the proportion of heavy commercial vehicles. This ensured that the one corridor could be used to quantify traffic impacts for a range of conditions.
- **Geometry:** The corridor should contain sections of different grade in order to account for this in the model. Grades of up to ±10% are considered to be representative of the majority of Australia's urban traffic corridors carrying heavy vehicles (Austroads 1997).
- **Turning Traffic:** The site would have a relatively low proportion of turning heavy vehicle traffic compared to through traffic. This would ensure that there was a strong likelihood of a heavy vehicle being followed proceeding all the way along the corridor.

### 6.3.1 Candidate corridors

Three urban arterial traffic corridors were identified as likely candidates for this project. All of these corridors are designated B-double routes through suburban Brisbane. They all were located in Brisbane's southern suburbs, and are shown in a map in Figure 6.2.

- Brisbane Urban Corridor (BUC), between Ipswich Motorway and Gateway Motorway
- Mount Lindesay Highway (Beaudesert Road), south of Granard Road
- Lytton Road, towards the Port of Brisbane

This figure is not available online. Please consult the hardcopy thesis available from the QUT Library

*District 13 Map: Department of Main Roads, 2003*

**Figure 6.2 – Candidate urban traffic corridors around Brisbane**

Upon examination of these alternative corridors, the Brisbane Urban Corridor most closely met the above criteria. It forms part of the National Highway network, and is managed by Queensland Department of Main Roads. There had been recent concerns about traffic operations on the corridor, particularly relating to heavy vehicles (see, for example Jan Taylor and Associates 2003).

Mount Lindesay Highway had three-lanes in each direction, and had many turning movements of heavy vehicles. It was considered too large and having too high a probability of followed vehicles not travelling the entire length of the corridor.

Lytton Road did not offer the appropriate mixture of traffic. As the major access road to the Port of Brisbane, this route had too many heavy vehicles to investigate their impacts on urban traffic consisting predominantly of light vehicles.

### 6.3.2 Brisbane Urban Corridor

The Brisbane Urban Corridor provided a toll-free connection between the Ipswich Motorway and the Gateway Motorway. There were 18 signalised intersections along its 11.5 kilometre length (Figure 6.3). The corridor was essentially flat in the industrial western end, hilly in the commercial middle and undulating in the residential eastern end, as shown in Figure 6.4. The corridor was well suited to studying effects of heavy vehicles on different traffic conditions – having few mid-corridor access points for LFVs, the same mixture of heavy vehicles was subjected to a wide range of traffic conditions.

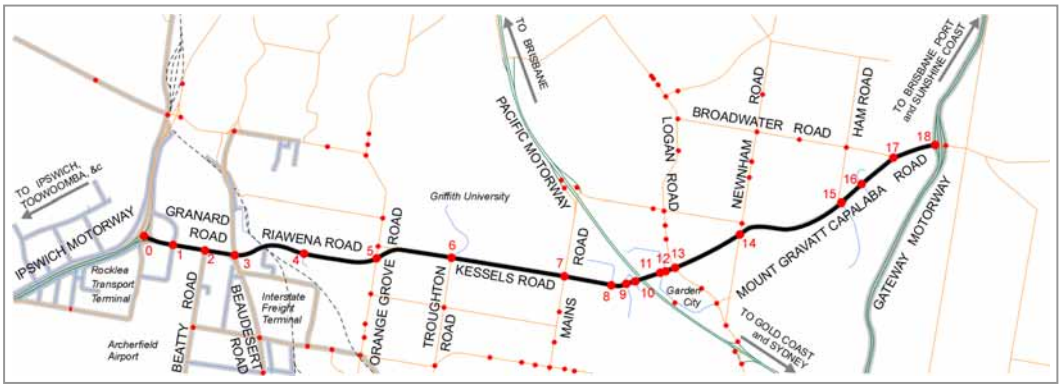


**Figure 6.3 – Plan of the Brisbane Urban Corridor**

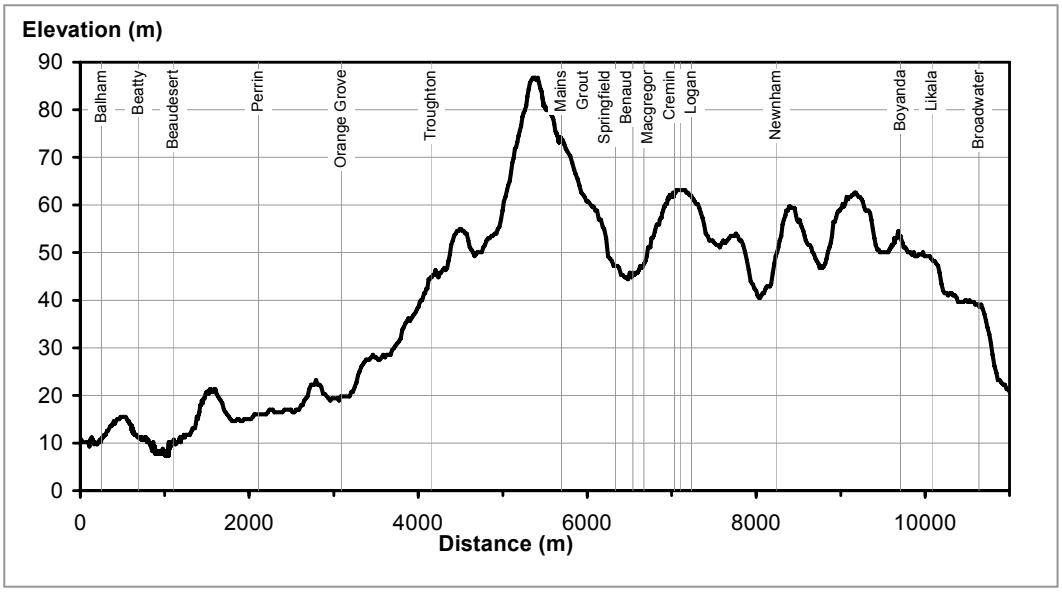


**Figure 6.4 – Elevation profile of the Brisbane Urban Corridor**

## 6.4 Traffic Volumes on the Brisbane Urban Corridor

The results of an extensive traffic survey on the BUC were examined to determine the expected traffic composition.

The survey was conducted in 2002 as part of an investigation of traffic operations on the BUC (Jan Taylor and Associates 2003). Surveys were conducted at four locations, automatically recording the hourly volumes of vehicles into each of 13 vehicle classifications in each direction over a one week period.

Table 6.1 and Figure 6.5 show the locations and average weekday bidirectional volumes at each of the four survey sites. Repeat surveys were undertaken at two of the sites. The highest traffic volumes were recorded in the middle of the corridor at Kessels Road east of Mains Road whereas the highest proportion of heavy vehicles was recorded at the western end of the corridor at Granard Road west of Beatty Road.

**Table 6.1 – Brisbane Urban Corridor Study traffic surveys**

*Source: Jan Taylor and Associates (2003)*

This table is not available online.
Please consult the hardcopy thesis
available from the QUT Library

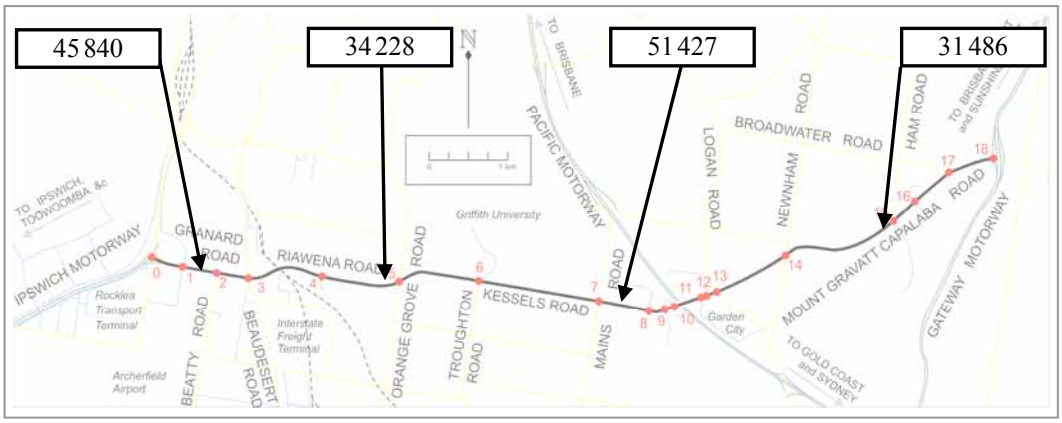


*Average weekday bidirectional volume (AWDT)*

**Figure 6.5 – Average weekday bi-directional volume on Brisbane Urban Corridor**

The hourly traffic volumes at Riawena Road west of Orange Grove are shown in Table 6.2 and Figure 6.6. Traffic volumes were relatively constant through the daylight hours; however, a slight 'tidal' flow is evident, with more westbound traffic in the morning peak and more eastbound traffic in the afternoon peak. The proportion of trucks increased in the off-peak periods, as shown in Figure 6.7.

**Table 6.2 – Brisbane Urban Corridor Study vehicle classification split**

| | *Average Traffic Volumes (vehicles per hour)* | | | | | | | |
|---|---|---|---|---|---|---|---|---|
| | *AM Peak (0700-1000)* | | *Midday (1000-1500)* | | *PM Peak (1500-1900)* | | *Night (other times)* | |
| *Vehicle Type* | *WB* | *EB* | *WB* | *EB* | *WB* | *EB* | *WB* | *EB* |
| Car | 1414 (84%) | 1010 (88%) | 1040 (78%) | 1141 (88%) | 1103 (85%) | 1548 (94%) | 498 (83%) | 388 (82%) |
| Rigid Truck | 218 (13%) | 114 (10%) | 239 (18%) | 117 (9%) | 157 (12%) | 75 (5%) | 61 (10%) | 56 (12%) |
| Articulated Truck | 40 (2.4%) | 21 (1.8%) | 50 (3.8%) | 23 (1.8%) | 25 (2.0%) | 11 (0.7%) | 35 (5.9%) | 27 (5.6%) |
| B-double | 8 (0.5%) | 9 (0.8%) | 9 (0.7%) | 9 (0.7%) | 6 (0.5%) | 6 (0.4%) | 6 (1.0%) | 3 (0.7%) |
| **Total** | **1679** | **1153** | **1339** | **1291** | **1292** | **1641** | **601** | **475** |

*Location: Kessels Road, West of Orange Grove, 23-30 April 2002*

*WB = Westbound, EB = Eastbound*

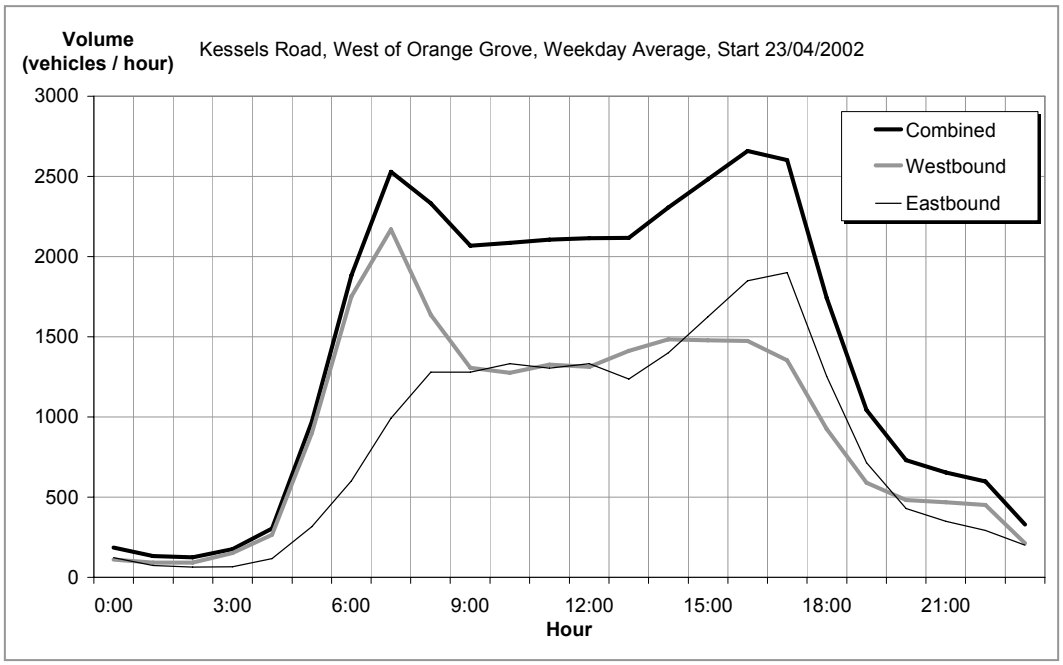


**Figure 6.6 – Hourly traffic volumes on the Brisbane Urban Corridor**

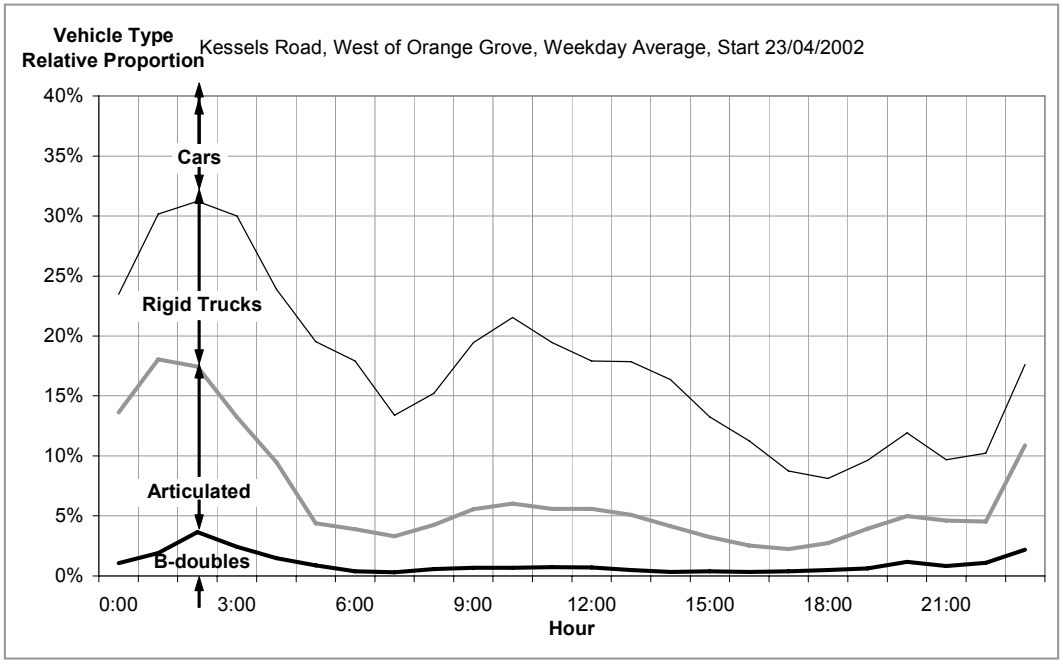


**Figure 6.7 – Relative proportions of vehicle types through the day**

The following four distinct operating conditions were identified from this survey data:

- **Peak periods:** high overall volume, low truck proportion (7am – 10am and 3pm – 7pm)
- **Inter peak:** medium overall volume, high truck proportion (10am – 3pm)
- **Pre- and post-peak:** medium overall volume, medium truck proportion (4am – 7am and 7pm – 10pm)
- **Night time:** low overall volume, relatively high truck proportion (10pm – 4am)

These periods have been represented diagrammatically in Figure 6.8. Weekends provided additional operating conditions, however these were of lesser interest due to their generally lower commercial traffic levels.

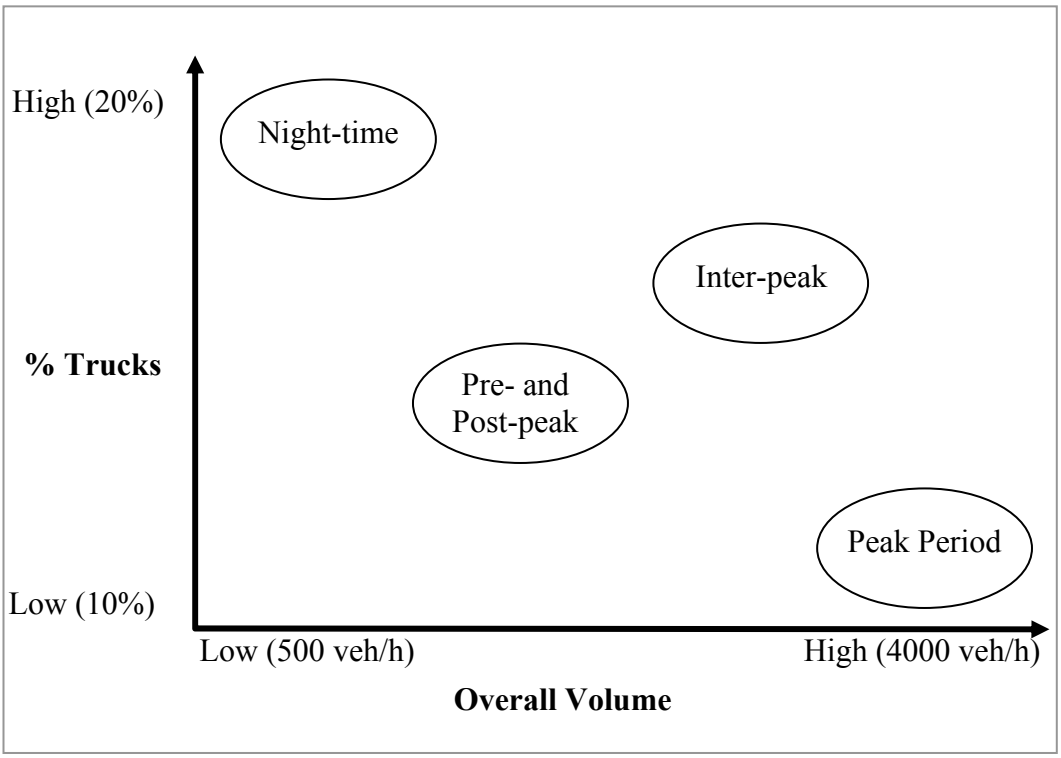


**Figure 6.8 – Major identifiable weekday traffic operating conditions**

## 6.5 Traffic Volume Survey

The traffic volume surveys conducted in 2002 for the Brisbane Urban Corridor Study did not include headway information. A current survey was required to estimate the vehicle type proportions in existence at the same time that the other surveys were being conducted.

A **Vehdat** automatic traffic counter-classifier unit from Australasian Traffic Surveys (ATS) was purchased for this purpose, and another unit was borrowed from ATS to record traffic in an adjacent lane. Technical specifications of the Vehdat unit are available from ATS' internet site (http://www.austraffic.com.au).

### 6.5.1 Survey method

The automatic traffic counter-classifiers were installed on Riawena Road, eastbound, approximately 300 metres west of Perrin Place and 700 metres east of Beaudesert Road. As seen in Figure 6.9, a two-metre wide raised concrete median separated the two carriageways. Traffic signs at this location, directing trucks to limit compression braking, were used to secure the equipment.


**Figure 6.9 – Traffic counter/ classifier location: Riawena Road, looking east towards Perrin Place**

The traffic counter was housed inside a lockable stainless steel box, and connected to two rubber hoses stretched across the road surface perpendicular to the direction of traffic (Figure 6.10).


**Figure 6.10 – Typical installation of the automatic traffic counter**

These two detector tubes were nailed onto the road surface (Figure 6.11) early in the morning of Sunday 12th September 2004. A laptop computer (Figure 6.12) was used to set up the traffic counter and to download data during the survey.

In order to collect sufficient data and to determine the variation between different days of the week, the counter-classifiers were intended to be set up for a period of one week. However, due to the large volume traffic on the road, the detector tubes became dislodged on Thursday 16th September.

The four full days of data that was collected was sufficient to enable an accurate characterisation of the volumes, headways, speeds and vehicle classifications at the survey site. Variations between the different days of the week could be estimated from the BUC Study data collected in 2002.


**Figure 6.11 – Installing the automatic traffic counters**


**Figure 6.12 – The automatic traffic counter locked to a road sign base during the survey, and the laptop computer used for downloading the data**

### 6.5.2 Survey data

A sample of the axle data file recorded by the Vehdat counter-classifier is shown in Figure 6.13. Each line displays the time in seconds at which one of the two detectors (0 or 1) was activated. Times are relative to the start time and date shown in the third and fourth lines of the file.

```
TITLE: Riawena Road, Lane 1
 RUN 1 Version 108
TIME 09:03:29
DATE 2004-09-12

(many other axle records)

1  0  125414.22457886
1  1  125414.32611084
1  0  125414.38589478
1  0  125414.45590210
1  1  125414.48834229
1  1  125414.55496216
1  0  125414.76995850
1  0  125414.83428955
1  1  125414.87115479
1  0  125414.89599609
1  1  125414.93710327
1  1  125414.99710083
```

**Figure 6.13 – Extract from sample axle data file**

The axle detections recorded by the counter-classifier were combined into individual vehicle records. Details of the vehicle classification algorithm used to do this are given in Appendix A. The resultant vehicle data file contains the date, time, lane, classification, number of axles and axle groups, the speed, headway and wheelbase of each classifiable vehicle that drove over the detector tubes. An extract of a vehicle data file is shown in Figure 6.14, the bold record indicating the 6-axle vehicle assembled from the 12 axle detection records in Figure 6.13.

```
___DATE___ ____TIME___ LA CL AXGP KM/H  H/WAY  OAWB
2004/09/13 19:53:33.093 2  1 0202 77.20 0.999  2.79
2004/09/13 19:53:40.226 2  1 0202 93.44 7.133  2.36
2004/09/13 19:53:43.326 1  9 0603 70.91 11.12 13.23 o oo    ooo
2004/09/13 19:53:45.122 2  1 0202 83.43 4.897  2.26
2004/09/13 19:53:58.080 2  1 0202 64.87 12.96  2.39
2004/09/13 19:53:58.082 1 10 0904 68.50 14.76 21.51 o oo    ooo    ooo
2004/09/13 19:54:03.203 2  1 0202 81.16 5.123  2.35
2004/09/13 19:54:12.292 1  1 0202 71.91 14.21  2.59
2004/09/13 19:54:14.343 2  1 0202 77.79 11.14  2.47
2004/09/13 19:54:16.848 1  9 0603 70.96 4.556 14.22 o  oo     ooo
2004/09/13 19:54:55.354 2  1 0202 84.08 41.01  2.44
```

**Figure 6.14 – Extract from sample vehicle data file**

## 6.6 Travel Time Survey

### 6.6.1 Background and benefits of each survey method

Table 6.3, taken from NAASRA (1988), shows several methods of conducting travel time surveys. The methods utilising a moving observer are more appropriate for long road sections, such as an urban traffic corridor; and give a greater level of detail, including the number of stops and stopped time. Stationary observation methods, such as a number plate survey, will generally give a much larger sample size but with less information about what actually happened within the road section.

Of the two moving observation methods, the chase car method was considered more appropriate for use in this study. Generally, drivers of the vehicle being followed would be unaware that their position and speed were being recorded, which might otherwise have an influence of the outcomes of the survey. Further, since a range of different vehicle types were studied, a floating vehicle survey would require that equipment be fitted to several vehicles.

**Table 6.3 – Travel time survey methods**

*Source: NAASRA (1988)*

This table is not available online.
Please consult the hardcopy thesis
available from the QUT Library

### 6.6.2 Equipment

The travel time survey method outlined in NAASRA (1988) predated the widespread availability of Global Positioning Systems (GPS). There are considerable advantages in using GPS for moving observer traffic surveys; particularly in regards to the ease of installation and calibration of the equipment, their accuracy and low cost. Alternative methods have been used in the past to measure the vehicle's speed and distance travelled. These have usually required a dedicated data logger connected to an external 'fifth wheel' or a sensor on the test vehicle's driveshaft.

A relatively simple GPS-based equipment set up was used to record the instantaneous position and speed of the chase car, using the following equipment:

- Garmin GPSMAP 76S GPS receiver
- Garmin GA-27C external antenna, mounted on the vehicle's roof
- Combined 12 volt power and serial data cable
- Laptop computer, having a serial port and Garmin MapSource® software
- Inverter to provide power for the laptop from the car's electrical system

Only the GPS receiver was required; however an external antenna provided a better GPS signal strength and greater accuracy. The power cable enabled longer travel surveys to be completed without needing to change batteries in the GPS receiver. The laptop computer and power inverter were only required if it was necessary to download the GPS track logs in the field.

A picture of the equipment installed in the cabin of a B-double is shown later in this chapter in Figure 6.22.

The Garmin GPSMap 76S GPS receiver could record up to 10,000 track points. At a rate of one track point per second, this gave approximately 2 hours and 45 minutes of data logging before having to download the data to the laptop personal computer. Typically, four downloads were conducted in an 8-hour survey session.

Additionally, the GPSMap76S had an inbuilt barometric altimeter and compass, which provided greater accuracy for altitude and heading angle than that provided by GPS receiver alone.

Technical specifications of the Garmin GPSMap76S GPS receiver and of the Garmin Mapsource software are available from Garmin's internet site (http://www.garmin.com).

### 6.6.3 Method

The chase car repeatedly was driven along the Brisbane Urban Corridor in alternating eastbound and westbound directions, following different vehicles.

Vehicle selection was conducted by firstly deciding which vehicle type to follow next, parking the vehicle at a safe location before the start of the corridor, waiting for an example of the selected vehicle type to appear, and then following the selected vehicle along the corridor.

If the vehicle being followed turned off before reaching the end of the corridor, the closest vehicle of the same type was located and that vehicle followed along the remainder of the corridor. Sometimes the closest vehicle was in front of the chase car, other times it was behind it. This ensured that travel time estimations were not excessively biased by always choosing an alternative vehicle either in front of or behind.

If the vehicle being followed passed through a traffic signal as it was changing to red, the chase car stopped at the intersection and attempted to rejoin the vehicle being followed further downstream. Care was taken not to exceed the speed limit at any time, including when trying to catch the following vehicle.

It took approximately 15 minutes for the chase car to reach the end of the corridor. The driver then stopped the chase car and checked the remaining memory in the GPS receiver. The GPS track log was downloaded to the laptop if there was not enough memory for a return run. The driver turned the vehicle around past the end of the corridor, selected the next vehicle type, and repeated the process.

### 6.6.4 Results

Garmin's MapSource program was used to download the GPS track logs to a laptop computer, to view the track logs on a map and to save the track logs to a text file for further analysis. Figure 6.15 shows a MapSource map of the area surrounding the Brisbane Urban Corridor, with the dotted line indicating a track log recorded by the chase vehicle.

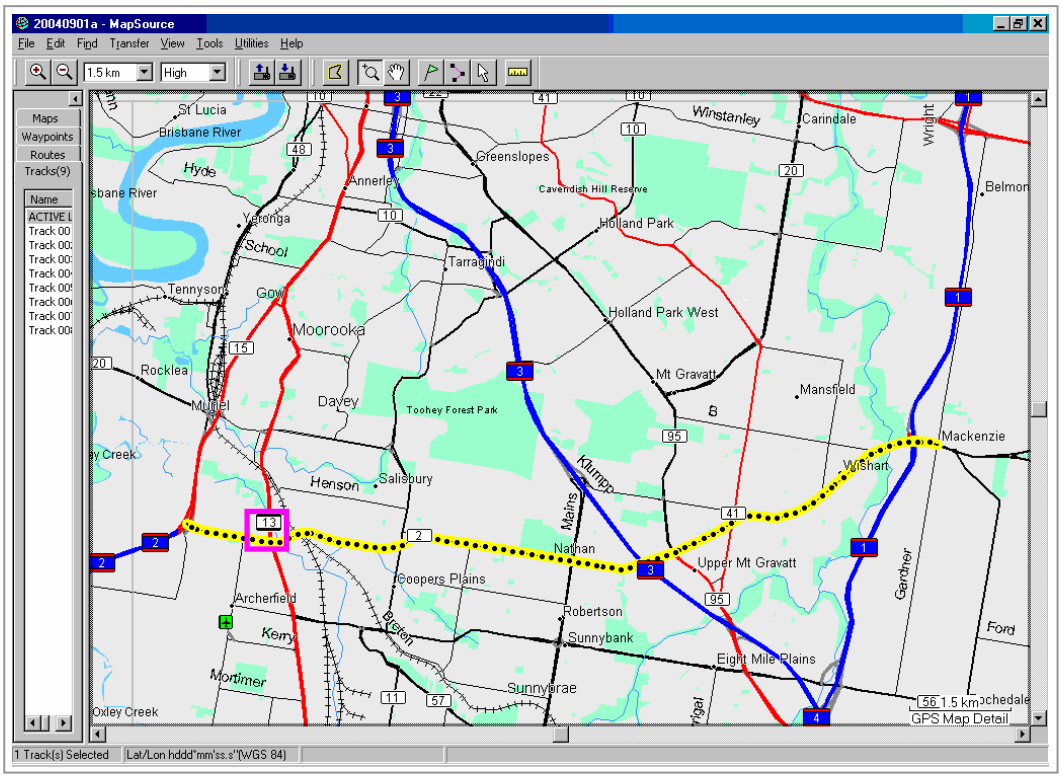


**Figure 6.15 – GPS track log on the Brisbane Urban Corridor**

Figure 6.16 is an enlargement of the western approach to the intersection of Granard Road and Beaudesert Road, indicated by the rectangle in the left of Figure 6.15. Several tracks can be seen in both lanes of the eastbound and westbound carriageways, corresponding to following different vehicles.

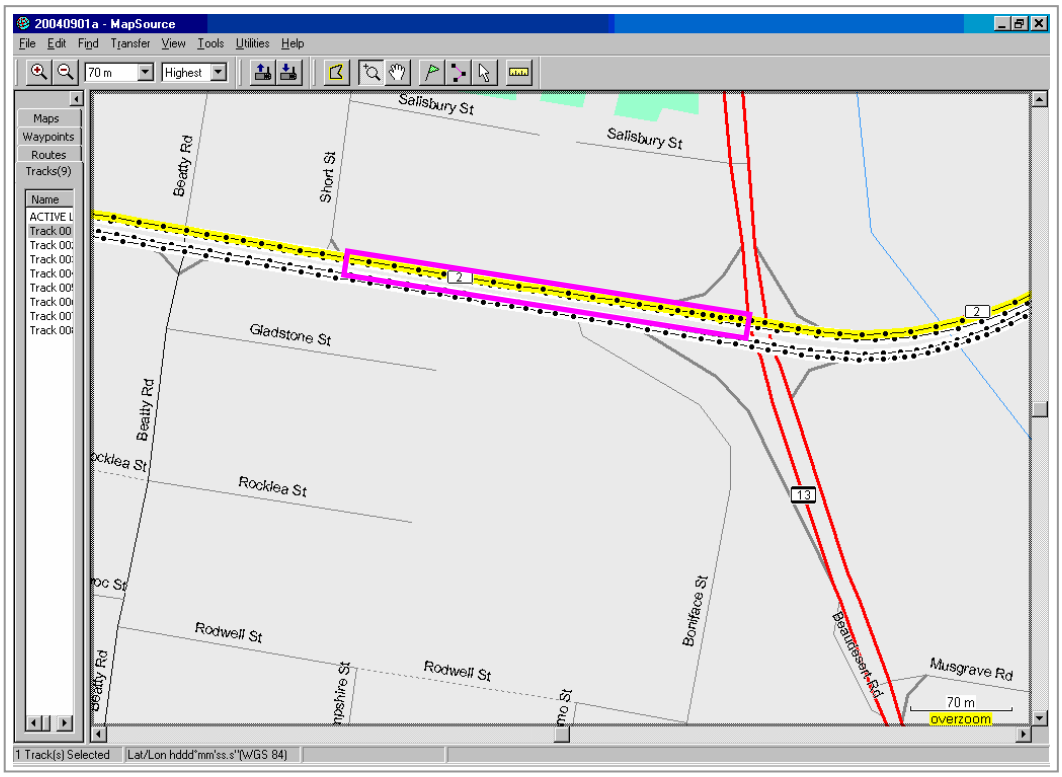


**Figure 6.16 – GPS track log, eastbound at Granard Road & Beaudesert Road**

The elongated rectangle to the left of the intersection in Figure 6.16 surrounds 22 track points that correspond to the chase car decelerating and stopping at the intersection. Figure 6.17 shows the MapSource track properties dialog box containing the track points highlighted in the previous figure.

Coordinates could be displayed as either latitude / longitude pairs, or in Universal Traverse Mercator (UTM) map coordinates. The latter coordinate system was preferred since it corresponded to a 1 metre Cartesian grid. This simplified the calculation of distances between consecutive points, eliminating the need to use spherical trigonometry. These coordinates were exported to a text file for further analysis in a spreadsheet. The spreadsheet was used to graph the plan (Figure 6.18) and profile (Figure 6.19). These can be compared to the plan and profile given in Figure 6.3 and Figure 6.4 earlier in this chapter.

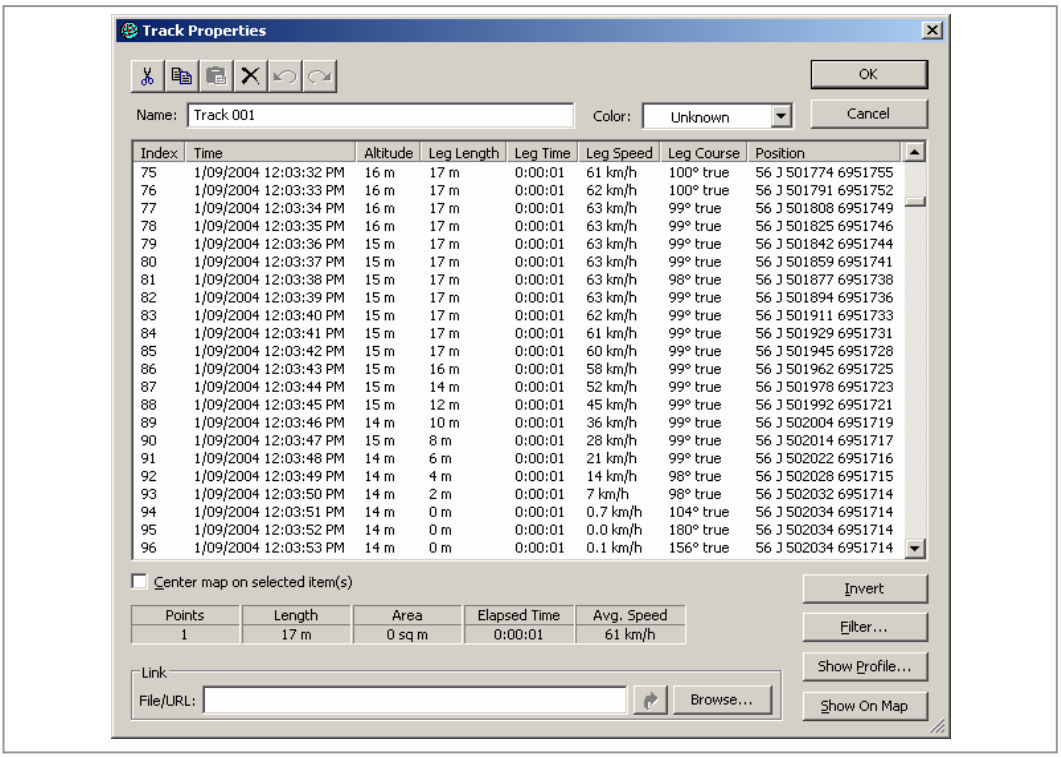


| Index | Time | Altitude | Leg Length | Leg Time | Leg Speed | Leg Course | Position |
|---|---|---|---|---|---|---|---|
| 75 | 1/09/2004 12:03:32 PM | 16 m | 17 m | 0:00:01 | 61 km/h | 100° true | 56 J 501774 6951755 |
| 76 | 1/09/2004 12:03:33 PM | 16 m | 17 m | 0:00:01 | 62 km/h | 100° true | 56 J 501791 6951752 |
| 77 | 1/09/2004 12:03:34 PM | 16 m | 17 m | 0:00:01 | 63 km/h | 99° true | 56 J 501808 6951749 |
| 78 | 1/09/2004 12:03:35 PM | 16 m | 17 m | 0:00:01 | 63 km/h | 99° true | 56 J 501825 6951746 |
| 79 | 1/09/2004 12:03:36 PM | 15 m | 17 m | 0:00:01 | 63 km/h | 99° true | 56 J 501842 6951744 |
| 80 | 1/09/2004 12:03:37 PM | 15 m | 17 m | 0:00:01 | 63 km/h | 99° true | 56 J 501859 6951741 |
| 81 | 1/09/2004 12:03:38 PM | 15 m | 17 m | 0:00:01 | 63 km/h | 98° true | 56 J 501877 6951738 |
| 82 | 1/09/2004 12:03:39 PM | 15 m | 17 m | 0:00:01 | 63 km/h | 99° true | 56 J 501894 6951736 |
| 83 | 1/09/2004 12:03:40 PM | 15 m | 17 m | 0:00:01 | 62 km/h | 99° true | 56 J 501911 6951733 |
| 84 | 1/09/2004 12:03:41 PM | 15 m | 17 m | 0:00:01 | 61 km/h | 99° true | 56 J 501929 6951731 |
| 85 | 1/09/2004 12:03:42 PM | 15 m | 17 m | 0:00:01 | 60 km/h | 99° true | 56 J 501945 6951728 |
| 86 | 1/09/2004 12:03:43 PM | 15 m | 16 m | 0:00:01 | 58 km/h | 99° true | 56 J 501962 6951725 |
| 87 | 1/09/2004 12:03:44 PM | 15 m | 14 m | 0:00:01 | 52 km/h | 99° true | 56 J 501978 6951723 |
| 88 | 1/09/2004 12:03:45 PM | 15 m | 12 m | 0:00:01 | 45 km/h | 99° true | 56 J 501992 6951721 |
| 89 | 1/09/2004 12:03:46 PM | 14 m | 10 m | 0:00:01 | 36 km/h | 99° true | 56 J 502004 6951719 |
| 90 | 1/09/2004 12:03:47 PM | 15 m | 8 m | 0:00:01 | 28 km/h | 99° true | 56 J 502014 6951717 |
| 91 | 1/09/2004 12:03:48 PM | 14 m | 6 m | 0:00:01 | 21 km/h | 99° true | 56 J 502022 6951716 |
| 92 | 1/09/2004 12:03:49 PM | 14 m | 4 m | 0:00:01 | 14 km/h | 98° true | 56 J 502028 6951715 |
| 93 | 1/09/2004 12:03:50 PM | 14 m | 2 m | 0:00:01 | 7 km/h | 98° true | 56 J 502032 6951714 |
| 94 | 1/09/2004 12:03:51 PM | 14 m | 0 m | 0:00:01 | 0.7 km/h | 104° true | 56 J 502034 6951714 |
| 95 | 1/09/2004 12:03:52 PM | 14 m | 0 m | 0:00:01 | 0.0 km/h | 180° true | 56 J 502034 6951714 |
| 96 | 1/09/2004 12:03:53 PM | 14 m | 0 m | 0:00:01 | 0.1 km/h | 156° true | 56 J 502034 6951714 |

| Points | Length | Area | Elapsed Time | Avg. Speed |
|---|---|---|---|---|
| 1 | 17 m | 0 sq m | 0:00:01 | 61 km/h |

**Figure 6.17 – Track properties dialog box, corresponding to track points in the rectangle in Figure 6.16**

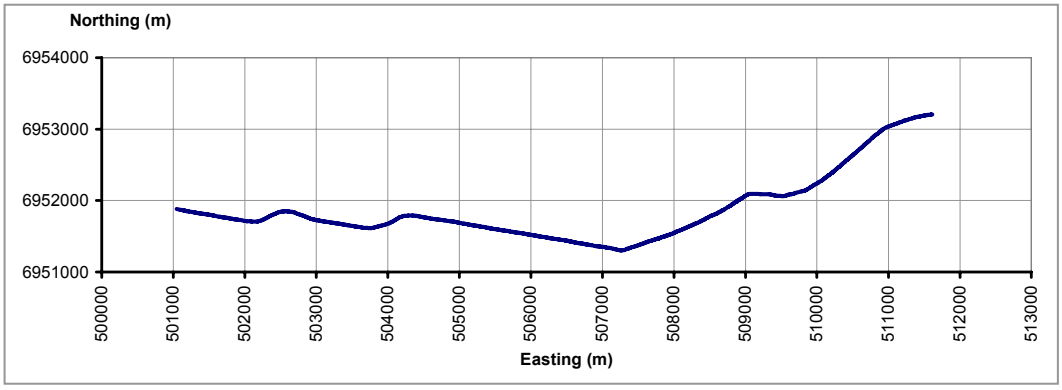


**Figure 6.18 – Plan of test drive recorded by GPS**

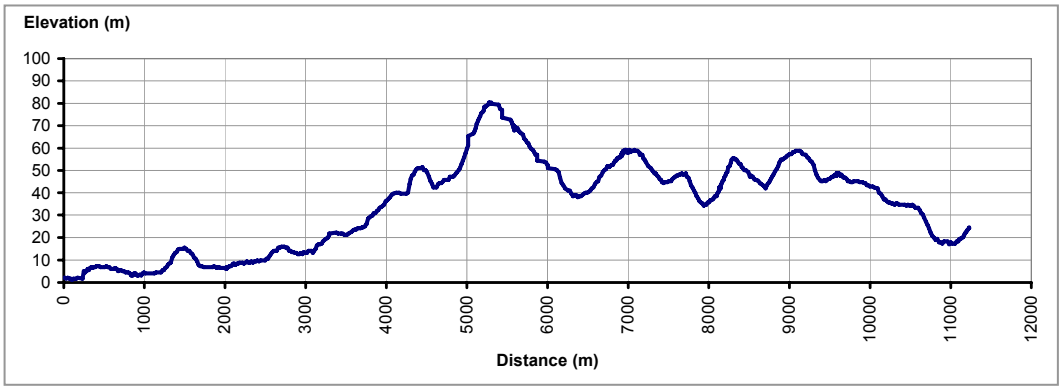


**Figure 6.19 – Profile of test drive recorded by GPS**

## 6.7 STREAMS Intersection Cycle Analysis Data

STREAMS is Queensland Main Roads' traffic management system. It controls the majority of the traffic signals operated by Main Roads, including those along the Brisbane Urban Corridor. Amongst its many functions, it records the instantaneous status of traffic signals, and can save that information for future use.

Concurrent with the chase car surveys, the instantaneous status of all of the traffic signals along the corridor was being recorded by STREAMS. The intersection status data was downloaded in the day after the survey from a STREAMS Explorer terminal located at Main Roads' head office.

A sample STREAMS intersection status file is shown in Figure 6.20. It shows the time of day that each cycle commenced, the time taken to complete the cycle, and the times taken by each phase that ran during the cycle.

| Time | Cycle Length | A len | B len | C len | D len | Phase Combo | Plan |
|---|---|---|---|---|---|---|---|
| 07:20:04 | 92 | 40 | 40 | 12 | 0 | ABC | 5 |
| 07:21:36 | 108 | 46 | 62 | 0 | 0 | AB | 5 |
| 07:23:24 | 100 | 38 | 42 | 0 | 20 | ABD | 5 |
| 07:25:04 | 110 | 38 | 72 | 0 | 0 | AB | 5 |
| 07:26:54 | 92 | 28 | 50 | 0 | 14 | ABD | 5 |
| 07:28:26 | 90 | 36 | 42 | 12 | 0 | ABC | 5 |
| 07:29:56 | 118 | 46 | 72 | 0 | 0 | AB | 5 |
| 07:31:54 | 94 | 28 | 42 | 0 | 24 | ABD | 5 |

**Figure 6.20 – Sample STREAMS intersection status file**

This data was used to construct a signal offset diagram, showing the position of each intersection along the corridor and the times at which the through movement on the corridor was active at each of those intersections. This was overlaid with the trajectory diagram recorded by GPS unit fitted to the chase car, as illustrated in Figure 6.21.

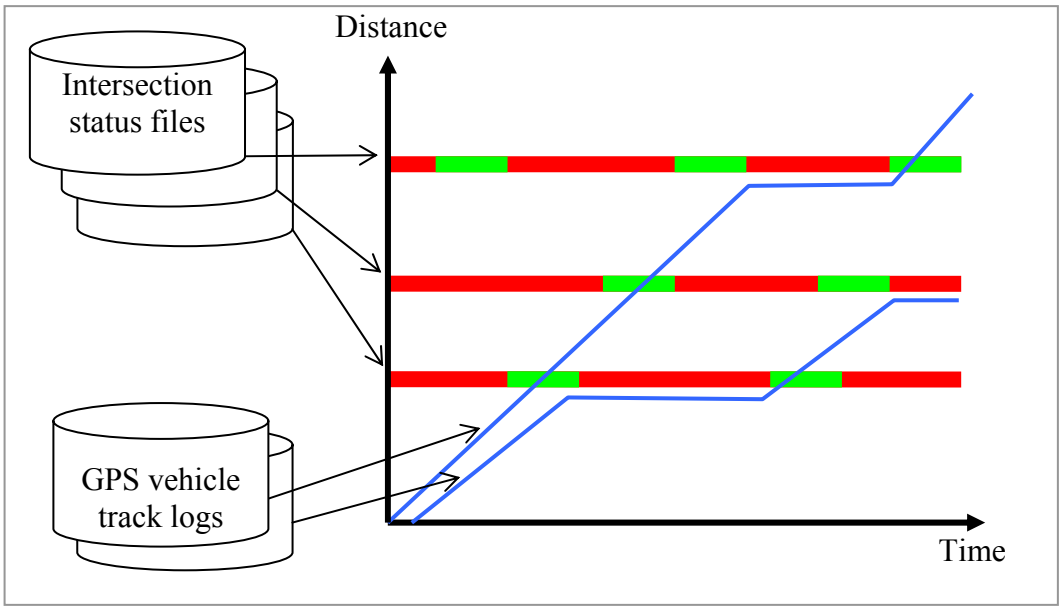


**Figure 6.21 – Constructing the trajectory diagrams**

## 6.8 Verification of the Chase Car Survey Method

### 6.8.1 Purpose

The method of estimating the longitudinal performance of a vehicle from a chase car has advantages in the lead vehicle driver remaining anonymous and generally being unaware of the experiment being conducted, and in the ability to survey a greater number of vehicles than other methods permit. However, it has the potential of being less accurate since the performance of the lead vehicle is being estimated remotely from another vehicle. This additional experiment was conducted to alleviate any concerns that the chase car survey method may not actually be giving a true representation of the in-service capabilities of the vehicle being followed.

### 6.8.2 Method

GPS units were fitted to a B-double and a chase car. Figure 6.22 shows the equipment mounted in front of the passenger's seat in the cabin of a B-double. The equipment setup in the chase vehicle was identical to that in the B-double.

The B-double had a 279 kW (375 hp) engine and was laden with zinc ingots to a gross vehicle mass of 62,500 kg. This gave a power-to-mass ratio of 4.46 W/kg, which was rather low for typical B-double operations.

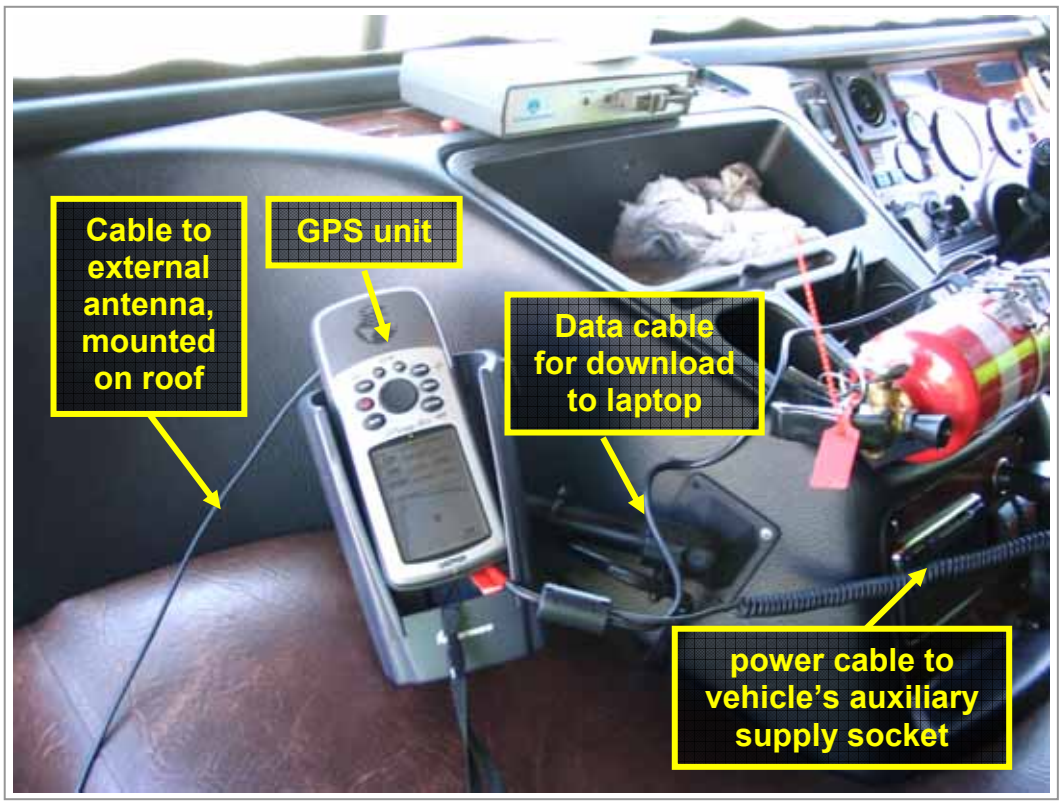


**Figure 6.22 – Garmin GPSMap 76S GPS unit mounted inside the cabin of a B-double**

The B-double test vehicle and chase car were driven over the Brisbane Urban Corridor in both eastbound and westbound directions. The driver of the chase vehicle was instructed to follow closely behind the B-double at a spacing that would prevent other vehicles from merging between them. If the B-double passed through a yellow or red traffic signal, the following vehicle was to stop at the traffic signal and to rejoin the B-double further along the route. Further, the chase car driver was instructed not to exceed the posted speed limit, even when attempting to catch up with the B-double if they become separated.

Two circuits of the Brisbane Urban Corridor were completed with the B-double fully laden. The vehicle was then unloaded, and a further circuit completed at a mass of approximately 25,000 kg.

### 6.8.3 Separation and travel time results

The GPS track logs were downloaded from the two GPS units to a laptop computer whilst the B-double was being unloaded and again at the completion of the testing. The track logs were then imported into a spreadsheet for analysis.

Figure 6.23 shows the easting coordinates recorded by the GPS units in the B-double and chase car, plotted against the time of day on the y-axis. The vehicles can be seen to move repeatedly between the left and rights end of the corridor.

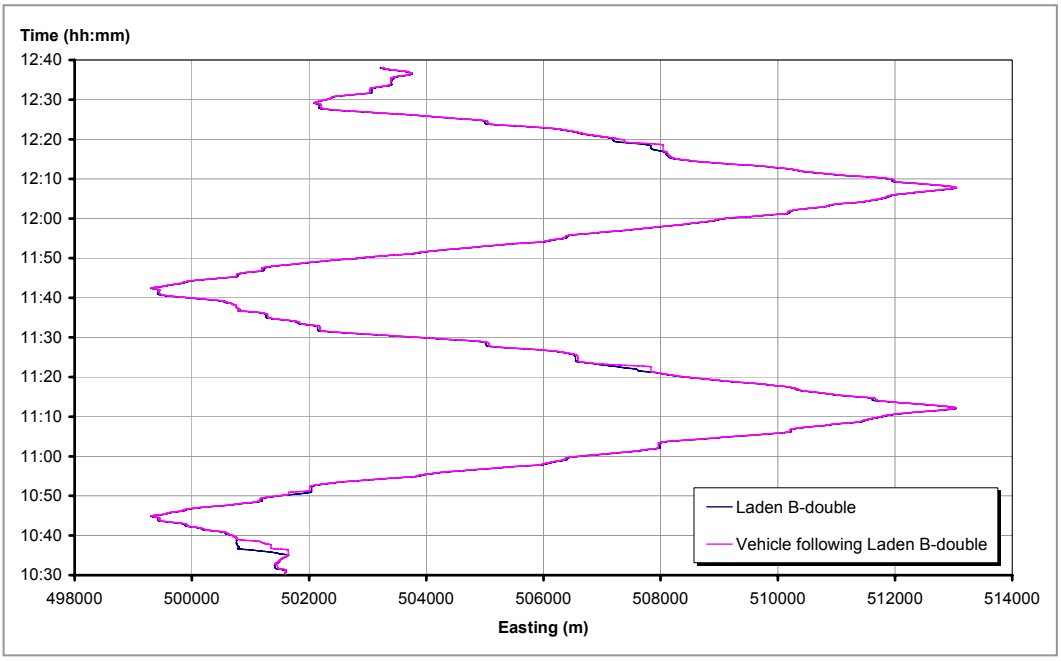


**Figure 6.23 – Easting coordinates of lead and following vehicle plotted against time**

Little difference can be seen between the easting coordinates of the two vehicles, except on the few occurrences when the lead vehicle passed through a changing traffic signal and the following vehicle was unable to do so.

The distance between the external antennae of the two GPS units was calculated in the spreadsheet. A histogram of these distances is shown in Figure 6.24. The distribution appears to follow a skewed normal distribution. A group of outliers at a spacing of more than 80 metres coincided with times that the vehicles were separated when the B-double passed through a changing traffic signal.

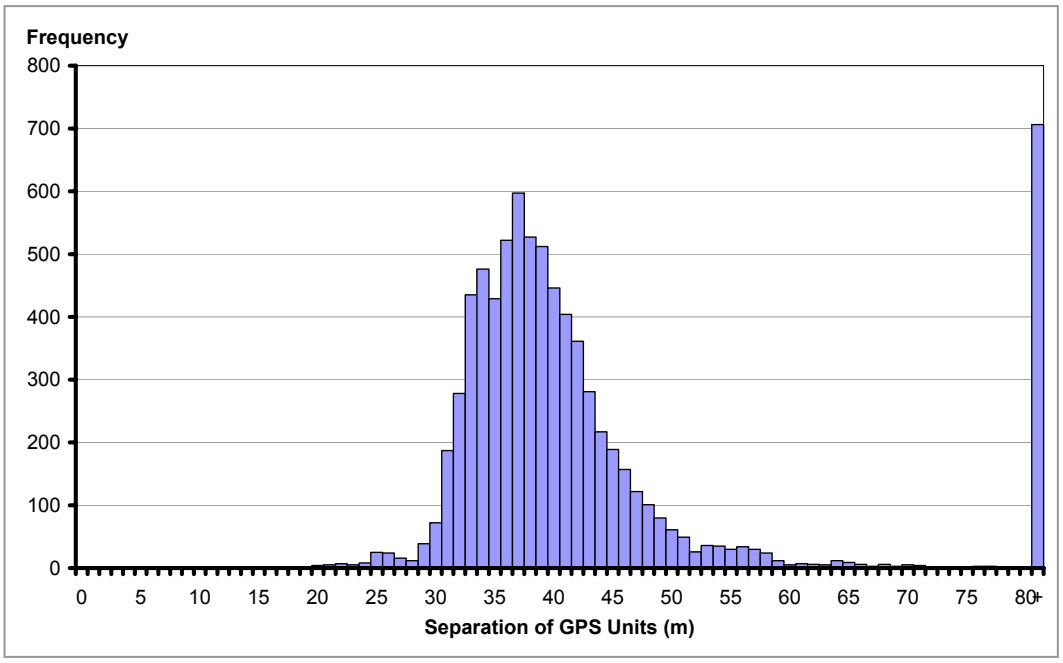


**Figure 6.24 – Histogram of the separation of the GPS units between the laden B-double and the chase car**

Table 6.4 shows the summary statistics for the separation between the GPS units on the B-double and the chase vehicle, for both laden and unladen conditions. By removing the data points when the GPS units were separated by more than 80 metres (when the vehicles became separated due to traffic), the average and standard deviation of the separation reduces considerably. The chase vehicle was separated from the unladen B-double for a large proportion of the time (92%), resulting in much larger separation values.

**Table 6.4 – Analysis of the separation of the GPS units between the lead and chase vehicles**

| *Data* | *n* | *average (m)* | *standard deviation (m)* | *median (m)* |
|---|---|---|---|---|
| **Laden B-double** | | | | |
| All data | 3990 | 76.00 | 124.63 | 38.84 |
| Separation < 80 m | 3546 | 39.01 | 6.70 | 37.79 |
| **Unladen B-double** | | | | |
| All data | 3905 | 635.17 | 385.07 | 604.69 |
| Separation < 80 m | 301 | 43.17 | 13.81 | 35.40 |

The B-double was 25 metres long, with the GPS antenna mounted on the cabin roof, 1 metre rearward of the front of the vehicle, and the GPS antenna on the roof of the chase vehicle was mounted 3 metres rearward of the front of the vehicle. Excluding times that the vehicles were separated by more than 80 metres, the median distance between the two GPS units was 37.8 metres, giving a median spacing between the rear of the B-double and the front of the chase car of 10.8 metres, as shown in Figure 6.25.

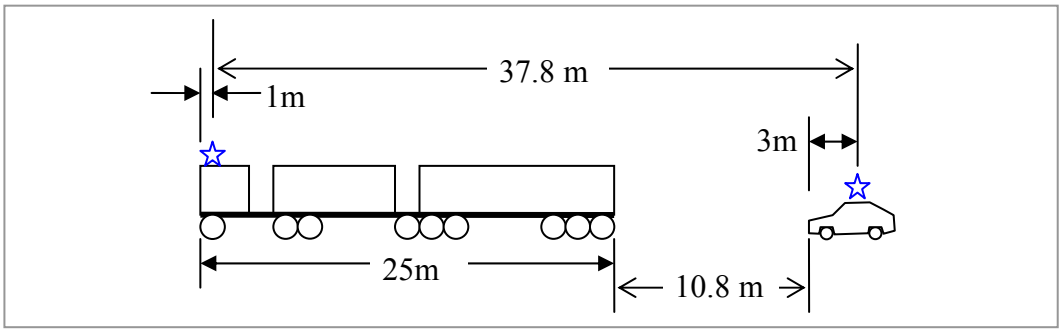


**Figure 6.25 – Calculation of the spacing between the vehicles from the separation of the GPS units**

Much of the spread in the vehicle separation data can be attributed to the spacing increasing with speed. Figure 6.26 shows the separation between the GPS units plotted against speed, indicating the increase in separation with speed.

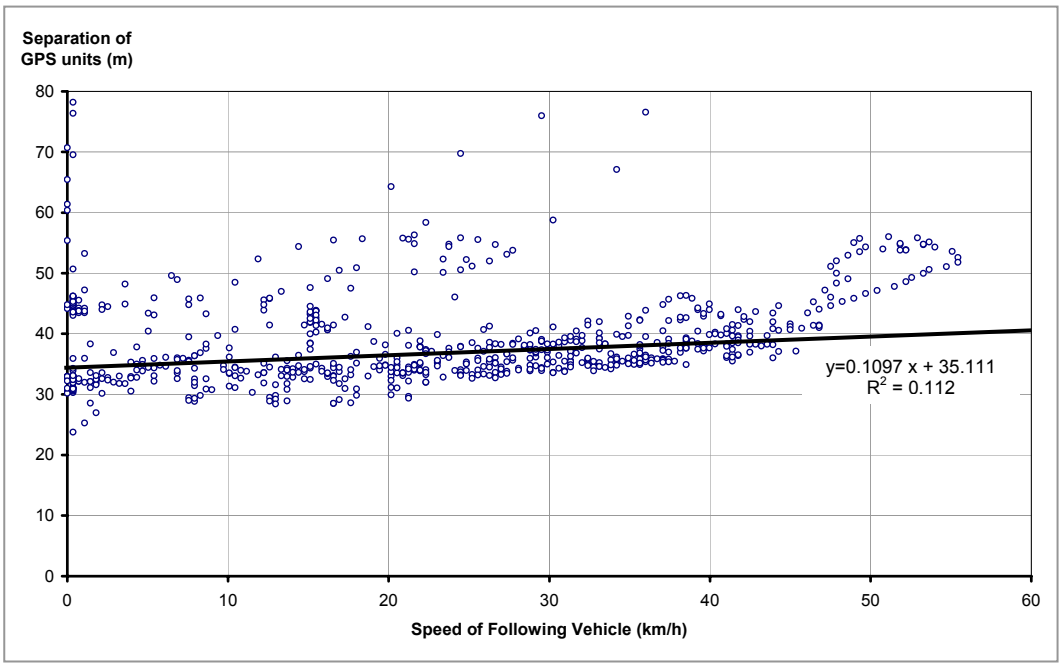


**Figure 6.26 – Increase in the separation of the GPS units with increasing speed**

Table 6.5 shows the coefficients of the linear regression of separation with speed for both the laden and unladen data. Data from times at which the vehicles were separated by more than 80 metres has been excluded from this analysis. There is little difference between laden and unladen data for either the separation at zero speed or its sensitivity to speed, with all coefficients statistically significant.

**Table 6.5 – Results of the regression of separation versus speed**

| *Model and Parameter* | *Coefficient* | *Standard Error* | *Significance (t-Statistic)* |
|---|---|---|---|
| **Following laden B-double** | **(n = 6959, $r^2$ = 0.11)** | | |
| Intercept | 35.110 | 0.139 | 252.324 |
| X Variable | 0.110 | 0.004 | 29.624 |
| **Following unladen B-double** | **(n = 3399, $r^2$ = 0.17)** | | |
| Intercept | 33.260 | 0.250 | 132.703 |
| X Variable | 0.164 | 0.006 | 26.751 |

*Note: Cases where the GPS units were separated by more than 80 metres have been excluded*

For most runs, the overall travel times between the two ends of the corridor were nearly identical between the B-double and chase vehicle. One exception occurred when the vehicles were separated and the chase vehicle completed the trip several seconds later.

The number of stops and stopped time were slightly greater for the chase car, once again due to the vehicles being separated at intersections.

### 6.8.4 Comparison of acceleration characteristics

The purpose of this additional experiment was to determine if differences existed between the acceleration characteristics measured in the two vehicles.

As an example, the speed and distance travelled as the vehicles leave a signalised intersection are shown in Figure 6.27 and Figure 6.28, respectively. Both the speed and distance traces are similar, there being slightly more variation in the speed of the chase car as its driver attempted to regulate the spacing between the vehicles.

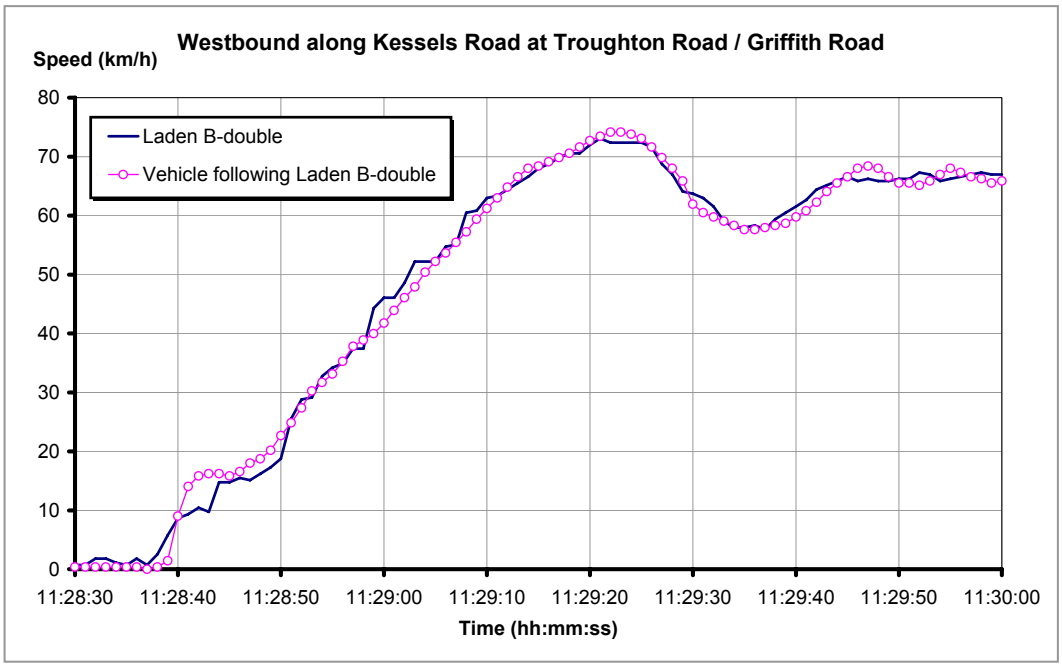


**Figure 6.27 – Speed plotted against time for leading and following vehicles**

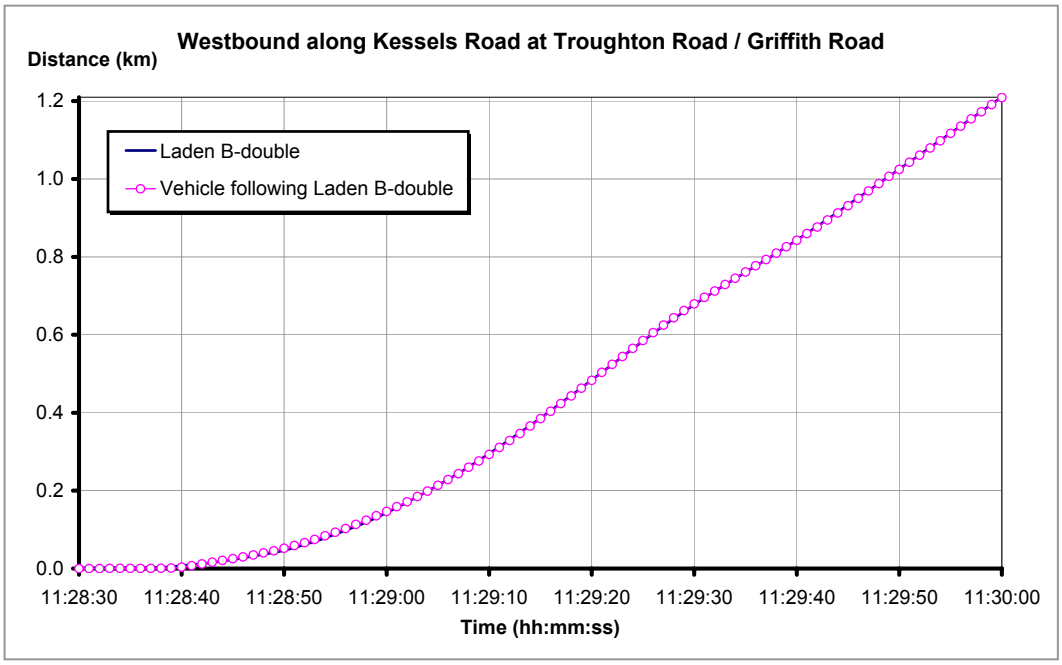


**Figure 6.28 – Distance plotted against time for leading and following vehicles**

The average acceleration of the vehicles was determined at each time the two vehicles started from rest at any signalised intersection on the corridor. The grade at the intersection was determined from the differences in elevation recorded by the GPS units.

Figure 6.29 shows the average accelerations as recorded by the two vehicles, plotted against the average grade at each intersection for the laden B-double (solid symbols) and the chase car (hollow symbols), whilst Figure 6.30 shows the same chart for the unladen B-double and the chase car. Linear regression lines have been added to the figures, solid lines representing the regression for the B-double and dashed lines representing the regression for the chase car.

The coefficients of these regression lines are presented in Table 6.6, together with the standard errors and statistical significance of the regression model parameters. The intercept was strongly significant for each of the four models, whilst the sensitivity of acceleration to grade was less so, particularly for the unladen B-double and the chase car following it.

The acceleration of the laden B-double was much more sensitive to grade than the unladen B-double, as indicated by the larger X-variables for the laden cases. There differences between the relationships between acceleration and grade for the B-double and the for the chase car were not significantly different, with less than one standard error difference in parameters from the B-double and chase car under both laden and unladen conditions.

**Table 6.6 – Results of the regression of average acceleration versus grade**

| *Model and Parameter* | *Coefficient* | *Standard Error* | *Significance (t-Statistic)* |
|---|---|---|---|
| **Laden B-double** | **(n = 35, $r^2$ = 0.29)** | | |
| Intercept | 0.326 | 0.012 | 28.045 |
| X Variable | -2.150 | 0.587 | -3.662 |
| **Following laden B-double** | **(n = 31, $r^2$ = 0.41)** | | |
| Intercept | 0.317 | 0.012 | 27.035 |
| X Variable | -2.495 | 0.560 | -4.455 |
| **Unladen B-double** | **(n = 20, $r^2$ = 3.2 x $10^{-6}$)** | | |
| Intercept | 0.410 | 0.023 | 18.062 |
| X Variable | -0.008 | 0.990 | -0.008 |
| **Following unladen B-double** | **(n = 18, $r^2$ = 0.10)** | | |
| Intercept | 0.406 | 0.020 | 20.406 |
| X Variable | -1.453 | 1.066 | -1.362 |

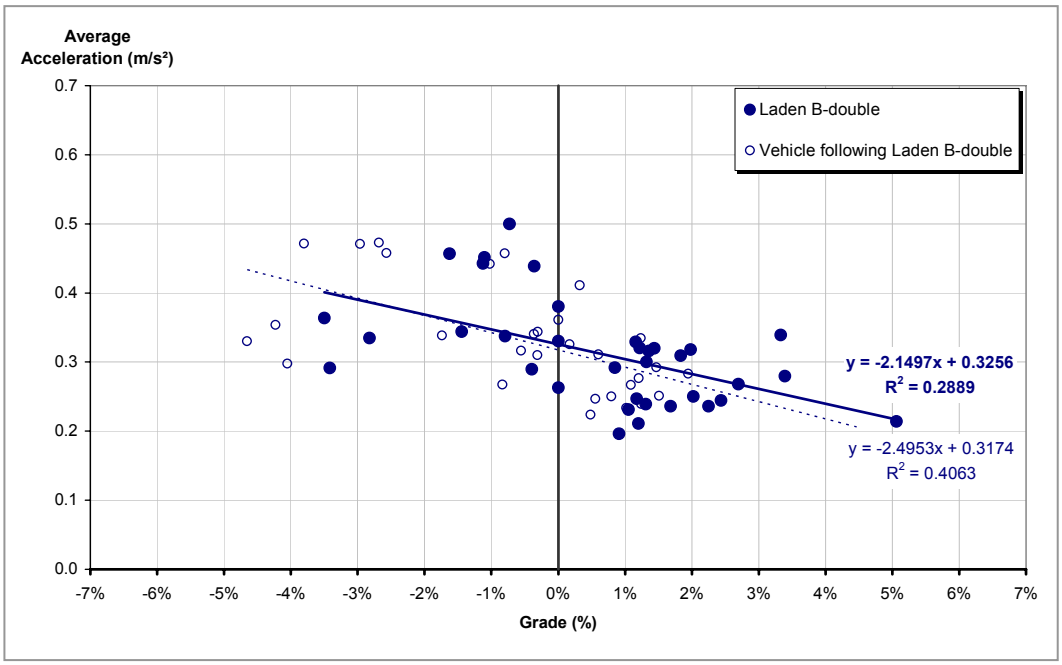


**Figure 6.29 – Reduction in average acceleration with measured grade for laden B-double**

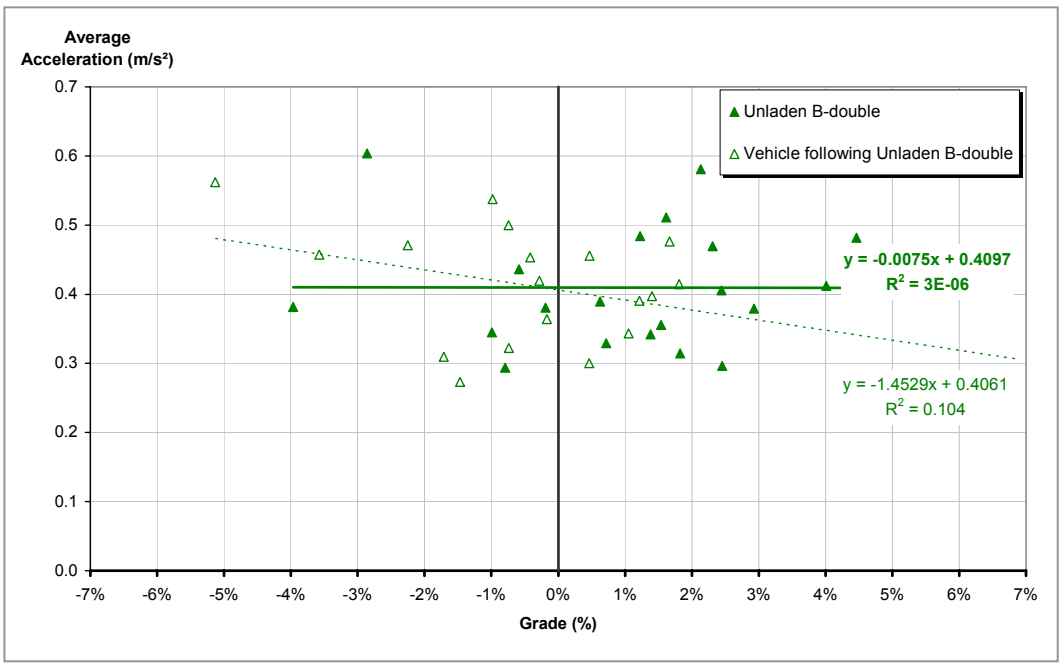


**Figure 6.30 – Reduction in average acceleration with measured grade for unladen B-double**

### 6.8.5 Implications on estimating characteristics of the lead vehicle

The following vehicle would only be able to provide exact speed and acceleration measurements of the leading vehicle if a constant separation was able to be maintained at all times, as if they were connected by a rigid pole. Figure 6.26 shows that the separation between the vehicles increases with increasing speed, with the regression line indicating an increase in separation of 6.58 m as speed increases from 0 to 60 km/h. Figure 6.27 shows that the B-double typically took 35 seconds to accelerate to 60 km/h from rest, whilst Figure 6.28 shows that it covered a distance of 300 metres in doing so.

Assuming this relationship between speed separation holds generally, the following vehicle would only travel a distance of 293.42 metres compared to the 300 metres travelled by the lead vehicle.

The constant acceleration rate required to cover these distances in the 35 seconds taken is 0.489 $m/s^2$ for the leading vehicle and 0.479 $m/s^2$ for the following vehicle. Conversely, calculating the acceleration required to accelerate to 60 km/h in these distances results in 0.463 $m/s^2$ for the leading vehicle and 0.473 $m/s^2$ for the following vehicle.

Because the acceleration rate is not constant, it is difficult to say whether the following vehicle will underestimate or overestimate the acceleration of the leading vehicle. In the previous chapter, an acceleration model that decreases linearly with increasing speed was found to be the most appropriate for use in this project. This acceleration model will be calibrated in the next chapter, and the corresponding acceleration relationships for these two examples will be compared.

## 6.9 Summary and Conclusions of this Chapter

This chapter describes the experiments undertaken to provide data used to calibrate the traffic corridor model developed in this project.

The Brisbane Urban Corridor was selected as the most appropriate urban arterial traffic corridor for the study. It had a high, but not excessive, proportion of heavy vehicles (including LFVs), that travelled through a range of traffic and road geometric conditions. Previous traffic surveys had been conducted on the corridor, giving an indication of the conditions to be expected.

An automatic traffic counter-classifier was used to record precisely the passage of vehicles at one location on the corridor, enabling the distributions of vehicles, headways and speeds to be characterised for the model.

A series of GPS-equipped chase car surveys were conducted at the same time, giving the trajectories of a range of vehicles using the corridor. These trajectories were then used to determine travel time and stopping characteristics, as well as estimating the behaviour of vehicles as they departed from signalised intersections.

The accuracy of the chase car method for estimating lead car behaviour was addressed in a separate experiment that used GPS units on both leading and following vehicles.

The next chapter describes the calibration of the parameters in the corridor-level traffic model, using the data collected in these experiments.

# CHAPTER 7 ANALYSIS OF THE TRAFFIC AND VEHICLE DATA

## 7.1 Introduction

This chapter describes the analysis of the data that was collected as discussed in the previous chapter. The purpose of this analysis is to provide the major input parameters for the corridor-level traffic model that was specified in an earlier chapter.

Data was collected from several sources:

- an automatic traffic counter-classifier on the test corridor
- a series of GPS-equipped chase car surveys, following different vehicle types along the test corridor
- the instantaneous status of the signalised intersections along the corridor

These were used to determine the following characteristics used in the model:

- the proportion of the different vehicle types in existence on the corridor
- the distribution of headways and speeds of each of those vehicle types
- the acceleration characteristics of each of the vehicle types

Additionally, the travel times and stop rates of each vehicle type were obtained, providing valuable information on their travel characteristics and a data set for which to compare model results.

## 7.2 Traffic Composition

### 7.2.1 Aggregating vehicle types

The vehicle classification algorithm described in Appendix A classifies vehicles according to the 12 classes in the Austroads ’94 vehicle classification scheme (Peters 1993). A computer program using this algorithm was used to process the raw axle detections recorded by the Vehdat traffic counter-classifiers. Ten of

those classes were present in significant numbers in the data; classes 11 and 12 (double and triple road trains, respectively) were not allowed on the test corridor.

Having ten vehicle classes was considered too many to handle efficiently through the project. There is a considerable range of performance capabilities within each of these vehicle classes, especially since they encompass both laden and unladen vehicles. This variation would mask any smaller differences that may occur between similar vehicle classes – for example between five-axle and six-axle articulated trucks. In addition, it would be difficult to obtain a statistically significant sample size for some of the rarer vehicle classes.

Aggregating several classes with similar characteristics would result in a more manageable and understandable outcome based on a more reliable data set.

Table 7.1 shows the relationships between the 12 Austroads vehicle classes and the 5 vehicle types used in this project. Generally, these form a many-to-one relationship, except for cars, four-wheel drives and light commercial vehicles.

**Table 7.1 – Aggregating the 12 Austroads vehicle classes into 5 vehicle types**

| | *Austroads Vehicle Classification* | *Vehicle Type* |
|---|---|---|
| 1 | Short Vehicle | Car |
| 2 | Short Vehicle Towing | 4WD/LCV |
| 3 | Two Axle Truck or Bus | Rigid truck |
| 4 | Three Axle Truck or Bus | |
| 5 | Four or Five Axle Truck | |
| 6 | Three Axle Articulated | Articulated truck |
| 7 | Four Axle Articulated | |
| 8 | Five Axle Articulated | |
| 9 | Six Axle Articulated | |
| 10 | B-Double | B-double |
| 11 | Double Road Train | -n/a- |
| 12 | Triple Road Train | |
| | Unclassifiable | |

The traffic counter-classifier was unable to differentiate between different vehicle types having similar wheelbases, for example between a passenger car and a four-wheel drive. With different power-to-mass ratios, these vehicle types were likely to have different performance characteristics, so it was appropriate to consider them as different vehicle types. Thus, Austroads vehicle classes 1 and 2 were pooled together, with a fixed proportion being considered passenger cars and the remainder being four wheel drives or light commercial vehicles.

### 7.2.2 Estimating the proportions of each vehicle type

The times of the day in which LFVs are having the greatest impact on traffic performance are determined by finding times at which there is a significant overall traffic volume *and* a significant proportion of heavy vehicles amongst that volume. Table 7.2 shows the average hourly traffic distribution of the traffic counts recorded by the automatic traffic counter-classifier on Riawena Road.

Figure 7.1 shows the distribution throughout the day for each of the four aggregated vehicle types. Short vehicles (cars, 4WDs, LCVs) have a strong peak in the afternoon and a lesser peak in the morning, corresponding to the two commuter peak periods. Peak volumes for all truck types occurred during the daytime inter-peak periods, typically 9am to 3pm. Peak volumes for cars occurred in the afternoon peak period, 3pm to 6pm. This site had a strong peak tidal flow, with the morning peak period being higher in the westbound direction, and the afternoon peak period being higher in the eastbound direction (as measured).

Figure 7.2 shows the relative proportions of the aggregated vehicle types at each hour through the day. Short vehicles are excluded from this figure because there are so many more of them than the other vehicle types. The proportion of B-doubles was highest at night time, particularly from 2am to 4am, but overall volumes of all vehicle types were low at this time. Note that, since this survey was conducted, tolls on an adjacent motorway have been eliminated for heavy trucks at night time in order to encourage use of the motorway and thus reduce truck noise at night on residential sections of the BUC.

Both articulated trucks and rigid trucks had their peak volumes in the daytime inter peak period, when there is still a substantial traffic level. The morning and afternoon peak periods both had relatively low proportions of truck traffic.

Thus, the baseline proportions of each vehicle type to be used in this project were selected to be those of the daytime inter-peak period, from 9am to 3pm.

**Table 7.2 – Classified traffic volumes**

*Riawena Road, Eastbound, 2 lanes, 13-15 September 2004*

| *Hour Ending* | *Car, 4WD, LCV* | *Rigid Truck* | *Articulated Truck* | *B-double* | *All vehicles* |
|---|---|---|---|---|---|
| 01:00 | 181 | 19 | 20 | 8 | 228 |
| 02:00 | 105 | 17 | 30 | 8 | 160 |
| 03:00 | 99 | 28 | 23 | 16 | 166 |
| 04:00 | 145 | 16 | 30 | 17 | 208 |
| 05:00 | 255 | 68 | 50 | 14 | 387 |
| 06:00 | 881 | 170 | 105 | 24 | 1180 |
| 07:00 | 1752 | 275 | 138 | 36 | 2201 |
| 08:00 | 2889 | 289 | 129 | 30 | 3337 |
| 09:00 | 3100 | 362 | 198 | 35 | 3695 |
| 10:00 | 2725 | 397 | 206 | 53 | 3381 |
| 11:00 | 2593 | 436 | 218 | 54 | 3301 |
| 12:00 | 2645 | 399 | 218 | 56 | 3318 |
| 13:00 | 2538 | 350 | 168 | 47 | 3103 |
| 14:00 | 2792 | 328 | 208 | 44 | 3372 |
| 15:00 | 3102 | 308 | 159 | 36 | 3605 |
| 16:00 | 3999 | 239 | 157 | 37 | 4432 |
| 17:00 | 4753 | 217 | 118 | 27 | 5115 |
| 18:00 | 4526 | 206 | 74 | 29 | 4835 |
| 19:00 | 2746 | 127 | 80 | 32 | 2985 |
| 20:00 | 1331 | 69 | 60 | 21 | 1481 |
| 21:00 | 902 | 30 | 53 | 22 | 1007 |
| 22:00 | 733 | 23 | 37 | 11 | 804 |
| 23:00 | 600 | 24 | 25 | 14 | 663 |
| 0:00 | 377 | 8 | 49 | 12 | 446 |
| **Total** | **45769** | **4405** | **2553** | **683** | **53410** |

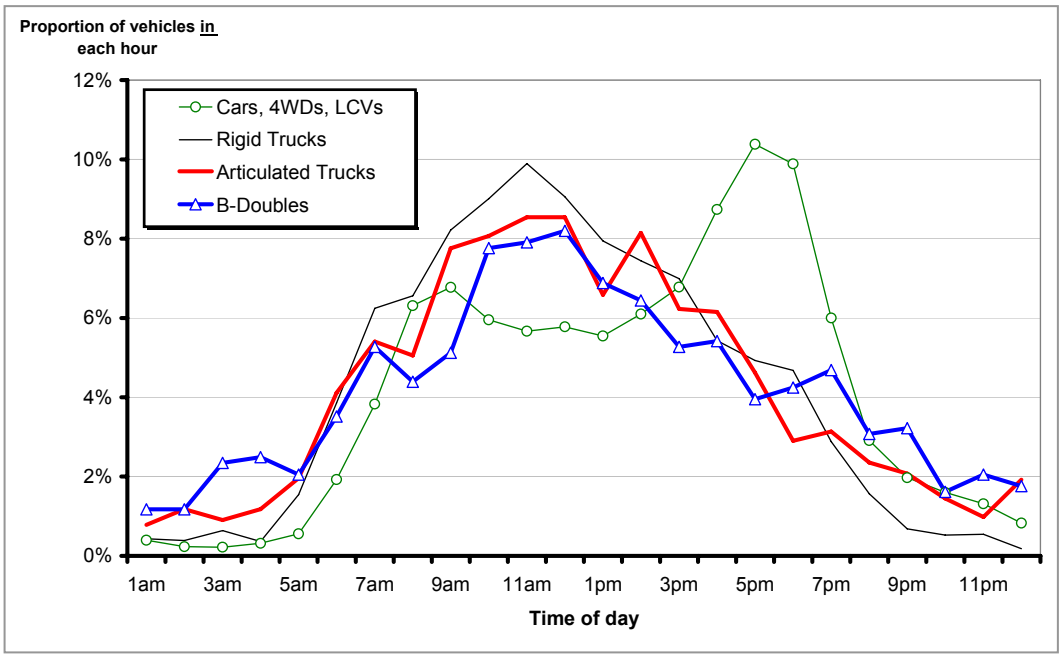


**Figure 7.1 – Distribution throughout the day for each vehicle type**

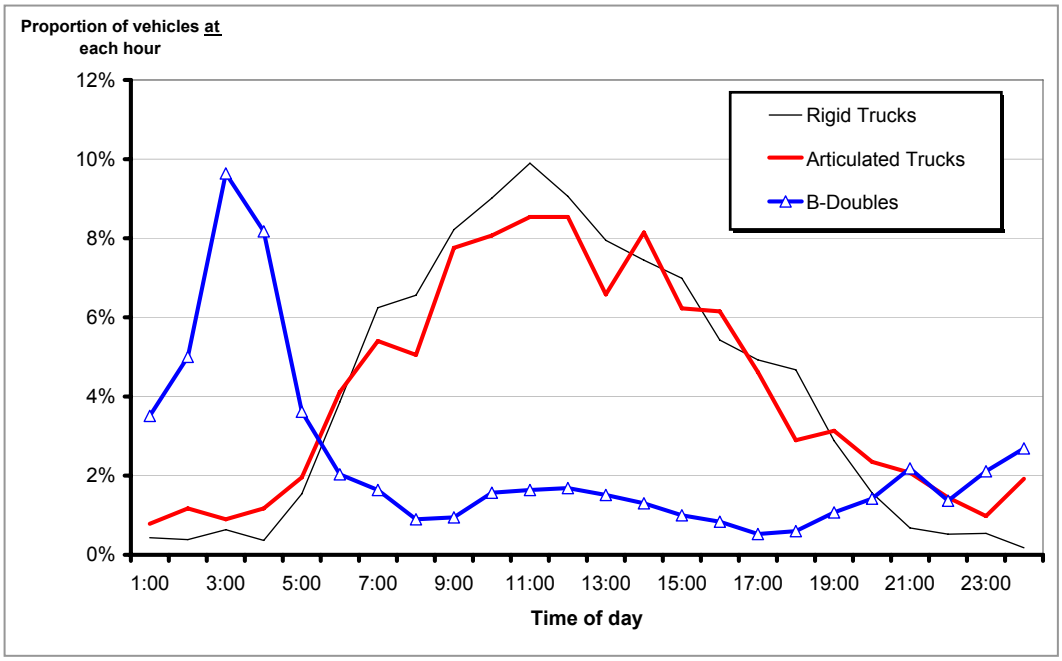


**Figure 7.2 – Variation of the proportion of vehicle types at each hour**

To distinguish between passenger cars and 4WD / LCVs, 80% of those vehicles in Austroads classes 1 and 2 were considered passenger cars. This is a similar proportion to that found in vehicle registration statistics collected by the Australian Bureau of Statistics (ABS 2006).

The proportions of each vehicle type for each hour in this analysis period were averaged to give the baseline proportions presented in Table 7.3.

**Table 7.3 – Proportions of each vehicle type used in the baseline arrival flow characterisation**

| *Vehicle Type* | *Proportion* |
|---|---|
| Passenger Car | 65.0% |
| 4WD/ Light Commercial Vehicle | 16.6% |
| Rigid Truck | 11.1% |
| Articulated Truck | 5.9% |
| B-double | 1.5% |

### 7.2.3 Headway characterisation

The data collected by the automatic traffic counters contained accurate headway information, which was used to characterise the distribution of headways by vehicle type and by lane. These different headway distributions were used in the corridor-level microsimulation model to determine the times at which vehicles enter the corridor. Headways were defined as being from the front axle of the leading vehicle to the front axle of the following vehicle, following the convention used in HCM2000 (Transportation Research Board 2000).

Headway distributions for each vehicle type in each lane were obtained by extracting the headways for the specific vehicle type and lane into a separate spreadsheet page and sorting them into ascending order. Since the classifier was unable to differentiate between cars, four-wheel drives and LCVs (all appearing as Austroads classes 1 and 2), the headway data for these two vehicle types were combined. A uniformly-spaced sequence of numbers ranging from zero to one was plotted against these sorted headways to give the cumulative probability distribution function of the headways.

Figure 7.3 shows the measured headway distributions for the four vehicle types in one of the surveyed lanes, using data from the daytime inter-peak period (9:00am to 3:00pm). Headways were generally greater for the larger vehicle types, with the median headway for B-doubles being approximately twice that of short vehicles.

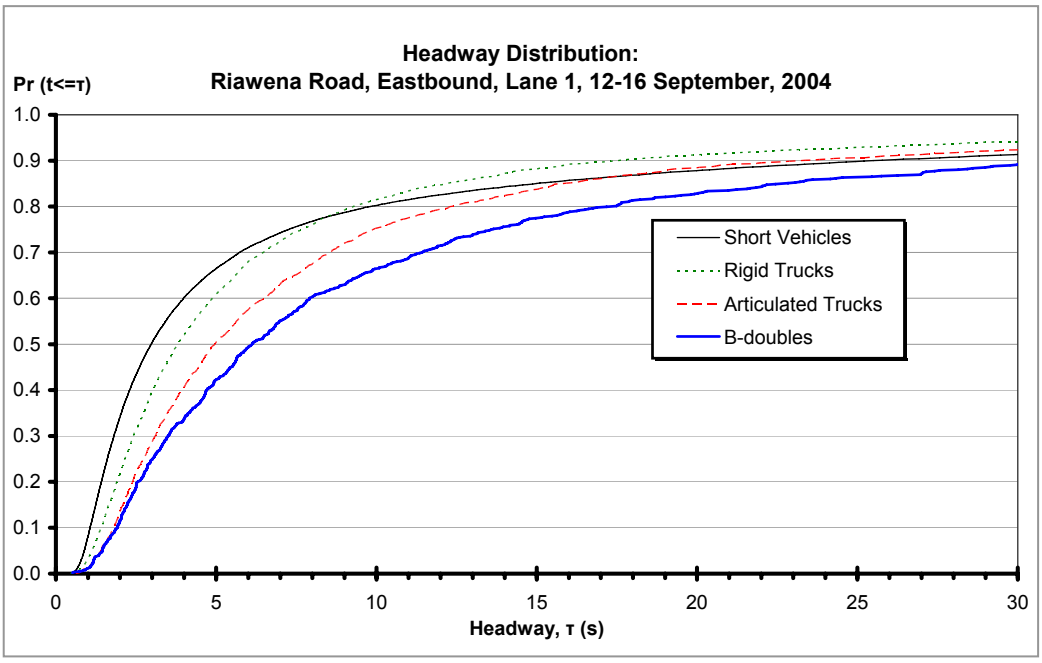


**Figure 7.3 – Cumulative probability distribution of headways for each vehicle type in lane 1**

As described in an earlier chapter, Cowan's M3 model (Cowan 1975) was considered to be the most appropriate formulation for the headway distribution model. However, in recognition of the differences in the measured headway distributions found in Figure 7.3, different model parameters would be determined for each of the four distinguishable vehicle types (combining cars with 4WDs and LCVs).

The parameters for the headway distribution functions were obtained by minimising the sum of the squares of the differences between the measured and modelled headways. Microsoft Excel's Solver function was used to minimise this error term by varying the parameters $\alpha$ and $\lambda$. Alternative methods exist for estimating headway distribution parameters in general traffic flow, including a maximum likelihood method used by Troutbeck (1997). Most of these estimate the proportion of unbunched vehicles (parameter $\alpha$ in Cowan's model) from the flow rate (for example, Akçelik 2006). This method would not be suitable for calculating vehicle type-specific headway distributions since the flow rate is a characteristic of the traffic stream in general, and not directly of the composition of vehicle types within the stream.

For single lane data the minimum headway, Δ, was held constant at 2 seconds, corresponding to the value recommended (Sullivan and Troutbeck 1994) for a multi-lane arterial road. A minimum headway of 1 second was used when both lanes were considered. Table 7.4 shows the model parameters used to minimise the root-mean-square error term (the square root of the sum of the squares of the differences between measured and modelled results divided by the number of terms being summed over). Figure 7.4 shows the headway distribution functions for each vehicle type in lane 1.

**Table 7.4 – Cowan's M3 model parameters for each vehicle type and lane**

*Daytime inter-peak data (9:00am-3:00pm)*

| *Headway Data* | *Count* | *Model Parameter* | | | *RMS Error* |
|---|---|---|---|---|---|
| | | *Δ (s)* | *α* | *λ ($s^{-1}$)* | |
| ***Lane 1*** | | | | | |
| Short Vehicle | 28,042 | 2 | 0.553 | 0.152 | 0.137 |
| Rigid Truck | 3,021 | 2 | 0.741 | 0.195 | 0.064 |
| Articulate Truck | 2,130 | 2 | 0.825 | 0.153 | 0.039 |
| B-double | 643 | 2 | 0.831 | 0.109 | 0.031 |
| **All vehicle types** | **33923** | **2** | **0.592** | **0.155** | **0.120** |
| ***Lane 2*** | | | | | |
| Short Vehicle | 30,150 | 2 | 0.461 | 0.147 | 0.190 |
| Rigid Truck | 2,067 | 2 | 0.667 | 0.158 | 0.093 |
| Articulate Truck | 771 | 2 | 0.746 | 0.118 | 0.058 |
| B-double | 148 | 2 | 0.767 | 0.138 | 0.020 |
| **All vehicle types** | **33173** | **2** | **0.481** | **0.145** | **0.179** |
| ***Both Lanes*** | | | | | |
| Short Vehicle | 58,192 | 1 | 0.564 | 0.432 | 0.140 |
| Rigid Truck | 5088 | 1 | 0.621 | 0.334 | 0.114 |
| Articulate Truck | 2091 | 1 | 0.679 | 0.224 | 0.084 |
| B-double | 791 | 1 | 0.710 | 0.168 | 0.060 |
| **All vehicle types** | **67096** | **1** | **0.572** | **0.395** | **0.135** |

The proportion of unbunched vehicles (parameter α) is higher for the larger vehicles, indicating that they are less likely to be travelling at very short headways behind the vehicle in front. This corresponds to these vehicles being more likely to be at front of a platoon of vehicles.

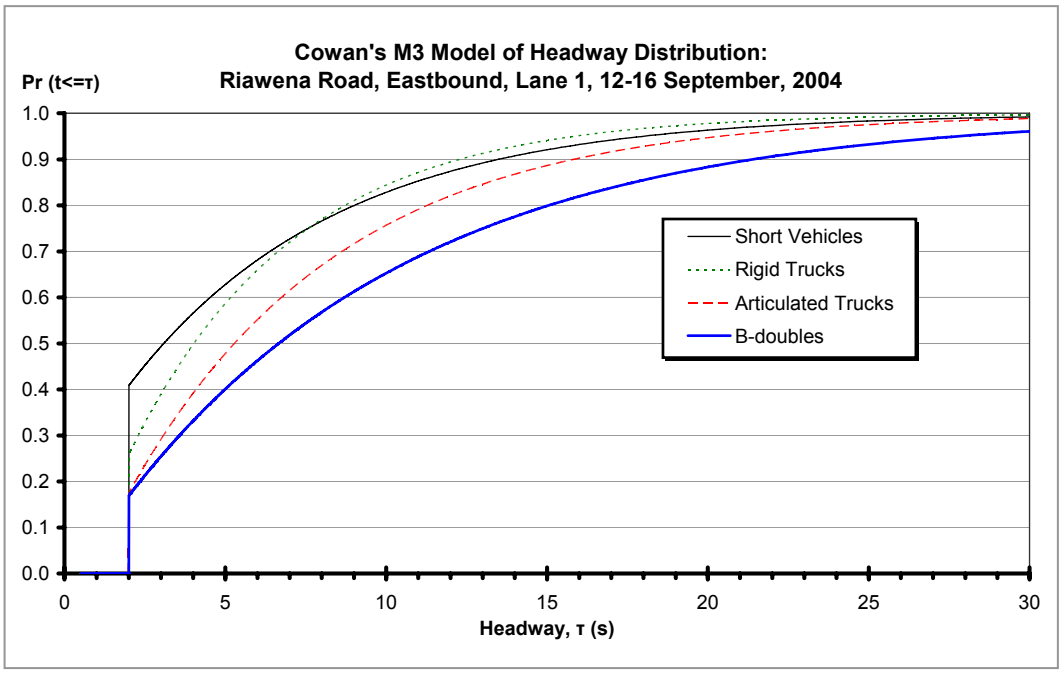


**Figure 7.4 – Cowan's M3 model of headway distribution for each vehicle type in lane 1 (Δ = 2 s)**

### 7.2.4 Following behaviour of different vehicle types

The automatic traffic counter data was also used to estimate the probability of a vehicle type occurring after another vehicle type. This probability distribution was considered for use in the corridor microsimulation model to determine the next vehicle type to be generated based on the vehicle type previously generated in the same lane.

Table 7.5: shows that heavy vehicles have greater likelihood of being followed by another heavy vehicle than the proportion of heavy vehicles in the general population. For example, 9.2% of articulated trucks were being followed by another articulated truck, whereas there were only 4.5% of articulated trucks in the sample population.

This probability table would be able to be used in a Markov chain application within the vehicle generation part of the simulation model in order to determine the type of each vehicle being generated based on the type of the vehicle preceding it.

**Table 7.5 – Following behaviour of different vehicle types**

| *Following Vehicle Type* | *Leading Vehicle Type* | | | | *All Vehicle Types* |
|---|---|---|---|---|---|
| | *Short Vehicle* | *Rigid Truck* | *Articulated Truck* | *B-double* | |
| Short Vehicle | 49 345 (87.7%) | 4 013 (79.3%) | 2 233 (75.9%) | 606 (76.9%) | 56 249 (86.4%) |
| Rigid Truck | 3 996 (7.1%) | 602 (11.9%) | 361 (12.3%) | 87 (11.0%) | 5 058 (7.8%) |
| Articulated Truck | 2 246 (4.0%) | 351 (6.9%) | 270 (9.2%) | 69 (8.8) | 2 941 (4.5%) |
| B-double | 609 (1.1%) | 76 (1.5%) | 75 (2.6%) | 26 (3.3%) | 788 (1.2%) |
| **Total** | **56 249 (100%)** | **5 058 (100%)** | **2 941 (100%)** | **788 (100%)** | **65 110 (100%)** |

### 7.2.5 Speed characterisation

The means and standard deviations of the speeds recorded by the automatic traffic counter for each vehicle type in each lane are shown in Table 7.6.

**Table 7.6 – Mean and standard deviation of speeds by vehicle type, all times**

*Data from all times of day, 12-16/09/2004*

| *Vehicle Type* | *Lane 1* | *Lane 2* | *Either Lane* |
|---|---|---|---|
| Short Vehicle | 75.8 ± 8.3 (n=27063) | 77.0 ± 8.5 (n=29186) | 76.4 ± 8.4 |
| Rigid Truck | 72.7 ± 8.0 (n=3004) | 73.9 ± 8.2 (n=2054) | 73.2 ± 8.1 |
| Articulated Truck | 73.1 ± 7.5 (n=2174) | 73.8 ± 8.7 (n=767) | 73.3 ± 7.9 |
| B-double | 72.8 ± 7.5 (n=641) | 73.2 ± 9.8 (n=147) | 72.9 ± 7.9 |
| **All classifiable vehicles** | **75.3 ± 8.2 (n=32882)** | **76.7 ± 8.4 (n=32154)** | **76.0 ± 8.3** |

*Notes: values are mean ± standard deviation (n=number of vehicles)*

*the number of vehicles in both lanes can be obtained by summing over the two lanes*

Two-sample t-tests were conducted to determine the significance of the differences in speeds of the different vehicle types and the different lanes. As shown in Table 7.7, the differences in speeds are statistically significant at the 5% significance level for comparisons between short vehicles and other vehicle types but not between the other vehicle types. Speed differences between lanes for the same vehicle type (excluding B-doubles) are also statistically significant at this level.

**Table 7.7 – Statistical comparisons of the speeds recorded by the Vehdat traffic counter, all times**

*Data from all times of day, 12-16/09/2004*
*Two-sample t-tests assuming unequal variances, $H_0$: $\mu_1 - \mu_2 = 0$ vs $H_1$: $\mu_1 - \mu_2 \neq 0$, $\alpha = 0.05$*

| *Vehicle Type* | *Lane* | *Mean* | *Std Dev.* | *Count* | *t Stat* | *P(T<=\|t\|)* | *Conclusion* |
|---|---|---|---|---|---|---|---|
| Short Vehicle | Either | 76.4 | 8.4 | 56249 | 26.83 | 6.0E-150 | **Reject Ho** |
| Rigid Truck | Either | 73.2 | 8.1 | 5058 | | | |
| Short Vehicle | Either | 76.4 | 8.4 | 56249 | 20.68 | 2.0E-89 | **Reject Ho** |
| Articulated Truck | Either | 73.3 | 7.9 | 2941 | | | |
| Short Vehicle | Either | 76.4 | 8.4 | 56249 | 12.34 | 3.5E-32 | **Reject Ho** |
| B-double | Either | 72.9 | 7.9 | 788 | | | |
| Rigid Truck | Either | 73.2 | 8.1 | 5058 | -0.54 | 5.9E-01 | Accept Ho |
| Articulated Truck | Either | 73.3 | 7.9 | 2941 | | | |
| Rigid Truck | Either | 73.2 | 8.1 | 5058 | 0.99 | 3.2E-01 | Accept Ho |
| B-double | Either | 72.9 | 7.9 | 788 | | | |
| Articulated Truck | Either | 73.3 | 7.9 | 2941 | 1.26 | 2.1E-01 | Accept Ho |
| B-double | Either | 72.9 | 7.9 | 788 | | | |
| Short Vehicle | 1 | 75.8 | 8.3 | 27063 | -16.93 | 3.59E-64 | **Reject Ho** |
| Short Vehicle | 2 | 77.0 | 8.5 | 29186 | | | |
| Rigid Truck | 1 | 72.7 | 8.0 | 3004 | -5.16 | 2.55E-07 | **Reject Ho** |
| Rigid Truck | 2 | 73.9 | 8.2 | 2054 | | | |
| Articulated Truck | 1 | 73.1 | 7.5 | 2174 | -1.98 | 0.048 | **Reject Ho** |
| Articulated Truck | 2 | 73.8 | 8.7 | 767 | | | |
| B-double | 1 | 72.8 | 7.5 | 641 | -0.46 | 0.064 | Accept Ho |
| B-double | 2 | 73.2 | 9.8 | 147 | | | |

It should be noted that the counter-classifier was located immediately downstream of a slight downgrade after a railway overpass. Vehicles (particularly heavy vehicles) are likely to have been travelling slightly faster than on an equivalent section without any grade.

The posted speed limit on this section of the BUC was 80 km/h, generally less than one standard deviation above the mean for all vehicle types.

Referring back to Figure 7.1, trucks were less prevalent during the morning and evening peak periods, when congestion is higher and speeds are generally lower. Thus, a simple average over the entire data set may be masking a difference in speeds between vehicle types.

To determine this, it is necessary to compare the speeds of different vehicle types under the same traffic conditions, i.e. in same time period.

This analysis was repeated using only data records from 9:00am to 3:00pm, the period identified earlier in this chapter when trucks numbers are highest. The revised mean and standard deviations of the speeds for each vehicle type are shown in Table 7.8.

**Table 7.8 – Mean and standard deviation of speeds by vehicle type, daytime inter-peak period**

*Data from 9:00am to 3:00pm each day, 12-16/09/2004*

| *Vehicle Type* | *Lane 1* | *Lane 2* | *Either lane* |
|---|---|---|---|
| Short Vehicle | 75.5 ± 7.4 (n=9229) | 76.4 ± 7.2 (n=10719) | 76.0 ± 7.3 |
| Rigid Truck | 72.3 ± 7.3 (n=1480) | 74.1 ± 7.6 (n=927) | 73.0 ± 7.5 |
| Articulated Truck | 72.6 ± 7.2 (n=920) | 73.0 ± 7.9 (n=340) | 72.7 ± 7.4 |
| B-double | 71.6 ± 7.4 (n=250) | 73.2 ± 9.5 (n=62) | 71.9 ± 7.9 |
| **All classifiable vehicles** | **74.8 ± 7.4 (n=11879)** | **76.1 ± 7.2 (n=12048)** | **75.5 ± 7.3** |

*Notes: values are mean ± standard deviation (n=number of vehicles)*

*the number of vehicles in both lanes can be obtained by summing over the two lanes*

Table 7.9 shows the results of the two-sample t-tests conducted to determine the significance of the speed differences indicated in Table 7.8. The differences in speeds between short vehicles and the other vehicle types are statistically significant at the 5% level, as those between rigid trucks and B-doubles. Speed differences are significant between lanes for all vehicle types except B-doubles.

**Table 7.9 – Statistical comparisons of the speeds recorded by the Vehdat traffic counter, daytime inter-peak period**

*Data from 9:00am to 3:00pm each day, 12-16/09/2004*
*Two-sample t-tests assuming unequal variances, $H_0$: $\mu_1 - \mu_2 = 0$ vs $H_1$: $\mu_1 - \mu_2 \neq 0$, $\alpha = 0.05$*

| *Vehicle Type* | *Lane* | *Mean* | *Std Dev.* | *Count* | *t Stat* | *P(T<=\|t\|)* | *Conclusion* |
|---|---|---|---|---|---|---|---|
| Short Vehicle | Either | 76.0 | 7.3 | 19948 | 18.59 | 4.4E-73 | **Reject Ho** |
| Rigid Truck | Either | 73.0 | 7.5 | 2407 | | | |
| Short Vehicle | Either | 76.0 | 7.3 | 19948 | 15.36 | 2.1E-49 | **Reject Ho** |
| Articulated Truck | Either | 72.7 | 7.4 | 1260 | | | |
| Short Vehicle | Either | 76.0 | 7.3 | 19948 | 9.11 | 9.6E-18 | **Reject Ho** |
| B-double | Either | 71.9 | 7.9 | 312 | | | |
| Rigid Truck | Either | 73.0 | 7.5 | 2407 | 1.16 | 0.25 | Accept Ho |
| Articulated Truck | Either | 72.7 | 7.4 | 1260 | | | |
| Rigid Truck | Either | 73.0 | 7.5 | 2407 | 2.33 | 0.02 | **Reject Ho** |
| B-double | Either | 71.9 | 7.9 | 312 | | | |
| Articulated Truck | Either | 72.7 | 7.4 | 1260 | 1.62 | 0.11 | Accept Ho |
| B-double | Either | 71.9 | 7.9 | 312 | | | |
| Short Vehicle | 1 | 75.8 | 8.3 | 27063 | -16.93 | 3.6E-64 | **Reject Ho** |
| Short Vehicle | 2 | 77.0 | 8.5 | 29186 | | | |
| Rigid Truck | 1 | 72.7 | 8.0 | 3004 | -5.16 | 2.6E-07 | **Reject Ho** |
| Rigid Truck | 2 | 73.9 | 8.2 | 2054 | | | |
| Articulated Truck | 1 | 73.1 | 7.5 | 2174 | -1.98 | 0.048 | **Reject Ho** |
| Articulated Truck | 2 | 73.8 | 8.7 | 767 | | | |
| B-double | 1 | 72.8 | 7.5 | 641 | -0.46 | 0.64 | Accept Ho |
| B-double | 2 | 73.2 | 9.8 | 147 | | | |

The average pace of B-doubles across both lanes can be calculated to be 50.1 s/km. This would lead to a 30 second travel time difference over the 11.3 length of the Brisbane Urban Corridor if these speeds could be maintained.

Speeds are generally higher in lane 2 (the offside or right lane) than in lane 1 (the kerbside or left lane), corresponding to a preference for overtaking on the offside.

## 7.3 Travel Times and Stop Rates

The travel times and stop rates of the different vehicle types are estimated from the GPS track logs recorded from a closely following "chase car".

### 7.3.1 Analysis method

The GPS track logs were segmented into a number of "trips", each corresponding to a single pass in either direction between two imaginary cordon lines at the eastern and western ends of the corridor.

The following performance measures were determined for each of the 63 eastbound and 63 westbound trips:

- The **travel time** between the two cordon lines
- The **average speed** between the two cordon lines (the distance travelled was relatively consistent between trips at 10,993 m ± 8 m eastbound and 11,005 m ± 13 m westbound)
- The **number of stops** (when speeds dropped below 5 km/h after having been above 25 km/h – this eliminated multiple stops when in a queue)
- The **stopped time** (when speed is below 5 km/h)
- The **vehicle type** (Car, 4WD, LCV, Rigid truck, Artic. truck, B-double)
- The **direction** of travel (eastbound / westbound)

Note that it was possible to distinguish between 4WDs and LCVs in this data, whereas other data sources have them aggregated together.

Figure 7.5 shows the average speeds of each run in the eastbound direction, with different symbols for each vehicle type. Results for the westbound direction are similar. Speeds are lower for the few runs conducted during the afternoon peak period, nominally from 3:00pm to 6:00pm. The vehicles followed during this period were all light vehicles or rigid trucks; there were few articulated trucks in the traffic during this period (indicted by the dashed rectangle in the figure).

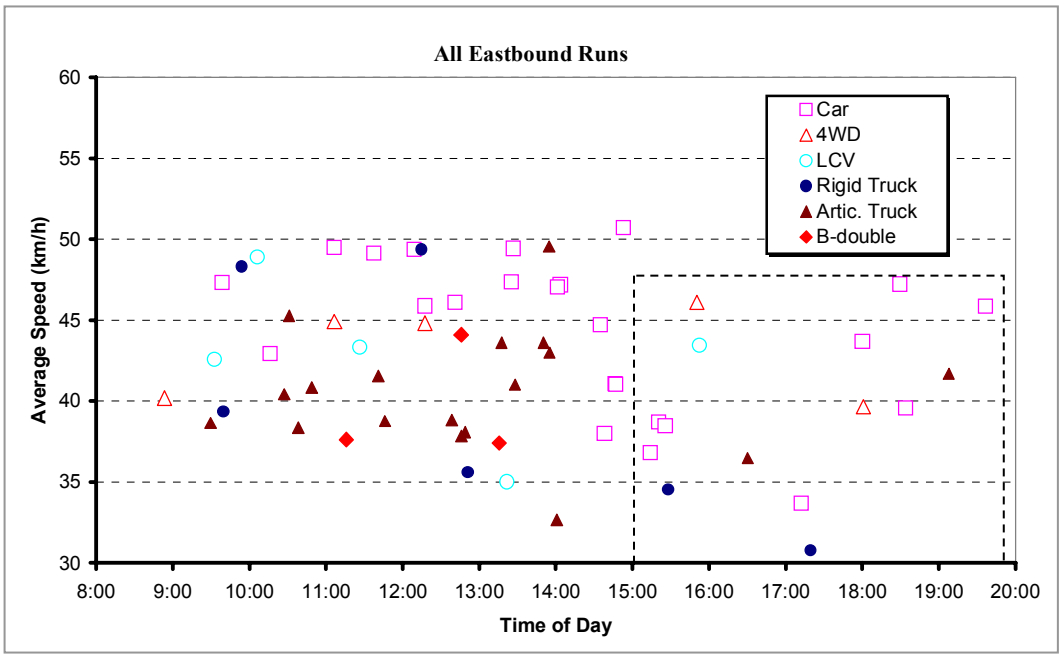


**Figure 7.5 – Variation in average speed with time for different vehicle types**

Runs conducted during the afternoon peak period were excluded from the analysis, since they would lead to a lower estimate of the average speeds of those vehicle types that were more prevalent in those times. Hence, only data collected in the daytime inter-peak period (9:00am to 3:00pm) was included in the analysis.

### 7.3.2 Results

Table 7.10 shows the number of trips conducted in each direction for each vehicle type in the day time inter-peak period (9:00am to 3:00 pm). The proportion of trips following each vehicle type is similar for the two directions, except for an inexplicable difference between the number of trips behind articulated trucks and B-doubles in each direction.

Table 7.11 shows the times taken by each vehicle type to travel between the two ends of the corridor, being followed by the chase car. There is little difference between the travel times of cars, 4wds and LCVs. Articulated trucks and B-doubles had comparable travel times, despite the greater mass of the B-doubles.

Any differences in travel times between the different vehicle types are of the same order of magnitude as the standard deviations of any of the vehicle types.

**Table 7.10 – Numbers of trips recorded in each direction for each vehicle type**

| | *Number of Trips* | |
|---|---|---|
| *Vehicle Type* | *Eastbound (towards Gateway Mwy)* | *Westbound (towards Ipswich Mwy)* |
| Car | 22 | 16 |
| 4WD | 3 | 5 |
| LCV | 5 | 4 |
| Rigid Truck | 4 | 8 |
| Articulated Truck | 17 | 7 |
| B-double | 3 | 10 |
| **All vehicle types** | **54** | **50** |

**Table 7.11 – Travel times recorded in each direction for each vehicle type**

| | *Mean ± standard deviation of travel time (mm:ss)* | |
|---|---|---|
| *Vehicle Type* | *Eastbound (towards Gateway Mwy)* | *Westbound (towards Ipswich Mwy)* |
| Car | 15:24 ± 02:21 | 14:06 ± 01:52 |
| 4WD | 15:21 ± 01:06 | 14:57 ± 01:09 |
| LCV | 15:39 ± 01:58 | 15:13 ± 02:05 |
| Rigid Truck | 15:35 ± 02:30 | 15:35 ± 02:02 |
| Articulated Truck | 16:18 ± 01:30 | 16:48 ± 03:13 |
| B-double | 16:43 ± 01:32 | 15:40 ± 03:08 |
| **All vehicle types** | **15:47 ± 01:58** | **15:12 ± 02:26** |

Table 7.12 shows the results of the statistical comparisons of the travel times for different vehicle types in each direction. The differences in travel times between vehicle types were not statistically significant at a level of significance of 0.05 for both the eastbound and westbound (not shown) direction. Similarly, the differences between travel times in the eastbound and westbound direction were not statistically significant for all vehicle types.

**Table 7.12 – Statistical comparison of the travel times recorded in each direction for each vehicle type**

*Two-sample t-tests assuming unequal variances, $H_0$: $\mu_1 - \mu_2 = 0$ vs $H_1$: $\mu_1 - \mu_2 \neq 0$, $\alpha = 0.05$*

| *Vehicle Type* | *Direction* | *Mean* | *Std Dev.* | *Count* | *t Stat* | *P(T<=\|t\|)* | *Conclusion* |
|---|---|---|---|---|---|---|---|
| Car | East | 924 | 141 | 22 | 0.06 | 0.95 | Accept Ho |
| 4WD | East | 921 | 66 | 3 | | | |
| Car | East | 924 | 141 | 22 | -0.25 | 0.81 | Accept Ho |
| LCV | East | 939 | 118 | 5 | | | |
| Car | East | 924 | 141 | 22 | -0.14 | 0.90 | Accept Ho |
| Rigid Truck | East | 935 | 150 | 4 | | | |
| Car | East | 924 | 141 | 22 | -1.45 | 0.15 | Accept Ho |
| Articulated Truck | East | 978 | 90 | 17 | | | |
| Car | East | 924 | 141 | 22 | -1.29 | 0.29 | Accept Ho |
| B-double | East | 1003 | 92 | 3 | | | |
| Car | East | 924 | 141 | 22 | 1.90 | 0.07 | Accept Ho |
| Car | West | 846 | 112 | 16 | | | |
| 4WD | East | 921 | 66 | 3 | 0.49 | 0.65 | Accept Ho |
| 4WD | West | 897 | 69 | 5 | | | |
| LCV | East | 939 | 118 | 5 | 0.32 | 0.76 | Accept Ho |
| LCV | West | 913 | 125 | 4 | | | |
| Rigid Truck | East | 935 | 150 | 4 | 0.00 | 1.00 | Accept Ho |
| Rigid Truck | West | 935 | 122 | 8 | | | |
| Articulated Truck | East | 978 | 90 | 17 | -0.39 | 0.71 | Accept Ho |
| Articulated Truck | West | 1008 | 193 | 7 | | | |
| B-double | East | 1003 | 92 | 3 | 0.79 | 0.45 | Accept Ho |
| B-double | West | 940 | 188 | 10 | | | |

Table 7.13 shows the average speeds of each vehicle type travelling between the two ends of the corridor in front of the chase car. Since average speed is determined from the (fixed) distance between the cordons and the travel time described above, the conclusions are similar to those from the previous table.

**Table 7.13 – Average speeds recorded in each direction for each vehicle type**

| | *Mean ± standard deviation of average speed (km/h)* | |
|---|---|---|
| *Vehicle Type* | *Eastbound (towards Gateway Mwy)* | *Westbound (towards Ipswich Mwy)* |
| Car | 43.68 ± 5.69 | 47.52 ± 5.57 |
| 4WD | 43.13 ± 3.00 | 44.36 ± 3.61 |
| LCV | 42.65 ± 4.96 | 43.97 ± 5.67 |
| Rigid Truck | 43.17 ± 6.74 | 43.04 ± 5.73 |
| Articulated Truck | 40.81 ± 3.71 | 40.64 ± 8.09 |
| B-double | 39.70 ± 3.80 | 43.68 ± 8.68 |
| **All vehicle types** | **42.39 ± 4.93** | **44.47 ± 6.69** |

Table 7.14 shows the average and standard deviation of the number of stops recorded when following each vehicle type in either direction. The low stopping rate of eastbound B-doubles were confirmed by an examination of their trajectories, which indicated that they travelled slowly when approaching the back of queue at an intersection to avoid having to come to a complete stop.

**Table 7.14 – Number of stops recorded in each direction for each vehicle type**

| | *Mean ± standard deviation of number of stops* | |
|---|---|---|
| *Vehicle Type* | *Eastbound (towards Gateway Mwy)* | *Westbound (towards Ipswich Mwy)* |
| Car | 6.50 ± 2.54 | 4.81 ± 1.76 |
| 4WD | 6.00 ± 3.00 | 5.60 ± 2.51 |
| LCV | 6.00 ± 2.12 | 5.00 ± 1.41 |
| Rigid Truck | 5.75 ± 1.71 | 5.00 ± 2.20 |
| Articulated Truck | 5.35 ± 2.18 | 6.00 ± 2.31 |
| B-double | 3.67 ± 1.53 | 5.20 ± 2.66 |
| **All vehicle types** | **5.85 ± 2.33** | **5.18 ± 2.10** |

Table 7.15 shows the results of two-sample t-tests of the statistical significance of these stop rates. Generally the differences in stop rates were not statistically significant at the 0.05 level of significance, except for comparing cars and B-doubles in the eastbound direction and comparing eastbound and westbound cars.

**Table 7.15 – Statistical comparison of the number of stops recorded in each direction for each vehicle type**

*Two-sample t-tests assuming unequal variances, $H_0$: $\mu_1 - \mu_2 = 0$ vs $H_1$: $\mu_1 - \mu_2 \neq 0$, $\alpha = 0.05$*

| *Vehicle Type* | *Direction* | *Mean* | *Std Dev.* | *Count* | *t Stat* | *P(T<=\|t\|)* | *Conclusion* |
|---|---|---|---|---|---|---|---|
| Car | East | 6.50 | 2.54 | 22 | 0.28 | 0.81 | Accept Ho |
| 4WD | East | 6.00 | 3.00 | 3 | | | |
| Car | East | 6.50 | 2.54 | 22 | 0.46 | 0.66 | Accept Ho |
| LCV | East | 6.00 | 2.12 | 5 | | | |
| Car | East | 6.50 | 2.54 | 22 | 0.79 | 0.46 | Accept Ho |
| Rigid Truck | East | 5.70 | 1.71 | 4 | | | |
| Car | East | 6.50 | 2.54 | 22 | 1.59 | 0.12 | Accept Ho |
| Articulated Truck | East | 5.30 | 2.18 | 17 | | | |
| Car | East | 6.50 | 2.54 | 22 | 2.80 | 0.05 | **Reject Ho** |
| B-double | East | 3.60 | 1.53 | 3 | | | |
| Car | East | 6.50 | 2.54 | 22 | 2.44 | 0.02 | **Reject Ho** |
| Car | West | 4.80 | 1.76 | 16 | | | |
| 4WD | East | 6.00 | 3.00 | 3 | 0.19 | 0.86 | Accept Ho |
| 4WD | West | 5.60 | 2.51 | 5 | | | |
| LCV | East | 6.00 | 2.12 | 5 | 0.85 | 0.43 | Accept Ho |
| LCV | West | 5.00 | 1.41 | 4 | | | |
| Rigid Truck | East | 5.70 | 1.71 | 4 | 0.61 | 0.56 | Accept Ho |
| Rigid Truck | West | 5.00 | 2.20 | 8 | | | |
| Articulated Truck | East | 5.30 | 2.18 | 17 | -0.69 | 0.51 | Accept Ho |
| Articulated Truck | West | 6.00 | 2.31 | 7 | | | |
| B-double | East | 3.60 | 1.53 | 3 | -1.31 | 0.24 | Accept Ho |
| B-double | West | 5.20 | 2.66 | 10 | | | |

This higher stop rate of cars than B-doubles in the eastbound direction is likely to be due to the inclusion of surveys conducted in the afternoon peak period. The average stop rates of cars are likely to be increased by including peak period , whilst the average stop rates of trucks are less likely to be affected since they are not as prevalent in peak traffic.

Table 7.16 shows the distribution of the stopped time recorded by the chase car following each vehicle type. Stopped time is defined as the sum of the times with a speed of less than 5 km/h. Two-sample t-tests were conducted, finding that none of the differences in mean stopped times for different vehicle types or different directions were statistically significant.

**Table 7.16 – Stopped time recorded in each direction for each vehicle type**

| | *Mean ± standard deviation of stopped time (mm:ss)* | |
|---|---|---|
| *Vehicle Type* | *Eastbound (towards Gateway Mwy)* | *Westbound (towards Ipswich Mwy)* |
| Car | 03:06 ± 01:39 | 02:37 ± 01:16 |
| 4WD | 03:07 ± 01:15 | 02:41 ± 01:33 |
| LCV | 02:58 ± 01:23 | 02:44 ± 02:14 |
| Rigid Truck | 03:05 ± 01:39 | 03:05 ± 01:28 |
| Articulated Truck | 02:48 ± 00:57 | 03:34 ± 02:08 |
| B-double | 03:11 ± 01:16 | 02:56 ± 01:54 |
| **All vehicle types** | **03:00 ± 01:20** | **02:54 ± 01:37** |

### 7.3.3 Analysis

Generally, few differences were found between the different vehicle types for any of the performance measures derived from the chase car survey.

It was expected that the lower acceleration capability of LFVs and trucks in general would have contributed to a lower travel time and hence slower average speed over the corridor, but this was not generally supported by the travel time data.

It was found that during the inter-peak period, traffic as a whole is moving along the corridor in a consistent, relatively homogeneous fashion.

## 7.4 Intersection Status Data

The instantaneous status of all of the intersections along the test corridor was recorded by STREAMS, Queensland Main Roads' integrated traffic management system. This information was used to validate the chase car data, by checking to ensure that the recorded trajectories of the chase car indicated appropriate behaviour around each intersection.

This is illustrated in Figure 7.6, showing the trajectory diagram recorded by the GPS unit overlaid on the corridor timing diagram recorded by STREAMS. The trajectory of the chase car, and of the articulated truck that it was following, can be seen only to pass through each intersection on a green signal.

Figure 7.7 shows the speed of the chase car plotted against the distance that it had travelled. The locations of each intersection can be identified, as can whether of not the vehicle stopped at the intersection. The cumulative number of stops is plotted on the right y-axis. This figure is useful in showing *where* the vehicle stopped, but it does not show for *how long* the vehicle was stopped.

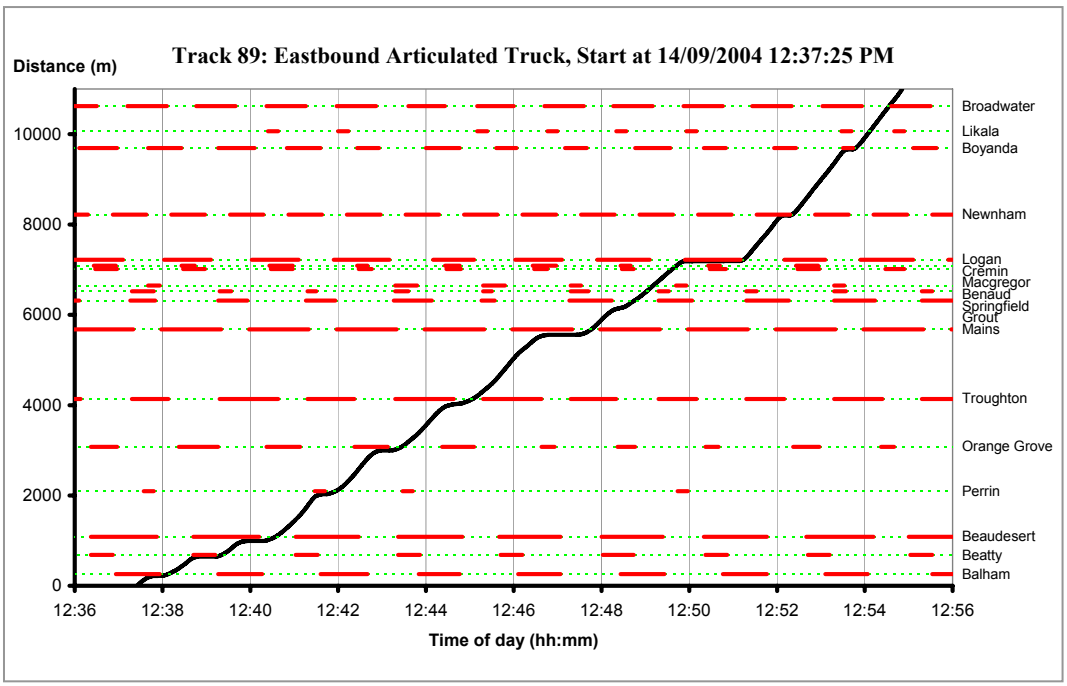


**Figure 7.6 – Vehicle trajectory (GPS data) superimposed on the corridor timing diagram**

The progression of the chase car through intersections on the corridor was checked using this method for all 126 runs, finding that it always passed through the intersections on a green signal.

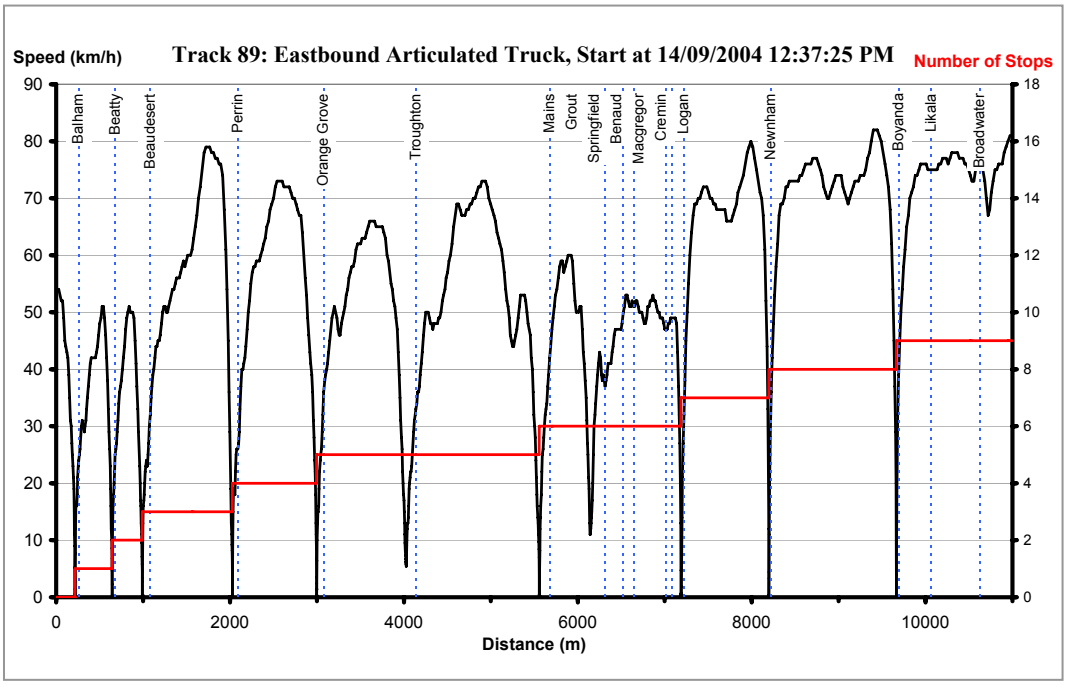


**Figure 7.7 – Typical speed and stopping profile from GPS data, corresponding to Figure 7.6**

## 7.5 Acceleration Profiles

### 7.5.1 Method

The 126 trips obtained from the GPS track logs were examined to give a number of representative samples of vehicles departing from the front of queues at signalised intersections along the test corridor. These were used to characterise the acceleration profiles for each vehicle and then for each vehicle type.

The following method was used:

1) For each instance of a vehicle accelerating uninterrupted from rest, such as would occur when departing from the front of a queue at a signalised intersection, determine the initial speed, $v_0$, and the time, $T$, distance, $x_T$, and speed, $v_T$, when acceleration ceases.

2) Determine the average grade that the acceleration was conducted on, by dividing the difference in elevations at the start and end of the acceleration by the distance travelled, $x_T$.

3) Fit a linearly decreasing acceleration model of the form given in Equation 7.1, which passes through the initial and final speeds and distances. This involves the following:

$$a(t) = \hat{\alpha} - \hat{\beta} v(t)/3.6 \qquad \text{Equation 7.1}$$

where $\hat{\alpha}$ is an estimate of the acceleration, $\alpha$, when speed, $v = 0$

$\hat{\beta}$ is an estimate of the rate of decrease of acceleration with speed, $\beta$.

Solve Equation 7.2 and Equation 7.3 (obtained by repeatedly integrating Equation 7.1) simultaneously, matching both the measured speed and distance at the end of the acceleration period:

$$v_T = v_0 \exp\left(-\hat{\beta}T\right) - 3.6\frac{\hat{\alpha}}{\hat{\beta}}\left[1 - \exp\left(-\hat{\beta}T\right)\right] \qquad \text{Equation 7.2}$$

$$x_T = \frac{\hat{\alpha}}{\hat{\beta}} T + \left( \frac{\hat{\alpha}}{\hat{\beta}} - \frac{v_0}{3.6} \right) \frac{1 - \exp\left(-\hat{\beta} T\right)}{\hat{\beta}} \qquad \text{Equation 7.3}$$

Equation 7.2 can be re-expressed to give $\hat{\alpha}$, as shown in Equation 7.4.

$$\hat{\alpha} = \frac{\left[ v_T - v_0 \exp\left(-\hat{\beta} T\right) \right] \hat{\beta}}{\left[ 1 - \exp\left(-\hat{\beta} T\right) \right] 3.6} \qquad \text{Equation 7.4}$$

Equation 7.3 can be re-expressed as an equation that may be used to find $\hat{\beta}$, as shown in Equation 7.5. Because of the indeterminate nature of this equation, $\hat{\beta}$ can be found using a numerical solver such as Microsoft Excel's Goal Seek command.

$$x_T - \frac{\hat{\alpha}}{\hat{\beta}} T - \left( \frac{\hat{\alpha}}{\hat{\beta}} - \frac{v_0}{3.6} \right) \frac{1 - \exp\left(-\hat{\beta} T\right)}{\hat{\beta}} \Rightarrow 0 \qquad \text{Equation 7.5}$$

4) Using the estimated model parameters derived above ($\hat{\alpha}$ and $\hat{\beta}$), for each sample of each vehicle type, determine an estimate of the time ($\hat{T}_{\mathbf{v}}$) and distance ($\hat{X}_{\mathbf{v}}$) taken to accelerate from rest to reach a nominal speed ($\mathbf{v}$) close to the speed limit (say 60 km/h).

$$\hat{T}_{\mathbf{v}} = -\frac{1}{\hat{\beta}} \ln\left( 1 - \frac{\mathbf{v}}{3.6} \frac{\hat{\alpha}}{\hat{\beta}} \right) \qquad \text{Equation 7.6}$$

$$\hat{X}_{\mathbf{v}} = \frac{\hat{\alpha}}{\hat{\beta}} \left[ \hat{T}_{\mathbf{v}} + \frac{1 - \exp\left(-\hat{\beta} \hat{T}_{\mathbf{v}}\right)}{\hat{\beta}} \right] \qquad \text{Equation 7.7}$$

5) Calculate the average time ($\overline{T}_{\mathbf{v}}$) and average distance ($\overline{X}_{\mathbf{v}}$) taken to reach this nominal speed for all vehicles of this type.

$$\overline{T}_{\mathbf{v}} = \sum_{i=1}^{n} \hat{T}_{\mathbf{v}i} \Big/ n \qquad \text{Equation 7.8}$$

$$\bar{X}_{\mathrm{v}} = \sum_{i=1}^{n} \hat{X}_{\mathrm{v}i} \Big/ n \qquad \text{Equation 7.9}$$

Note that the acceleration model (Equation 7.1) has a maximum speed of $v_{\max} = 3.6\ \alpha / \beta$. If the nominated speed exceeds 0.95 $v_{\max}$, then a large or infinite time would be required to reach the nominated speed. These cases should not be included in the average.

6) Repeat step 3), this time using the average time and average distance to reach the nominated speed. This gives the parameters $\alpha$ and $\beta$ for the vehicle type.

$$\alpha = \frac{\mathbf{v}\beta}{\left[1 - \exp\left(-\beta \bar{T}_{\mathrm{v}}\right)\right] 3.6} \qquad \text{Equation 7.10}$$

$$X_{\mathrm{v}} = \frac{\alpha}{\beta}\left[T_{\mathrm{v}} + \frac{1 - \exp\left(-\beta T_{\mathrm{v}}\right)}{\beta}\right] \qquad \text{Equation 7.11}$$

### 7.5.2 Example of applying the acceleration characterisation method

On 1/09/2004, an articulated truck was stopped at the signalised intersection at the corner of Granard Road and Beaudesert Road. It commenced accelerating through the intersection in an eastbound direction towards Riawena Road at 1:12:52 pm. The GPS-equipped survey car was closely following the articulated truck, recording position and speed at one-second intervals.

The initial speed of the vehicle, when the GPS device indicated that the following vehicle was no longer at rest, was $v_0$ = 0.39 km/h. The vehicle stopped accelerating after a time $T$ = 46 seconds. It had reached a speed of $v_T$ = 81 km/h, and travelled a distance of $x_T$ = 678 metres. The initial elevation was 16.5m, and final elevation was 23.7m, giving an average gradient of 1.06%.

A model of the form given in Equation 7.1 was fitted to the initial and final conditions. Solving numerically, the estimates of the coefficients were determined to be $\hat{\alpha} = 1.05776\ \mathrm{m/s^2}$ and $\hat{\beta} = 0.03788\ \mathrm{s^{-1}}$. As a check, both the predicted

speed and distance at the end of the acceleration matched those that were measured. The measured and modelled speeds and distances are shown in Figure 7.8 and Figure 7.9, respectively, confirming that the model closely matches the recorded profiles and exactly matches the end conditions.

Using these coefficients, the model predicts that the vehicle would accelerate from rest (not from the initial speed as measured by the GPS device) to a speed of 60 km/h in a time of $\hat{T}_v = 24$ seconds and a distance of $\hat{X}_v = 230$ metres on a grade of 1.06%.

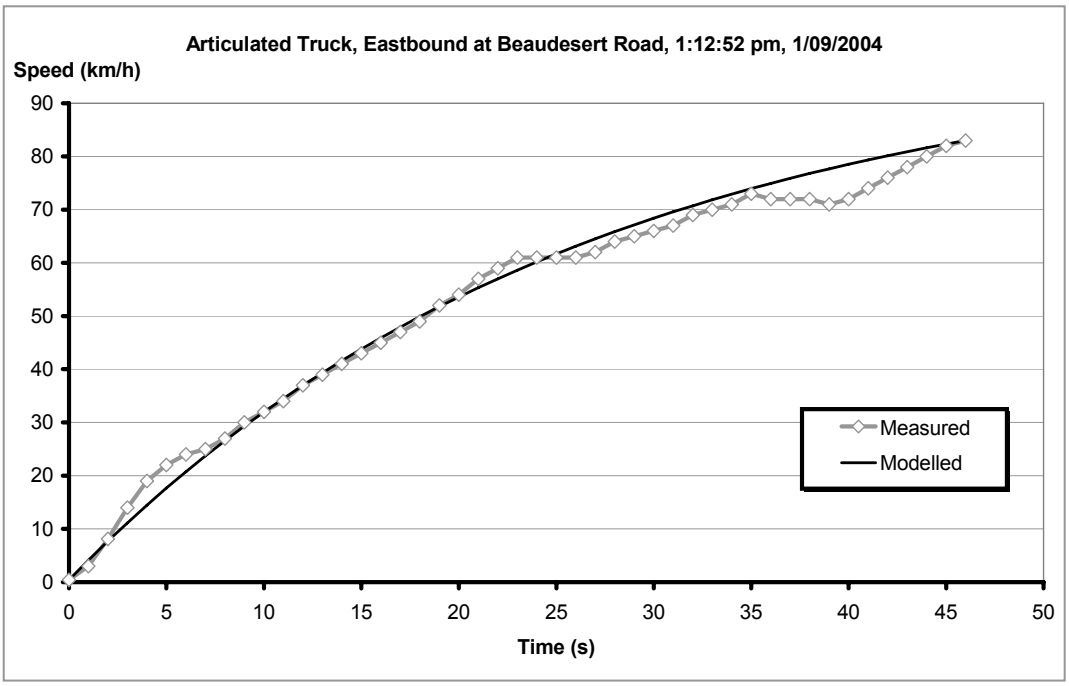


**Figure 7.8 – Measured and modelled speed when accelerating from rest for a typical vehicle being followed**

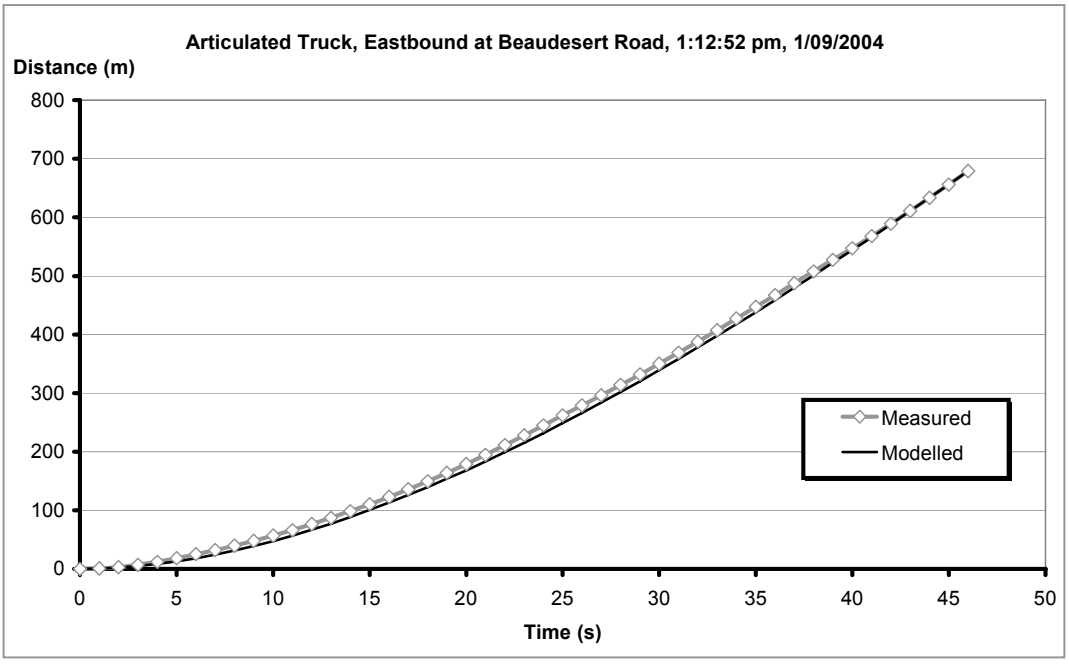


**Figure 7.9 – Measured and modelled distance travelled when accelerating from rest for a typical vehicle being followed**

### 7.5.3 Acceleration on grade

A vehicle's maximum acceleration capability reduces with increasing grade. This is particularly evident in the in-service performance of heavy vehicles, which use a greater proportion of their maximum acceleration capability in service. A free body diagram of the forces acting on a grade, such as presented at the beginning of Chapter 4 indicates that acceleration decreases by **g** sin θ when on an inclined plane at angle θ. That is, our acceleration model given in Equation 7.1 would become Equation 7.12.

$$a(t) = \alpha_0 - \beta v(t)/3.6 - \mathbf{g}\sin\theta \qquad \text{Equation 7.12}$$

The maximum gradeability of the vehicle, when the vehicle could climb at near-zero speed and not be able to accelerate, would then be given by substituting $a = 0$ and $v = 0$ into this equation, giving Equation 7.13.

$$\sin\theta_{max} = \alpha_0/\mathbf{g} \qquad \text{Equation 7.13}$$

Very importantly, note that this equation generally underestimates the gradeability of heavy vehicles. The example above predicts $\alpha$ = 1.05776 m/s$^2$; giving $\theta_{max}$ = 6.18°, or a maximum gradeability of $g_{max} = \tan(\theta_{max})$ = 10.8%.

For comparison, the performance-based standard for gradeability and startability for general access vehicles (NRTC 2003a) specifies that a vehicle must be able to commence forward motion on a grade of at least 15% and to maintain forward motion on a grade of at least 25%. In designing (rural) roads, a general maximum grade of 10% is specified in the worst case (mountainous) (Austroads 1997).

Thus, an alternative model was required that better accounted for the reduction of acceleration when a vehicle was on grade.

In order to still account for the reduction in acceleration capability with grade, the initial rate of acceleration, α, was assumed to decrease linearly with grade. That is, $\alpha = \alpha_0 - \gamma g$, where $\gamma$ is the rate of decrease in acceleration capability with grade, $g$. Note that $g = \tan(\theta)$.

The acceleration model then becomes:

$$a(t) = \alpha_0 - \beta v(t)/3.6 - \gamma g \qquad \text{Equation 7.14}$$

The maximum possible grade that the vehicle can start movement on is given by setting both the speed and acceleration to zero, giving:

$$g_{max} = \alpha_0/\gamma \qquad \text{Equation 7.15}$$

The coefficient $\gamma$ is estimated by minimising the standard deviation of the predicted times taken to accelerate from rest to 60 km/h. In the example above, the vehicle was modelled as being able to accelerate from rest to 60 km/h in a time of 24 seconds on a grade of 1.06%. With an initial value of $\gamma$ = 0, it would take the same time on level ground.

The maximum speed that a vehicle can maintain of a specified grade is given by setting $a(t) = 0$, resulting in Equation 7.16.

$$v_{\max} = \frac{\alpha_0 - \gamma g}{\beta} \qquad \text{Equation 7.16}$$

For the 54 articulated truck acceleration samples recorded, assuming that $\gamma = 0$, the average time to accelerate to 60 km/h was 34.8 seconds with a standard deviation of 12.3 seconds.

Increasing $\gamma$ from its initial value of 0 introduces an increasing amount of sensitivity of acceleration to grade. For the samples of accelerating vehicles measured on positive grades, the estimate of the vehicle's acceleration capability on level ground will increase; and for the samples of accelerating vehicles measured on negative grades, the estimate of the vehicle's acceleration capability on level ground will decrease. This leads to an overall reduction in the standard deviation of the time taken to accelerate to the free speed.

Figure 7.10 shows the change, as $\gamma$ is varied, in the standard deviation of the 54 articulated truck samples of the time taken to accelerate to 60 km/h. The figure shows that a minimum in the standard deviation exists, increasing $\gamma$ beyond this value leads to an increase in the standard deviation as the acceleration models for each vehicle become too sensitive to grade. Microsoft Excel's Solver Command was used to minimise this standard deviation, finding that a value of $\gamma$ = 3.612 m/s$^2$ gave a minimum standard deviation of 10.94 seconds.

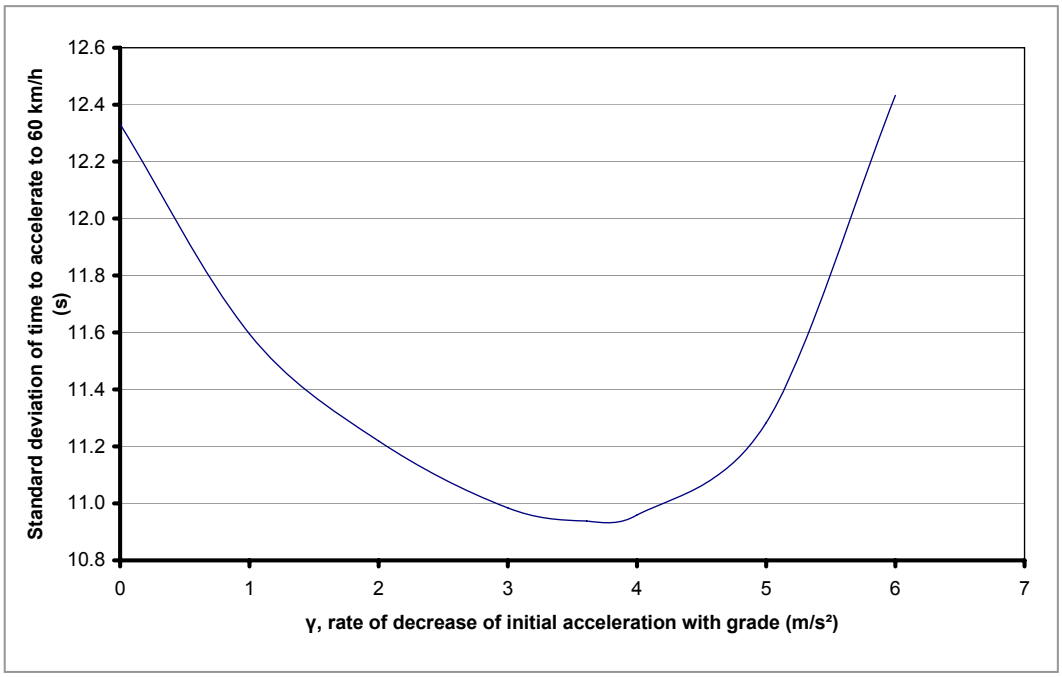


**Figure 7.10 – Finding the minimum standard deviation in acceleration time by varying $\gamma$**

Having determined the rate of change of initial acceleration with grade, the time and distance taken to accelerate from rest to a specified speed on level ground can be determined. For the 54 articulated truck samples, the average time to accelerate to 60 km/h on level ground was 35 seconds, in an average distance of 323 metres.

A similar process of determining the coefficients for the average vehicle was then undertaken, finding coefficients $\alpha_0$ and $\beta$ by matching both the distance and time taken to accelerate to speed on a level ground by solving Equation 7.10 and Equation 7.11 simultaneously.

Thus, the acceleration model for the average articulated truck is given by:

$$a(t) = 0.645 - 0.018\ v(t)/3.6 - 3.612\ g \qquad \text{Equation 7.17}$$

The maximum speed on level ground, $v_{max}$, is given by $v_{max} = 3.6\ \alpha_0 / \beta$, which is calculated to be 126 km/h.

The maximum grade, $g_{max}$, is calculated to be 17.9% using this method. Had we simply assumed that acceleration decreases by **g** sin θ when on an inclined plane, the maximum grade would be 6.6%, meaning the vehicle model would crawl to a standstill on a corridor with modest grades.

### 7.5.4 Acceleration model parameters for each vehicle type

This method was applied to calibrate the acceleration model parameters for each vehicle type. Table 7.17 shows the mean and standard deviation of the times and distances taken to accelerate to a speed of 60 km/h, from the 344 vehicle acceleration samples that were recorded. Accounting for the grade that the vehicles were on whilst accelerating, the equivalent times and distances are presented in Table 7.18.

**Table 7.17 – Time and distance to accelerate to 60 km/h, not accounting for grade**

| *Vehicle Type* | *Sample Size* | *Accelerating from rest to 60 km/h, γ = 0* | | | |
|---|---|---|---|---|---|
| | | *Time (s)* | | *Distance (m)* | |
| | | *Mean* | *Std Dev.* | *Mean* | *Std Dev.* |
| Passenger Car | 136 | 16.6 | 5.9 | 165 | 58 |
| 4WD / LCV | 69 | 20.6 | 6.7 | 209 | 68 |
| Rigid Truck | 59 | 30.9 | 12.1 | 301 | 118 |
| Articulated Truck | 54 | 34.9 | 12.3 | 321 | 99 |
| B-double | 26 | 47.5 | 24.8 | 431 | 224 |

**Table 7.18 – Time and distance to accelerate to 60 km/h, accounting for grade**

| *Vehicle Type* | *Sample Size* | *Accelerating from rest to 60 km/h, accounting for grade* | | | |
|---|---|---|---|---|---|
| | | *Time (s)* | | *Distance (m)* | |
| | | *Mean* | *Std Dev.* | *Mean* | *Std Dev.* |

| | | | | | |
|---|---|---|---|---|---|
| Passenger Car | 136 | 16.3 | 5.4 | 151 | 53 |
| 4WD / LCV | 69 | 20.2 | 6.3 | 205 | 65 |
| Rigid Truck | 59 | 29.0 | 9.1 | 280 | 83 |
| Articulated Truck | 54 | 35.0 | 10.9 | 323 | 93 |
| B-double | 26 | 43.2 | 17.1 | 397 | 155 |

The standard deviations of both the times and the distances are lower in this table than in Table 7.17, indicating that the variability of the predicted performance is reduced by accounting for grade.

The calibrated model parameters for each vehicle type are presented in Table 7.19, together with the maximum speeds and grades that the models predict. This is not to say that these vehicles are incapable of travelling faster than, or on grades steeper than these specified. These parameters were found to give the best fit to the measured data, and are applicable of urban traffic corridors having speeds and grades below these maxima.

**Table 7.19 – Model coefficients for each vehicle type**

| *Vehicle Type* | $\alpha$ *(m/s²)* | $\beta$ *(1/s)* | $\gamma$ *(m/s²)* | $v_{max}$ *(km/h)* | $g_{max}$ |
|---|---|---|---|---|---|
| Car | 1.725 | 0.071 | 2.51 | 88 | 68% |
| 4WD / LCV | 1.481 | 0.065 | 2.63 | 82 | 56% |
| Rigid Truck | 0.896 | 0.033 | 7.30 | 97 | 12% |
| Articulated Truck | 0.645 | 0.018 | 3.61 | 126 | 18% |
| B-double | 0.517 | 0.014 | 3.36 | 130 | 15% |

The low values of $v_{max}$, particularly for cars and 4WDs/LCVs may initially appear to be of concern. It should be noted that these simulations are based on samples of acceleration from vehicles travelling below the posted urban speed limit on the corridor of 60 km/h. The model is thus considered valid for applications up to this limiting speed.

This is similar to the limitations placed on the relationships developed by Bunker and Haldane (2003), in which acceleration was assumed to decrease linearly with elapsed time. A maximum valid time was specified to prevent the model predicting negative accelerations.

The times and distances for the current model formulation to reach this speed limit of 60 km/h, or even a higher speed limit of 75 km/h still increase with increasing vehicle size, as shown in Table 7.20.

**Table 7.20 – Time and distance to reach a limiting speed for each vehicle type**

| | *Speed limit=60 km/h* | | *Speed limit = 75 km/h* | |
|---|---|---|---|---|
| *Vehicle Type* | *time (s)* | *distance (m)* | *time (s)* | *distance (m)* |
| Car | 16.2 | 160 | 27.2 | 370 |
| 4WD / LCV | 20.3 | 204 | 37.9 | 543 |
| Rigid Truck | 29.0 | 280 | 44.6 | 576 |
| Articulated Truck | 35.0 | 323 | 48.9 | 585 |
| B-double | 43.2 | 397 | 60.0 | 714 |

Figure 7.11 and Figure 7.12 shows the acceleration predicted for each vehicle type when accelerating from rest up to a speed of 60 km/h on a level surface. Figure 7.13 and Figure 7.14 show the speed and distance predicted for each vehicle type, respectively.

For comparison, the B-double acceleration model used by Bunker and Haldane (2003) is shown alongside those derived in this study. This model decreases linearly with time, reaching low acceleration values more rapidly than the others do. Despite this, it gives a similar distance versus time plot (Figure 7.14) to the articulated truck in this study. Bunker and Haldane's tests used a high-powered prime mover (410 kW, or 550 hp), which is greater than that typically used for a B-double. Hence, the acceleration rate would be expected to be higher than that of a typical B-double.

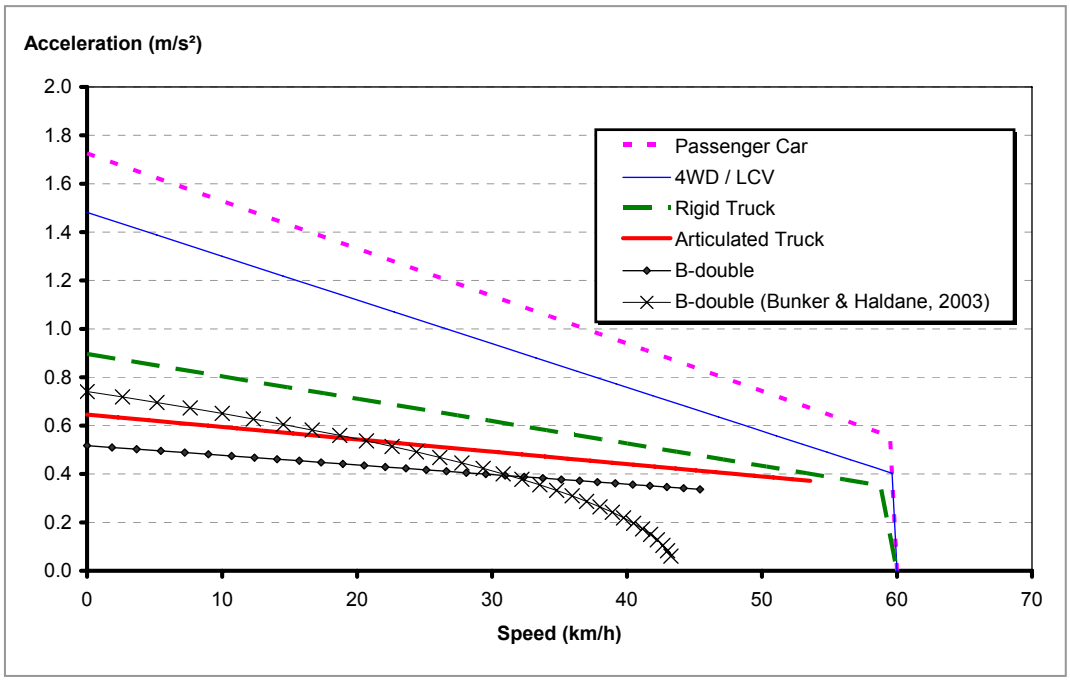


**Figure 7.11 – Decrease in acceleration with speed for each vehicle type when accelerating from rest to a speed of 60 km/h**

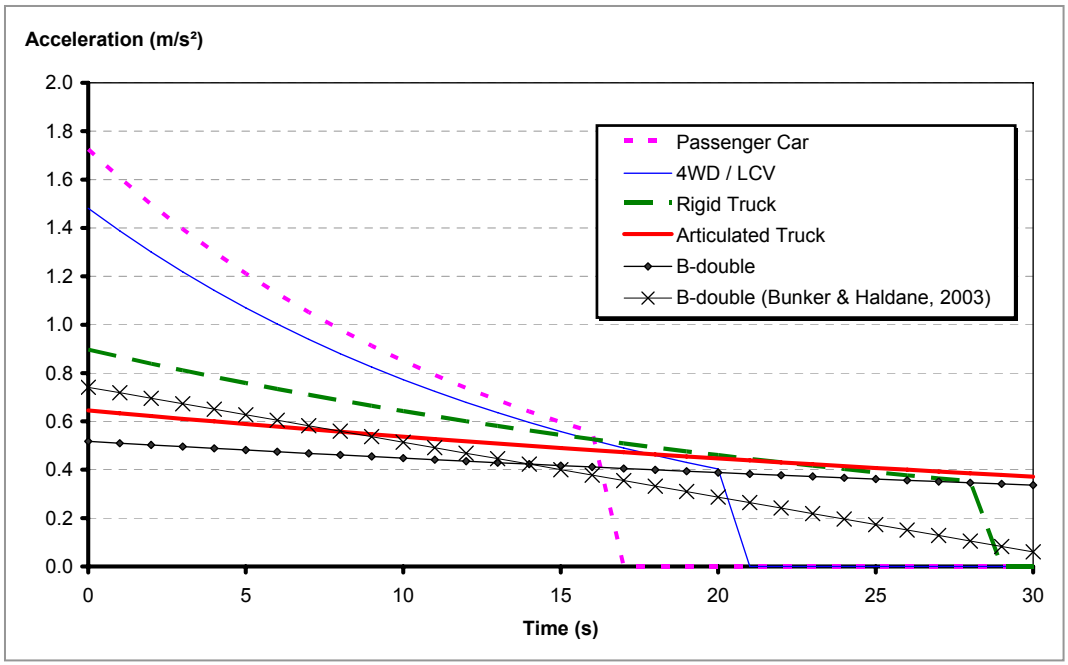


**Figure 7.12 – Acceleration of each vehicle type when accelerating from rest to a speed of 60 km/h**

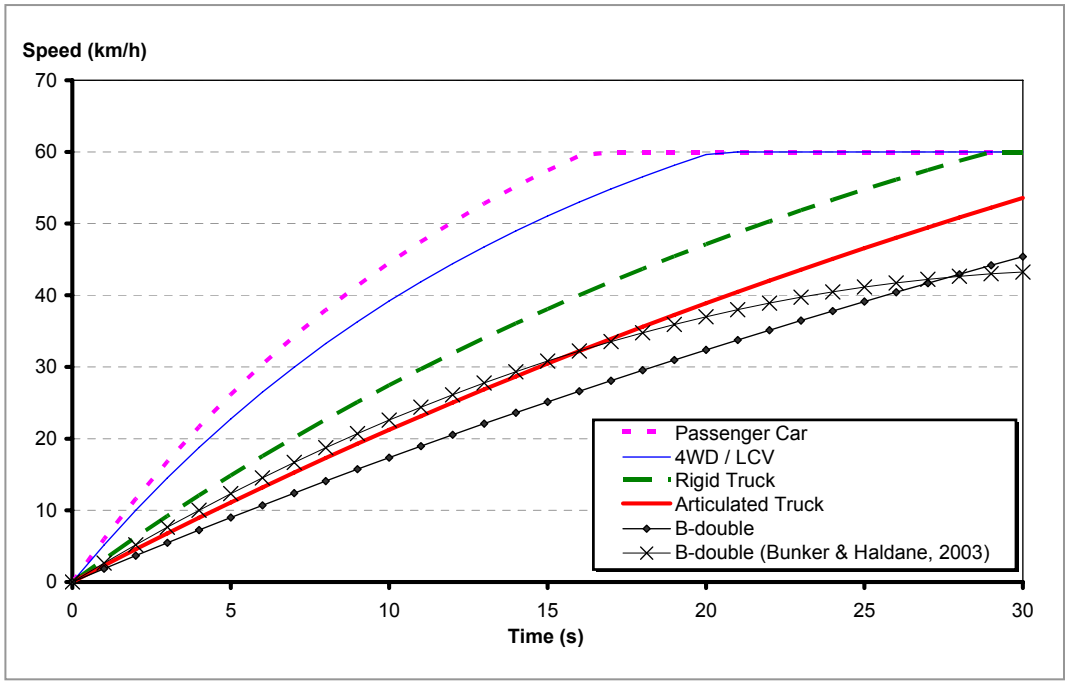


**Figure 7.13 – Speed of each vehicle type when accelerating from rest to a speed of 60 km/h**

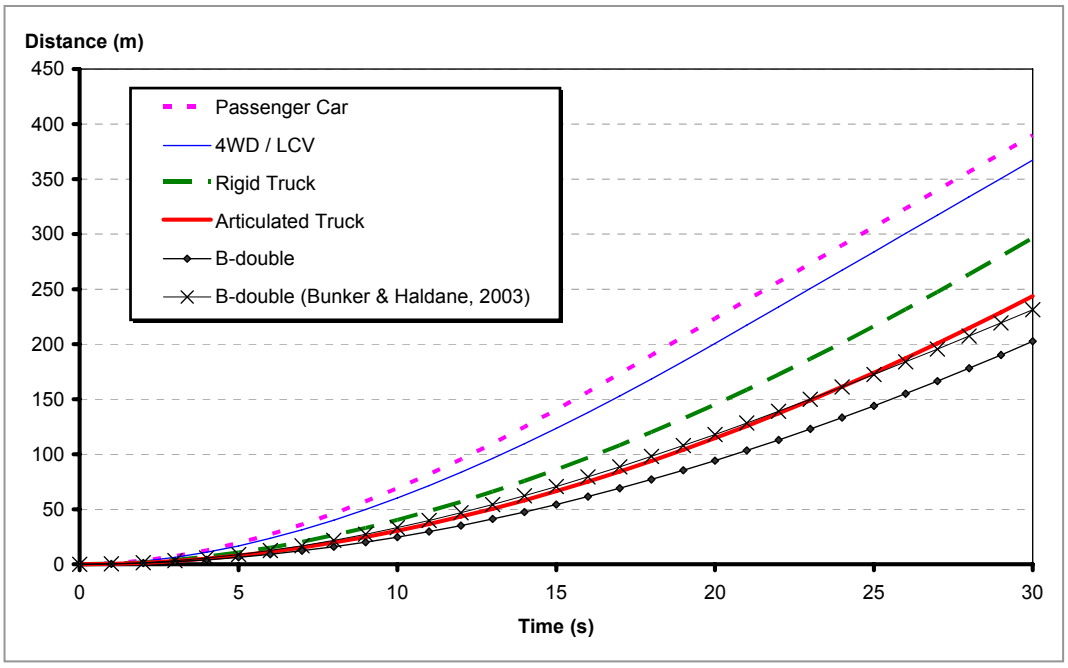


**Figure 7.14 – Distance travelled by each vehicle type when accelerating from rest to a speed of 60 km/h**

### 7.5.5 Comparison of leading and following vehicle acceleration

In the previous chapter it was found that the separation between the leading vehicle and the following vehicle increased with speed, an example showing that the following vehicle travelled 293.4 m when the leading vehicle travelled 300 m to accelerate from rest to 60 km/h in 35 seconds. The parameters for the acceleration model were determined for these two sample accelerations, with the results presented in Table 7.21.

**Table 7.21 – Acceleration model parameters for the leading and following vehicles**

| *Parameter* | *Leading* | *Following* |
|---|---|---|
| Final speed, $v_T$ (km/h) | 60 | 60 |
| Time taken, $T$ (s) | 35 | 35 |
| Distance, $x_T$ (m) | 300.0 | 293.4 |
| Max. acceleration, $\alpha$ (m/s$^2$) | 0.518 | 0.485 |
| Reduction rate, $\beta$ (s$^{-1}$) | 0.0049 | 0.0010 |

The model for the following vehicle has a lower initial acceleration, but the acceleration rate does not decrease as rapidly, as can be seen in Figure 7.15.

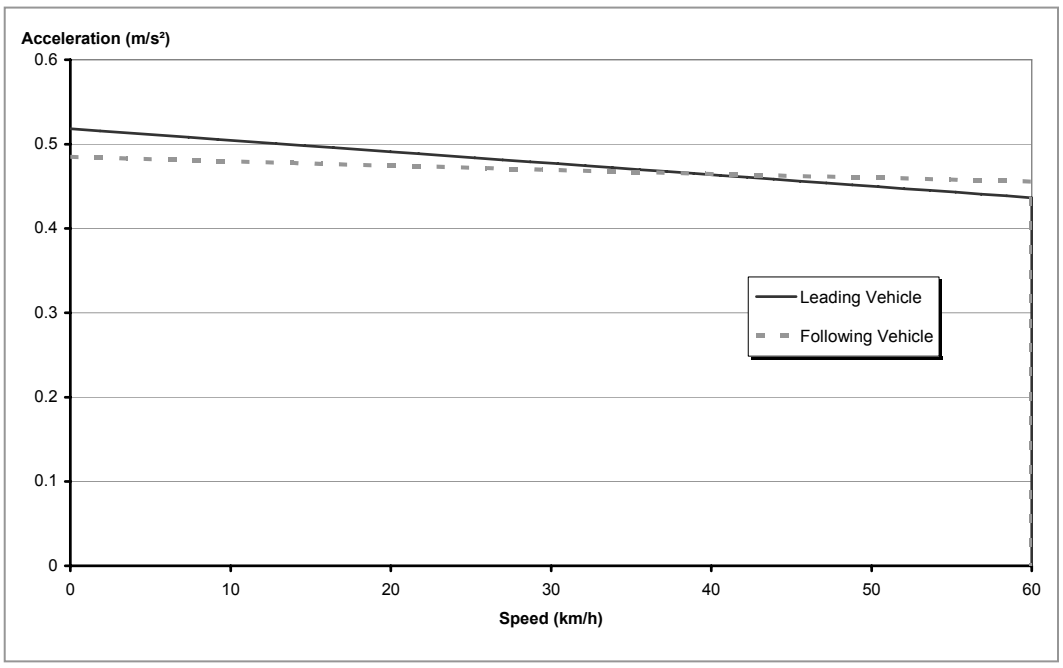


**Figure 7.15 – Acceleration versus speed for leading and following vehicles**

Figure 7.16 shows the speed predicted by the leading and following acceleration models when accelerating from rest to the speed limit of 60 km/h. The maximum difference in speeds of the two models is 1.01 km/h, occurring at 17.2 seconds; whilst the average difference in speeds is 0.66 km/h. These differences in speeds are small compared to the typical travel speeds on urban corridors.

It would be possible to account for this underestimation of the distance taken to accelerate simply by adding the estimated change in separation to the distance taken to accelerate. This was not done in the current project.

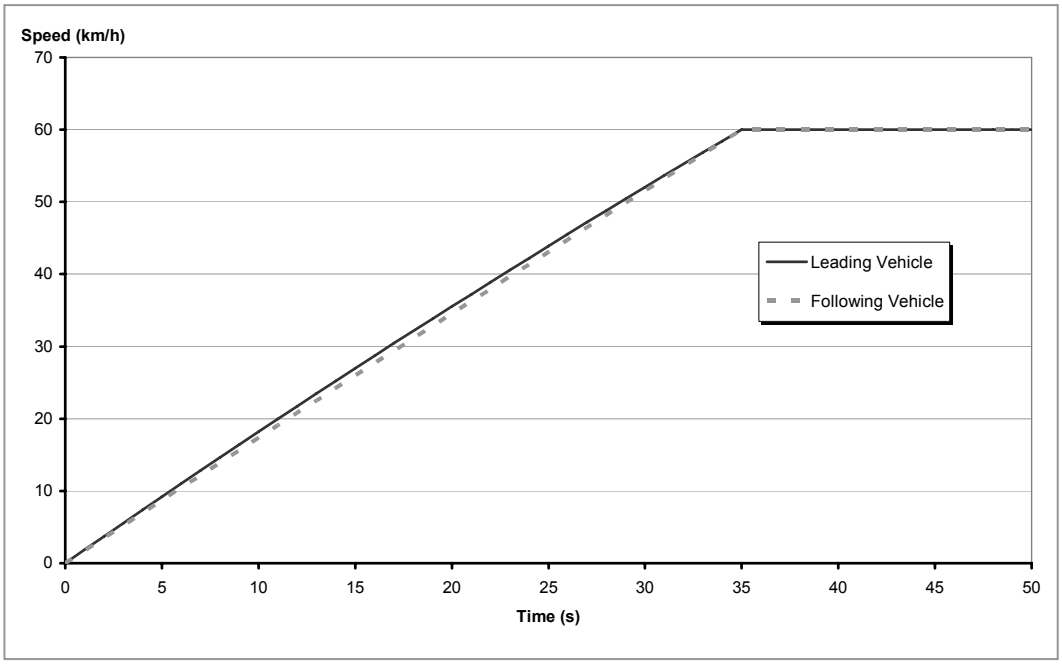


**Figure 7.16 – Speed versus time for leading and following vehicles**

## 7.6 Summary and Conclusions of this Chapter

This chapter describes the calibration of model parameters using the data collected in the previous chapter. Three data sources were used – an automatic traffic counter, a GPS-equipped chase car, and the status of the intersections on the corridor.

The composition of the traffic on the corridor was estimated using data from the automatic traffic counter. Volumes of each vehicle type at each hour of the day were analysed; finding that the distributions of the proportions of vehicle types throughout the day closely matched that recorded in an earlier survey as part of the BUC Study (Jan Taylor and Associates 2003). The peak period for interactions between LFVs and other traffic was identified as being the daytime inter-peak period.

The distribution of the proportion of vehicle types recorded in this period was used in the baseline model case. The probability distribution of vehicle types was found to depend upon the vehicle type being followed, with an articulated truck more likely to appear after another articulated truck than their proportion in the overall sample. A Markov chain probability distribution could be used to incorporate this into a simulation model – first determining the leading and following vehicle types and then calculating the headway from the appropriate distribution function.

The traffic count data was also used to model the distribution of the headways for each vehicle type. The parameters of the Cowan's M3 model used for this purpose were determined by minimising the errors between measured and modelled points. Headways were generally greater in front of the larger vehicles, and the proportion of un-bunched vehicles (parameter $\alpha$ in the model) was correspondingly greater for the larger vehicles.

Speeds recorded by the traffic counters did not vary much between vehicle types, although the location of the site immediately downstream of a railway overpass may have some influence on the speeds of some vehicle types.

Travel times and stop rates of each vehicle type were estimated from the GPS-equipped chase car, finding little difference between the vehicle types. Statistical t-tests of the differences in performance measures indicated that generally speaking, any differences were not statistically significant.

The trajectories recorded by the GPS-equipped chase car could be overlaid on a corridor timing diagram created using data from STREAMS. This proved the accuracy of the survey method in recording the vehicle's position and speed.

A method was defined and tested to estimate the in-service acceleration characteristics of a vehicle type based on the trajectories recorded by a chase car following a sample of those vehicles. This model also accounted for the grade upon which the vehicle was accelerating.

Lesser emphasis has been placed on the in-service braking performance of the different vehicle types. There is less difference in braking performance than acceleration performance, since all vehicles are required by the Australian Design Rules to meet similar braking requirements. Additionally, braking has less influence on control delay during a typical deceleration / acceleration cycle at a signalised intersection than acceleration does – even if a vehicle can brake faster it still has to stop at the same place in queue and leaves the queue at the same time. A constant value of -3.0 $m/s^2$ for deceleration on level ground was used for all vehicle types in the simulation model. This is the value for deceleration when approaching a signalised intersection used in the Guide to Traffic Engineering Practice Part 7: Traffic Signals (Austroads 2003). The magnitude of this deceleration increases with increasing grade.

The GPS data collected by the chase car following different vehicles along the corridor contains many samples of in-service braking performance, and the analysis method described in this chapter would be adaptable at a later stage to braking instead of to acceleration.

The next chapter describes the development of the corridor-level traffic microsimulation model that makes use of this data analysis.

# CHAPTER 8 DEVELOPMENT OF THE SIMULATION MODEL

## 8.1 Introduction

A corridor-level traffic simulation model was developed in this project to enable a controlled investigation of the effects of various freight policy and traffic management options to be undertaken.

Although several commercial traffic microsimulation software packages were available, a specific-purpose simulation tool was developed from first principles in this project. Several advantages and a few disadvantages were identified in choosing to do this, as was outlined at the start of Chapter 5; the most important advantages of doing so were the in-depth understanding and appreciation of the workings of traffic microsimulation models, and the opportunities to develop and implement innovative modelling techniques.

This chapter describes the development of that simulation model. It describes the modelling framework, building on the specifications described in a previous chapter, and then how it was implemented in the C++ programming language. Details of specific elements of the program are described, including the car-following and lane changing algorithms. The different variants of the program are described, and then several examples are presented to demonstrate its use.

The model is known as **CorMod**, an abbreviation of **Cor**ridor **Mod**el. It comprises a total of 3470 lines of C++ code for the console version of the program, with an extra 1705 lines of code added for a version with a rudimentary Windows interface.

## 8.2 Model Framework

The methodology of implementing a corridor-level traffic model was described in a previous chapter, prior to describing the data collection and analysis that provided model calibration parameters. All of these were required before the model development and testing stages described in this chapter.

Initial prototyping of the application was undertaken in a spreadsheet, using Visual Basic for Applications. This interpreted macro language was found to be too slow for the multiple-runs that were required in the final application, with a single run with very few vehicles taking several seconds to execute. A compiled computer program was required rather than an interpreted spreadsheet macro language.

The application is built around an object-oriented model framework, in which multiple objects, specifically the vehicles, intersections and road sections on the corridor interact with each other as the simulation proceeds.

The program uses standard C++ syntax and standard function calls. It was developed in Microsoft Visual C++, but was able to be recompiled with both Borland and Intel compilers resulting in executable programs that both produced identical results to the Microsoft version. If required, it would be expected to be readily portable to non-Windows based computer architectures.

## 8.3 Data Classes and Structures

Prior to describing the relationships between the data elements in the program, it is appropriate to distinguish between **structures** and **classes** in an object-oriented computer program. A structure is a collection of data attributes that logically belong together and are most efficiently handled together. In the context of this current application; a vehicle has certain attributes such as its speed, position and lane – it is more efficient to specify an array of vehicle structures than to manage separate arrays of speeds, positions and lanes.

Classes are the object-oriented extensions of structures. In addition to encapsulating various common attributes together, a class has methods permitting those attributes to be accessed and modified. Continuing with the vehicle example, a structure for a vehicle may contain elements `x`, `v` and `a` for the position, speed and acceleration respectively. Without using object oriented programming, the vehicle is moved forward a time step of `dt` with the following two lines:

```
Vehicle.x += Vehicle.v * dt + 0.5 * Vehicle.a * dt * dt;
Vehicle.v += Vehicle.a * dt;
```

Whereas using object oriented programming, a method `Move(dt)` can be defined within the class that contains `x += v*dt+ 0.5*a*dt*dt` and `v += a*dt`. The vehicle is then moved forward by simply calling:

```
Vehicle.Move(dt)
```

Generally, direct access to data elements within a class is not permitted, thus limiting the risk of that data being inadvertently changed.

## 8.4 Data Classes and Structures used in this Program

### 8.4.1 Corridor class

The **Corridor** class encapsulates the behaviour of the entire traffic corridor in one object. It contains the data elements used in the simulation, as well as functions to specify what occurs as the simulation proceeds.

The data in the corridor is represented as arrays of pointers to other data elements, including the vehicles and intersections on the corridor. These data elements contain their own pointers to other data elements of interest such as the vehicle in front of the current vehicle, the next intersection, or the characteristics of the vehicle. Some of these pointers change as the simulation proceeds – vehicles change lanes and pass through intersections, requiring updating of some pointers. Other pointers remain constant throughout the simulation, such as the characteristics of a particular vehicle or the intersection located downstream of a particular intersection.

Figure 8.1 represents the encapsulation of the major data elements in the Corridor data class. The corridor consists of a number of **Vehicles**, each having dynamic pointers to the surrounding vehicles, the current **Intersection** and the current road **Section**. Pointers to vehicle and driver types do not change during the simulation, nor do those between adjacent intersections or sections.

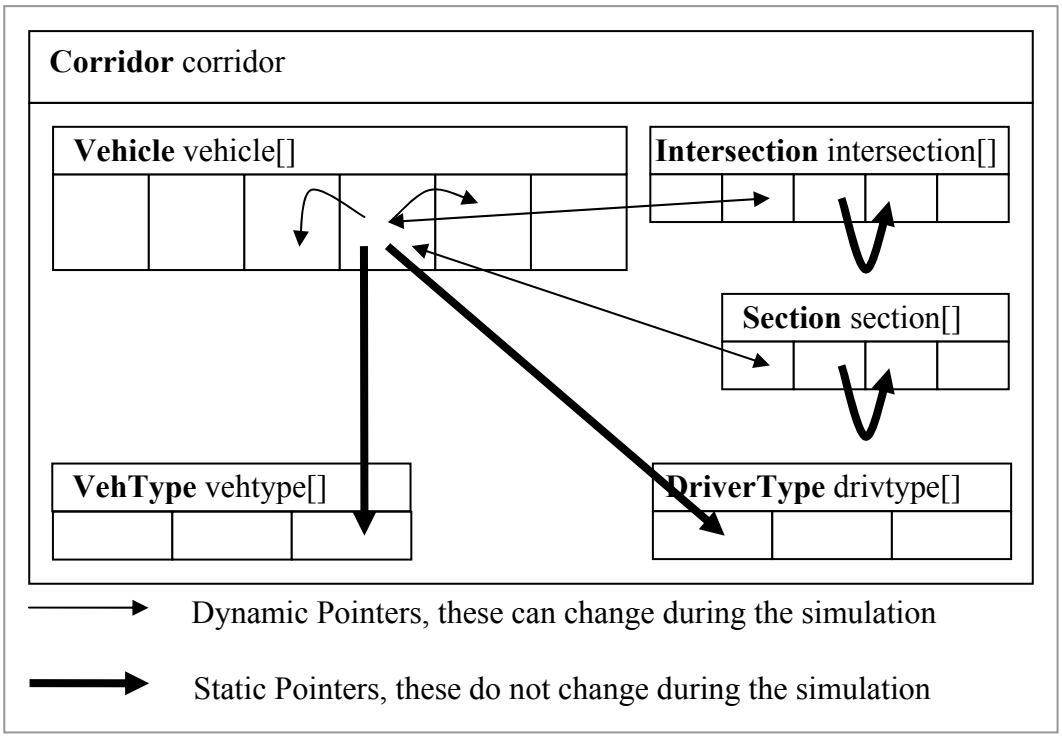


**Figure 8.1 – Objects and the pointers between them in the Corridor data class**

The **Corridor** class contains several functions that are called during program execution. These are outlined in Table 8.1, presented in order of program execution. In a multiple simulation run, the functions `Initialise()`, `Run()` and `AccumulateStatsCounters()` are executed repeatedly in a loop, providing for several simulations to be initialised and run sequentially and the statistics calculated for each run and averaged over all the runs.

**Table 8.1 – Major functions in the Corridor data class**

| *Function* | *Purpose* |
|---|---|
| `Corridor()` | Constructor: initialises variables |
| `ReadIniFile()` | Reads parameters from initialisation file |
| **`Initialise()`** | Initialises the vehicles and intersections prior to running a simulation |
| **`Run()`** | Runs the simulation, updating the vehicles and intersections at fixed time increments |
| **`AccumulateStatsCounters()`** | Calculates summary statistics for the run just completed |
| `Summarise()` | Prepares a report summarising the run |
| `~Corridor()` | Destructor: cleans up after completion |

The **CorridorW** class is a descendent of the Corridor data class. It is only used in the graphical interface version of the program, and contains additional methods to draw the corridor trajectory diagram on the computer screen.

### 8.4.2 Vehicle class

The Vehicle data class contains variables x and v, representing the vehicle's current longitudinal position and speed. These are updated at every time step. Speed is constrained to be zero or positive at all times, and the position cannot decrease between simulation time steps.

Each vehicle contains pointers to the vehicles immediately in front of and immediately behind it in the current lane. These pointers are used to determine the headway and relative speed of the vehicle, both of which are used in the car following model. These pointers only require changing when a lane change occurs. Pointers to the next intersection and to the current road section are updated as the vehicle passes the intersection stop line or moves onto a new road section.

### 8.4.3 VehicleType structure

The **VehicleType** structure contains vehicle type-specific information, such as the vehicle length, the maximum acceleration, maximum speed and maximum gradeability. Each vehicle is assigned a VehicleType, which does not change during the simulation. Since this is a structure, the data elements may be accessed directly rather than having to use data access method functions.

### 8.4.4 DriverType structure

The **DriverType** structure contains driver behaviour information, such as the car following sensitivity and the propensity to use maximum acceleration. Currently this is set to a constant value, but the code has been implemented so that a range of different driver types may be used, and possibly randomly allocated to vehicles at the program initialisation stage.

### 8.4.5 Intersection class

The **Intersection** class keeps track of the vehicles in each lane about to cross its stop line and about to cross its detector loops. The status of the intersection is updated as the simulation proceeds, changing the signal status on either a fixed-time or vehicle-actuated basis. The default is vehicle-actuated, where the allocated green time ranges between minimum and maximum values and is extended as vehicles pass the intersection detector location. Full details of the vehicle actuated signal algorithm is given in Austroads (2003), default parameter values used to set the "personality" of the intersection controller are presented in Table 8.2.

**Table 8.2 – Intersection controller "personality" default values**

*Refer also to Austroads (2003)*

| *Variable* | *Value* |
|---|---|
| Cycle Time (s) | 90.0 |
| Gap (s) | 35.0 |
| Headway (s) | 0.8 |
| Minimum Green Time (s) | 8.0 |
| Maximum Initial Green Time (s) | 30.0 |
| Maximum Extension (s) | 40.0 |
| Maximum Green Time (s) | 60.0 |
| Progression Design Speed (km/h) | 60.0 |
| Yellow Time (s) | 4.5 |
| All-Red Time (s) | 2.0 |

Each intersection maintains pointers to the vehicles about to cross its detector location and its stop line location. These are checked at each time step and updated if the vehicle has crossed the location. This method was found to be more efficient than having to check through every vehicle at each time step.

### 8.4.6 Section class

The **Section** class represents a road section, having specified start and end points, a speed limit and a gradient. Each section contains a pointer to the next section, as well as pointers to the next vehicle in each lane about to leave the section. At each time step, a check is made if the distance travelled by that vehicle exceeds the end of the section – if so, the vehicle's section pointer is set to the next section. The

section's speed limit and gradient are used in calculating the vehicle's instantaneous acceleration.

## 8.5 How the Program Works

### 8.5.1 Initialisation

The initialisation routines make extensive use of random numbers that are generated using the functions given in "Numerical Recipes in C" (Press *et al.* 1992). The random number seed can be either explicitly specified in the input file, ensuring the same random number sequence is used if the simulation is repeated; or the random number seed is based on the system clock, giving different random number sequences if the simulation is repeated.

A queue of vehicles is generated in each lane prior to starting the actual corridor simulation. Vehicle types are randomly assigned according to the proportions specified in the input file.

A Cowan's M3 distribution was used to generate the vehicles' initial headways. The default minimum headway was set to $\Delta = 2$ seconds, and the default proportion of unbunched vehicles decreased with increasing flow according to $\alpha = 1800 / q$. (Tanner 1962). These parameters may be specified in the input file, overruling the default values.

Although the previous chapter describes the derivation of vehicle type-specific headway distributions, these were not used in the final version of CorMod. These headways are only used at initialisation, the headways are determined by queue discharge characteristics once the vehicles have stopped at the first intersection.

Headways are tested to ensure that they are not less than the length of the preceding vehicle divided by its speed.

### 8.5.2 System updates

As the simulation proceeds, vehicles are actuated in each approach lane when the simulation time exceeds their designated activation time, determined from their headway from the previous vehicle in the same lane.

At each time step, the required accelerations of all of the vehicles are first calculated and then the speeds and positions of all of the vehicles are updated. The acceleration required to maintain the appropriate car-following behaviour depends on the speeds and positions of other vehicles, so these must not be updated before calculating the accelerations of vehicles that depend upon them.

Each vehicle maintains a pointer to the intersection currently in front. As each vehicle passes an intersection, this pointer is replaced by a pointer to the next intersection downstream. At the same time, the intersection detector loop modelled at the stop line is actuated.

### 8.5.3 The flow chart

Figure 8.2 shows the flow chart for the CorMod program. Three loops are used by the program:

The outer-most loop represents an individual simulation of the traffic on the corridor. Typically, multiple simulations are conducted and their results averaged.

The middle loop represents what happens during a single time step, typically lasting 0.1 seconds:

The status of each intersection is first updated to ensure that vehicles will stop at or leave the front of the queue as appropriate during the current time step.

The inner-most loop updates the positions and speeds of all of the vehicles in the current time step:

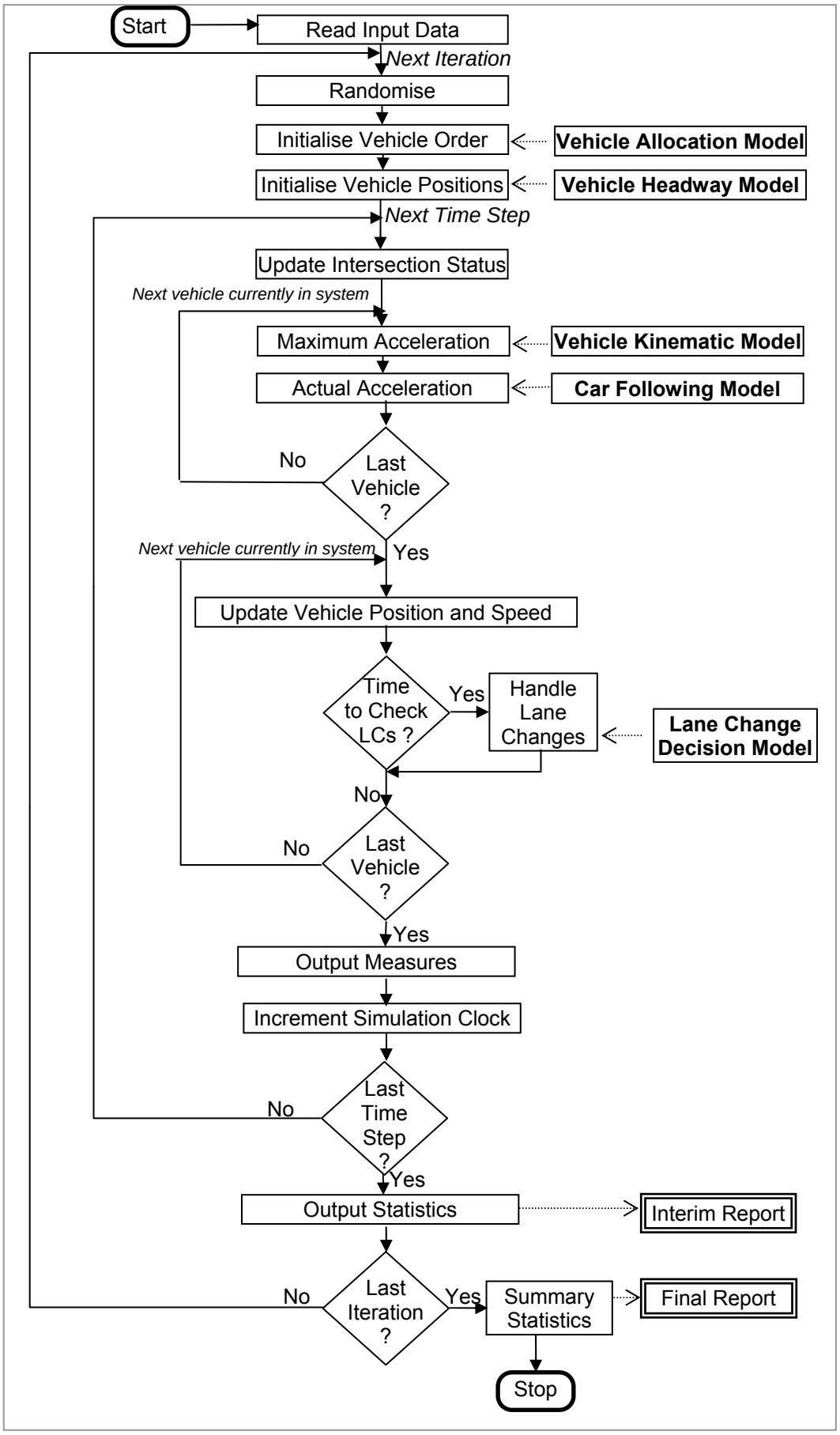


**Figure 8.2 – CorMod program flowchart**

All active vehicles in the system are processed at each time step. This involves firstly determining each of their required accelerations, then checking if any vehicle passed an intersection or moved on to a new section of road. The vehicles are then moved forwards and their speeds adjusted.

After handling all of the vehicles, checks are made to see what lane changes should be performed (the process being described shortly).

Output measures are recalculated and finally the system time clock is updated, ready for the next time step.

When the simulation has reached the last time step, the final output measures are calculated and displayed if required to an interim report for the current simulation.

At the completion of the last simulation, the summary statistics are calculated and reported before the program stops.

### 8.5.4 Car-following

A major component of the corridor level model is ensuring that the individual vehicles appropriately follow their leaders as they travel along the corridor. This behaviour is based upon:

- The capabilities of the vehicle
- Maintaining an appropriate flow / density profile at a macroscopic level
- Ensuring that safe stopping speeds and distances are maintained
- Obeying traffic control measures (specifically speed limits and intersection controls)

Vehicle capabilities have been described in depth in earlier chapters.

The spacing between vehicles is assumed to increase linearly with increasing speed up to the free-flow speed, as indicated in Figure 8.3. This linear relationship results in a triangular flow-density profile (Figure 8.4), which has been used in the analysis of shock waves in traffic flow (see, for example Daganzo 1997).

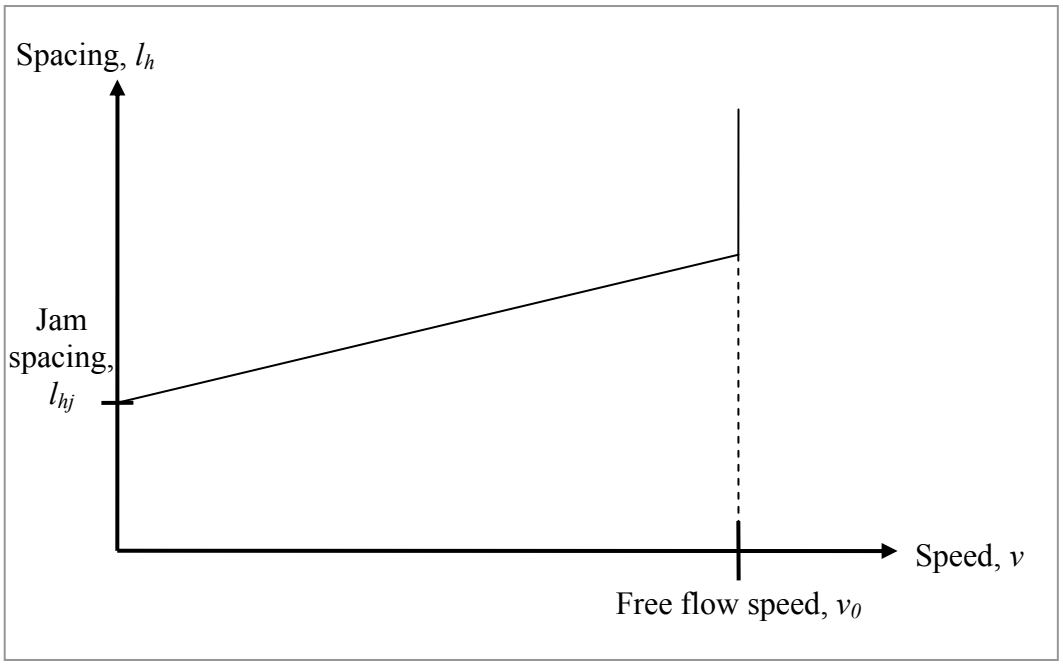


**Figure 8.3 – Spacing / speed relationship**

The spacing between vehicles at a specified speed can be related to the jam spacing, saturation flow and free-flow speed using Equation 8.1.

$$l_h = l_{hj} + \left( \frac{1}{q_s} - \frac{l_{hj}}{v_0} \right) v \text{, for } v < v_0 \qquad \text{Equation 8.1}$$

where $l_h$ is the spacing between vehicles at speed $v$

$l_{hj}$ is the jam spacing between stationary vehicles

$q_s$ is the saturation flow rate

$v_0$ is the free-flow speed.

In addition, each vehicle must maintain a headway and a speed that would enable it to stop safely if the vehicle in front was to decelerate at its maximum rate.

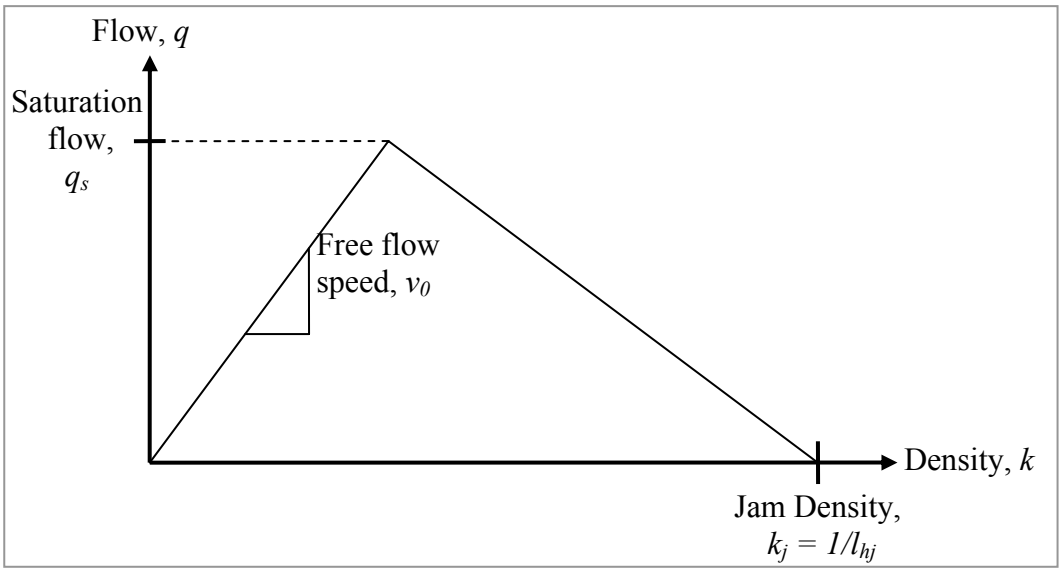


**Figure 8.4 – Triangular flow / density profile corresponding to Figure 8.3**

Furthermore, the vehicle must stop if it is approaching a red traffic light. If the vehicle in front also is stopping then normal car following behaviour will ensure this happens. However, the case of arriving at the front of a queue must be considered as a separate case.

### 8.5.5 Verification of the car-following model

A spreadsheet was used to test the correct operation and stability of the car-following algorithm prior to implementing it in the C++ program.

The test used two vehicles. The lead vehicle was initially at rest, then accelerated up to the speed limit, stopping at a signalised intersection and then accelerating back up to the speed limit. The following vehicle was initially travelling at the speed limit towards the rear of the lead vehicle; it had to decelerate to avoid a collision with the lead vehicle, which it then followed through the intersection.

Figure 8.5 shows the trajectory diagrams of the lead and following vehicles, and Figure 8.6 shows the actual and desired spacing between the two vehicles. If the spacing was below the desired spacing then the following vehicle would decelerate, if above it the vehicle would accelerate. This desired spacing was the maximum of the safe stopping distance and the distance required to maintain the flow / density profile given in Figure 8.4.

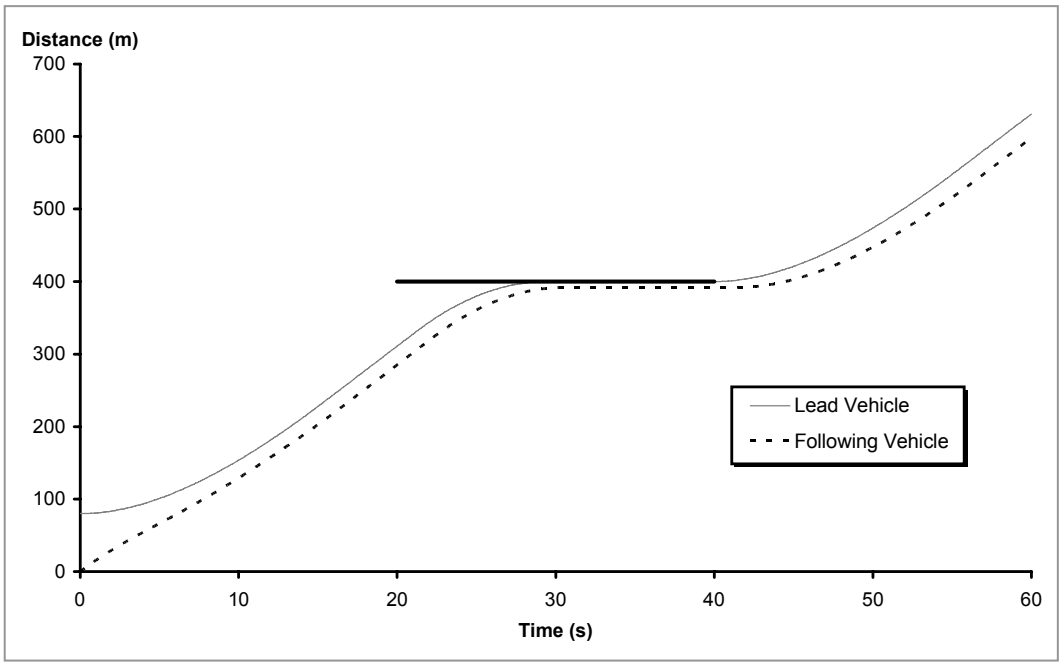


**Figure 8.5 – Trajectories of lead and following vehicles during testing of the car following model**

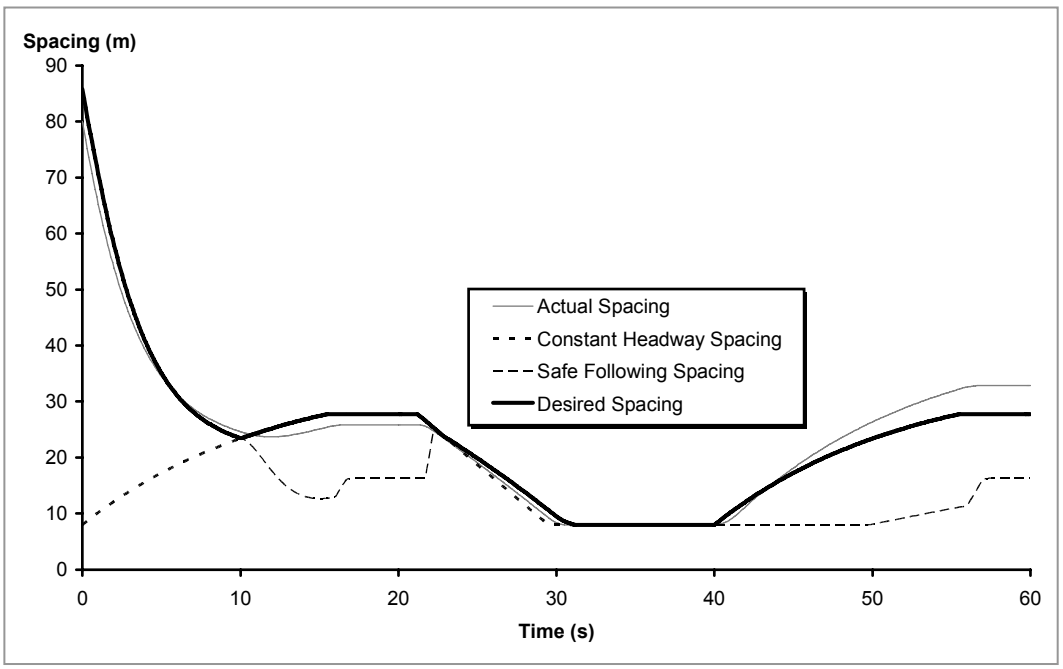


**Figure 8.6 – Spacing between lead and following vehicles during testing of the car following model**

Figure 8.7 and Figure 8.8 show the acceleration and speeds, respectively, for the two vehicles. They indicate that the maximum and minimum acceleration rates and the speed limit were never exceeded. This latter figure also shows the safe stopping speed, i.e. the maximum speed that the following vehicle could travel at and still be able to stop without colliding with the lead vehicle. This can be seen always to exceed the instantaneous speed of the following vehicle.

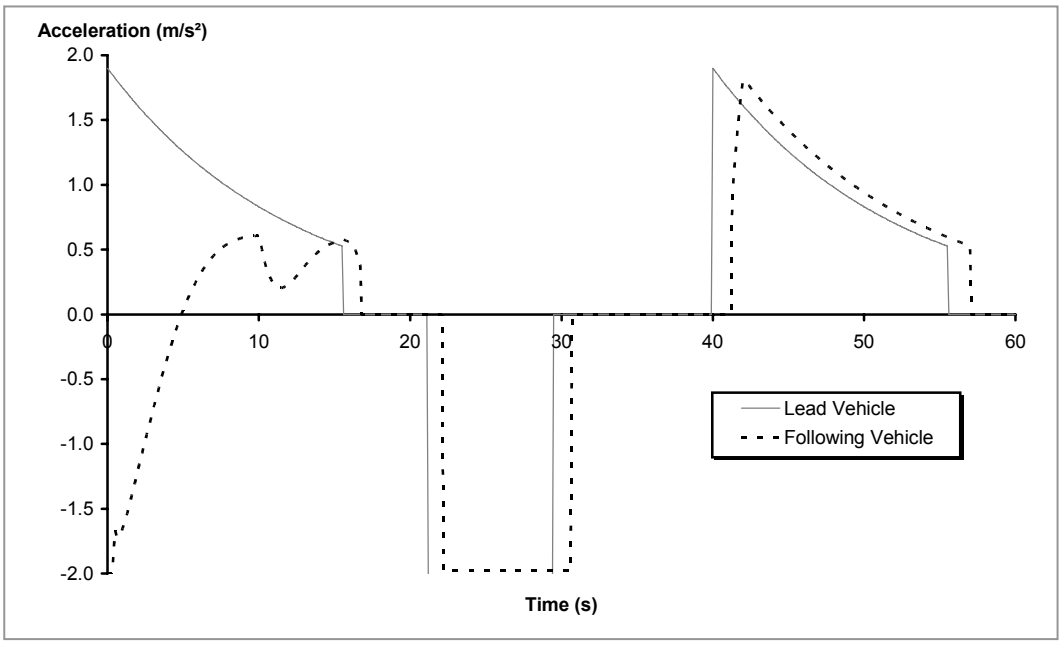


**Figure 8.7 – Acceleration of lead and following vehicles during testing of the car following model**

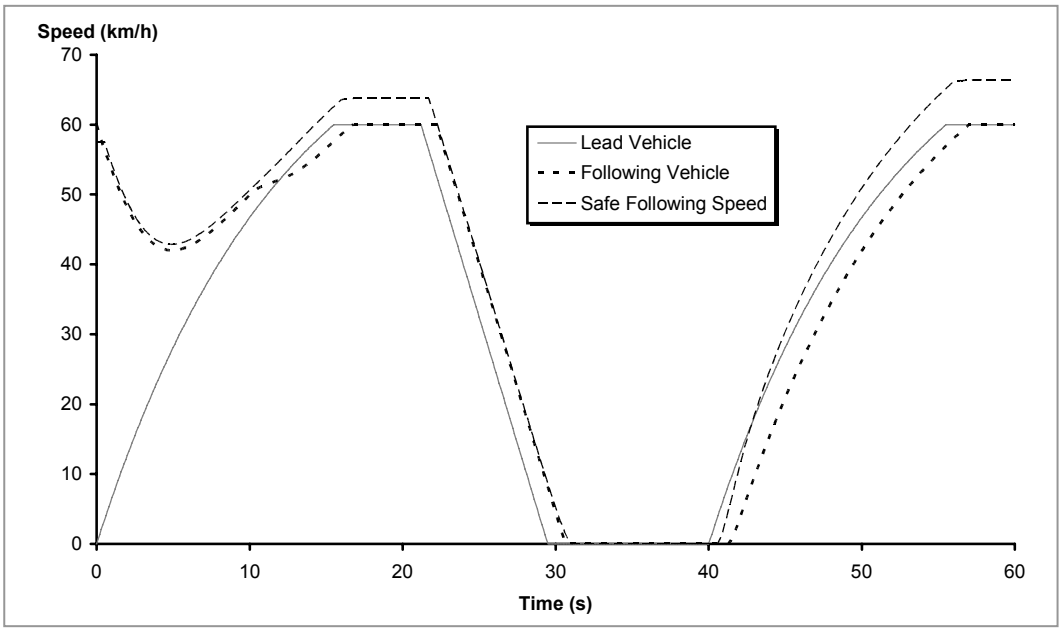


**Figure 8.8 – Speed of lead and following vehicles during testing of the car following model**

### 8.5.6 Handling lane changes

Each vehicle maintains pointers to the vehicles immediate in front of and behind it, and to the next intersection to be crossed. Intersections also maintain pointers to the next vehicle to cross their stop line in each lane. The vehicles in an adjacent lane (either to the right or to the left) of a vehicle considering a lane change are obtained by finding the vehicle about to cross the next intersection in the adjacent lane, and repeatedly finding that vehicle's follower until its longitudinal position is not greater than that of the vehicle considering the lane change.

This method required that the surrounding vehicles were identified only when considering a lane change. It was found to be more efficient than constantly maintaining pointers to adjacent vehicles at each time step.

The logic used to handle lane-change decisions is outlined in Figure 8.9 and described briefly below.

Lane changing opportunities are not considered every time step. Just as a real driver has many other tasks to conduct, opportunities to change lanes are sought at a less frequent rate than the simulation time step rate. When each vehicle is initiated at the start of the simulation, a counter for that vehicle is set to a uniform random deviate (ranging from 0 to 1) multiplied by the desired lane changing consideration rate (typically 10 seconds). At each time step, the counter is decremented by the time-step value. When the counter reaches zero, the vehicle will look for a lane change opportunity, and then resets the counter to the lane change consideration rate. This ensures that lane changes occur less frequently than the simulation time step and that not all vehicles try to change lanes at the same time step.

If the vehicle's speed is less than desired when considering a lane-change, the vehicle will then look for opportunities to change lanes. Opportunities consist of gaps in adjacent lanes into which the vehicle may merge without a collision. Except in the case of the vehicle being in the far-right or far left lane; a preferred lane is identified either to the left of right of the current lane.

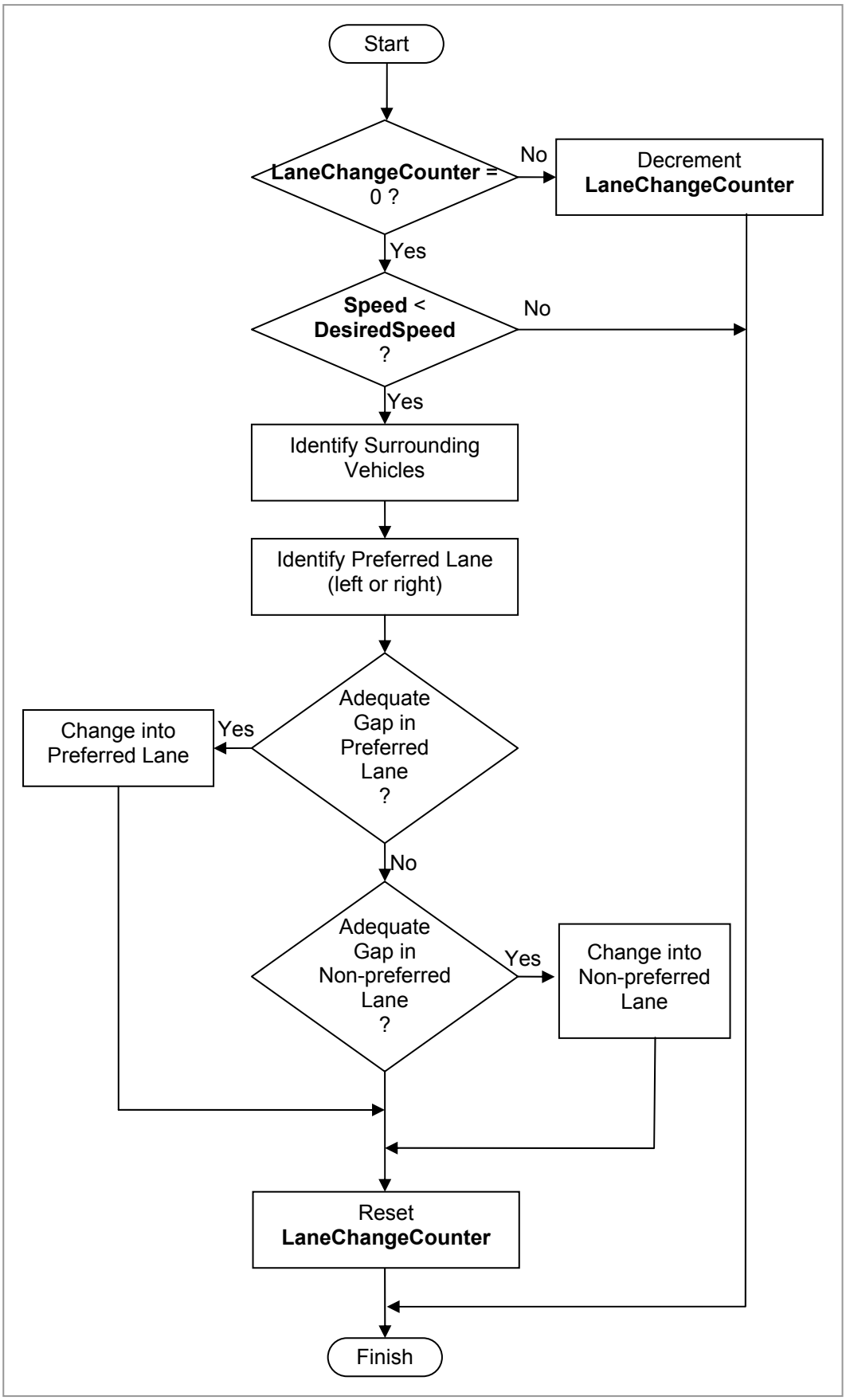


**Figure 8.9 – CorMod lane changing decision flowchart**

If the vehicle is approaching a queue at an intersection, the preferred lane is selected based on the differences in expected queue clearance times of the candidate lanes. A longer queue length or the presence of a slower-accelerating vehicle in the queue will lead to a greater expected queue clearance time, and greater incentive to use another lane. Just as a real driver subconsciously evaluates queue lengths and compositions in the various lanes when approaching an intersection, the program predicts how long the vehicle would take to clear the intersection if it was to remain in the existing lane or change to the left or the right. When approaching the back of queue, the slowest-accelerating vehicle in the queue is identified. The distance from the back of queue to the stop line is also identified, and used to calculate the time that the back of queue would take to reach the stop line, accelerating at the rate given by the slowest-accelerating vehicle. This time is compared to similarly calculated times in adjacent lanes to determine whether a lane change would be advantageous.

Having identified a preferred lane to change into, a check is made to ensure that the lane change can be made safely without colliding with either the vehicle in front or behind in the candidate lane. A physical gap of adequate size must exist, and the vehicles must be able to match their speeds without exceeding their braking and acceleration limits. Even though a large gap may exist for a vehicle to merge into, if the lead vehicle is slow or stationary then the vehicle changing lanes may not be able to decelerate in the available distance to avoid a collision – similarly a suitable gap must exist to allow a faster vehicle behind the vehicle changing lanes to decelerate without a collision. If not suitable gap exists in the preferred lane, then opportunities to change into the non-preferred lane are sought.

The lane change itself was handled by revising the pointers between the vehicles and possibly the pointers from the next intersection to the vehicles in each approaching lane. The vehicle changing lanes had to update both its leader and follower pointers to vehicles in the new lane, the previous leader's follower had to be set to the previous follower, the previous follower's leader had to be set to the previous leader, and the new leader's follower and new follower's leader had to be set to the vehicle changing lanes.

If either the vehicle changing lanes or the new follower were the next vehicle to cross an intersection stop line or intersection detector, then the intersection's pointers would need to be changed.

## 8.6 Implementation

Two versions of the corridor model program were developed:

- A command-line version (**CorModC**) which does not have the computational overhead of a graphical output and was used for lengthy simulation runs, such as multiple replications with different random number seeds.
- A Microsoft Windows-based graphical version (**CorModW**), which was intended for model verification and graphical presentation purposes.

Both versions used the same fundamental source code for model operation, but had different output stages.

### 8.6.1 Command line version (CorModC)

The command line version of the program is shown during a simulation in Figure 8.10. The program took the name of the model configuration file as its first parameter on the command line, and the program output was printed to the standard output stream. As is shown in this example, output could be redirected to a file for further analyses.

Unlike the graphical version, the console version ran multiple simulations, each with a different random number sequence. Progress through the simulations was indicated on-screen, showing the current run number, current execution time, number of vehicles that had entered the corridor, and the number of vehicles that were currently active in the corridor.

During execution, the program accumulated various performance-related statistics; these were used at the end of the simulations to calculate averages and standard deviations of a number of performance measures.

For example, the program accumulated the number of cycles at each intersection, together with the sum and sum-of-squares of the queue lengths in each cycle, for each lane at each intersection. These were used to calculate the mean and standard deviation of the queue length at each lane and each intersection.

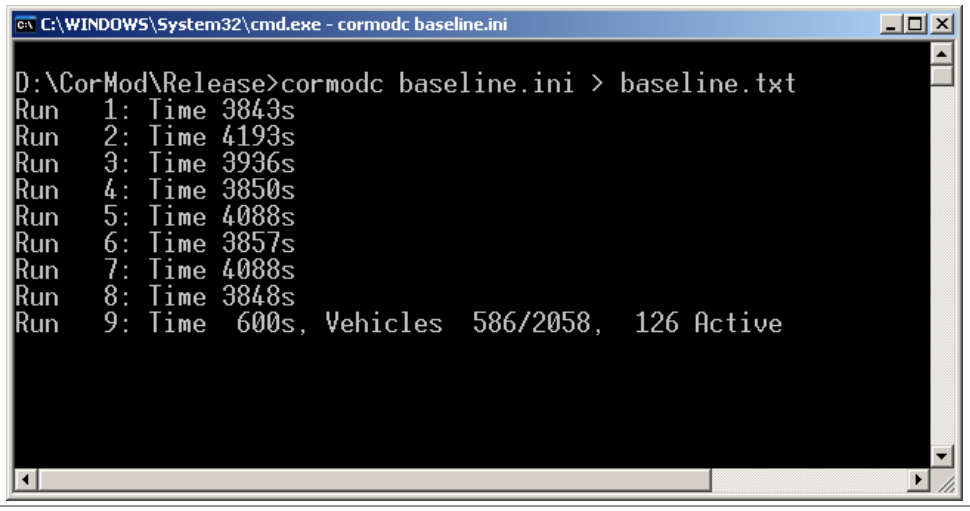


**Figure 8.10 – Running CorModC, the command-line version of the model**

### 8.6.2 Graphical interface version (CorModW)

The graphical interface version displayed the trajectories of the vehicles as they moved along the corridor, together with the status of the traffic signals at the intersections on the corridor.

**CorModW** displays a window on the corridor trajectory and timing diagram, as is shown in Figure 8.11 and described below:

- The simulation starts at time `TInit` and position `XInit`, and finishes when time `TEnd` has been reached *and* the all of the vehicles have passed position `XEnd`.
- The CorModW screen only displays sections of trajectories between times `TMin` and `TMax`, and between positions `XMin` and `XMax`.
- The corridor performance statistics, such as travel times and number of stops, are calculated between two cordon lines at positions `XStart` and `XFinish`; these cordon lines are only active between times of `TStart` and `TFinish`.

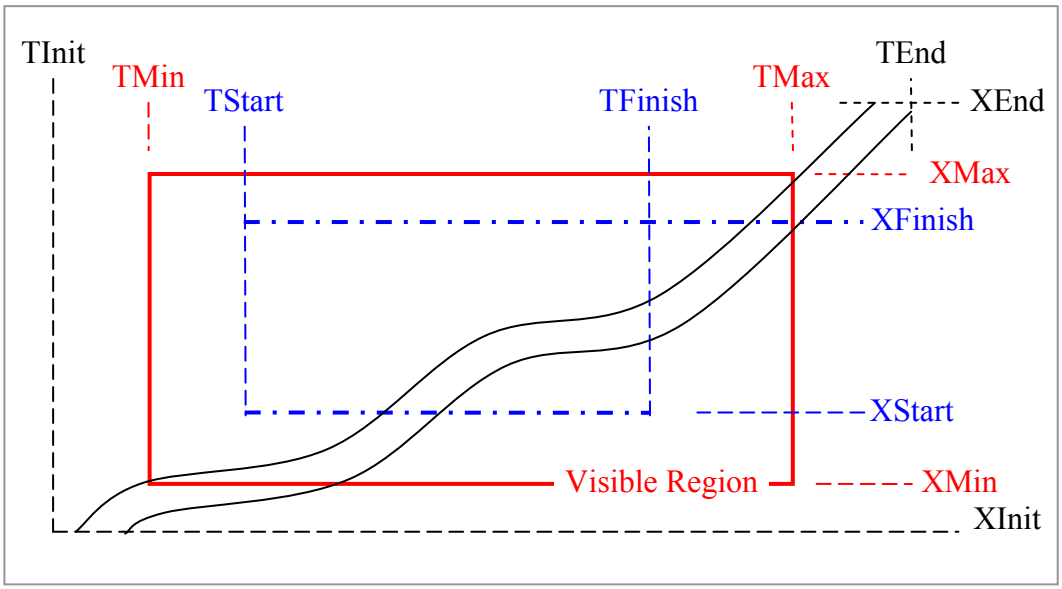


**Figure 8.11 – Spatial and temporal extents of a CorModW simulation**

The CorModW display of the trajectory diagram may be printed or copied to the Windows clipboard for pasting into other applications as a Windows metafile.

Figure 8.12 shows an example **CorModW** window. Vehicles already on the corridor at time `TMin` are shown in their positions between `XMin` and `XMax`. Other vehicles appear on the screen at position `XMin` between time `TMin` and `TMax`. All vehicles proceed along the corridor, disappearing from view when they reach `TMax` or `XMax`.

Different vehicle types are represented by lines having different patterns. A legend is used to show which line corresponds to each vehicle type. The cross-hatched rectangles represent a red signal at an intersection being displayed to the corridor through movement and gaps between the rectangles represent a green signal being displayed.

Only one lane of the corridor is visible on screen at a time, other lanes can be selected by choosing the lane under the View menu. Vehicles changing into or out of the current lane during the simulation are indicated by trajectories appearing and disappearing from the trajectory diagram. Checking of adjacent lanes will show from where the lane changing vehicle has come or to where it has gone.

By adjusting the `TMin`, `TMax`, `XMin` and `XMax` display parameters, the **CorModW** screen can show a different part of the diagram. For example, the display can zoom in on the black rectangle in Figure 8.12 to give the screen shown in Figure 8.13. At this level of detail, it is possible to distinguish the trajectories of different vehicles, and to check the correct queue formation and discharge behaviour at signalised intersections. Larger jam spacings are evident behind heavy vehicles, as can their slower acceleration rate.

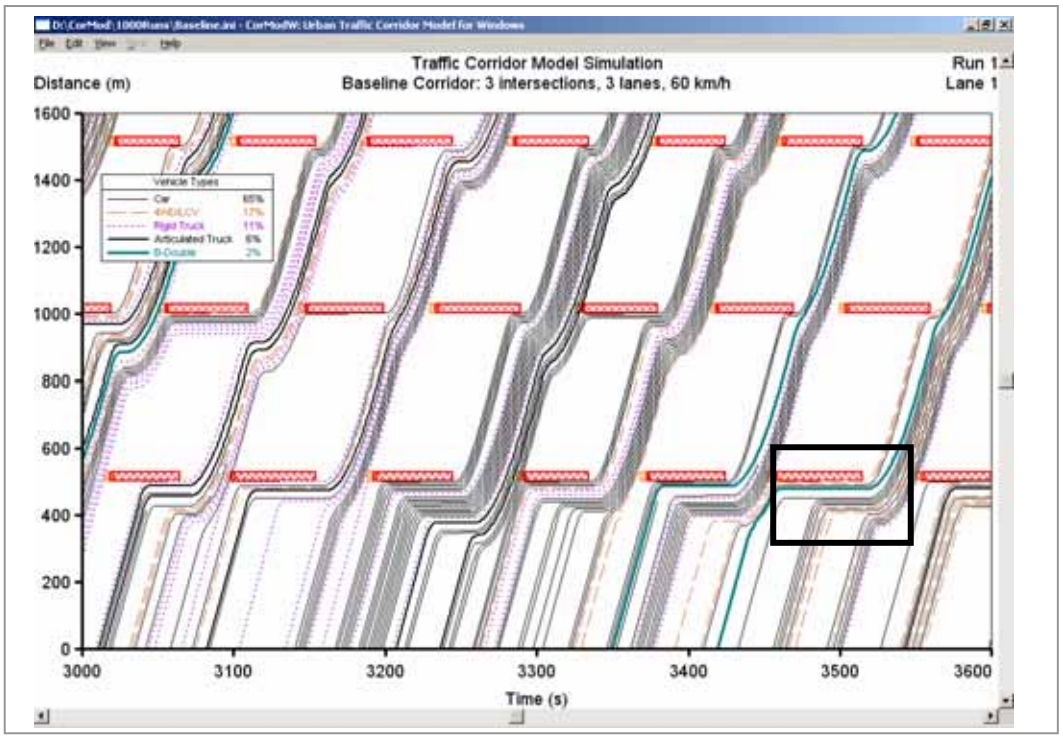


**Figure 8.12 – CorModW display, rectangle is shown in detail in Figure 8.13**

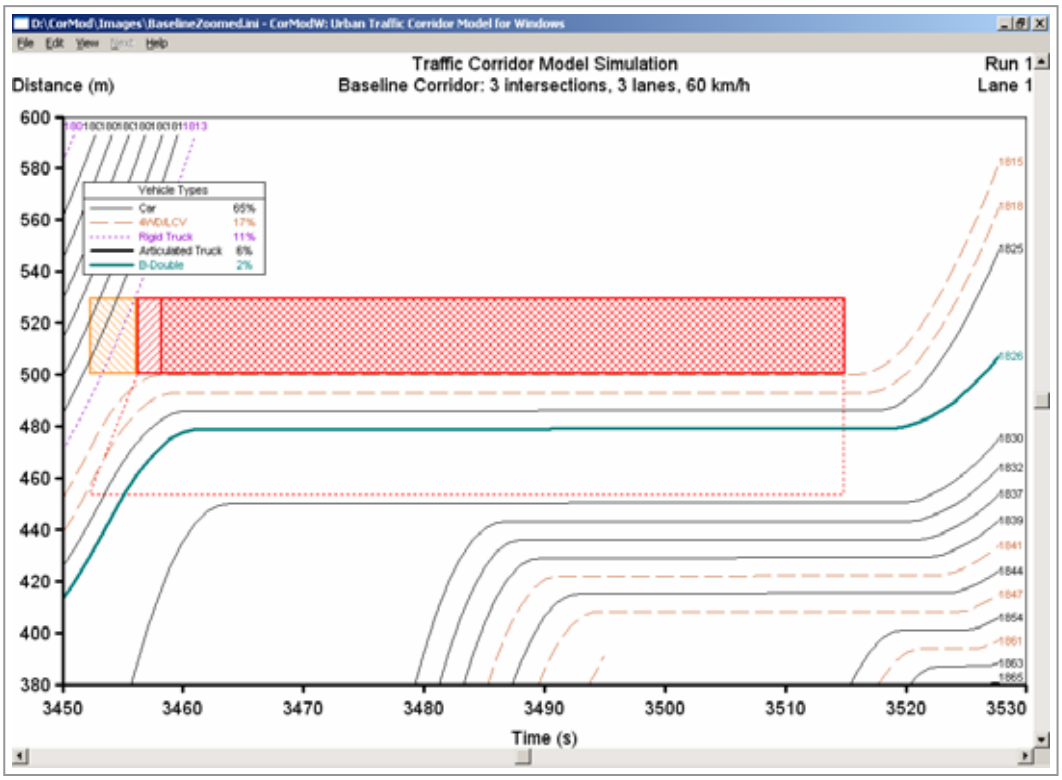


**Figure 8.13 – CorModW display, zoomed in on the rectangle highlighted in Figure 8.12**

## 8.7 Using the Program

### 8.7.1 Input data file format

**CorMod** uses a similar file format to the configuration settings files used by Microsoft Windows. These files usually have a `.ini` file extension.

The files are standard ASCII text files, divided into several sections that are indicated by rectangle braces. Within each section, there may be a number of keys that are assigned values.

```
[section]
key=value
```

A complete **CorMod** configuration settings file is shown in Figure 8.14. Separate sections are provided for headings, displays, location of the cordon lines, initialisation simulation and control parameters, the proportions and details of the vehicle types, the intersections, lanes and road sections. This figure provides most of the syntax for the configuration settings file.

```
;Corridor Model Initialisation File
;Euan Ramsay, Queensland University of Technology, 2006

;Note: Any characters after a semicolon are treated as a comment

[heading]
Title=Traffic Corridor Model Simulation
Subtitle=Baseline Corridor: 3 intersections, 3 lanes, 60 km/h

[display]
XMin=0
XMax=1600
XInc=200
TMin=3000
TMax=3600
TInc=100

[cordons]
XStart=100          ; position of start cordon line, metres
XFinish=2100        ; position of finish cordon line, metres
TStart=0            ; starting time for both cordon lines
TFinish=3600        ; finishing time for start cordon line
                    ;     finish cordon line is active until the very end

[initial]
TInit=-400          ; warm-up time
XInit=-100          ; vehicle generation position, metres
Flow=600            ; vehicles per hour per lane

[simulation]
Seed=1234567890     ; random number seed
DeltaT=0.1          ; time step, seconds
DeltaTLC=10         ; time between checking for lane changes, seconds
XEnd=2200           ; simulation stops when all vehicles pass this point,
metres
TEnd=4800           ; ... or when this time is reached

[control]
NRuns=1000          ; number of runs
ShowEachRun=false   ; display results of each run?
ShowExecTime=true   ; display how long the simulation took to execute?
PauseAtEnd=false    ; pause at end of simulation (useful if running
interactively)
ShowProgress=true   ; show current simulation time (console version)

[vehicletypes]      ; matches recorded vehicle proportions
Proportion1=0.65
Proportion2=0.165
Proportion4=0.111
Proportion9=0.059
Proportion10=0.015
```

**Figure 8.14 – Example CorMod input file**

**(continued on next page…)**

```
[vehicletype1]
Name=Car           ; name of this vehicle type
VehicleLength=5    ; vehicle length in metres
JamSpacing=7       ; queue length (jam spacing) in metres
MaxAccel=1.77      ; maximum acceleration (when v=0), in m/s^2
MaxSpeed=86        ; maximum speed (when a=0), in km/h
Deceleration=-3    ; constant deceleration (when stopping at signals), in m/s^2
MaxGrade=50        ; maximum grade (at which v=0), percentage
StartResponseTime=1 ; delay between green signal and start of acceln, seconds

[vehicletype2]
Name=4WD/LCV
VehicleLength=5
JamSpacing=7
MaxAccel=1.50
MaxSpeed=81
Deceleration=-3
MaxGrade=40
StartResponseTime=1

[vehicletype4]
Name=Rigid Truck
VehicleLength=9
JamSpacing=13
MaxAccel=0.89
MaxSpeed=96
Deceleration=-3
MaxGrade=30
StartResponseTime=4

[vehicletype9]
Name=Articulated Truck
ShortName=Artic Tr
VehicleLength=19
JamSpacing=23.3
MaxAccel=0.75
MaxSpeed=97
Deceleration=-3
MaxGrade=25
StartResponseTime=4

[vehicletype10]
Name=B-Double
VehicleLength=25
JamSpacing=29
MaxAccel=0.68
MaxSpeed=109
Deceleration=-3
MaxGrade=19
StartResponseTime=4

[intersection1]
Location=500           ; location of signal stop-line, metres
CycleTime=90           ; in seconds [same for downstream intersections]
MaxGreen=0.667         ; maximum green time, in seconds
;                        or as a proportion of cycle time
ProgressionSpeed=40    ; speed at which signals are coordinated to, in km/h

[intersection2]        ; takes default parameters from upstream intersection
Location=1000

[intersection3]
Location=1500

[lanes]
NumLanes=3
AllowLaneChanges=yes

[section1]
Start=0                ; (finishes when next section starts), metres
SpeedLimit=60          ; speed limit, km/h
Elevation=0            ; elevation at section start, metres
                       ;     used to calculate grade on previous section
```

**Figure 8.14 – Example CorMod input file (continued)**

### 8.7.2 Running CorModC and CorModW

The command line version **CorModC** is run from a Windows command line prompt. In Microsoft Windows, a command-line prompt can be started by selecting `Run` from the Windows Start menu, typing `cmd`, and pressing enter.

The default input file name is `Cormod.ini` – if this file does not exist and no input file name was specified on the command line, then the program will prompt for an input file name.

Output would normally be redirected to a text file, as shown below.

```
CorModC configuration_settings_file.ini > outputfile.txt
```

**CorModW** is a Windows program, the configuration file is selected by choosing File | Open… from the menu. Note that **CorModW** only executes one simulation of the traffic corridor, whereas **CorModC** typically executes multiple replications and reports the average results of these.

When the simulations have completed, the program outputs the summary results for the combined simulations. This is shown in Figure 8.15, representing the summary of 1000 simulation runs. Output consisted of the following tables:

The **Corridor Performance Table,** showing the average speed, travel time, stopped time and number of stops for each vehicle type.

The **Intersection Timing Table,** showing the cycle time and green time distributions for each intersection.

The **Lane Performance Table,** showing the queue length, delay and capacity of each lane at each intersection. Saturation flow and start loss were calculated using the method described in Appendix E of ARR-123 (Akçelik 1995).

The **Intersection Delay Tables,** showing the control delay and stopped time for each vehicle type at each intersection.

```
CorModC - Urban Traffic Corridor Model - console version
Traffic Corridor Model Simulation
No B-Doubles, replaced by artics & rigids

Over all 1000 runs:

                              Space Mean  Travel       Stopped      Number of
      Vehicle     Number of    Speed     Time (s)     Time (s)     Stops
       Type       Vehicles     (km/h)    Avg   SD.    Avg   SD.    Avg   SD.
------------------+----------+--------+------------+------------+------------
 1 Car               1168332   33.18   217.0  42.5   50.2  35.5   2.11  1.09
 2 4WD/LCV            298251   33.08   217.6  42.7   50.2  35.4   2.10  1.09
 4 Rigid Truck        232280   32.63   220.7  43.8   50.4  36.1   1.85  0.97
 9 Articulated Truck  140377   32.10   224.3  44.7   51.8  36.5   1.85  0.96
   All Vehicle Types 1839240   33.01   218.1  42.9   50.4  35.6   2.05  1.07
------------------+----------+--------+------------+------------+------------

                       Number    Average Cycle   Green Time (s)      Average
Intersection           of Cycles   Time (s)    Average   Std.Dev.   G/C Ratio
----------------------+----------+----------+----------+----------+----------
     1                   40000       90.0       34.6        5.9       0.385
     2                   40000       90.0       32.3        7.5       0.359
     3                   40000       90.0       32.6        6.2       0.362
----------------------+----------+----------+----------+----------+----------

                   Queue      Queued   QueueClear  Satn  Start  Lost
                 Length (m)  Vehicles   Time (s)   Flow  Loss   Time Capacity
                  Avg  SD.   Avg  SD.   Avg  SD. (veh/h)  (s)    (s)  (veh/h)
----------------+----------+----------+----------+------+------+------+------
Intersection 1
Lane 1            130   63  11.0  4.9  24.6  8.4   1814   6.03  10.05    616
Lane 2            126   59  10.7  5.1  24.4  8.7   1768   5.93   9.89    604
Lane 3            130   62  10.9  5.0  24.6  8.5   1816   6.03  10.05    617
All Lanes         163    0  32.6  0.0  29.7  0.0   5398    n/a    n/a   1837
----------------+----------+----------+----------+------+------+------+------
Intersection 2
Lane 1             99   94   6.2  5.2  13.1  9.8   1877   4.25   8.33    625
Lane 2             95   89   6.3  5.2  13.5  9.8   1858   4.19   8.25    620
Lane 3             99   94   6.2  5.2  13.1  9.7   1878   4.25   8.33    625
All Lanes         144    0  18.7  0.0  20.7  0.0   5612    n/a    n/a   1870
----------------+----------+----------+----------+------+------+------+------
Intersection 3
Lane 1             73   68   5.9  4.3  13.2  9.0   1968   4.51   8.68    654
Lane 2             74   66   6.1  4.4  13.8  9.2   1960   4.49   8.65    652
Lane 3             74   68   6.0  4.4  13.4  9.1   1967   4.51   8.68    654
All Lanes         112    0  17.9  0.0  20.4  0.0   5896    n/a    n/a   1961
----------------+----------+----------+----------+------+------+------+------

                      Control Delay / Cycle (s)   Control Delay / Stopped Veh
                      _______Intersection_______   _______Intersection_______
Vehicle Type             1        2        3         1        2        3
---------------------+--------+--------+--------+++--------+--------+--------
 1 Car                 628.9    543.3    639.4       46.7     34.2     22.7
 2 4WD/LCV             175.6    147.3    161.5       47.4     34.1     22.8
 4 Rigid Truck         166.2    132.6    123.9       49.5     33.5     23.3
 9 Articulated Truck   138.0     96.2     76.5       49.2     36.4     26.1
   All Vehicle Types  1108.6    919.5   1001.3       47.5     34.3     23.0
---------------------+--------+--------+--------+++--------+--------+--------

                       Stopped Time / Cycle (s)    Stopped Time / Stopped Veh
                      _______Intersection_______   _______Intersection_______
Vehicle Type             1        2        3         1        2        3
---------------------+--------+--------+--------+++--------+--------+--------
 1 Car                 440.5    300.3    226.0       32.7     18.9      8.0
 2 4WD/LCV             122.7     80.8     55.9       33.1     18.7      7.9
 4 Rigid Truck         110.0     69.1     40.5       32.7     17.5      7.6
 9 Articulated Truck    86.9     51.8     26.7       31.0     19.6      9.1
   All Vehicle Types   760.1    502.0    349.1       32.6     18.7      8.0
---------------------+--------+--------+--------+++--------+--------+--------
```

**Figure 8.15 – Output file produced by CorModC**

An additional output table, the **Queue Position Classification Matrix** was used in some cases to display the proportion of vehicles of each type appearing in each queue position of a specified lane (see Figure 8.16). This required that the following command be included in the intersection section of the input file:

`QueuePosClassLane`*n*`=true`

If *n* = 0 then the queue position classification matrix was displayed for all lanes at the specified intersection, otherwise it was only displayed for the $n^{th}$ lane.

```
Queue Position Classification Matrix, Intersection 1, All Lanes:

Queue    Class 1     Class 2     Class 4     Class 9    Class 10      Total
Pos.      n   %       n   %       n   %       n   %       n   %         n
-----+-----------+-----------+-----------+-----------+-----------+-----------
 1     8751 63.0   2212 15.9   1531 11.0   1114  8.0    277  2.0     13885
 2     8949 66.0   2303 17.0   1429 10.5    705  5.2    164  1.2     13550
 3     8657 65.4   2251 17.0   1470 11.1    680  5.1    184  1.4     13242
 4     8428 65.3   2145 16.6   1417 11.0    718  5.6    189  1.5     12897
 5     8142 65.3   2096 16.8   1371 11.0    687  5.5    175  1.4     12471
 6     7761 65.0   1994 16.7   1290 10.8    692  5.8    200  1.7     11937
 7     7360 65.3   1880 16.7   1188 10.5    676  6.0    166  1.5     11270
 8     6828 64.5   1795 16.9   1187 11.2    635  6.0    148  1.4     10593
 9     6364 64.7   1662 16.9   1081 11.0    574  5.8    161  1.6      9842
10+   43519 64.5  11062 16.4   7716 11.4   4137  6.1   1061  1.6     67495
-----+-----------+-----------+-----------+-----------+-----------+-----------
Green Hold actuated 674 times. Average hold time 2.98 s.
```

**Figure 8.16 – Queue position classification matrix produced by CorModC**

## 8.8 Verification and Testing of the Program

Several basic tests of the program were undertaken in order to confirm its correct operation in simulating traffic progressing along an urban corridor.

The details of some of those tests are included below.

### 8.8.1 Test of queue formation and release at a signalised intersection

Figure 8.17 shows a CorModW display of a short single lane corridor with fixed-time signalised intersection. All vehicles arrive at a uniform headway of 6 seconds, corresponding to a flow of 600 vehicles per hour. The vehicles are all designated as cars, having the same acceleration and jam spacing. Vehicles can be seen to decelerate to stop at the signalised intersection, and to form a growing queue whilst there are stationary vehicles in front of them.

Queue discharge commences a short time (a specifiable reaction time) after the signal turns to green. Following vehicles start accelerating shortly after their leaders do, resulting in saturation flow until the queue clears. There is a period of unsaturated flow, followed by the red signal in the next cycle.

This behaviour corresponds with the queue formation and release behaviour that is the basis for much of the signalised intersection theory described in Chapter 3. This is a strong indication of the appropriateness of the car-following model implementation in this program.

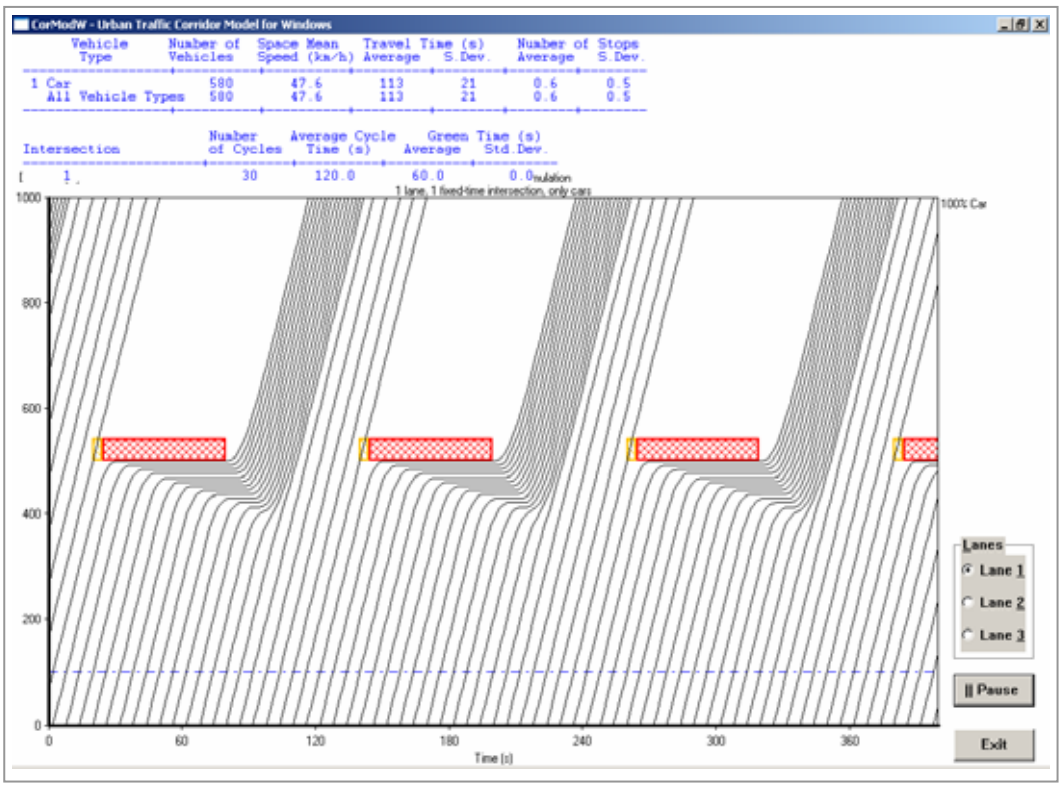


**Figure 8.17 – Test of car following model implementation in CorModW**

### 8.8.2 Trace of vehicles through a queue

**CorMorC** includes an option to produce a detailed trace of vehicles passing through a specified intersection in a specified lane. A multi-lane corridor with several intersections was created, and the behaviour of vehicles recorded as they passed through one of the intersections.

Figure 8.18 is the corresponding **CorModC** intersection queue output, showing the times that each vehicle passes the intersection stop line if it is green, or starts to decelerate, stops, starts to accelerate and reaches the free flow speed if the signal is red.

Vehicles #256 and #277 may be traced through the intersection queue output; their records are **bold** and boxed, respectively. Vehicle #277 can be seen to have made an incomplete stop, decelerating to 36 km/h at a distance of 87 m from the intersection stop line.

At the end of each cycle, the intersection queue output reports the number of queued vehicles, queue length, and queue clearance time. The current estimates of the saturation flow, start loss and capacity are reported, using the method given in Appendix E of ARR-123 (Akçelik 1995).

Figure 8.19 shows the corresponding **CorModW** display zoomed in on the intersection. Each vehicle is numbered, as indicated when their trajectories leave the graph windows. Vehicle #253 is a car that enters the intersection towards the end of the yellow period, exiting the other end of the intersection during the all-red time. The next vehicle, #256 is a rigid truck that must stop, arriving at the front of the queue, and vehicle #277 is an articulated truck arriving at the back of the queue but not having to stop. This confirms the information presented in the intersection queue output.

```
T= 233.60 I=1 L=1 Veh  250 Passes intxn. NX=11 TX=28.70s v=60km/h
T= 238.30 I=1              Show   YELLOW. G=33.4s. [Lane 3 Gapped Out]
T= 240.80 I=1 L=1 Veh  253 Passes intxn. NX=12 TX=35.90s v=60km/h
T= 242.30 I=1              Show   RED.   AR=2.0s
T= 244.30 I=1              Start  Opposing Movement.
T= 245.00 I=1 L=1 Veh  256 Brakes approaching queue  from  60km/h at 450m
T= 249.00 I=1 L=1 Veh  238 Has reached a cruising speed of 60km/h at 887m
T= 251.00 I=1 L=1 Veh  256 Starts queue. NQ= 1, LQ=13.0m
T= 251.20 I=1 L=1 Veh  259 Brakes approaching queue  from  60km/h at 433m
T= 258.00 I=1 L=1 Veh  259 Joins  queue. NQ= 2, LQ=20.0m
T= 258.00 I=1 L=1 Veh  262 Brakes approaching queue  from  60km/h at 427m
T= 264.40 I=1 L=1 Veh  265 Brakes approaching queue  from  60km/h at 413m
T= 264.70 I=1 L=1 Veh  262 Joins  queue. NQ= 3, LQ=33.0m
T= 271.20 I=1 L=1 Veh  265 Joins  queue. NQ= 4, LQ=40.0m
T= 271.20 I=1 L=1 Veh  268 Brakes approaching queue  from  60km/h at 407m
T= 277.90 I=1 L=1 Veh  268 Joins  queue. NQ= 5, LQ=47.0m
T= 278.00 I=1 L=1 Veh  271 Brakes approaching queue  from  60km/h at 400m
T= 284.40 I=1 L=1 Veh  274 Brakes approaching queue  from  60km/h at 387m
T= 284.70 I=1 L=1 Veh  271 Joins  queue. NQ= 6, LQ=60.0m
T= 284.90 I=1              End of Cycle.  C=80.0s

T= 284.90 I=1              Show   GREEN.
T= 288.90 I=1 L=1 Veh  256 Leaves queue.
T= 288.96 I=1 L=1 Veh  256 Passes intxn. NX= 1 TX= 4.06s v= 0km/h
T= 289.70 I=1 L=1 Veh  259 Leaves queue.
T= 290.50 I=1 L=1 Veh  262 Leaves queue.
T= 291.10 I=1 L=1 Veh  274 Joins  queue. NQ= 7, LQ=67.0m
T= 291.20 I=1 L=1 Veh  277 Brakes approaching queue  from  60km/h at 380m
T= 291.30 I=1 L=1 Veh  265 Leaves queue.
T= 292.10 I=1 L=1 Veh  268 Leaves queue.
T= 292.90 I=1 L=1 Veh  271 Leaves queue.
T= 293.70 I=1 L=1 Veh  274 Leaves queue. End of Queue
T= 293.70 I=1 L=1 Veh  277 Incomplete stop, starting from  36km/h at 413m
T= 295.14 I=1 L=1 Veh  259 Passes intxn. NX= 2 TX=10.24s v=16km/h
T= 297.46 I=1 L=1 Veh  262 Passes intxn. NX= 3 TX=12.56s v=20km/h
T= 300.21 I=1 L=1 Veh  265 Passes intxn. NX= 4 TX=15.31s v=25km/h
T= 301.96 I=1 L=1 Veh  268 Passes intxn. NX= 5 TX=17.06s v=27km/h
T= 303.79 I=1 L=1 Veh  271 Passes intxn. NX= 6 TX=18.89s v=29km/h
T= 305.99 I=1 L=1 Veh  274 Passes intxn. NX= 7 TX=21.09s v=33km/h Queue Cleared
T= 307.81 I=1 L=1 Veh  277 Passes intxn. NX= 8 TX=22.91s v=32km/h
T= 310.82 I=1 L=1 Veh  280 Passes intxn. NX= 9 TX=25.92s v=37km/h
T= 313.49 I=1 L=1 Veh  283 Passes intxn. NX=10 TX=28.59s v=49km/h
T= 318.20 I=1 L=1 Veh  256 Has reached a cruising speed of 60km/h at 784m
T= 320.00 I=1 L=1 Veh  286 Passes intxn. NX=11 TX=35.10s v=60km/h
T= 321.70 I=1              Show   YELLOW. G=36.8s. [Lane 3 Gapped Out]
T= 324.20 I=1 L=1 Veh  289 Brakes approaching queue  from  60km/h at 450m
T= 325.70 I=1              Show   RED.   AR=2.0s
T= 327.70 I=1              Start  Opposing Movement.
T= 327.80 I=1 L=1 Veh  277 Has reached a cruising speed of 60km/h at 765m
T= 328.40 I=1 L=1 Veh  259 Has reached a cruising speed of 60km/h at 929m
T= 328.90 I=1 L=1 Veh  265 Has reached a cruising speed of 60km/h at 891m
T= 329.60 I=1 L=1 Veh  271 Has reached a cruising speed of 60km/h at 858m
T= 330.20 I=1 L=1 Veh  289 Starts queue. NQ= 1, LQ=7.0m

Cycle #5, Lane 1
For the queue which discharged in the preceding green period...

Max Queue Length     = 67.0 m
Max Queued Vehicles  =    7
Queue Clearance Time = 21.1 s

Queue discharge counters (Refer ARR123, Appendix E):
x1=17, x2=18, x3=1, x4=82, n1=5, n3=1, n4=5
Saturation Flow = 2032 veh/h  Start Loss   =  4.7 s  Inter Green  =  6.0 s
Start Lag       = 10.7 s      End Lag      =  1.8 s  Lost Time    =  8.9 s
Displayed Green = 36.8 s   Effective Green = 33.9 s  Cycle Time   = 80.0 s
Capacity        =  861 veh/h
```

**Figure 8.18 – Extract of intersection queue output, matching Figure 8.19**

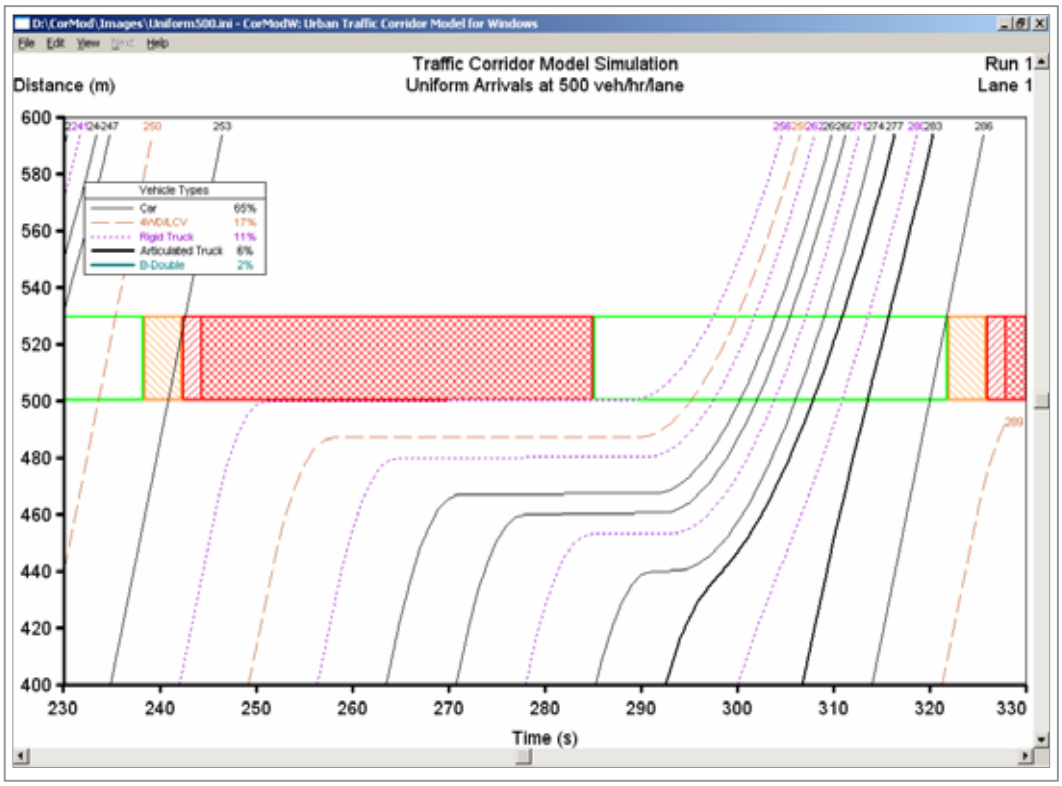


**Figure 8.19 – Vehicle trajectories corresponding to Figure 8.18**

### 8.8.3 Demonstration of the "Red Wave"

Figure 8.20 shows a theoretical demonstration of the "Red Wave" that was reported earlier (TTM Consulting 1987; Ramsay 1998).

Several specific conditions were used to ensure that the Red Wave would appear:

- Intersection timing parameters were selected to give a limited bandwidth for traffic progression, by specifying a short cycle time of 60 seconds and green time of 25 seconds
- The progression design speed (PDS), specifying the offsets between adjacent traffic signals on a common timing plan, was set to match the posted speed limit. Common practice would be to set the PDS at a lower value than the speed limit.
- A constant gradient of 5% was used on the corridor to further reduce the heavy vehicle acceleration rates

- A single lane corridor was used, preventing the lane changing that would otherwise occur around a slow-moving vehicle

Traffic arrives at uniform headways, progressing along the corridor at the same speed to which the signals are coordinated. A B-double, indicated by the thick dark line in the figure, stops at one of the intersections and having a slower acceleration rate than the cars, takes a longer time to accelerate up to the desired speed. This results in it arriving at the next signalised intersection just as it had changed to red. The same occurs at all of the intersections on the corridor. Cars are prevented from changing lanes in this simulation, and so form an ever-increasing queue behind the slow vehicle.

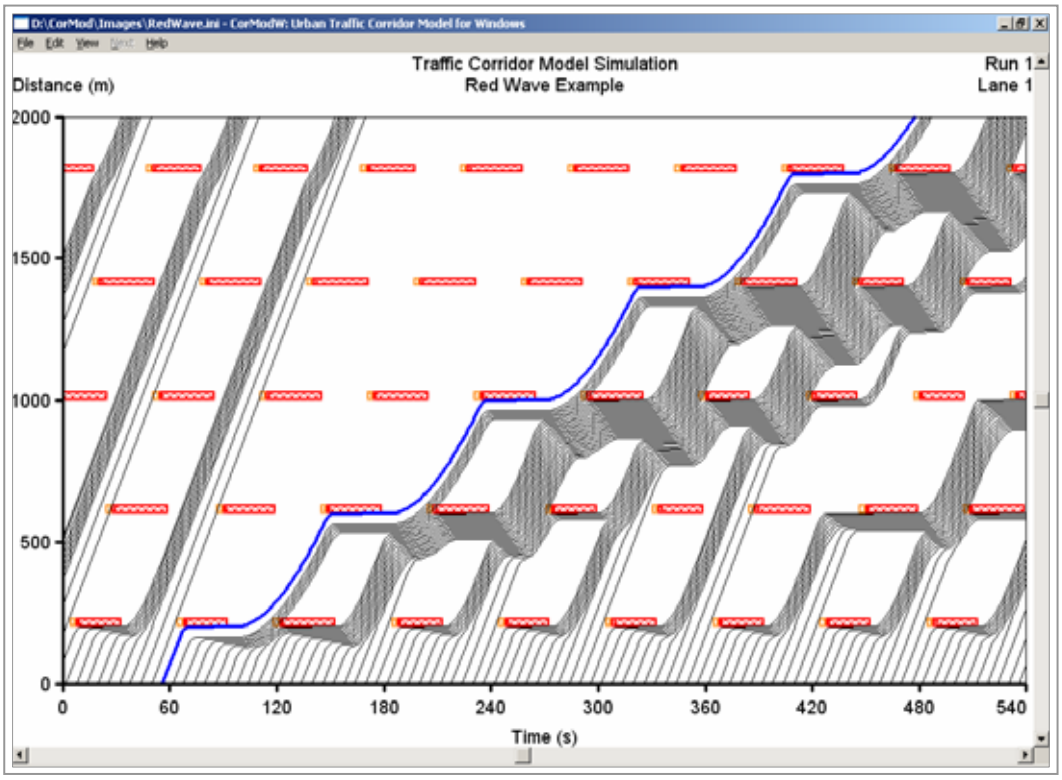


**Figure 8.20 – Demonstration of the "Red Wave" using CorModW**

It should be noted that this extremity of traffic operation has only been presented to illustrate a specific concept. As listed above, several undesirable traffic operational practices were required for the Red Wave to appear; in normal traffic operations such an extreme condition would not occur, and was not evident in CorMod simulations of more realistic traffic conditions.

## 8.9 Conclusions of this Chapter

A corridor-level traffic model has been developed, that is capable of simulating the progression of vehicles having different characteristics along a multi-lane corridor. Each vehicle moves along the corridor from start to finish, obeying speed limits and signalised intersections, maintaining a safe headway to the vehicle in front, and changing lanes when it is advantageous and safe to do so.

Two versions of the program have been developed: The first (**CorModC**) is an efficient command-line based program that intended to perform multiple replications of the same simulation using different random numbers. The second version (**CorModW**) is a Windows program that displays the trajectory diagram of the simulation for interpretation, debugging and presentation purposes.

Operation of the model has been verified by examining its behaviour in both theoretical and realistic situations.

The next chapter describes the parametric study that was undertaken to test the model in detail, and examines sensitivities of model outputs to the input parameters.

# CHAPTER 9 PARAMETRIC STUDY USING THE TRAFFIC CORRIDOR SIMULATION MODEL

## 9.1 Introduction to this Parametric Study

This chapter describes the application of the model to a simple urban traffic corridor. This is to ensure the correct operation of the model and to determine the sensitivity to input parameter values.

## 9.2 Baseline Test Conditions

### 9.2.1 Test corridor

The test corridor consisted of a three-lane single-direction road section, as shown in Figure 9.1. Three intersections, spaced 500 metres apart, were included on the corridor. The intersections operated at a common cycle time, with the offsets between adjacent intersections being specified by dividing the relative distance by the progression design speed (PDS).

Two cordon lines were placed on the corridor, spaced 2000 metres apart and encompassing all three intersections. The travel times, speeds and stop rates were measured between these two cordons.

This baseline corridor was on a level surface, without any grade. The effect of grade is examined separately in a section of this chapter.

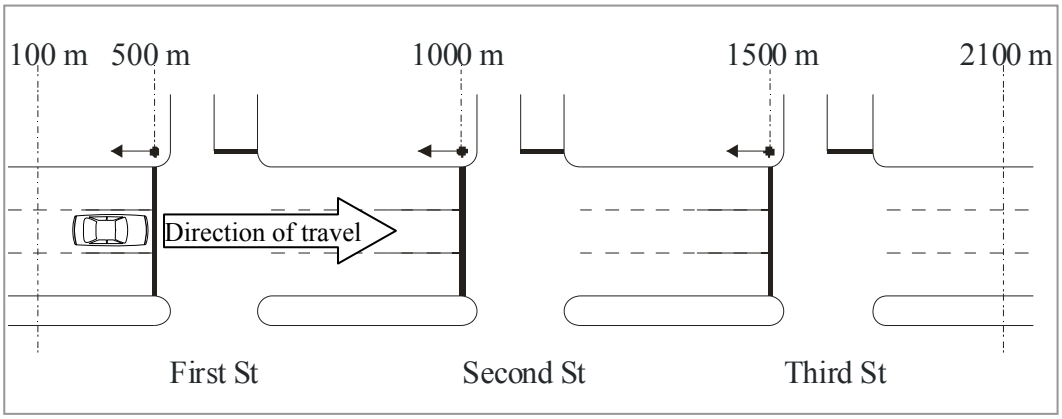


**Figure 9.1 – Test corridor**

There was no alternative corridor for the vehicles to use. In reality, it would be expected that some diversion to alternative routes would occur, and even long-term land-use patterns may occur, because of a reduction in the level of service on a route. Conversely, improvements to the corridor would be expected to lead to additional traffic being attracted to the corridor.

## 9.3 Test Traffic Composition

Vehicle proportions were as recorded by the automatic traffic counter-classifier (see Chapter 6) in the daytime inter-peak period. Heavy vehicles were found to be less numerous during either the morning or afternoon peak periods, so it was considered to be a more appropriate test of their effect on traffic performance if the daytime inter-peak vehicle composition was used as the base case.

**Table 9.1 – Proportion of each vehicle type used in the baseline simulation**

| *Vehicle Type* | *Austroads Classes* | *Proportion* |
|---|---|---|
| Car | 1 | 65.0 % |
| 4WD/ LCV | 1,2 | 16.5 % |
| Rigid Truck | 3, 4, 5 | 11.1 % |
| Articulated Truck | 6, 7, 8, 9 | 5.9 % |
| B-double | 10 | 1.5 % |
| B-triple | 11 | 0.0 % |

### 9.3.1 Base case scenario

A warm-up time of 400 seconds was used, representing at least twice the time taken for a typical vehicle to travel over the corridor. This allowed time for traffic to reach an equilibrium state before recording of vehicle travel statistics was commenced. The actual recording of travel statistics ran for 3600 seconds, and the simulation terminated after all vehicles had passed through the corridor or the time limit of 6000 seconds was exceeded.

A total of 1000 repeat runs were conducted for each scenario, each using a different random number seed. This large number of simulations was used to minimise the inter-run variability associated with stochastic simulations.

### 9.3.2 Performance measures

**CorMod** records the instantaneous positions and speeds of each vehicle on the corridor, and reports many intersection- and vehicle type-specific performance measures (see Figure 8.15 in the previous chapter). In order to provide a more concise and readily-interpretable comparison of parameter sensitivities and of alternative scenarios, the following two primary performance measures were used in this and following chapters:

- The average speed of each vehicle type between the two ends of the corridor. This is also referred to as "space mean speed", to indicate that the average is being taken of the speeds of all vehicles in the space between the two ends of the corridor.
- The average number of stops of each vehicle in each vehicle type in travelling between the two ends of the corridor.

It should be noted at this stage that delay is one of the more commonly used performance measure for comparison of alternative scenarios, being the performance measure used by the Highway Capacity Manual to determine the Level of Service of a facility. Delay was not used as a primary performance measure in this project since it is dependent upon the length and number of intersections on the corridor, and it can be easily derived from the average speed of vehicles on the corridor.

The average speed was considered to be a more appropriate measure since it is normalised, being independent of the length or number of intersections on the corridor and is more-readily interpretable – a specified average speed on the corridor is generally better understood by both technical and lay audiences than a specified number of seconds delay.

Travel time may also be derived from the average speed by multiplying it by the corridor length. Costs associated with travel time for passenger and freight vehicles can then be calculated, as has been done at the end of the next chapter.

The number of stops is also used as a primary performance measure, since it is closely related to the acceleration and braking requirements and hence to several secondary measures such as noise, fuel consumption and emissions, pavement wear and vehicle maintenance costs.

Problems may arise in having two primary performance measures, particularly when trying to optimise for multiple objectives. It is common practice to consider a weighted average of the various performance measures, finding an optimum that maximises (or minimises if appropriate) the weighted average measure.

It should also be noted that these two primary performance measures are closely related – increasing the number of stops generally decreases the average speed along the corridor. Thus, an optimum solution that minimises the number of stops would be expected to be close to that which maximises the average speed. This was found when optimising the progression design speed of signals along the corridor, as reported in the next chapter.

## 9.4 Effect of Varying Traffic Volume

The traffic volume was varied from 100 to 900 vehicles per hour per lane in increments of 100. In reality, with a fully vehicle-actuated signal system, the green times on all approaches would increase with the approach flows; resulting in an increase in cycle time. Since **CorMod** did not explicitly model the opposing traffic, an external means of replicating this increase in cycle time was required.

### 9.4.1 Estimating the appropriate cycle time as volume is varied

The intersection cycle analysis data recorded by STREAMS was used to estimate how the cycle time varied throughout the day as approach volumes changed.

Figure 9.2 shows an example of this variation in cycle time with approach volume. Cycle times are lowest during off-peak periods when volumes are low, and increase with increasing volumes towards a maximum value.

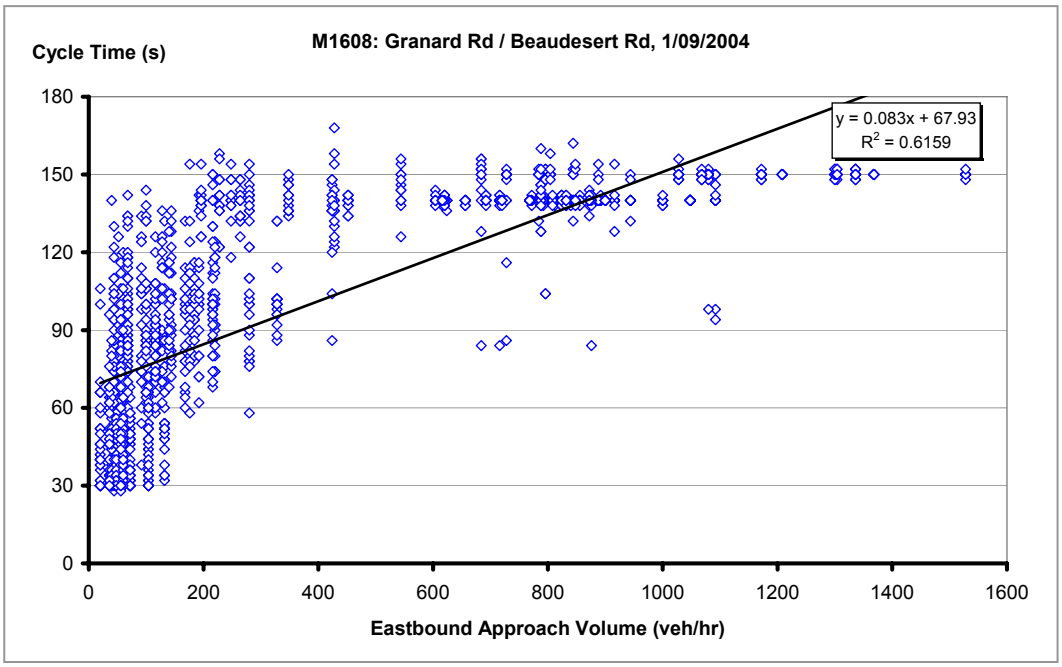


**Figure 9.2 – Typical variation in cycle time with approach volume**

An examination of STREAMS data for a range of typical intersections on the Brisbane Urban Corridor indicated that cycle times varied from approximately 40 seconds at night through to 130 seconds in peak periods. Corresponding volumes typically varied from 100 through to 900 vehicles per hour per lane. Based on these ranges, an empirical relationship (Equation 9.1) was used to relate cycle time, $C$, to the volume per lane, $q$, on the arterial corridor.

$$C = 40 + 0.1\,q \qquad \text{Equation 9.1}$$

This replicated the greater green times allocated to both the corridor and opposing traffic as volumes increase with a vehicle-actuated signal system. Maintaining the same inter-green times, the cycle times increase accordingly. This removes the need to model the opposing traffic within **CorMod** explicitly.

The intention of varying cycle time with volume was to maintain a relatively constant $G$ / $C$ ratio. As described in an earlier chapter, **CorMod** used a vehicle-actuated signal algorithm to determine the green time for the through movement. Green time was initially set at a minimum value and extended by a fixed amount with the passing of each vehicle until a maximum is reached. As shown in Figure 9.3, this simple linear relationship between cycle time and volume gave a $G$ / $C$ ratio of between 0.32 and 0.41 as the volume of traffic on the corridor was varied.

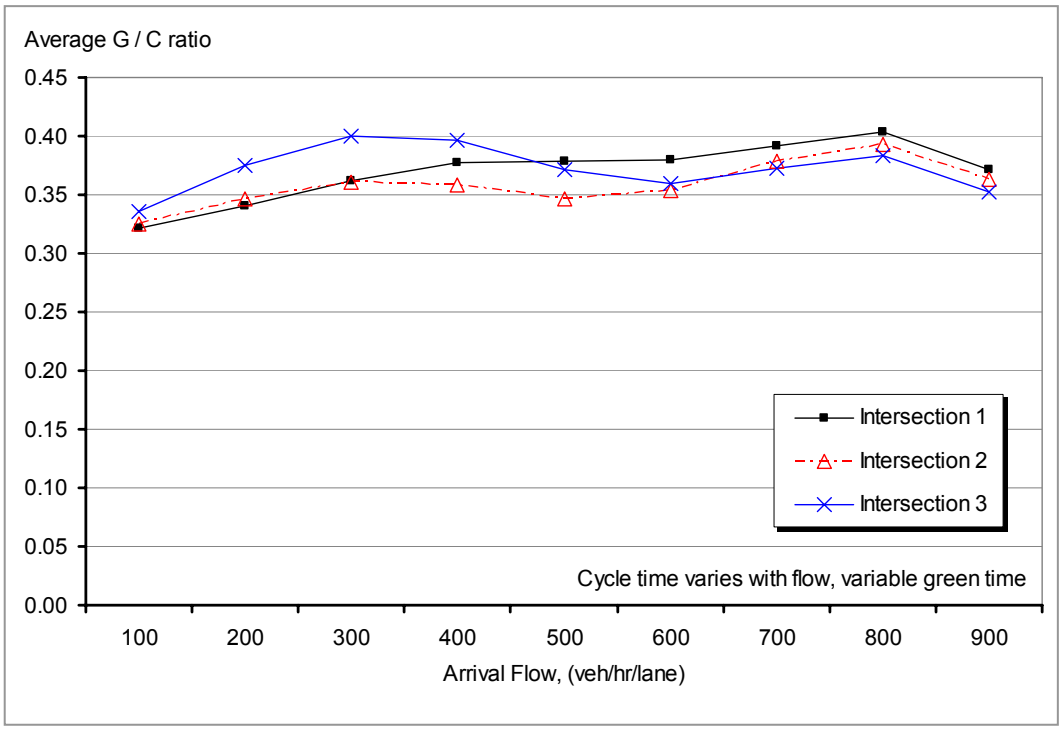


**Figure 9.3 – Ratio of green time to cycle time plotted against arrival flow**

Table 9.2 shows the general decrease in space mean speeds for all vehicle types as the arrival flow was increased. In the context of this chapter, space mean speed is approximated as the distance between the two cordon lines divided by the average travel time taken for vehicles to travel between them.

**Table 9.2 – Speeds of different vehicle types at various arrival flows**

| | *Space Mean Speed (km/h) by Arrival Flow (veh/h/lane)* | | | | | | | | |
|---|---|---|---|---|---|---|---|---|---|
| *Vehicle Type* | *100* | *200* | *300* | *400* | *500* | *600* | *700* | *800* | *900* |
| Car | 38.7 | 40.5 | 40.8 | 40.1 | 37.6 | 33.5 | 27.3 | 19.1 | 16.1 |
| 4WD / LCV | 38.3 | 40.2 | 40.5 | 39.9 | 37.5 | 33.4 | 27.3 | 19.1 | 16.1 |
| Rigid Truck | 37.4 | 39.3 | 39.7 | 39.1 | 36.9 | 32.9 | 27.0 | 19.0 | 16.0 |
| Articulated Truck | 36.8 | 38.7 | 39.1 | 38.6 | 36.3 | 32.4 | 26.6 | 18.9 | 15.9 |
| B-Double | 37.2 | 38.7 | 38.9 | 38.3 | 36.0 | 32.0 | 26.2 | 18.6 | 15.7 |
| All Vehicle Types | 38.3 | 40.2 | 40.5 | 39.8 | 37.4 | 33.3 | 27.2 | 19.1 | 16.0 |

### 9.4.2 Vehicle type-specific results

Speeds of all vehicle types can be seen to have generally decreased with increasing flow on the corridor, as is also shown in Figure 9.4.

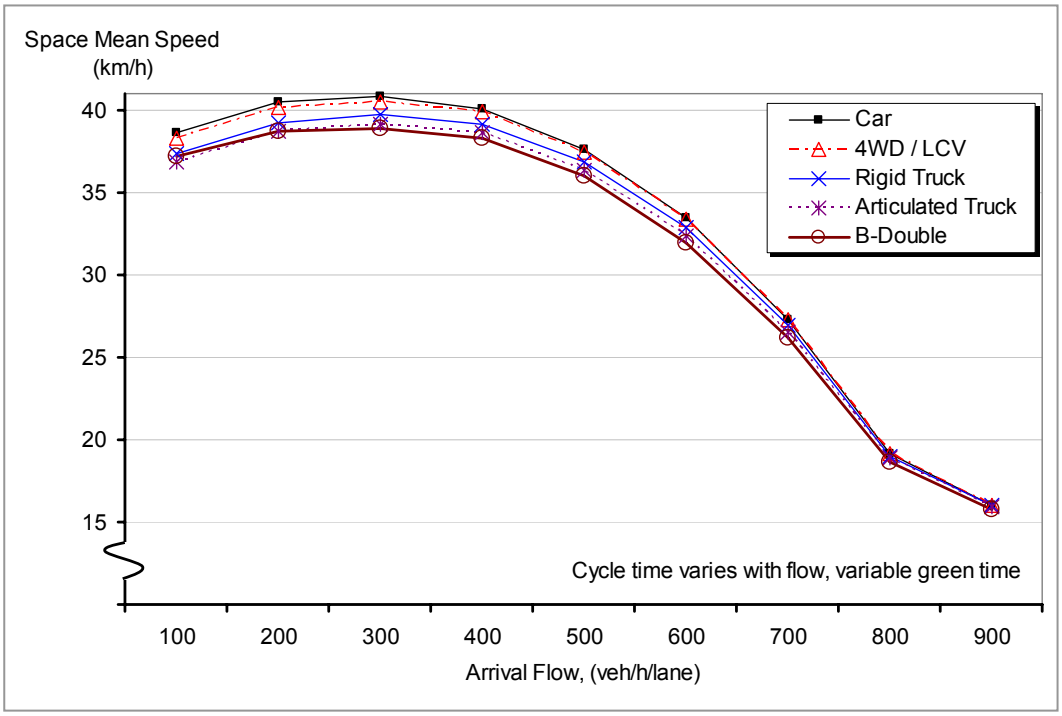


**Figure 9.4 – Speeds of different vehicle types at various arrival flows**

The slight increase in speeds at low flow rates (from 100 to 300 vehicles per hour) was an outcome of the vehicle-actuated signal control strategy, resulting in the slight increase in the green time ratio between these flows (Figure 9.3). Although the empirical linear relationship between flow and cycle time intended to maintain a relatively constant $G$ / $C$, it did not do so at low flows.

Few differences are evident in the speeds of the different vehicle types, particularly at very high flow rates, where congestion levels reduce speeds significantly for all vehicles.

Stop rates also increased dramatically with increasing arrival flow, as can be seen in Figure 9.5. At low flows, heavy vehicles had a slightly lower stop rate than light vehicles. This is attributed to the greater headway being maintained by the heavy vehicles leading to them being less likely to come to a complete stop when

arriving at the back of a queue at a signalised intersection. Stopped time also increases with arrival flow, as seen in Figure 9.6.

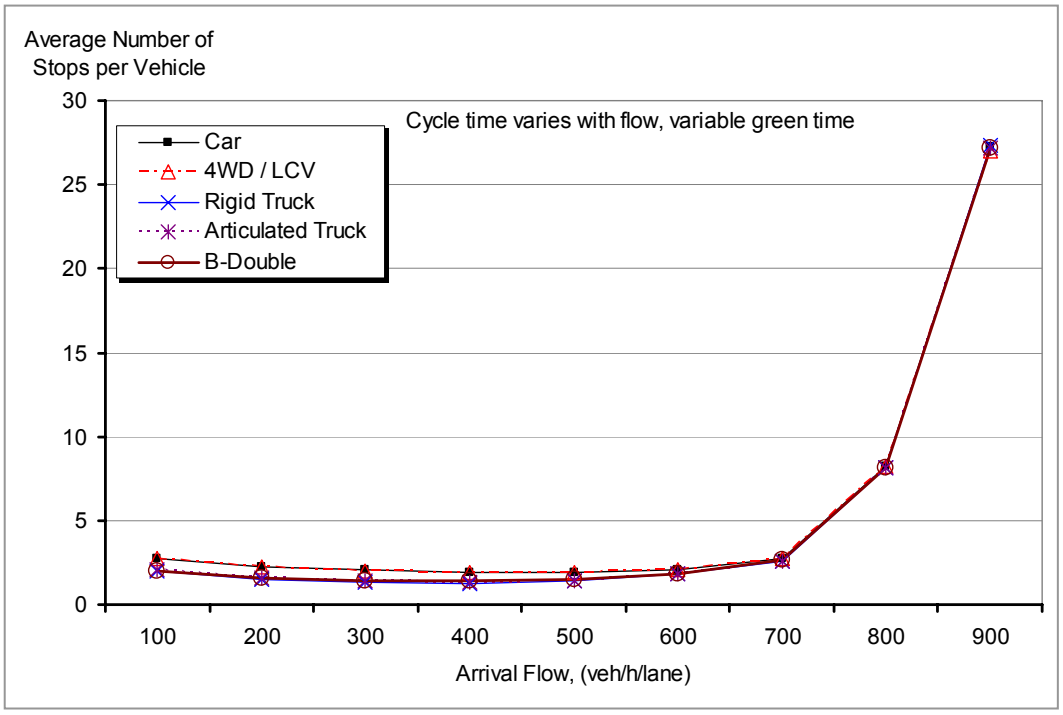


**Figure 9.5 – Stop rates of different vehicle types at various arrival flows**

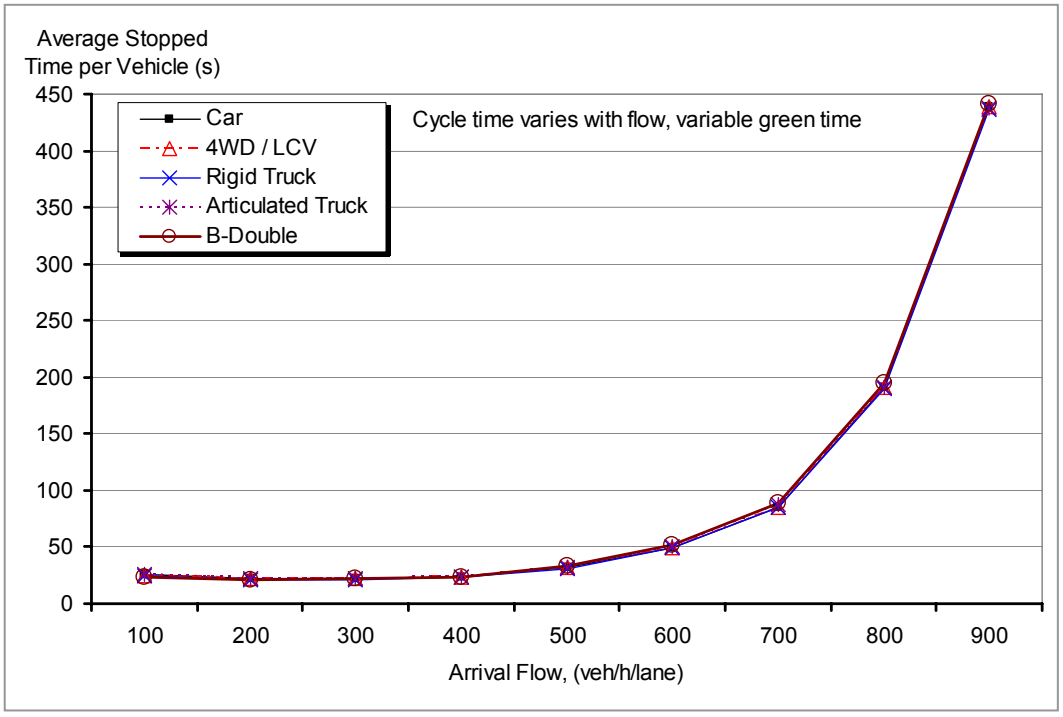


**Figure 9.6 – Stopped time per vehicle for different vehicle types at various arrival flows**

There is negligible difference in the stopped time between the vehicle types, despite the lower stop rate of heavy vehicles. This is attributed to the greater time taken to start a heavy vehicle than a light vehicle after the signal changes to green or the leading vehicle starts, as described in Chapter 2. The net effect of having fewer stops due to the greater headway in front of a heavy vehicle but each stop lasting longer is to have a comparable stopped time for heavy and light vehicles.

### 9.4.3 Intersection-specific results

Figure 9.7 shows the increase in the number of queued vehicles (averaged across the three lanes) at each of the intersections as the arrival flow rate increases. The greater queue length at intersection 1 was due the random arrivals at this intersection. Downstream intersections (2 and 3) had platooned arrivals, and the timing of signals modelled on the corridor ensured that a majority of the arrivals at these intersections were during the green period. This resulted in lower queue lengths and delays at these downstream intersections.

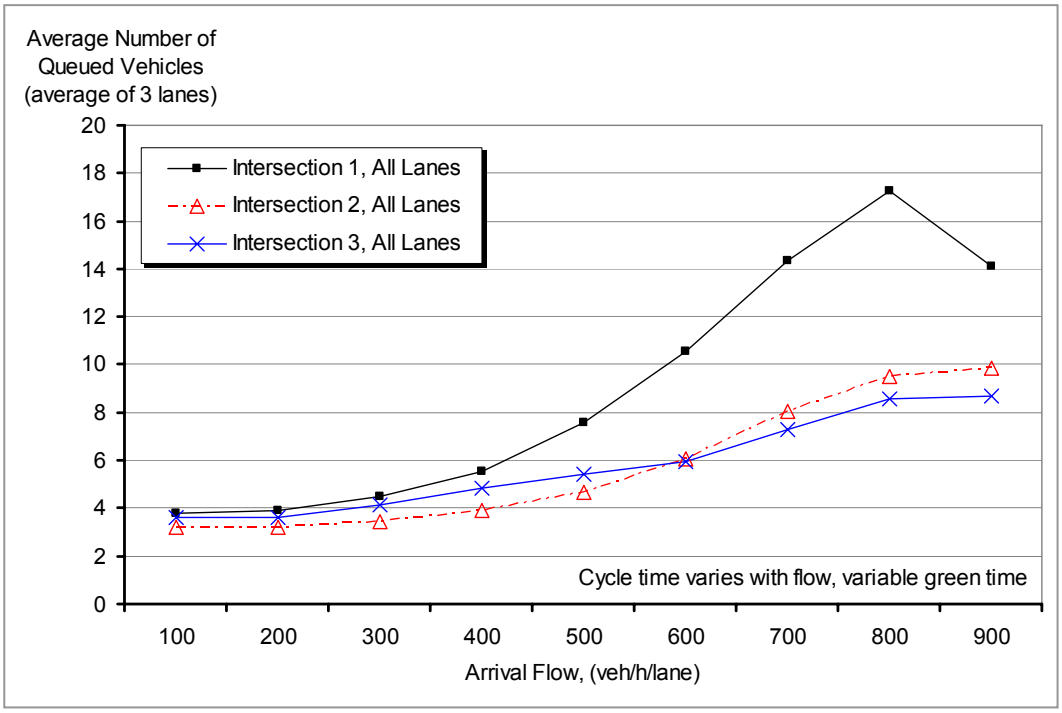


**Figure 9.7 – Number of queued vehicles plotted against arrival flow**

This is also evident in Figure 9.8, which shows that the queue clearance times for the downstream intersections (having more arrivals during their green periods) were lower than for intersection 1 with random arrivals.

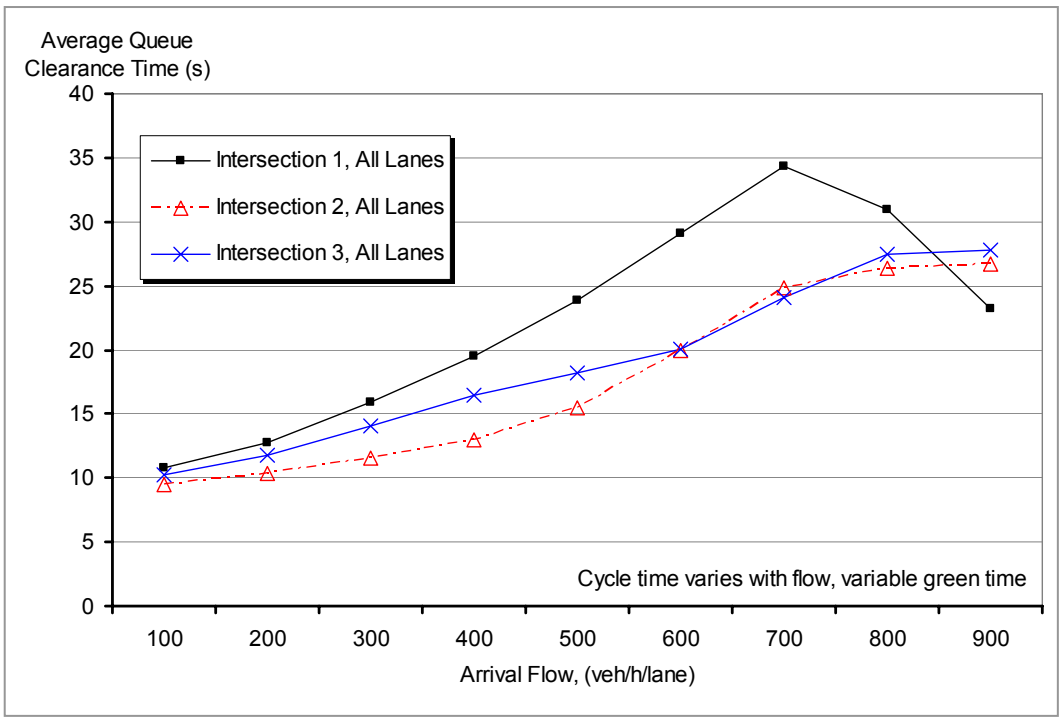


**Figure 9.8 – Queue clearance time plotted against arrival flow**

The reduction in queue length and clearance time at intersection 1 at very high arrival flows (800+ vehicle per hour per lane) was attributed to the queue building p beyond the point at which vehicles were being generated, leading to an under estimation of the number of queued vehicles and queue length. Intersections 2 and 3 did not exhibit this, since their approach volumes were limited by what could be discharged from intersection 1. Figure 9.9 demonstrates this, showing the trajectory diagram of an oversaturated corridor. The queue continuously builds up at intersection 1, which was only able to release a limited number of vehicles in each cycle. This was sufficient for the downstream intersections to service.

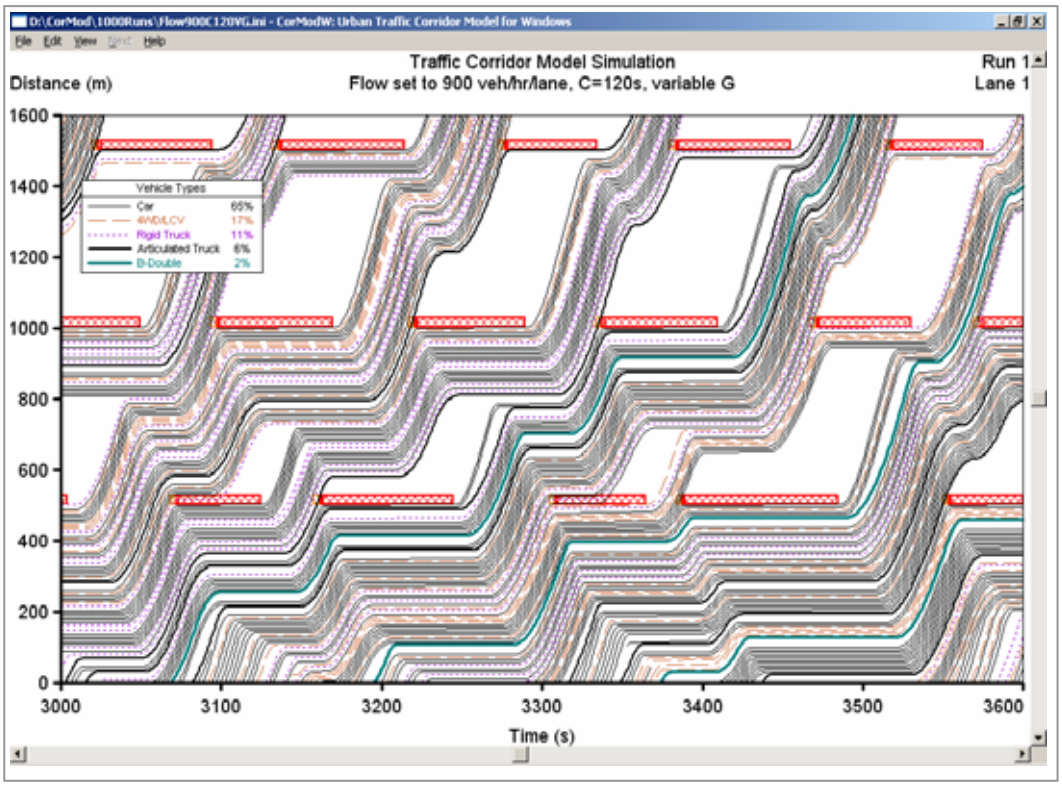


**Figure 9.9 – Trajectory diagram of an oversaturated corridor**

## 9.5 Effect of Cycle Time

A range of simulations was conducted, varying the cycle time used by all three intersections on the corridor. The arrival flow was held constant at 600 veh/h/lane for all of these simulations, and the maximum green time was maintained at 2/3 of the cycle time. These conditions represent the daytime inter-peak period, in which there is a large proportion of heavy vehicles in a relatively large traffic volume.

Figure 9.10 shows the decrease in space mean speed for all vehicle types as the cycle time is increased. Figure 9.11 shows the increasing number of stops for all vehicle types as the cycle time is increased.

There was a general decrease in speeds and increase in number of stops as the cycle time was increased. The increase in red time at each signalised intersection leads to increases in delay and queue length, and thence to lower speeds and increased number of stops. The generally lower stop rate for heavy vehicles than for light vehicles was attributed to heavy vehicles being less likely to need to come to a complete stop when arriving at the rear of a queue.

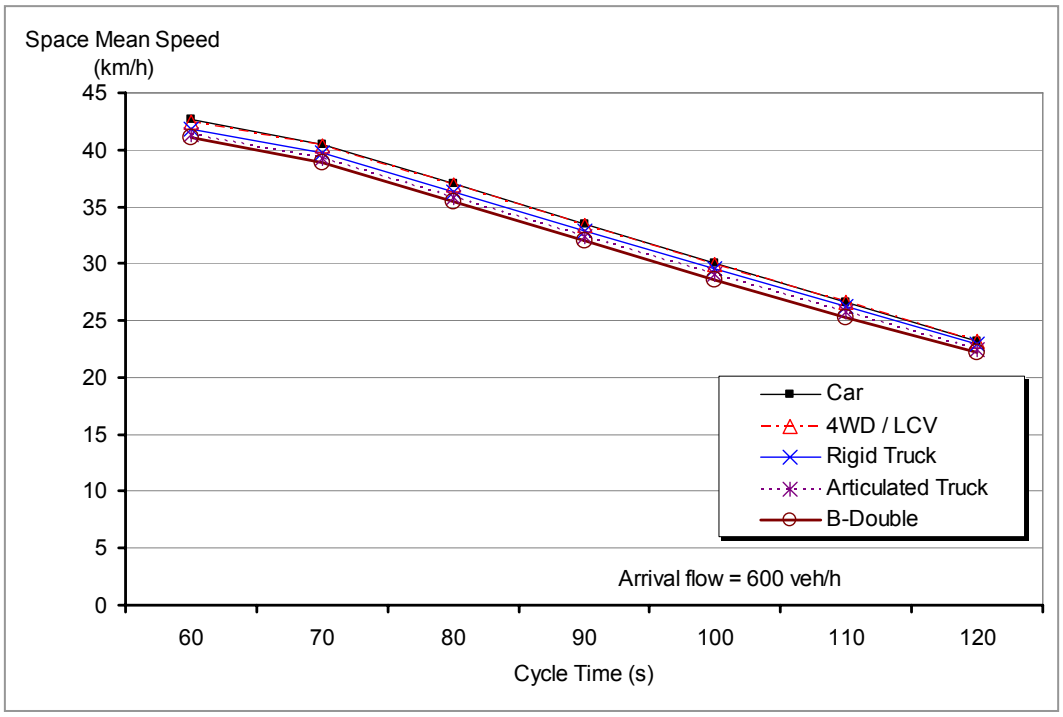


**Figure 9.10 – Variation of speed with cycle time**

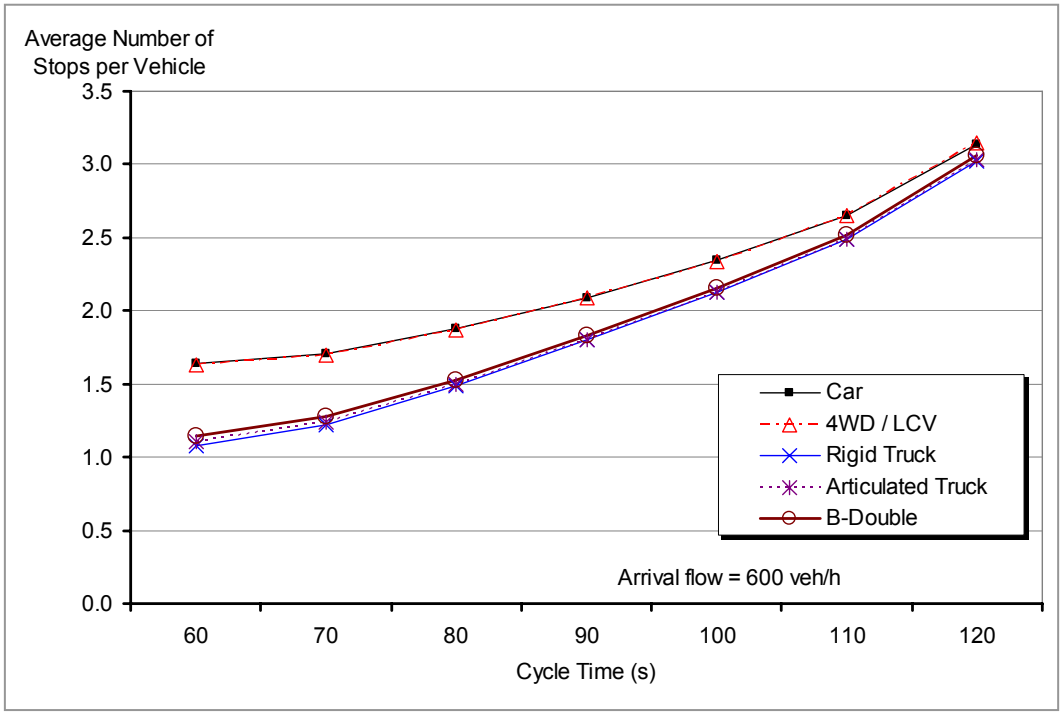


**Figure 9.11 – Variation of stop rate with cycle time**

As the cycle time increases, the ratio of incomplete stops to total stops decreases; resulting in the stop rate increasing at a faster rate for heavy vehicles than for light vehicles as cycle time increases. This supports the assertion that:

> *"Most (signal linking design) problems for trucks are caused by the generally long cycle times operating with signal linking compared to vehicle-actuated signals.*
>
> *(TTM Consulting 1987)*

Conversely, longer cycle times lead to a proportional reduction in lost time, increasing the capacity of the signalised intersection.

## 9.6 Effect of Lane Changing

Figure 9.12 shows that the space mean speeds of all vehicle types are higher when vehicles are allowed to change lanes (the default case in **CorMod**). Figure 9.13 indicates a reduction in the number of stops for all vehicle types with lane changing enabled.

Even though heavy vehicles undertook relatively fewer lane changes than light vehicles, the removal of light vehicles from in front of their paths benefited their progress as well.

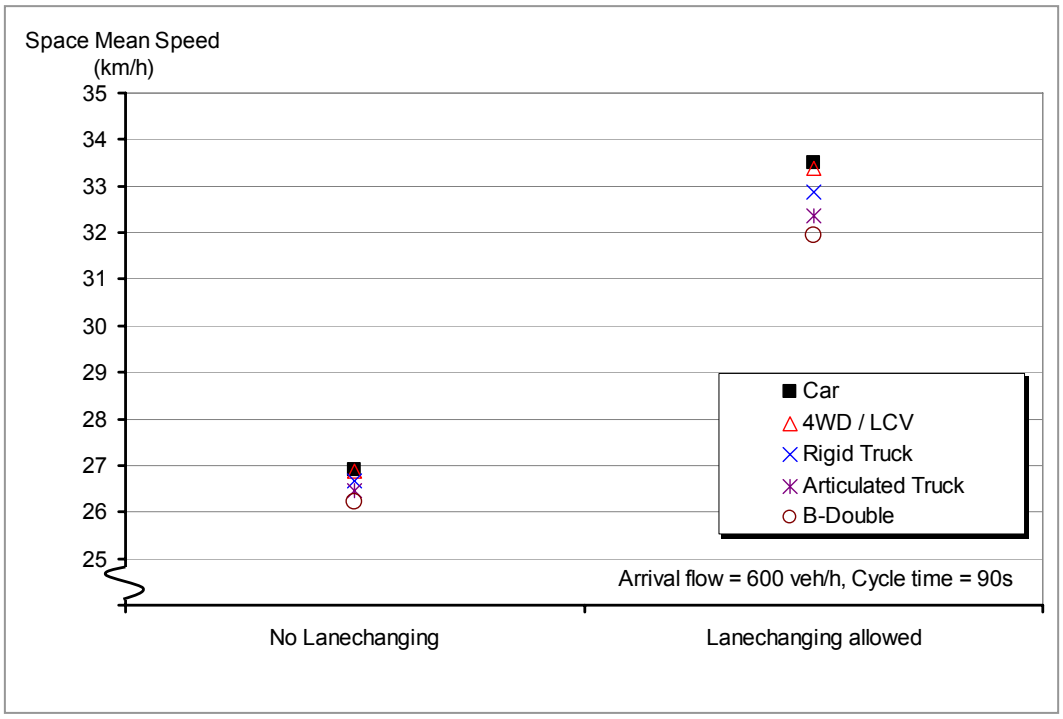


**Figure 9.12 – Higher speeds for all vehicle types with lane changing**

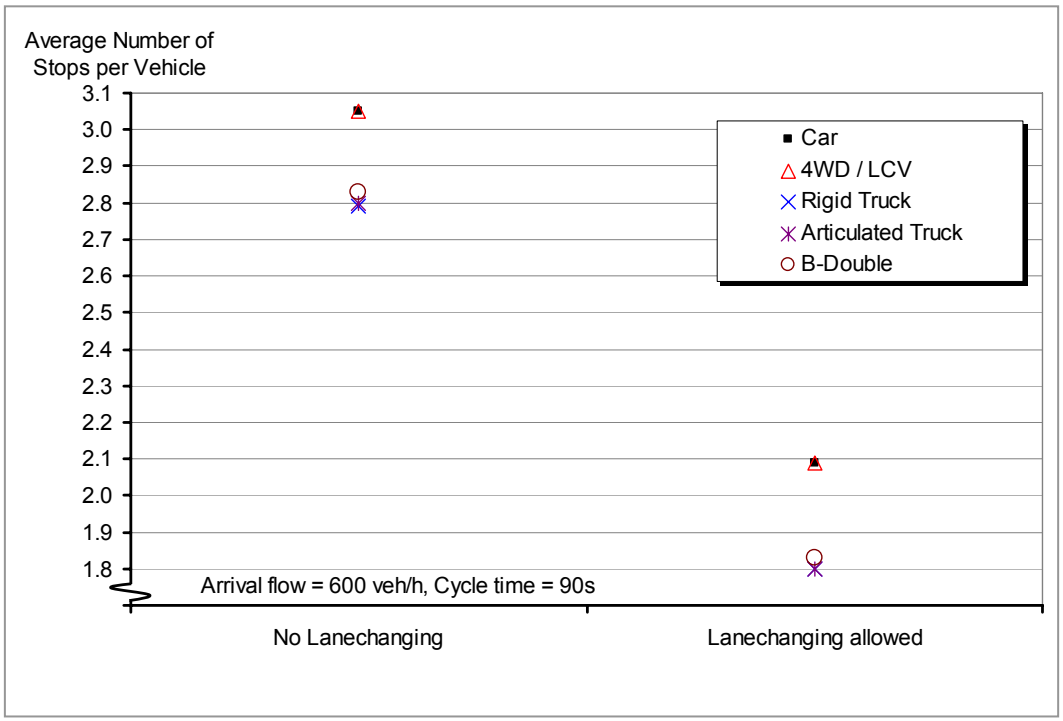


**Figure 9.13 – Fewer stops for all vehicle types with lane changing**

## 9.7 Effect of Grade

### 9.7.1 Method

The effect of grade on the progression of vehicles along a corridor was examined next. Within the **CorMod** program, grade is determined by the elevations at the start and end of road sections. Each vehicle keeps track of the current road section, using the current grade in the calculation of its maximum acceleration and maximum speed.

Grade was generally assumed constant along the corridor, with different scenarios considering grades ranging from -10% to +10% in 2% increments. As shown in Figure 9.14, an additional scenario considered a corridor having varying grades – starting at 4%, increasing to 10% and then returning to 4%. This corridor had the same overall change in elevation as a corridor with a constant grade of 6%, and is useful in comparing an undulating road profile with a uniform gradient profile.

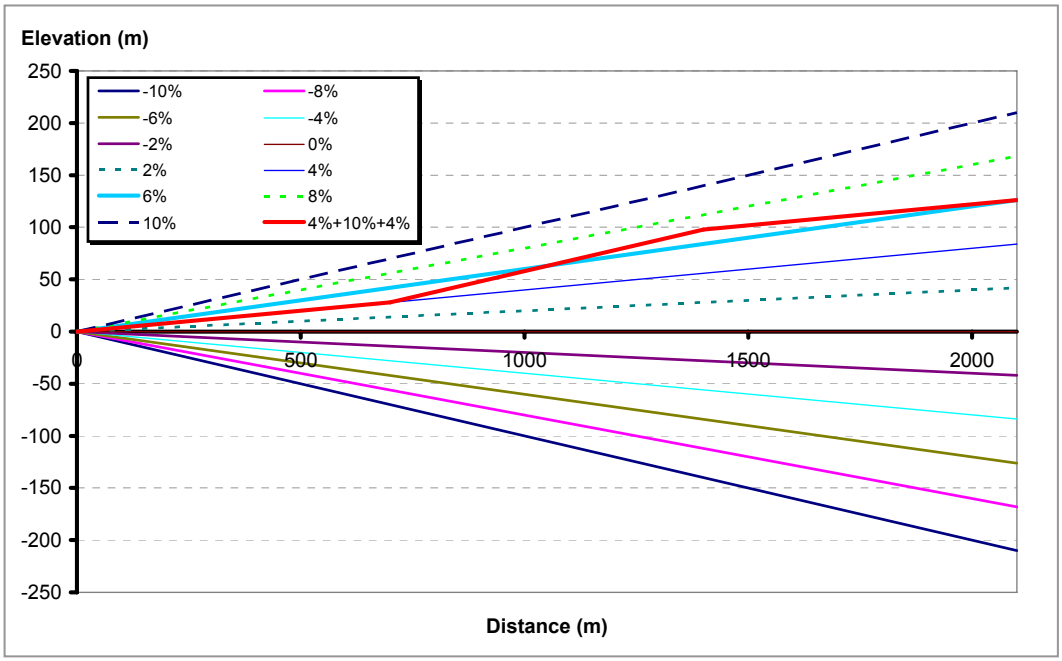


**Figure 9.14 – Uniform and undulating gradient profiles**

### 9.7.2 Results and analysis

Figure 9.15 shows the decrease in space mean speed with increasing gradient. This reduction was greater for heavy vehicles, being more influenced by grade.

Figure 9.16 shows the increasing stop rate for all vehicle types as grade increases. Examination of the trajectory diagrams found that there were relatively few overtaking opportunities under the prevailing traffic conditions, and cars were being slowed down by heavy vehicles on the grade.

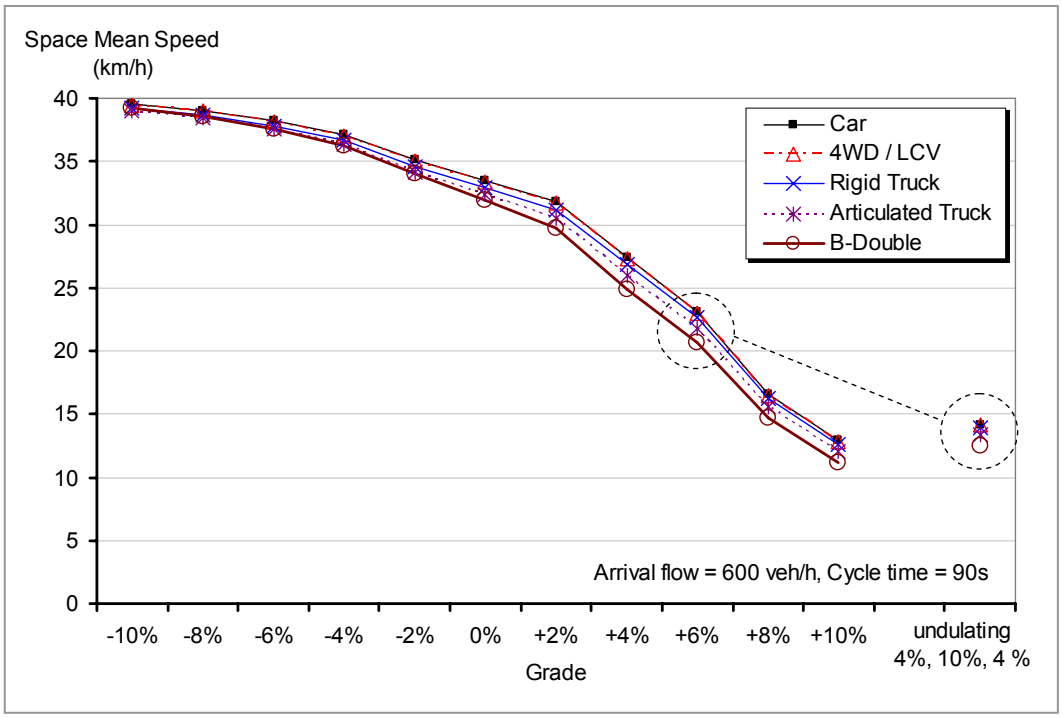


**Figure 9.15 – Decreasing space mean speed with increasing grade**

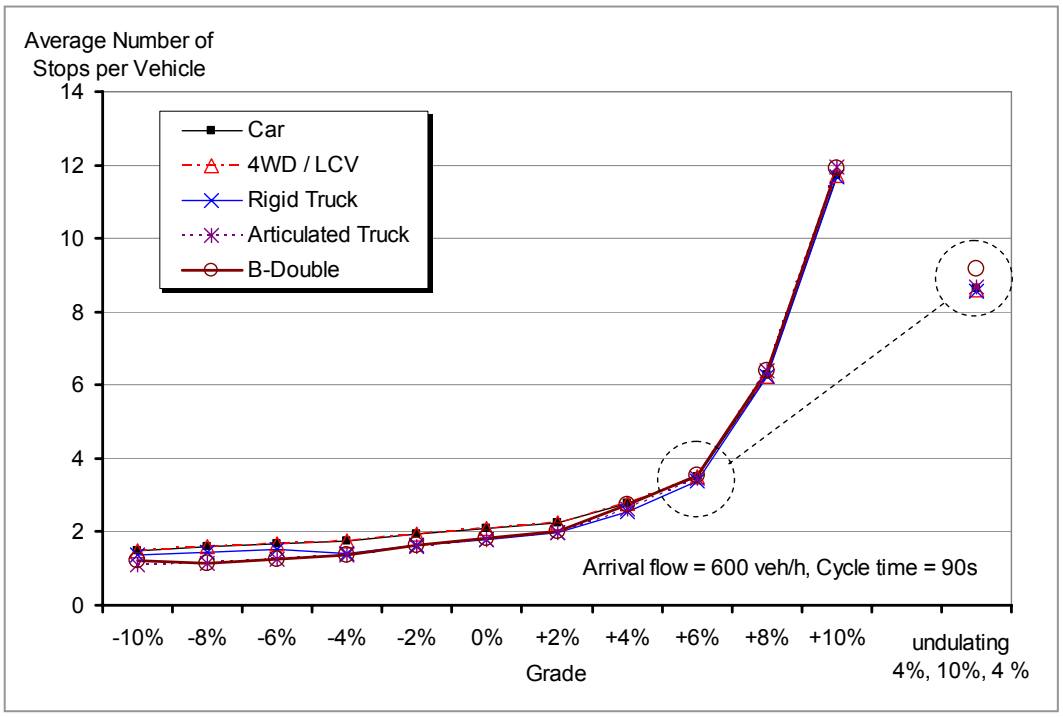


**Figure 9.16 – Increasing stop rate with increasing grade**

Note that on severe down grades, this simple acceleration model predicts similar acceleration rates and speeds for heavy and light vehicles. In reality, speeds of heavy vehicles on severe down grades (typically over 10%) are intentionally kept low to limit the risk of brake failure.

The simulation with an undulating profile (circled by dashed lines in Figure 9.15 and Figure 9.16) had a much lower average speed and a greater stop rate than for an equivalent constant grade profile of 6%. Examination of the trajectory diagram indicated that the steeper gradient section (10%) was forming a bottleneck that prevented vehicles from making use of the lower upstream gradient. Having a constant gradient or having the steeper section at the start rather than the end or middle of the corridor would be likely to benefit all vehicle types.

Saturation flow was seen to decrease as grade increased at all intersections (Figure 9.17). This was attributed to the lower accelerations of heavy vehicles at intersections on grade leading to greater headways during queue discharge. Start loss was also seen to increase with increasing grade.

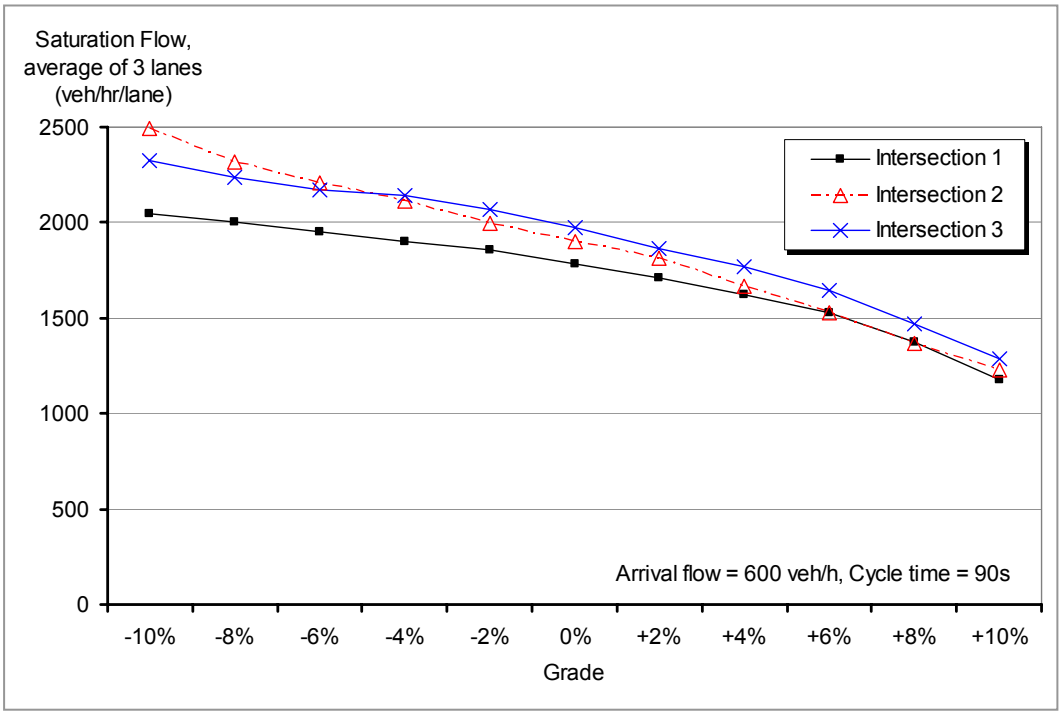


**Figure 9.17 – Saturation flow plotted against grade**

## 9.8 Summary and Conclusions of the Parametric Study

This chapter examines the sensitivity of the corridor model's outputs to a number of input parameters. A hypothetical 3-lane, 3-intersection corridor was used in this study.

Increasing traffic arrival volumes on the corridor were found to result in lower speeds and higher stop rates for all vehicle types. Differences were found between the first intersection on the corridor and downstream intersections at very high arrival flows, primarily because downstream intersections had a limit on their approach volumes due the limited capacity of the first intersection.

Lengthy cycle times were found to affect all vehicles adversely, particularly heavy vehicles that were less likely to come to a partial stop when approaching the rear of a queue at a signalised intersection that is red for a longer time.

Allowing vehicles to change lanes whilst travelling along the corridor was seen to improve travel speeds and reduce stop rates for all vehicle types.

Grade was seen to have a significant effect on travel times and stop rates for all vehicle types, with a constant gradient being preferable to an undulating gradient that has the same overall change in elevation but a steeper mid-section.

The next chapter continues to use the same hypothetical corridor to examine several freight policy and traffic management scenarios.

# CHAPTER 10 APPLICATION OF THE MODEL TO A HYPOTHETICAL URBAN CORRIDOR

## 10.1 Introduction

This chapter describes the application of the corridor-level traffic model to the assessment of several freight policy and traffic management scenarios.

The Bureau of Transport and Regional Economics (BTRE 2006) predicted a continuing increase of capital city road freight, growing in Brisbane at 3.7% per annual (p.a.), compared to an average rate of 3.1% p.a. across all 8 capital cities. This represents more than double the 2003 volume of road freight being moved through urban areas by 2020.

Several scenarios are examined in this chapter to estimate the likely effects of this growth rate on urban traffic corridor performance; and the effects of measures having the potential to lessen the negative impacts.

### 10.1.1 Test corridor

The same test corridor was used for this application as was used in the previous chapter. Repeated in Figure 10.1, the model represents a 2-kilometre long section of an urban arterial freight corridor that is three lanes wide and has three signalised intersections at equal spacings of 500 metres.

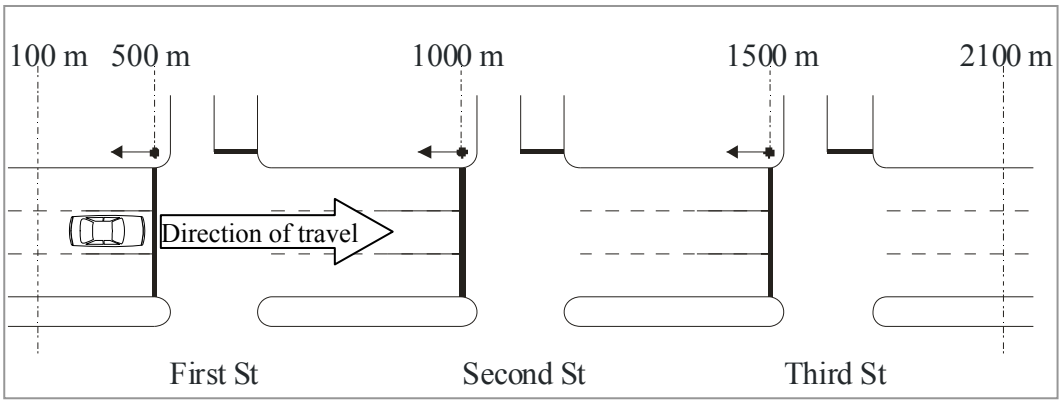


**Figure 10.1 – Test corridor**

### 10.1.2 Scenarios examined

Several scenarios within the following groups were examined for this hypothetical corridor:

- Changes in freight volumes
- Freight policy, freight vehicle mode split
- Traffic management – lane utilisation
- Traffic management – corridor progression
- Heavy vehicle detection and green time extension

The savings in the value of travel time under each of these scenarios were estimated and are reported later in the chapter.

### 10.1.3 Evaluation criteria

The following measures were used to compare the performance of the different scenarios

- Space Mean Speed for each vehicle type
- Number of stops per vehicle for each vehicle type
- Queue lengths for lanes having different vehicle types
- Queue clearance times for lanes having different vehicle types
- Saturation flows for lanes having different vehicle types

The first two of these are user-related traffic performance measures, being directly felt by road users travelling along the corridor. The remaining measures are of more use to the traffic engineering practitioner, and are useful in explaining *why* the particular scenario behaves differently to the baseline case.

Additionally, a monetary value of travel time is reported in the last part of this chapter. Although only considering one component of the cost of travel, it enables a direct comparison between scenarios across a number of vehicle types.

## 10.2 Increasing Freight Volumes

### 10.2.1 Background

The effects of altering the volumes of freight moved along the corridor were investigated, without including the effects of any freight policy or traffic management measures.

### 10.2.2 Method

The freight volumes carried by all heavy vehicles (Rigid trucks, Articulated trucks and B-doubles) were varied from 60% to 200% of the current base case. An arrival flow of 600 veh/h/lane was used in the base case; this was varied with the freight volume.

The same number of Cars and 4WDs/LCVs was maintained, whilst the numbers of Rigid Trucks, Articulated Trucks and B-doubles all were adjusted to the specified proportion of the base case freight volume.

Under a typical freight growth projection, the number of cars and 4WDs/LCVs would increase along with the number of freight-carrying vehicles. BTRE (2002) forecast a 'doubling of the freight task' by the year 2020, based on a growth rate of 2.2 per cent per annum; whilst the passenger car fleet was expected to have a slower rate of growth of around 1 per cent per annum. An alternative strategy would be to have different growth rates for different vehicle types. However, the emphasis of this project is on the management of freight movements along a corridor, rather than future projected traffic growth. As such, the number of cars and 4WDs/LCVs was held constant for these scenarios. The sensitivity of output measures to varying arrival flow volumes was covered in the previous chapter.

The proportions of each vehicle type used in these simulations are presented in Table 10.1, together with the arrival flow rates on the corridor.

**Table 10.1 – Vehicle type distributions for changed freight volumes**

| *Vehicle type* | *Proportion of current heavy vehicle freight volume* | | | | | | | |
|---|---|---|---|---|---|---|---|---|
| | *60%* | *80%* | *100%* | *120%* | *140%* | *160%* | *180%* | *200%* |
| Car | 70.2% | 67.5% | 65.0% | 62.7% | 60.5% | 58.5% | 56.7% | 54.9% |
| 4WD / LCV | 17.9% | 17.2% | 16.5% | 16.0% | 15.4% | 14.9% | 14.5% | 14.0% |
| Rigid Truck | 7.2% | 9.2% | 11.1% | 12.8% | 14.5% | 16.0% | 17.4% | 18.7% |
| Articulated Truck | 3.8% | 4.9% | 5.9% | 6.8% | 7.7% | 8.5% | 9.2% | 9.9% |
| B-double | 0.9% | 1.2% | 1.5% | 1.7% | 1.9% | 2.1% | 2.3% | 2.5% |
| **All Vehicle Types** | **100%** | **100%** | **100%** | **100%** | **100%** | **100%** | **100%** | **100%** |
| | | | | | | | | |
| *Flow (veh/h/lane)* | *556* | *578* | *600* | *622* | *644* | *666* | *688* | *710* |

### 10.2.3 Results

A total of 1000 repetitions of each simulation were conducted, with the results being averaged to give the following findings:

Figure 10.2 shows the decrease in space mean speed for all vehicle types as the number of freight vehicles was increased. This decrease in speed was attributed to the increase in the overall volume of vehicles, and not specifically to the type of vehicles being added.

For comparison, Figure 9.4 in the previous chapter showed a decrease in average space mean speed across all vehicle types from 37 km/h to 25 km/h as the arrival flow was increased from 600 veh/h/lane to 700 veh/h/lane, whilst maintaining the same vehicle type proportions. This current figure shows a similar decrease in speed as flow was increased by a comparable amount by adding only heavy vehicles.

Figure 10.3 shows the increase in the stop rates of all vehicle types as the freight volume is increased. The stop rate of heavy vehicles was generally lower than that of light vehicles at the same freight volume, as was found in the previous chapter. The stop rate for heavy vehicles increased at a faster rate than for light vehicles as their proportion was increased and they became a greater proportion of the overall number of vehicles on the corridor.

These simulations indicate that doubling the freight task alone (as per BTRE's (2006) predictions for the year 2020) would reduce corridor speeds for all vehicles by an average of 23% and increase the average number of stops by 58%.

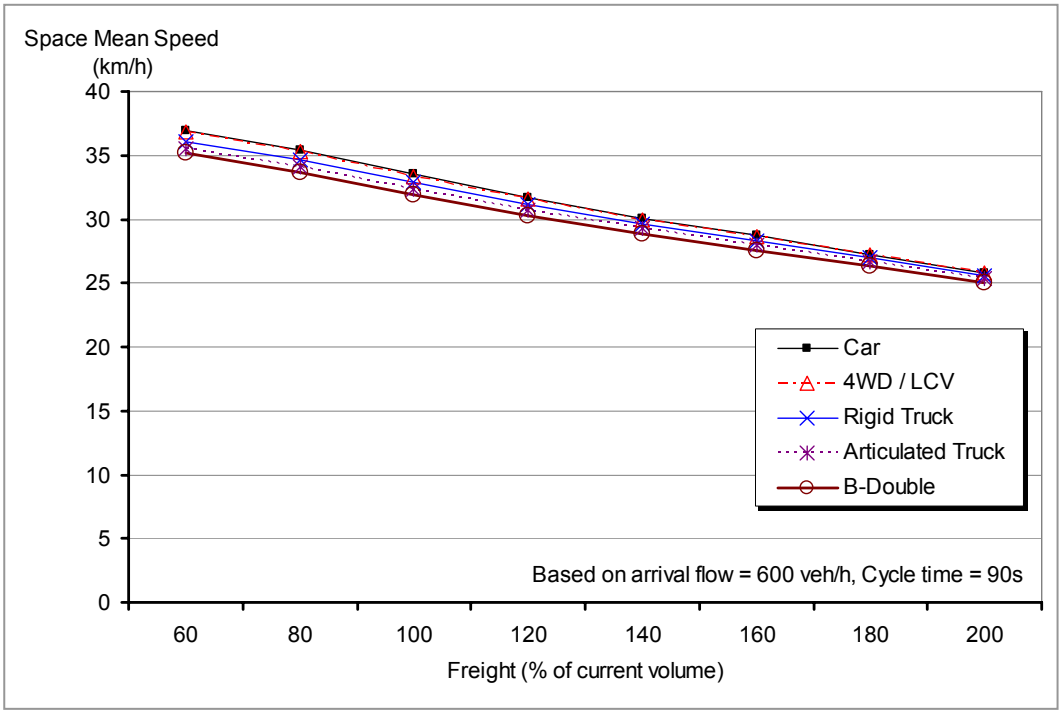


**Figure 10.2 – Decrease in space mean speed with increasing freight volume**

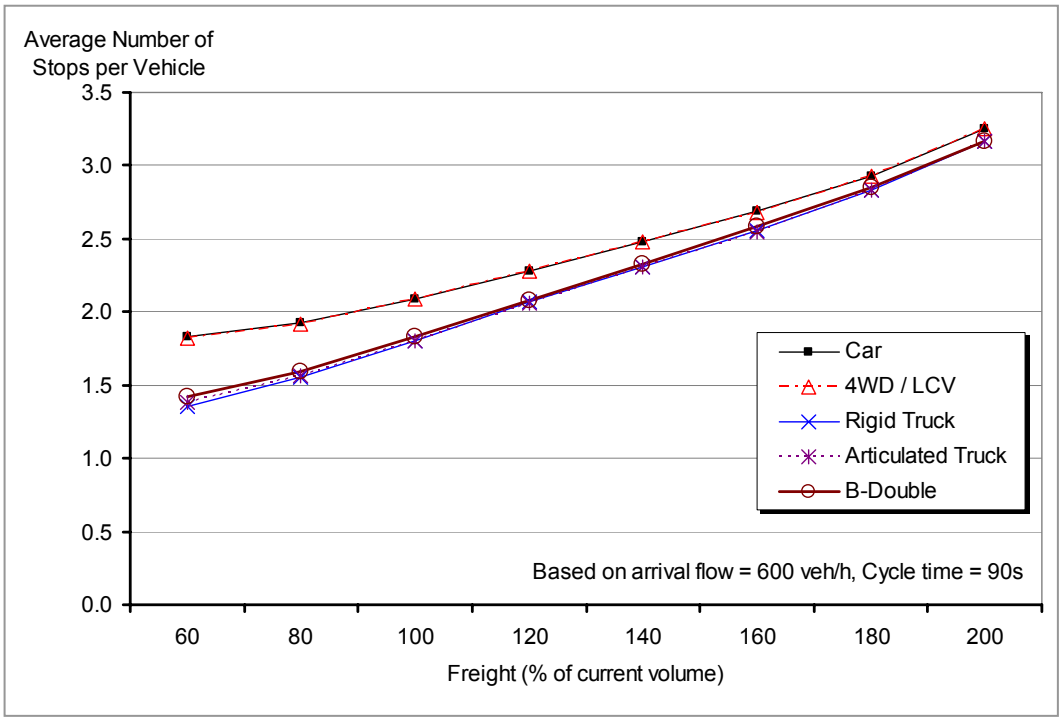


**Figure 10.3 – Increase in stop rate with increasing freight volume**

## 10.3 Freight Vehicle Mode Selection

### 10.3.1 Background

In recognising, the problems associated with the predicted increase in road freight volumes, NTC and others are working towards a greater use of more-innovative vehicles capable of carrying a greater payload. This section investigates the implications of several freight vehicle mode policies, such as prohibition of certain vehicle types from using the corridor, or introduction of new vehicle types.

### 10.3.2 Method

The following freight vehicle mode scenarios were examined:

**Cars Only** All heavy vehicles have been removed from the corridor to an alternative route. The overall traffic volume remains the same as for the base case, cars having been attracted to the corridor to replace the freight vehicles.

**Base Case** Existing freight volumes and mode split

**No B-doubles** The freight volume remains the same as in the base case. 75% of the freight originally carried by B-doubles was carried by articulated trucks and 25% carried by rigid trucks. This would require more vehicles to carry the freight, and hence higher arrival flows on the corridor.

**More B-doubles** The freight volume remains the same as in the base case. 25% of the freight originally carried by rigid trucks and 33% of the freight originally carried by articulated trucks was carried by B-doubles. This would require fewer vehicles to carry the freight, and hence a lower arrival flow on the corridor.

**Some B-triples** The freight volume remains the same as in the base case. 33% of the freight originally carried by B-doubles and 33% of the freight originally carried by articulated trucks was carried by B-triples. This would require fewer vehicles to carry the freight, and hence a lower arrival flow on the corridor.

The average payload carried by each vehicle type was estimated from various sources (including Ramsay 1998; Haldane and Bunker 2002), and are presented in Table 10.2.

**Table 10.2 – Average payloads carried by each vehicle type**

| *Vehicle type* | *Assumed average payload (t)* |
|---|---|
| Car | - |
| 4WD / LCV | - |
| Rigid Truck | 10 |
| Articulated Truck | 27 |
| B-double | 48 |
| B-triple | 68 |

Note that since B-triples were not able to be tested on the corridor, their performance characteristics were estimated from those of a B-double with a greater mass and the same engine power; leading to lower acceleration capability and gradeability.

The numbers of each vehicle type required to conduct the same freight task as in the baseline case were calculated for each scenario. These were converted to equivalent proportions of the total number of vehicles, resulting in the vehicle type distributions shown in Table 10.3.

These adjusted vehicle type proportions and arrival flows were incorporated into the model input files for these scenarios and 1000 repeat simulation of each scenario were conducted, with the averaged results shown below:

**Table 10.3 – Vehicle type distributions for changed freight vehicle mode**

| | *Freight vehicle mode scenario* | | | | |
|---|---|---|---|---|---|
| *Vehicle type* | *Cars only* | *Baseline* | *No B-doubles* | *More B-doubles* | *B-triples* |
| Car | 100% | 65.0% | 63.6% | 67.0% | 65.9% |
| 4WD / LCV | 0% | 16.5% | 16.2% | 17.1% | 16.8% |
| Rigid Truck | 0% | 11.1% | 12.6% | 8.6% | 11.2% |
| Articulated Truck | 0% | 5.9% | 7.6% | 4.0% | 4.0% |
| B-double | 0% | 1.5% | 0% | 3.2% | 1.0% |
| B-triple | 0% | 0% | 0% | 0% | 1.1% |
| **All Vehicle Types** | **100%** | **100%** | **100%** | **100%** | **100%** |
| | | | | | |
| *Flow (veh/h/lane)* | *600* | *600* | *613 (+2.1%)* | *582 (-3%)* | *592 (-1.3%)* |

### 10.3.3 Results

Figure 10.4 shows the space mean speed for the different vehicle types in each of the five scenarios, whilst Figure 10.5 shows the average number of stops per vehicle. The cars-only scenario did not include results for other vehicle types, and there was only one scenario that included B-triples.

Most significantly, the space mean speed was highest in the cars-only scenario. This was attributed to them not being impeded by the other vehicle types. There was little difference in stop rates for this scenario; cars were stopping a similar number of times but were able to maintain a higher speed between stops. It must be realised that, in relocating the freight traffic to an alternative route, the travel times and level-of service on that route are likely to be degraded.

Of the four scenarios in which freight continued to be carried along the corridor, the scenario involving a greater use of B-doubles gave the highest speeds and lowest stop rates. This was primarily attributed to the fewer number of vehicles being required to carry the same volume of freight.

Although the scenario involving the use of B-triples for some of the freight also had fewer vehicles than the baseline case, the assumed poorer performance of B-

triples in congested traffic results in overall lower speeds and higher stop rates for all vehicle types.

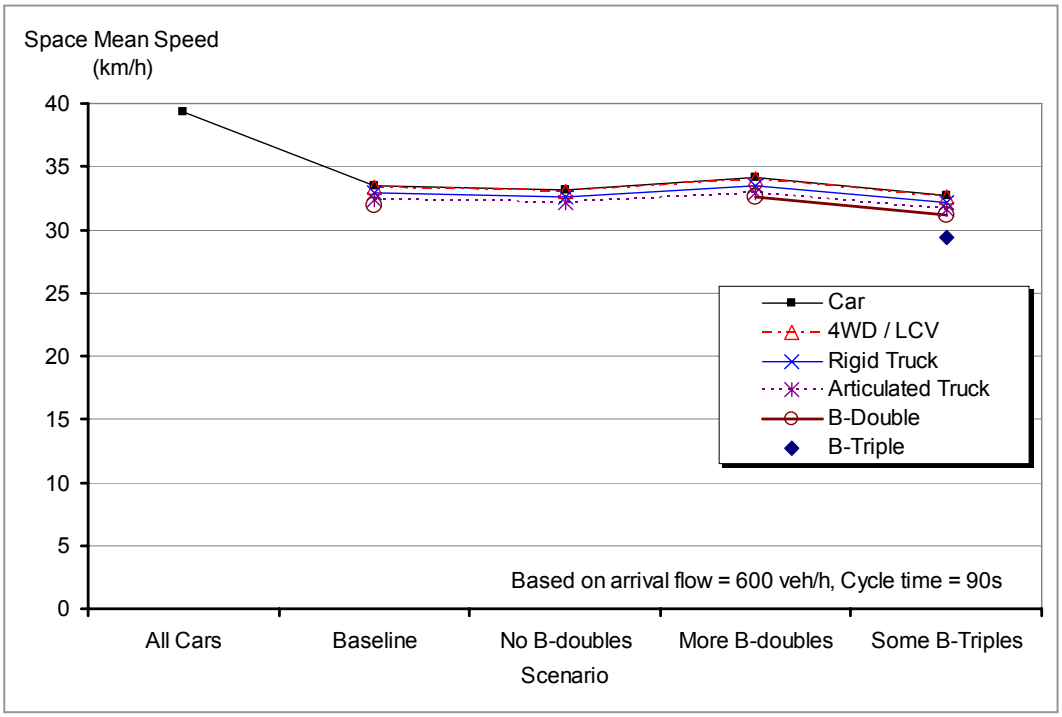


**Figure 10.4 – Space mean speed of each vehicle type under different freight vehicle mode scenarios**

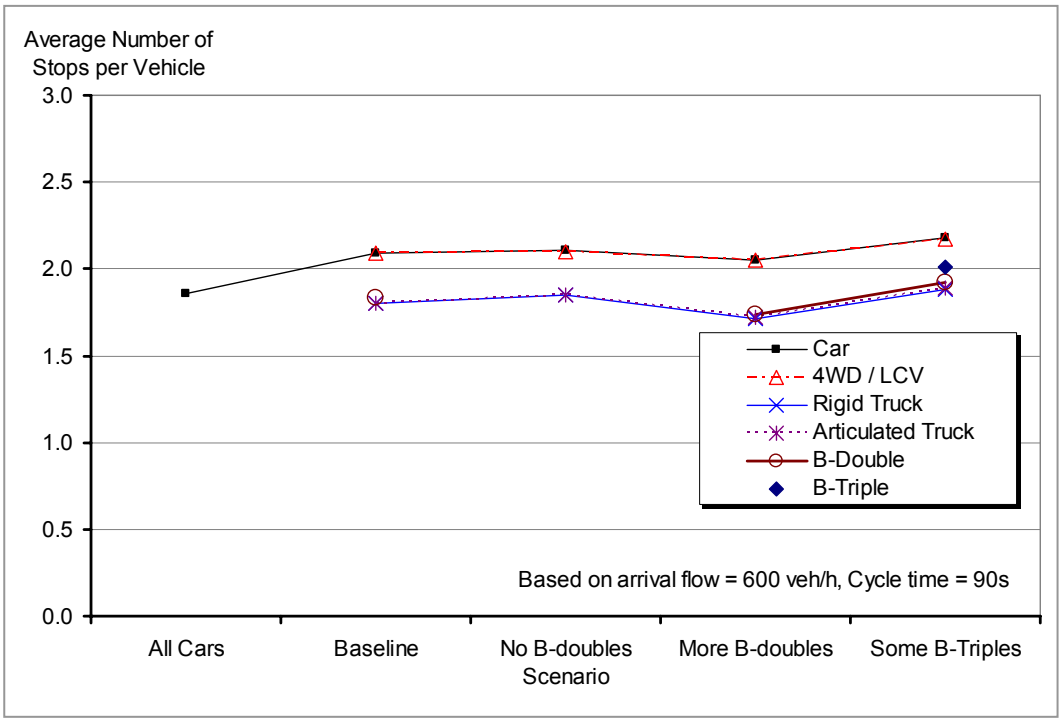


**Figure 10.5 – Number of stops per vehicle under different freight vehicle mode scenarios**

Figure 10.6 and Figure 10.7 show the queue clearance times and saturation flow rates at the three intersections under each of these freight vehicle mode scenarios.

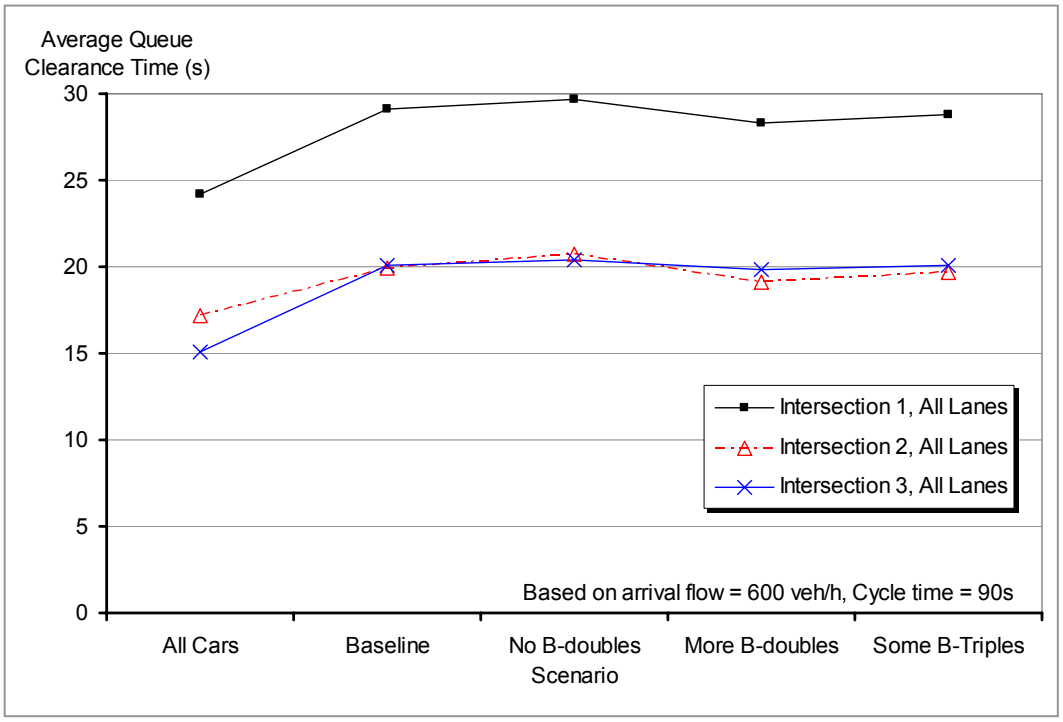


**Figure 10.6 – Average queue clearance times at all intersections under different freight vehicle mode scenarios**

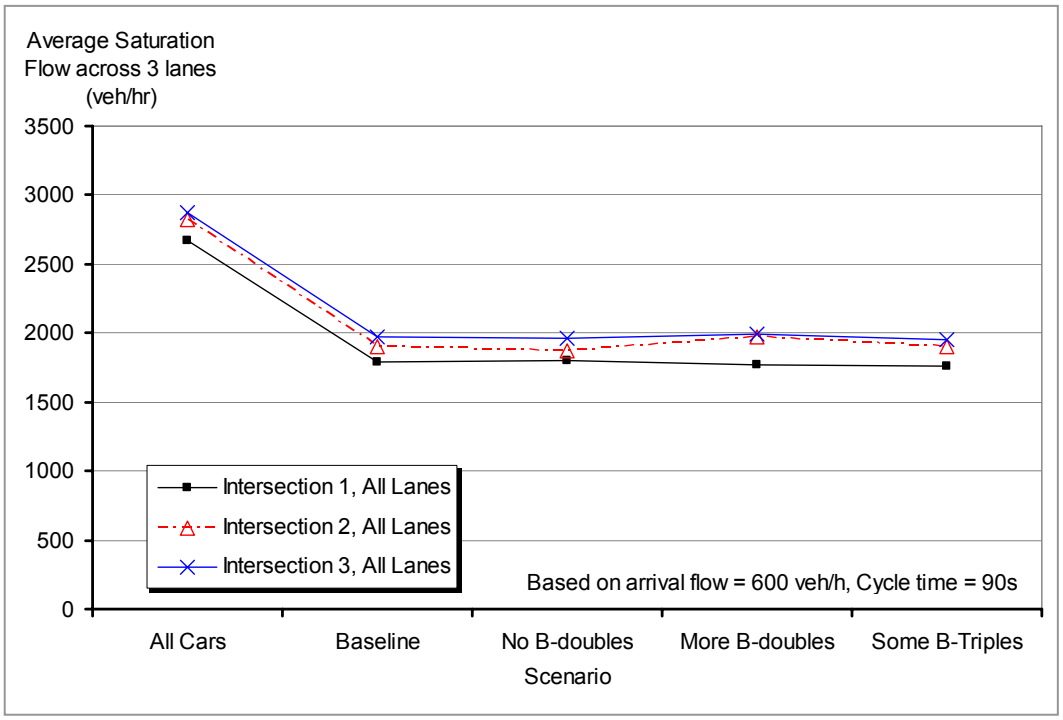


**Figure 10.7 – Average saturation flow per lane at all intersections under different freight vehicle mode scenarios**

The trends in intersection performance were found to be similar to those of corridor performance. The cars-only scenario had the fastest queue clearance times and highest saturation flows, whilst the scenario with more B-doubles was the best of those carrying freight on the corridor.

As found in the previous chapter, the queue clearance times of intersections 2 and 3 are less than for intersection 1, due to the high proportion of vehicles arriving during the green signal at those intersections.

## 10.4 Effect of Lane Allocation Strategies

### 10.4.1 Introduction

As reported earlier, Al-Kaisy (2004) conducted a number of microsimulation runs of heavy vehicles in congested freeway traffic, finding that lane allocation strategies offered benefits in congested urban freeway traffic.

This section aims to apply similar strategies to congested urban arterial corridors controlled by signalised intersections.

A similar set of four lane utilisation scenarios to Al-Kaisy's was used in these scenarios:

**Baseline** All vehicle types are permitted to use any of the three lanes

**All trucks use lane 1** All rigid trucks, articulated trucks and B-doubles must use lane 1. Cars and 4WDs/LCVs may use any lane

**All trucks use lanes 1 and 2** All rigid trucks, articulated trucks and B-doubles must use lane 1 or lane 2. Cars and 4WDs/LCVs may use any lane, but lane 3 is for their exclusive use.

**Big trucks in lane 1, small trucks in lanes 1 and 2** All articulated trucks and B-doubles must use lane 1. Rigid trucks must use lane 1 or lane 2. Cars and 4WDs/LCVs may use any lane, but lane 3 is for their exclusive use.

Implementation and enforcement of the more-complicated of these lane utilisation strategies would be a challenge. Due to the symmetry of this hypothetical corridor, it would not make much difference which of the three lanes was allocated to each vehicle type – having trucks use the right-most lane would be similar to having them use the left-most lane. In practice, it is generally observed that trucks tend to use the centre lane of a three-lane carriageway in order to avoid having to slow down or stop behind turning traffic. **CorMod** does not include traffic turning onto or off the corridor.

Table 10.4 shows the lanes permitted to be used by each vehicle type under these four different lane allocation strategies. Although cars and 4WDs/LCVs were free to use any lane, it was expected that they would tend to change lanes out of the generally slower lanes being used by trucks.

**Table 10.4 – Lane allocations for various traffic management strategies**

| | *Lanes permitted in each scenario* | | | |
|---|---|---|---|---|
| *Vehicle Type* | *Baseline* | *All trucks use lane 1* | *All trucks use lanes 1 & 2* | *Big trucks in lane 1, Small trucks in lanes 1&2* |
| Car | 1, 2, 3 | 1, 2, 3 | 1, 2, 3 | 1, 2, 3 |
| 4WD / LCV | 1, 2, 3 | 1, 2, 3 | 1, 2, 3 | 1, 2, 3 |
| Rigid Truck | 1, 2, 3 | 1 | 1, 2 | 1, 2 |
| Articulated Truck | 1, 2, 3 | 1 | 1, 2 | 1 |
| B-double | 1, 2, 3 | 1 | 1, 2 | 1 |

### 10.4.2 Method

The lane allocation restrictions were implemented in **CorMod** by specifying the lane(s) that each vehicle type is not permitted to use. Figure 10.8 shows an extract of an input file with the last line specifying that this vehicle type be not permitted to use lane number 2.

```
[vehicletype10]
Name=B-Double
VehicleLength=25
JamSpacing=29
MaxAccel=0.68
MaxSpeed=109
Deceleration=-3
MaxGrade=19
StartResponseTime=4
CanUseLane2=false
```

**Figure 10.8 – Commands used to restrict B-doubles from lane 2**

This restriction has the following two effects inside the **CorMod** program:

- It prevents these vehicle types from being generated in this lane
- It prevent these vehicle types from considering lane changes into this lane (this also prevents lane changes across this lane, e.g. from lane 1 to lane 3)

### 10.4.3 Results

A total of 1000 simulations of each scenario were conducted, each using a different random number seed. The results of the simulations were averaged.

Figure 10.9 shows the space mean speed of each vehicle type under each scenario, and Figure 10.10 shows the average number of stops per vehicle for each vehicle type in each scenario.

Both space mean speeds and stop rates were similar between vehicle types across three of the four lane utilisation scenarios. The scenario restricting all trucks to a single lane had the lowest speed for trucks and highest speed for cars. Stop rates for heavy vehicles was highest under this scenario as well.

The lane utilisation scenarios can be further examined by referring to the lane queue performance figures for intersection 1. Results for the other two intersections were similar to those at intersection 1.

Figure 10.11 shows the queue length in each lane, Figure 10.12 shows the number of queued vehicles in each lane, Figure 10.13 shows the average queue clearance time in each lane, and Figure 10.14 shows the saturation flow at each lane.

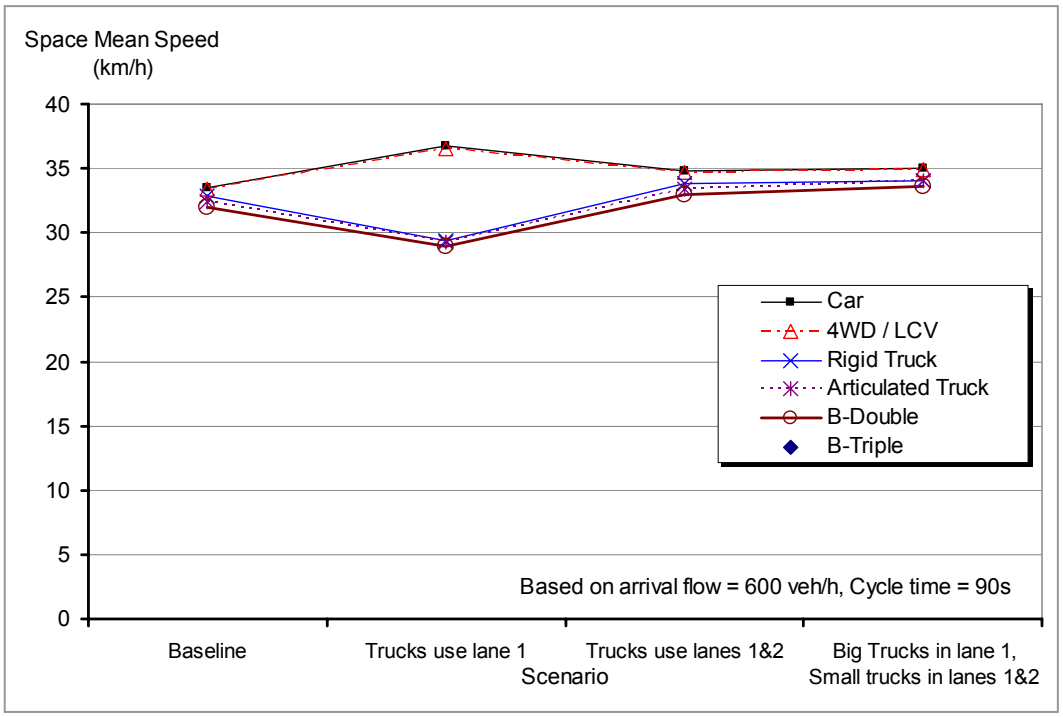


**Figure 10.9 – Space mean speed of each vehicle type under different lane utilisation scenarios**

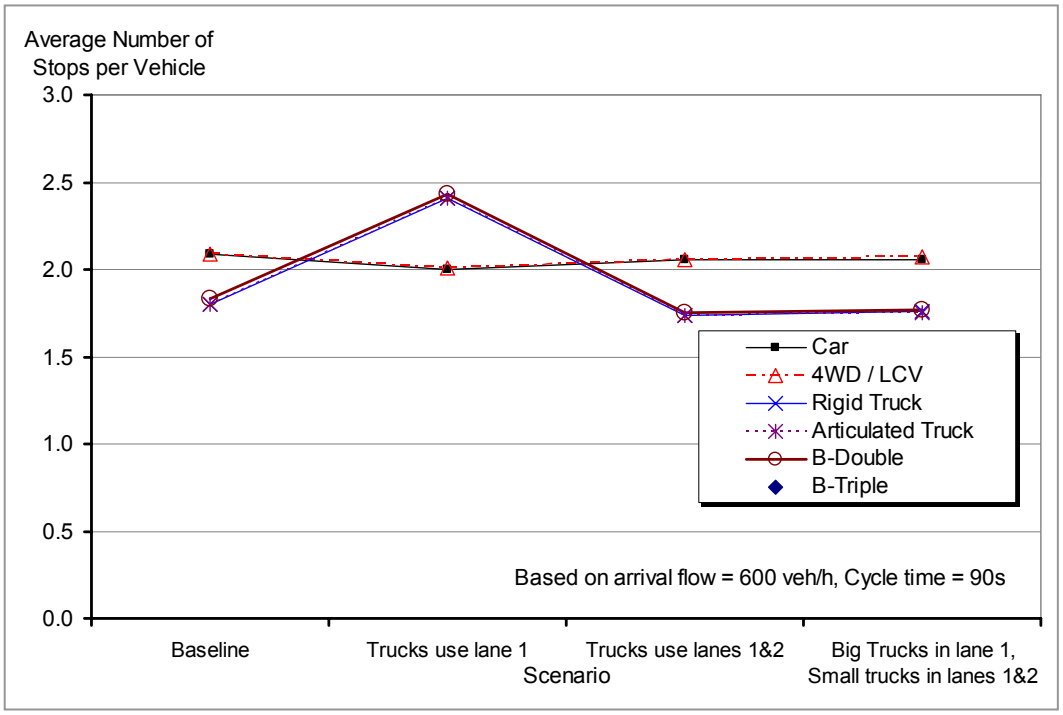


**Figure 10.10 – Number of stops per vehicle under different lane utilisation scenarios**

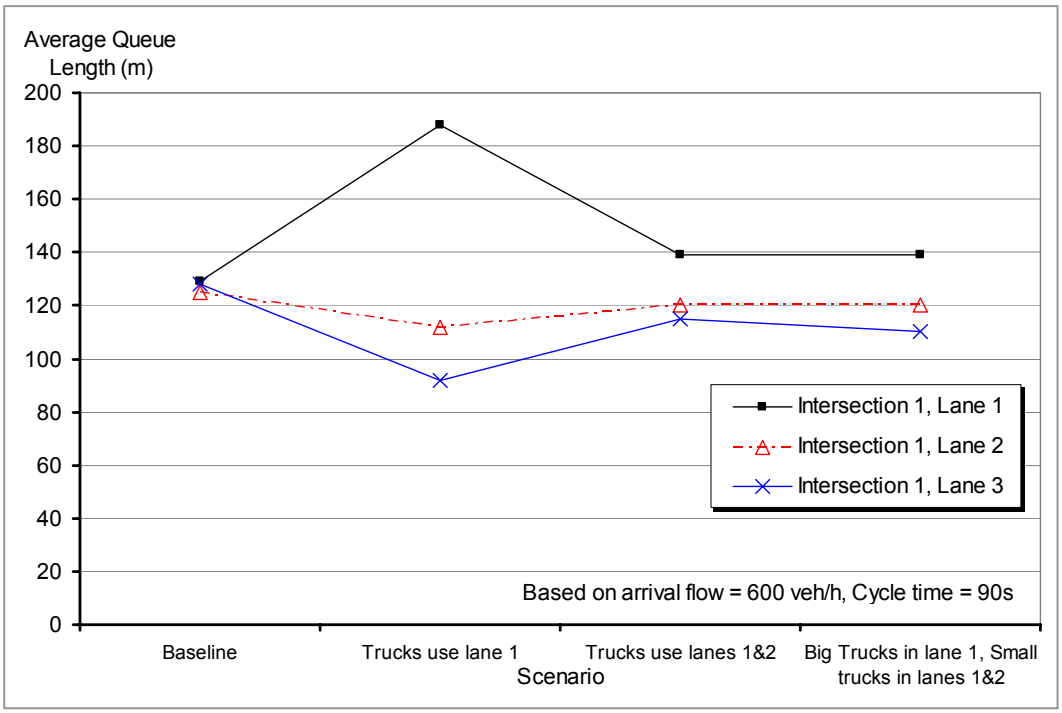


**Figure 10.11 – Length of each queue at intersection 1 under different lane utilisation scenarios**

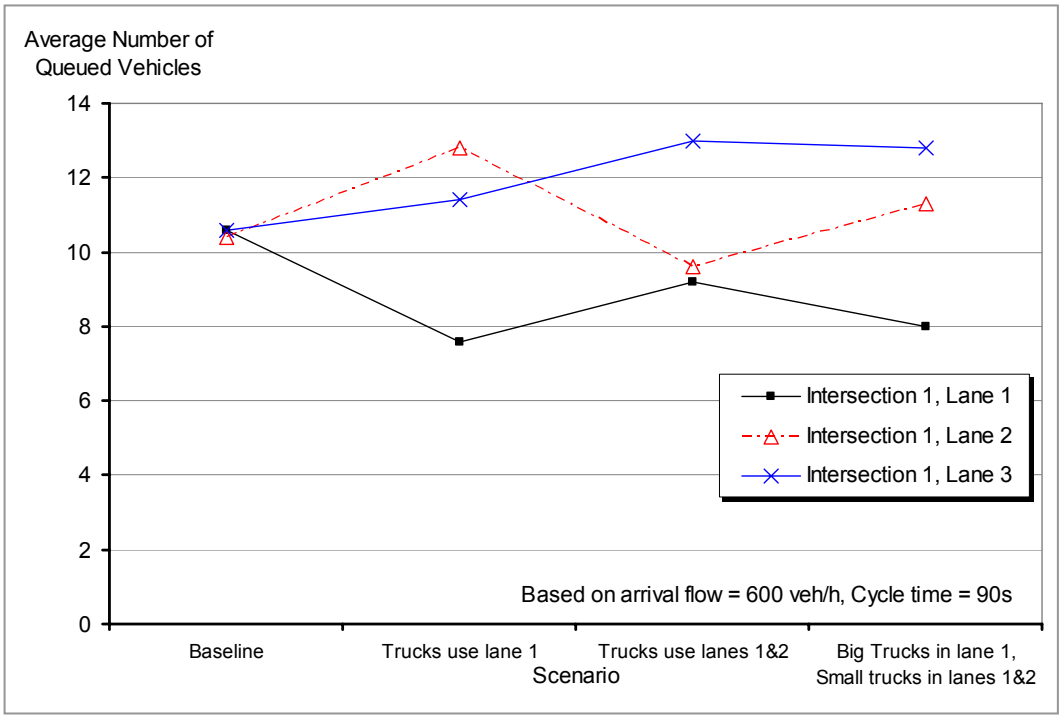


**Figure 10.12 – Number of vehicles in each lane at intersection 1 under different scenarios**

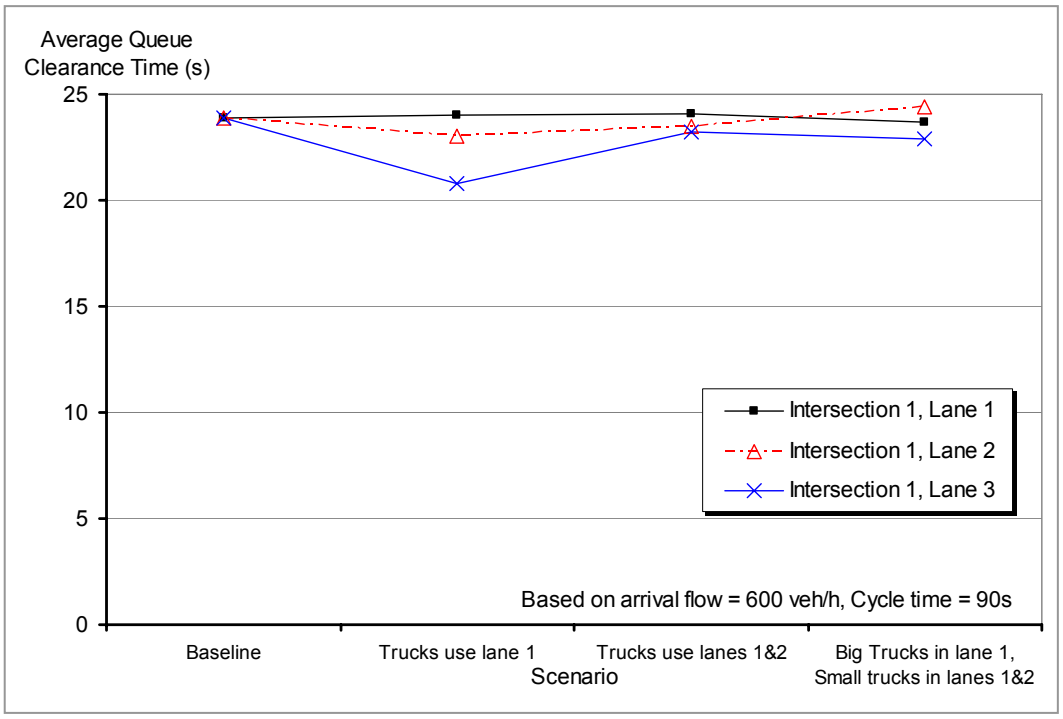


**Figure 10.13 – Queue clearance times at intersection 1 under different scenarios**

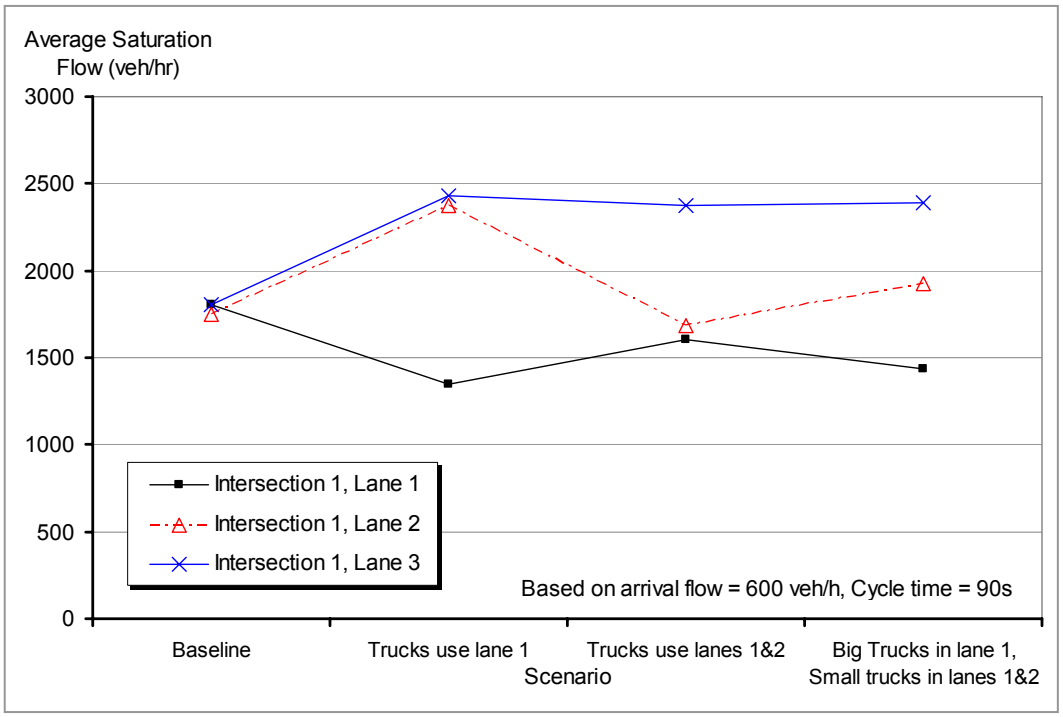


**Figure 10.14 – Saturation flows at intersection 1 under different scenarios**

### 10.4.4 Analysis and Discussion

**Restricting all trucks to using lane 1** gave a much longer queue in lane 1 than in the other lanes. There were two reasons for this. Firstly, the trucks were longer than cars so a queue of trucks would be longer than a queue of an equivalent number of cars. Secondly, the lane was operating at a higher degree of saturation than the other lanes. There were differences between lanes in the queue clearance times and saturation flows for this scenario, indicating that the single truck lane was serving more vehicles than its reduced capacity could handle.

A slight difference between lanes 2 and 3 was found, even though they had the same vehicle composition (no trucks). Some of the vehicles that were initially in lane 1 were likely to have changed lanes into lane 2 as the simulations progressed, and there was less impetus for them to change lanes once more into lane 3.

**Restricting all trucks to using lanes 1 and 2** also gave greater queue lengths in these lanes than in lane 3. The number of queued vehicles in these lanes was found to be less than in lane 3, primarily due to the differences in average vehicle lengths between the lanes. Queue clearance times were very similar between the three lanes, whilst lane 3 had a much higher saturation flow.

Figure 10.15 shows the **CorModW** display of the trajectory diagrams for lane 1 (top) and lane 2 (bottom) for the scenario restricting all trucks to lane 1. Lane 1 was often oversaturated, with lengthy queues developing and vehicles not being able to clear the queue in the available time. The queue discharge from intersection 1 often occurred into the back of a stationary queue at intersection 2. This being the critical lane, the vehicle-actuated signals would have been running to the maximum permitted green time in each cycle. Lane 2 (and lane 3, which is not shown) did not have this problem, and was able to discharge a large number of vehicles efficiently in each cycle due to the greater saturation flow rate and long green time available.

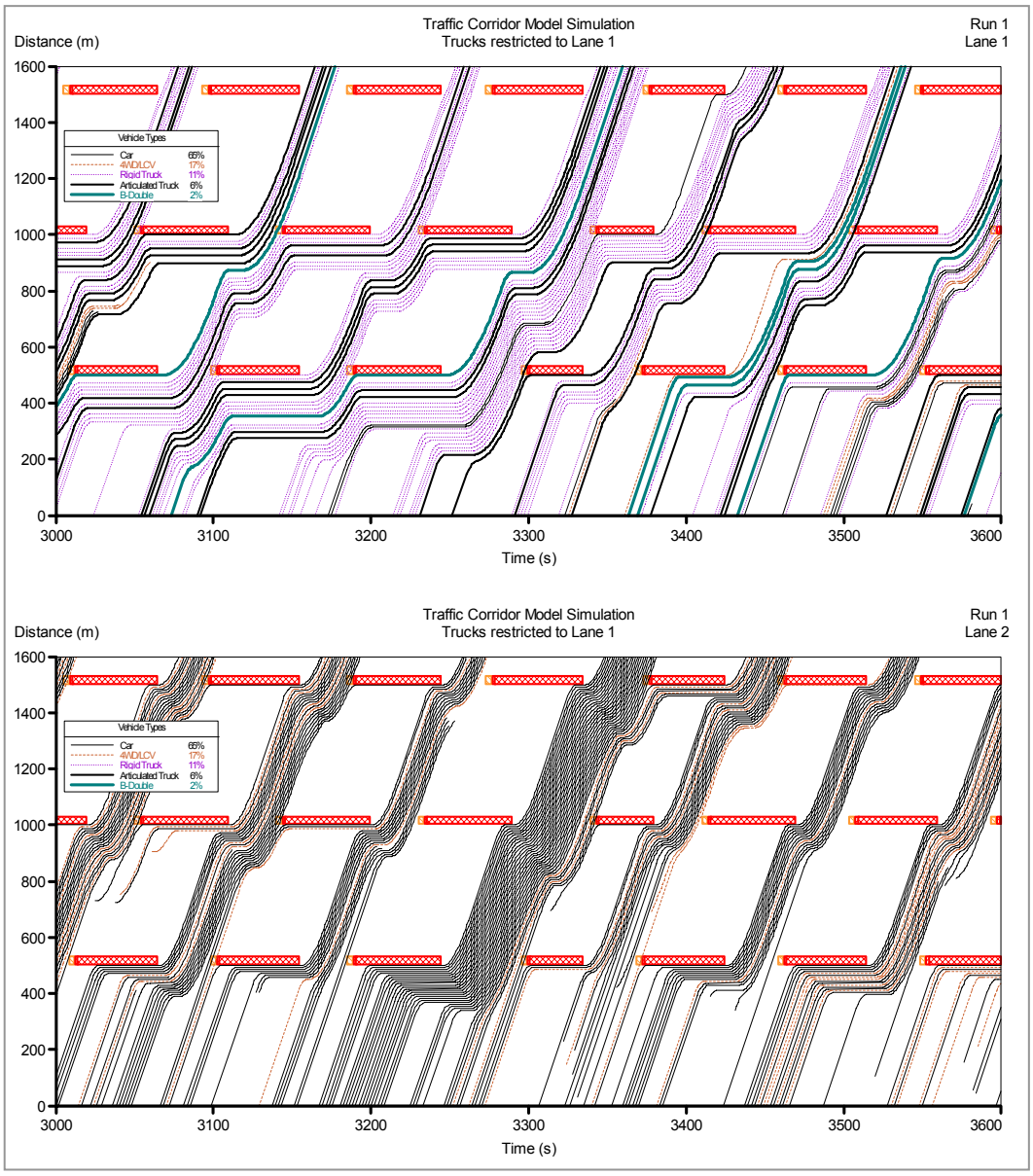


**Figure 10.15 – Effect of restricting all trucks to a single lane.**

The optimum lane utilisation strategy for this three-lane corridor was to segregate the different vehicle types to the greatest extent possible – by restricting large trucks to a single lane, smaller trucks to that lane and another, and permitting cars to use any lane (although tending to change into the car-only lane). Implementation and enforcement issues with such a lane utilisation policy would need to be considered.

## 10.5 Effect of Signalised Corridor Progression Design Speed

### 10.5.1 Introduction

Heavy vehicles are generally slower, and take a greater time to reach the prevailing speed environment. As such, it was thought likely that would benefit from a lower progression design speed (PDS) than that which best serves passenger cars (TTM Consulting 1987; Ogden 1999).

The effect on other vehicle types of optimising signals for heavy vehicle needs to be considered. The alternative theories are that:

- Cars are disadvantaged because the signals are being optimised for another vehicle type, or
- Cars perceive a benefit through the removal of impediments to their progress (fewer slowly-accelerating heavy vehicles at intersections).

This section investigates the effect of altering the progression design speed on the travel time and stop rate of different vehicle types.

### 10.5.2 Method

The temporal offsets between adjacent signals are generally specified to maximise the bandwidth of the platoons of vehicles able to pass through them. The progression design speed (PDS) is defined as the speed at which a vehicle driving through the signals will arrive at each signal at the same time after the green signal has commenced. It is the distance between the adjacent signals divided by temporal offset between them.

The PDS is specified is in **CorMod** by setting its value in the input file for the first intersection, as seen in Figure 10.16. Downstream intersections will use the same PDS as their predecessor, unless explicitly specified otherwise.

```
[intersection1]
Location=500            ; location of signal stop-line, metres
CycleTime=90            ; cycle time, [same for downstream intersections]
MaxGreen=0.667          ; maximum green time, in seconds
                        ; or as a proportion of cycle time
ProgressionSpeed=37     ; speed at which signals are coordinated to, in km/h

[intersection2]         ; takes default parameters from upstream interxn
Location=1000

[intersection3]
Location=1500

[section1]
Start=0                 ; section start (finishes when next section starts)
SpeedLimit=60           ; speed limit, km/h
Elevation=0             ; elevation at section start, metres
                        ;     used to calculate grade on previous section
```

**Figure 10.16 – Setting the progression design speed in CorMod**

A number of similar input files were created, having PDS varying from 25 km/h to 70 km/h in 5 km/h increments. PDS values in excess of the speed limit (60 km/h on this hypothetical corridor) would be an extreme traffic operation condition, expected to provide poor progression between adjacent signals since vehicles would be unable to keep pace with the wave of green signals on the corridor.

A total of 1000 simulations were conducted of each scenario, the averaged results of which are presented below:

### 10.5.3 Results

As seen in Figure 10.17, the PDS giving the highest space mean speed for all vehicle types was 35 km/h. Values of PDS approaching or exceeding the speed limit (of 60 km/h) gave consistently low space mean speeds, because vehicles cannot pass through consecutive signals without exceeding the speed limit.

Figure 10.18 shows that the PDS offering the lowest stop rate is different for light and heavy vehicles. The minimum stop rate for heavy vehicles occurred at a PDS of 40 km/h, whereas the minimum stop rate for cars occurred at a PDS of 45 km/h. Both of these were higher than the 35 km/h PDS which maximised the space mean speed for all vehicles.

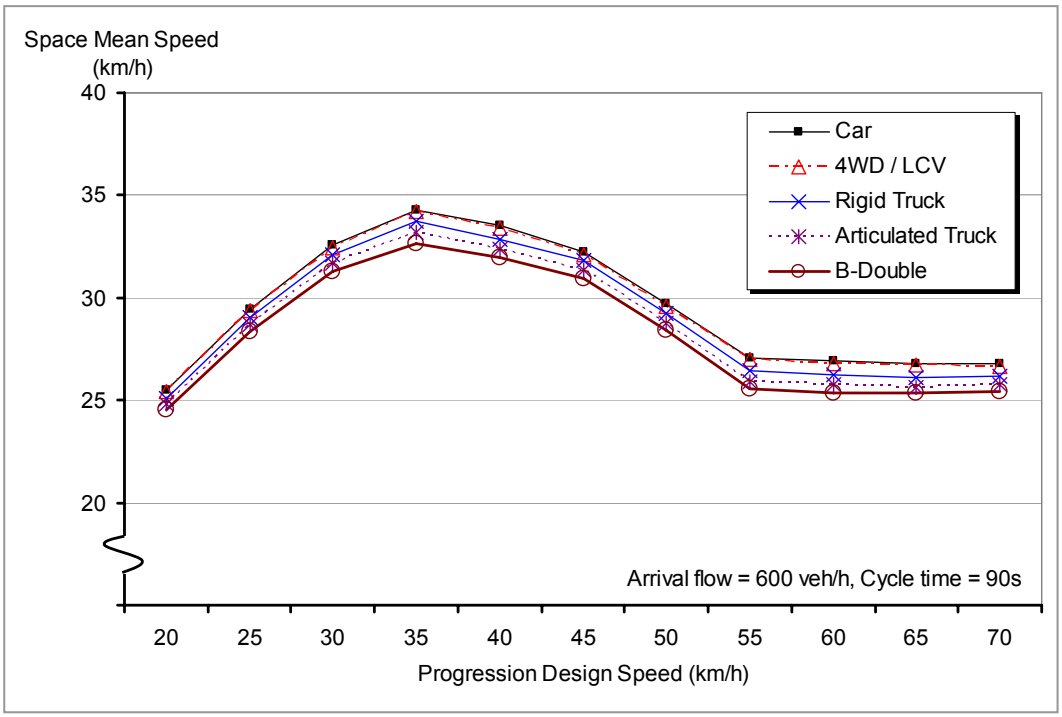


**Figure 10.17 – Variation of space mean speed with progression design speed for various vehicle types**

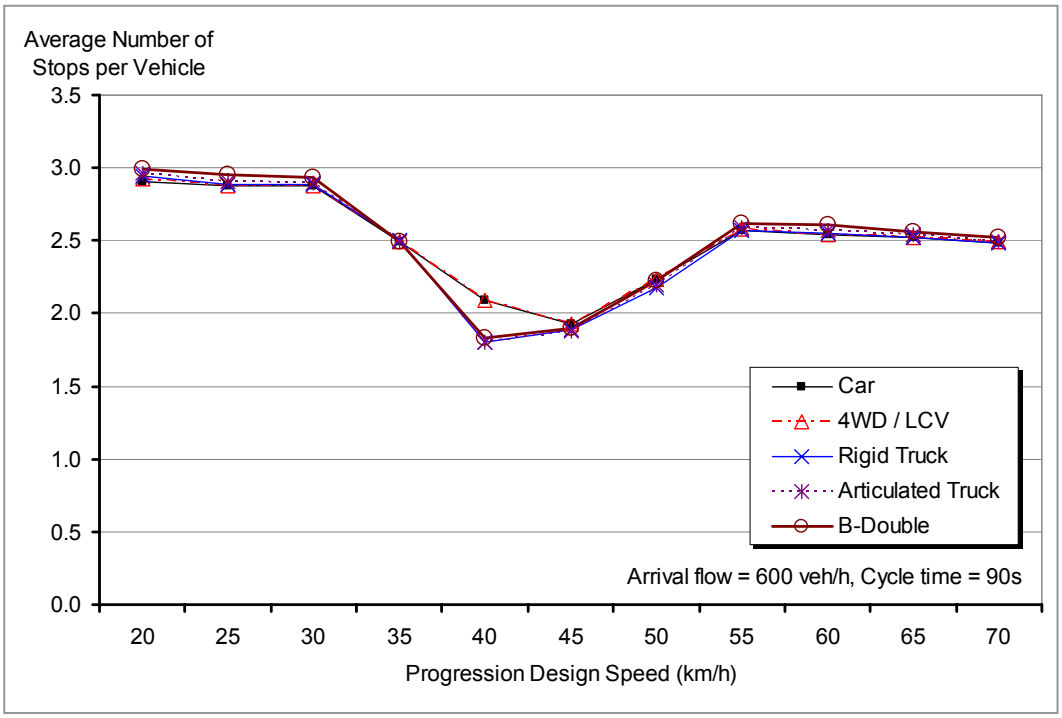


**Figure 10.18 – Variation of stop rate with progression design speed for various vehicle types**

The generally greater headway in front of a heavy vehicle means they are more likely to arrive at the back of a queue and not have to come to a complete stop (Figure 10.19). Anecdotally, heavy vehicles approaching a red traffic signal will slow down earlier and crawl towards the back of queue rather than having to come to a complete stop. This was not explicitly modelled in the program, and would not be expected to alter the control delay experienced by the heavy vehicle.

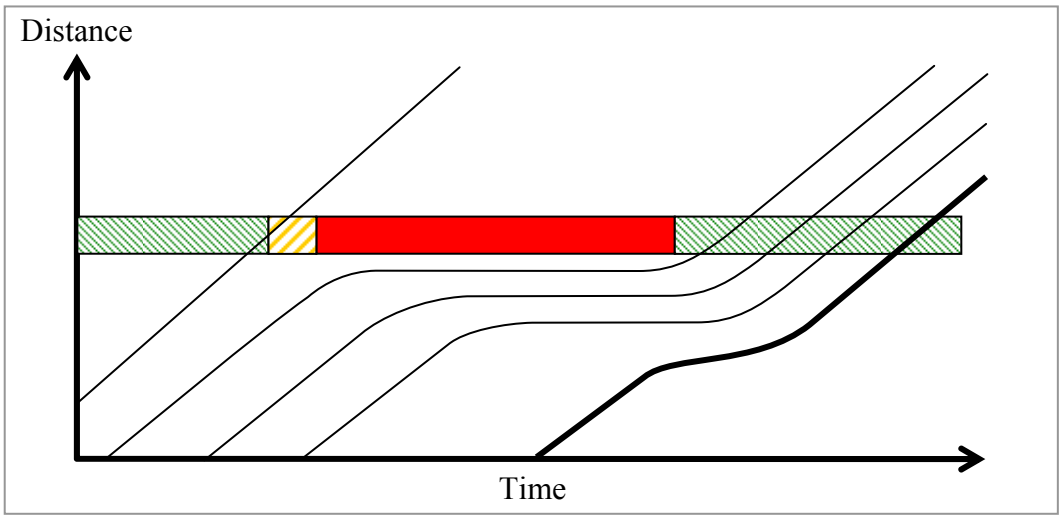


**Figure 10.19 – A large headway in front of a heavy vehicle reduces the need to come to a complete stop**

### 10.5.4 Is there an optimal progression design speed?

Progression design speed affects the speed, travel time and stop rate of vehicles in a corridor of coordinated traffic signals. There was little difference between the optimum setting for maximising the speeds of heavy vehicles and light vehicles; however, the stop rate of heavy vehicles was minimised at a lower progression design speed than that which minimised the stop rate of cars.

There were only slight differences between the optimum PDS for maximising speeds (35 km/h) and for minimising the number of stops for heavy vehicles (40 km/h). In deciding between the two of these, Figure 10.18 shows a large increase in number of stops (particularly for trucks) as PDS is decreased from 40 km/h to 35 km/h, whilst Figure 10.17 shows a lesser decrease in speeds as PDS is increased from 35 km/h to 40 km/h. Thus, an optimum PDS of 40 km/h based on the minimum stopping rate for trucks would also be close to optimum for maximising speeds and minimising the number of stops for cars.

The “Red Wave” that was mentioned in Ramsay (1998) was able to be reproduced with CorMod under carefully controlled conditions(including uniform headways and prohibiting lane changes). Under more general realistic conditions, heavy vehicles did not have to stop at the front of the queue at every intersection, and a queue of cars did not continually build up behind slow-moving heavy vehicles.

## 10.6 Advance Detection of Heavy Vehicles

### 10.6.1 Introduction

Figure 10.20 shows the Queue Position Classification Matrix for intersection 1 for the baseline case to which the other scenarios have been compared:

Queue Position Classification Matrix, Intersection 1, All Lanes:

| Queue Pos. | Car n | Car % | 4WD/LCV n | 4WD/LCV % | Rigid Tr n | Rigid Tr % | Artic Tr n | Artic Tr % | B-Double n | B-Double % | Total n |
|---|---|---|---|---|---|---|---|---|---|---|---|
| 1 | 89440 | 64.4 | 22156 | 15.9 | 15428 | 11.1 | 9191 | **6.6** | 2724 | **2.0** | 138939 |
| 2 | 88624 | 65.2 | 22400 | 16.5 | 14951 | 11.0 | 7861 | 5.8 | 2000 | 1.5 | 135836 |
| 3 | 86840 | 65.3 | 22035 | 16.6 | 14495 | 10.9 | 7561 | 5.7 | 1967 | 1.5 | 132898 |
| 4 | 84337 | 65.2 | 21443 | 16.6 | 14058 | 10.9 | 7531 | 5.8 | 1909 | 1.5 | 129278 |
| 5 | 81277 | 65.1 | 20889 | 16.7 | 13638 | 10.9 | 7281 | 5.8 | 1817 | 1.5 | 124902 |
| 6 | 77656 | 64.9 | 19802 | 16.5 | 13290 | 11.1 | 7249 | 6.1 | 1738 | 1.5 | 119735 |
| 7 | 74196 | 65.2 | 18638 | 16.4 | 12528 | 11.0 | 6706 | 5.9 | 1680 | 1.5 | 113748 |
| 8 | 69257 | 65.0 | 17697 | 16.6 | 11860 | 11.1 | 6259 | 5.9 | 1548 | 1.5 | 106621 |
| 9 | 63681 | 64.4 | 16587 | 16.8 | 11189 | 11.3 | 5911 | 6.0 | 1484 | 1.5 | 98852 |
| 10+ | 418236 | 64.4 | 107697 | 16.6 | 73808 | 11.4 | 39816 | 6.1 | 10211 | 1.6 | 649768 |

**Figure 10.20 – Baseline queue position classification matrix**

Although the proportion of articulated trucks is 5.9% and B-doubles is 1.5% in the population of vehicles generated for this scenario, this figure shows that both articulated trucks and B-doubles are more likely to appear at the front of queue. At this intersection, 6.6% of all vehicles arriving at the front of the queue were articulated truck, and 2.0% were B-doubles. Similar ratios were noticed at the other intersections. Implications for queue discharge and queue lengths would be expected to be greater than if proportions in the population were used. Additionally, as was reported in an earlier chapter, the PCE of heavy vehicles was found (Molina 1987; West and Thurgood 1995) to be greater when they are located at the head of a queue at a signalised intersection.

Particularly under random arrival conditions, heavy vehicles are more likely to appear at the head of the queue due to their maintaining a greater headway in front. These differences in headway distributions were confirmed from the automatic traffic counter data collected during this project. Having a greater headway, they are more likely to have the signal change from green in front of them. This assumes that HV & LV drivers have the same propensity to stop at a signal changing from green.

The detection of heavy vehicles approaching signalised intersections has been described in an earlier chapter. Researchers at Texas Transportation Institute has successfully applied it to isolated rural intersections, claiming benefits in reduced crash rates and pavement maintenance requirements (Middleton *et al.* 1997; Sunkari *et al.* 2000).

This section aims to extend this application to urban traffic corridor conditions, to determine whether it can be made to work, and to determine its effectiveness and the impacts that it may have on other road users on the corridor and crossing the corridor.

### 10.6.2 Details of the advance detection algorithm

The brief of this algorithm is to develop a means of extending the green time to allow the passage of an approaching heavy vehicle that otherwise would have to stop and restart.

The details of the advance detection algorithm are presented below, with Figure 10.21 illustrating the operation of the counter used to determine whether green time should be extended.

Additional vehicle detectors are located in each lane a distance upstream of each intersection. The existing inductive loops used for vehicle detection (located approximately 35 metres before the stop-line in Queensland and just before the stop-line in other Australian states) are too close to the intersection for use in this application. Detectors for a Sydney-based bus transit system were located beyond the safe stopping distance of the approaching bus (Vandebona and Rossi 2006).

Since this current application also records the length of the approaching heavy vehicle, it must be located at least the safe stopping distance plus the length of the longest vehicle likely to be detected. For a corridor design speed of 60 km/h, this was calculated to be 130 m.

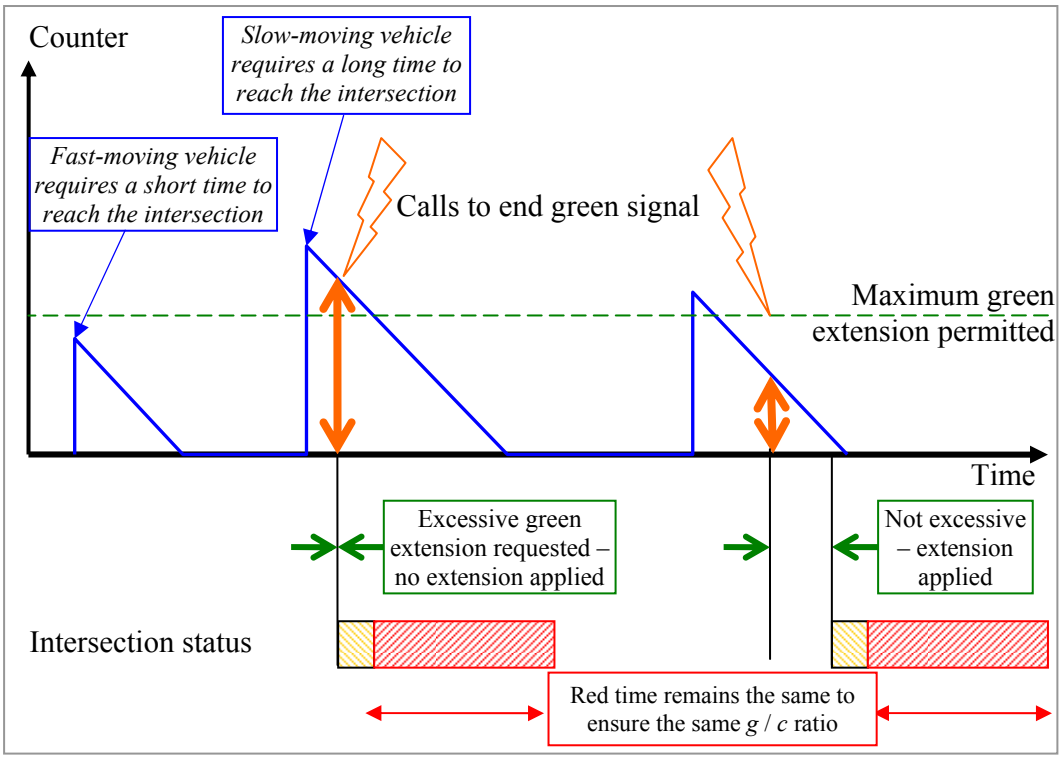


**Figure 10.21 – Logic used to extend the green time for an approaching heavy vehicle**

Unlike the Sydney bus priority system, the detectors do not rely on transponders being fitted to the vehicles. Pairs of standard inductive loops embedded in the pavement surface are used to estimate both the speed and length of a vehicle passing over it. Detections are only registered if the calculated length of the vehicle exceeds a specified minimum.

An estimate is made of the time taken for a long vehicle passing over the detector to reach the intersection at its current speed. Fast-moving vehicles would require a shorter time than slow-moving vehicles.

A counter is initialised to this estimated time, and is decremented as time passes. The counter is checked when an end-of-green is requested. If the counter has less than 10 seconds remaining, then the green signal is held on until the counter

reaches zero; enabling the long vehicle to pass through safely. If the counter has more than 10 seconds remaining then the green signal is not held and the approaching long vehicle would have to stop. Holding the green signal for an excessive length of time would take too much cycle time from the next movement.

After a green time extension, the time at which the next red signal terminates is delayed by the same amount as the green extension. This has the effect of maintaining the same $g$ / $c$ ratio, and not to disadvantage opposing movements.

### 10.6.3 Test of the heavy vehicle detection logic in CorMod

The **CorMod** program was enhanced to include the heavy vehicle detection and green time extension logic described in the previous section. Heavy vehicle detection is enabled by including the lines shown in Figure 10.22 in the **CorMod** initialisation file. These commands specify the position of the heavy vehicle detector relative to the intersection stop line, the maximum time that the green signal would be held for, the vehicle types that detection will work for, and whether or not the holds will be reported in the lane queuing display (Figure 10.25).

```
[advancedetectors]
Lead=130
MaxHold=10
VehicleType9=true
VehicleType10=true
VehicleType11=true
ReportHolds=true
```

**Figure 10.22 – Commands used to enable advance detection of heavy vehicles**

This sets the location of the heavy vehicle detector to be 130 metres before the stop line (the normal detectors, located 35 metres before the stop line, remain in use for normal vehicle-actuated signal operation). The maximum green hold time is set to 10 seconds, and the detector is only activated by vehicle types 9, 10 and 11 (articulated trucks, B-doubles and B-triples, respectively). For debugging purposes, reporting of detections and green holds is enabled.

Identical simulations were conducted with and without heavy vehicle detection enabled, as shown in Figure 10.23 and Figure 10.24 respectively.

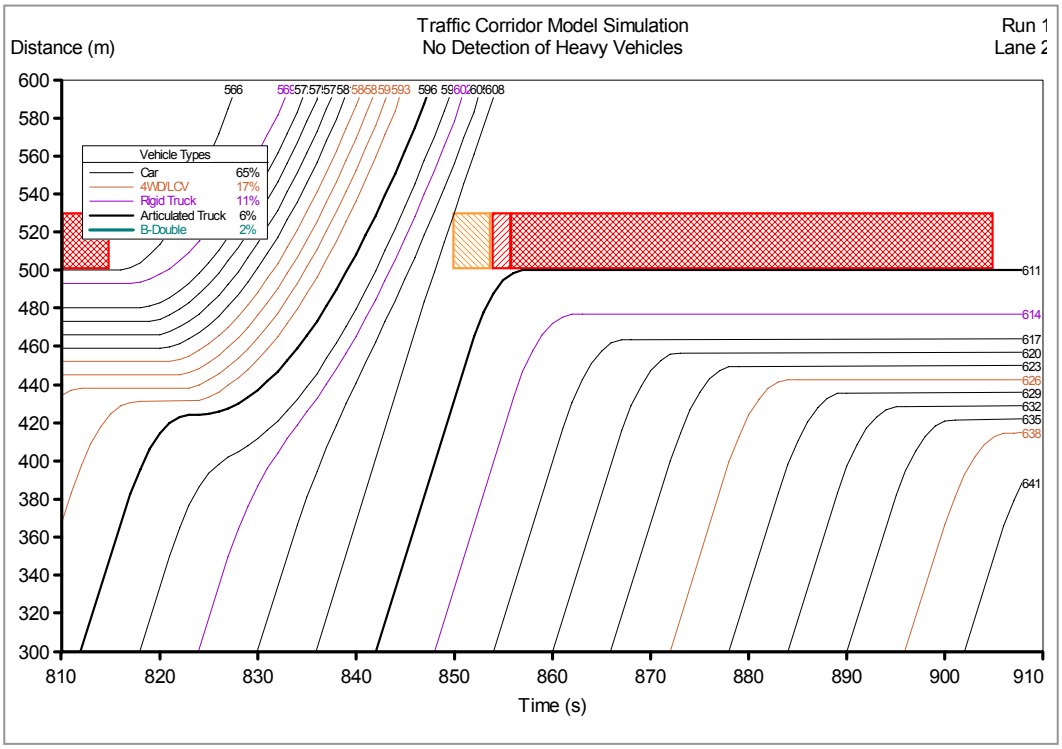


**Figure 10.23 – Heavy vehicle (#611) arriving at the front of a queue without green time extension**

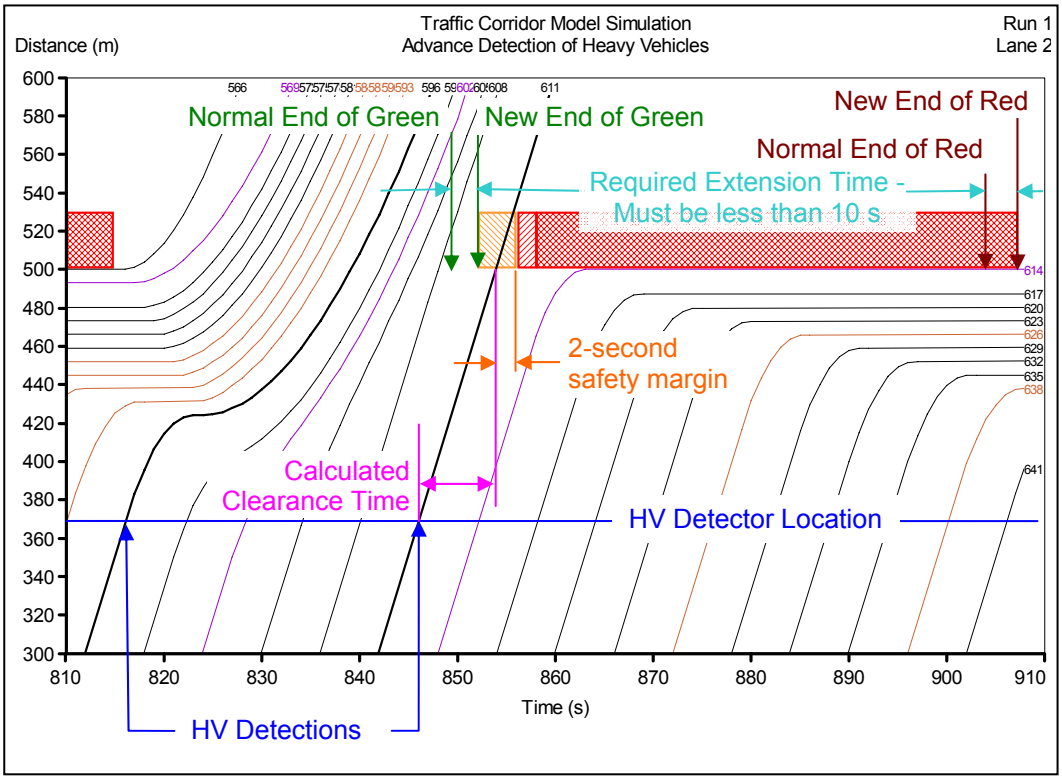


**Figure 10.24 – Detection of heavy vehicle and extending the green period**

Without heavy vehicle detection, vehicle #611 (an articulated truck) approaches the intersection as the green signal terminates and stops at the front of the queue. With heavy vehicle detection, the green time is extended by 2.4 seconds, permitting vehicle #611 to pass through the intersection. The heavy vehicle is no longer at the head of the queue, leading to a faster discharge of the queue when the next cycle starts.

Figure 10.25 shows an extract of the lane queuing display corresponding to the trajectory diagram shown in Figure 10.24. Three heavy vehicles (class 9) were detected at times of 816.14 s, 834.14 s and 864.14 s, each travelling at 60 km/h and requiring a hold time of 5.74 s. The normal end of green was signalled at 849.7 s, with the detection counter having 2.24 s remaining. This was less than the maximum hold time, so the green signal was held until 852 s. The front heavy vehicle passed the intersection stop line at 854 s in front of a yellow signal, with the red signal coming on at 856 s.

```
T= 816.14 I=1 L=2 Veh  596 [Class= 9] detected at -130m 60.0km/h. Hold=5.74s
T= 834.14 I=1 L=3 Veh  606 [Class= 9] detected at -130m 60.0km/h. Hold=5.74s
T= 846.14 I=1 L=2 Veh  611 [Class= 9] detected at -130m 60.0km/h. Hold=5.74s
T= 849.70 I=1              Hold   Green  for 2.24s. Veh 611 [Class= 9] Lane 2
T= 852.00 I=1              Show   YELLOW. G=37.1s. [Lane 3 Gapped Out]
T= 854.00 I=1 L=1 Veh  610 Passes intxn. NX=16 TX=39.10s v=60km/h
T= 854.00 I=1 L=2 Veh  611 Passes intxn. NX=16 TX=39.10s v=60km/h
T= 856.00 I=1              Show   RED.   AR=2.0s
T= 858.00 I=1              Start  Opposing Movement.
T= 865.18 I=2 L=2 Veh  596 [Class= 9] detected at -131m 59.3km/h. Hold=5.90s
T= 904.90 I=1              Hold   Red for 2.24s.
T= 907.20 I=1              Show   GREEN.
```

**Figure 10.25 – CorModC lane queuing display corresponding to Figure 10.24**

A fourth heavy vehicle (also class 9) was detected at a time of 865s. Its speed was marginally lower than the previously detected vehicles, so the required hold time is greater.

### 10.6.4 Effectiveness of heavy vehicle detection

The Queue Position Classification Matrix in Figure 10.26 shows that, with vehicle detection, 5.7% of all vehicles stopping at the head of the queue at this intersection were articulated trucks and 1.6% were B-doubles. Referring back to Figure 10.20, without detection these proportions were 6.6% and 2.0%, respectively.

The heavy vehicle detection and green time extension at this intersection was used 10507 times in a total of 1000 simulations each of 1 hour duration. This is an average of once every 342 seconds, with the green time being held for an average time of 4.36 seconds.

Queue Position Classification Matrix, Intersection 1, All Lanes:

| Queue Pos. | Car n | Car % | 4WD/LCV n | 4WD/LCV % | Rigid Tr n | Rigid Tr % | Artic Tr n | Artic Tr % | B-Double n | B-Double % | Total n |
|---|---|---|---|---|---|---|---|---|---|---|---|
| 1 | 90089 | 65.0 | 22689 | 16.4 | 15676 | 11.3 | 7924 | **5.7** | 2271 | **1.6** | 138649 |
| 2 | 89199 | 65.8 | 22720 | 16.8 | 15027 | 11.1 | 6823 | 5.0 | 1759 | 1.3 | 135528 |
| 3 | 86990 | 65.7 | 22106 | 16.7 | 14568 | 11.0 | 7057 | 5.3 | 1781 | 1.3 | 132502 |
| 4 | 84015 | 65.2 | 21430 | 16.6 | 14228 | 11.0 | 7372 | 5.7 | 1761 | 1.4 | 128806 |
| 5 | 81137 | 65.3 | 20605 | 16.6 | 13661 | 11.0 | 7114 | 5.7 | 1817 | 1.5 | 124334 |
| 6 | 77452 | 65.1 | 19560 | 16.4 | 13196 | 11.1 | 6941 | 5.8 | 1758 | 1.5 | 118907 |
| 7 | 73610 | 65.3 | 18434 | 16.3 | 12370 | 11.0 | 6648 | 5.9 | 1719 | 1.5 | 112781 |
| 8 | 68432 | 64.8 | 17630 | 16.7 | 11787 | 11.2 | 6258 | 5.9 | 1512 | 1.4 | 105619 |
| 9 | 63158 | 64.6 | 16234 | 16.6 | 10910 | 11.2 | 5942 | 6.1 | 1493 | 1.5 | 97737 |
| 10+ | 408641 | 64.3 | 105647 | 16.6 | 72231 | 11.4 | 38873 | 6.1 | 9964 | 1.6 | 635356 |

**Green Hold actuated 10507 times. Average hold time 4.36 s.**

**Figure 10.26 – Queue position classification matrix with heavy vehicle detection**

Figure 10.27 and Figure 10.28 show the proportion of vehicles arriving at the front of queues at each intersection that were articulated trucks and B-doubles, respectively. Heavy vehicles were more likely to appear at the front of the queue at high arrival flow rates, and their detection was unable to stop this. At more modest flow rates, heavy vehicles were less likely to appear at the front of queue and detection was able to reduce this even further.

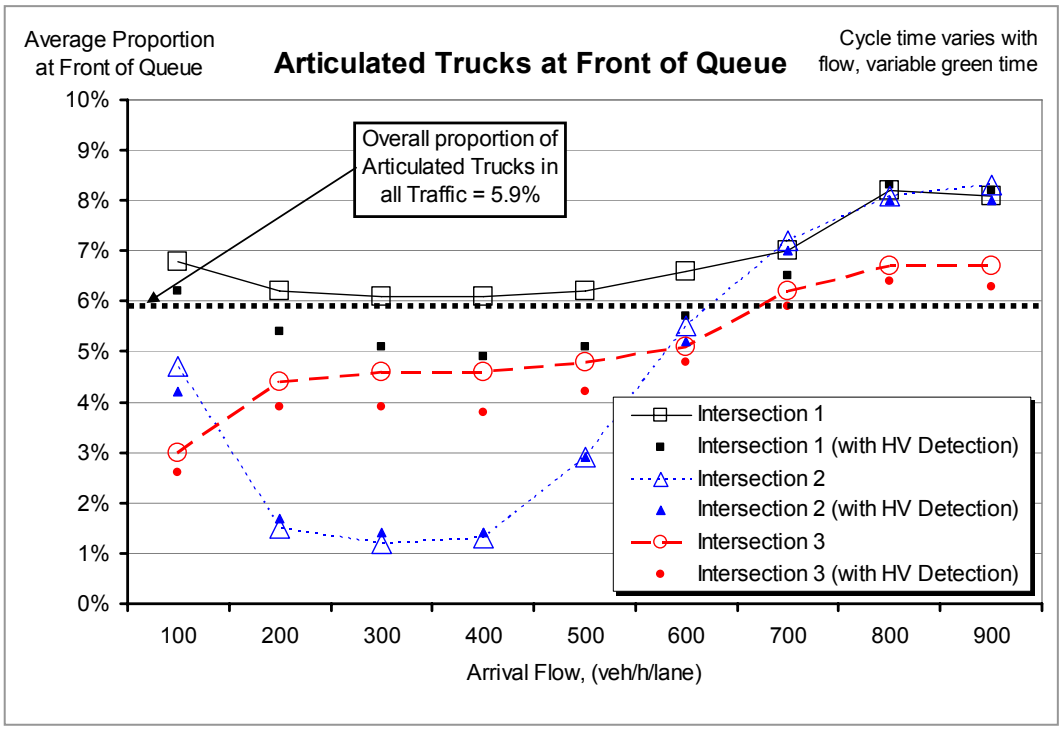


**Figure 10.27 – The proportion of vehicles at the front of intersection queues that were articulated trucks**

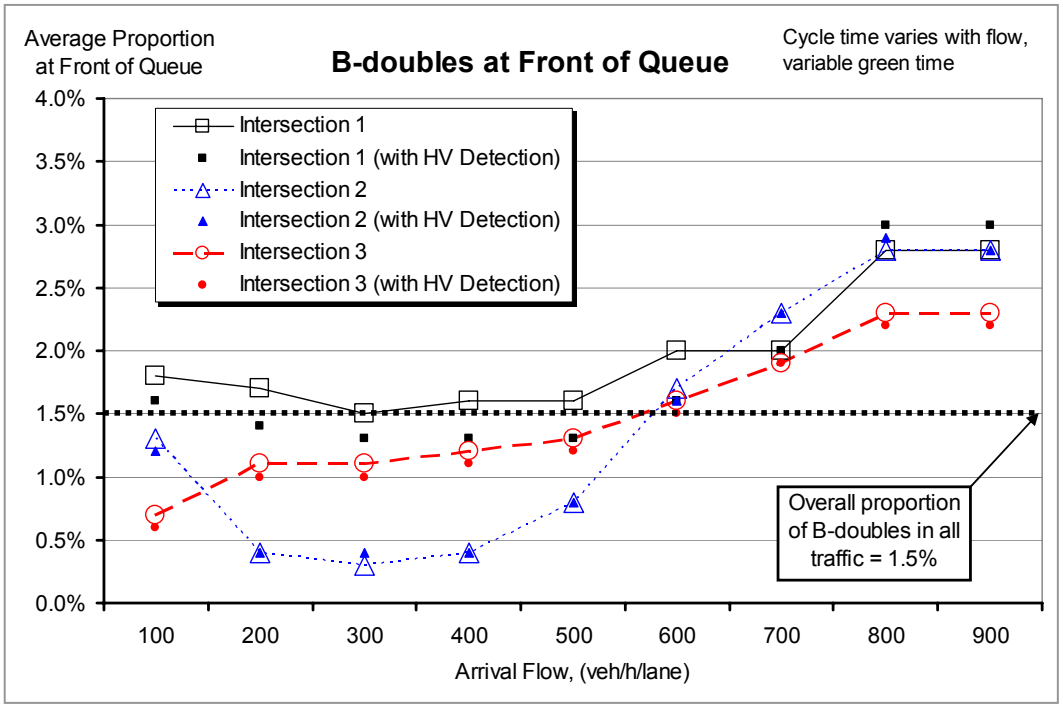


**Figure 10.28 – The proportion of vehicles at the front of intersection queues that were B-doubles**

### 10.6.5 Effect of heavy vehicle detection on other corridor traffic

Table 10.5 shows the speeds and average number of stops, averaged over all vehicle types, without and with heavy vehicle detection being used. Heavy vehicle detection can be seen to give a slight increase in speeds and reduction in the number of stops at low-to-medium flow. At higher flow rates, heavy vehicle detection decreases the speeds and increases stop rates.

**Table 10.5 – Change in speeds and stop rates with heavy vehicle detection**

| *Arrival flow (veh/h/lane)* | *Space mean speed (km/h)* | | | *Average stops per vehicle* | | |
|---|---|---|---|---|---|---|
| | *without detection* | *with detection* | *% change* | *without detection* | *with detection* | *% change* |
| 100 | 38.31 | 38.42 | 0.3% | 2.59 | 2.56 | -1.2% |
| 200 | 40.19 | 40.35 | 0.4% | 2.10 | 2.08 | -1.0% |
| 300 | 40.5 | 40.7 | 0.5% | 1.92 | 1.90 | -1.0% |
| 400 | 39.82 | 40.01 | 0.5% | 1.80 | 1.78 | -1.1% |
| 500 | 37.41 | 37.6 | 0.5% | 1.79 | 1.79 | 0.0% |
| 600 | 33.32 | 33.32 | 0.0% | 2.04 | 2.05 | 0.5% |
| 700 | 27.21 | 26.76 | -1.7% | 2.72 | 2.81 | 3.3% |
| 800 | 19.09 | 18.23 | -4.5% | 8.20 | 11.46 | 39.8% |
| 900 | 16.03 | 15.79 | -1.5% | 27.21 | 31.65 | 16.3% |

The following figures disaggregate the data in this table to show the speeds and stop rates for three vehicle types (cars, articulated trucks and B-doubles).

Figure 10.29 shows the decrease in the average speed of the different vehicle types as the arrival flow is increased, for cases without and with heavy vehicle detection (represented by hollow and solid symbols respectively).

This is also represented in Figure 10.30, plotting the space mean speed with heavy vehicle detection against the equivalent conditions without detection. The diagonal line across the graph represented the line of equality; any symbols above that line indicate conditions in which heavy vehicle detection is beneficial, and symbols below indicate a benefit in not using detection.

Detection was seen to be beneficial to all vehicle types at low to medium arrival flows, whereas at high arrival flows it lead to slightly lower speeds.

Figure 10.31 and Figure 10.32 show the stop rates for each vehicle type at different arrival flows both with and without heavy vehicle detection. The greatest reduction in stop rate is for articulated trucks and B-doubles at flows of between 200 and 500 vehicles per hour per lane.

Heavy vehicle detection was particularly effective in reducing the number of stops at low-to-medium arrival flow rates. At high flow rates (more than 700 veh/h/lane) it increased the number of stops for all vehicle types.

The change in the number of stops may not appear to be much, but it is the heavy vehicles at the front of the queue that are not being stopped to the same extent. This would lead to faster queue discharge at the signalised intersections.

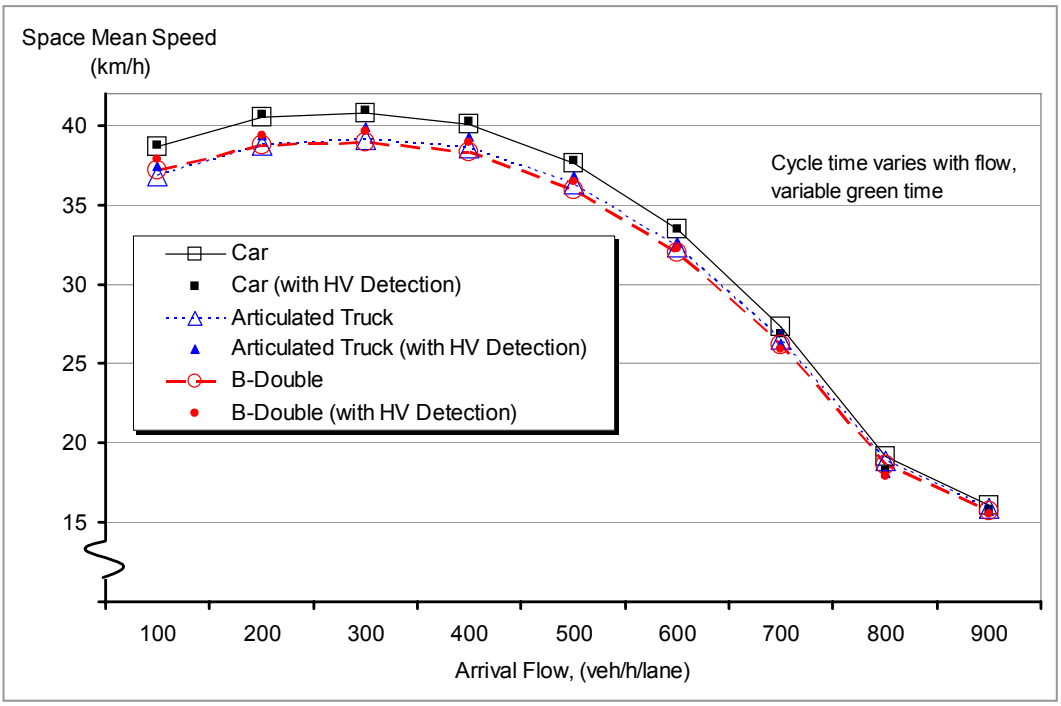


**Figure 10.29 – Effect of heavy vehicle detection on speeds of various vehicle types at different arrival flows**

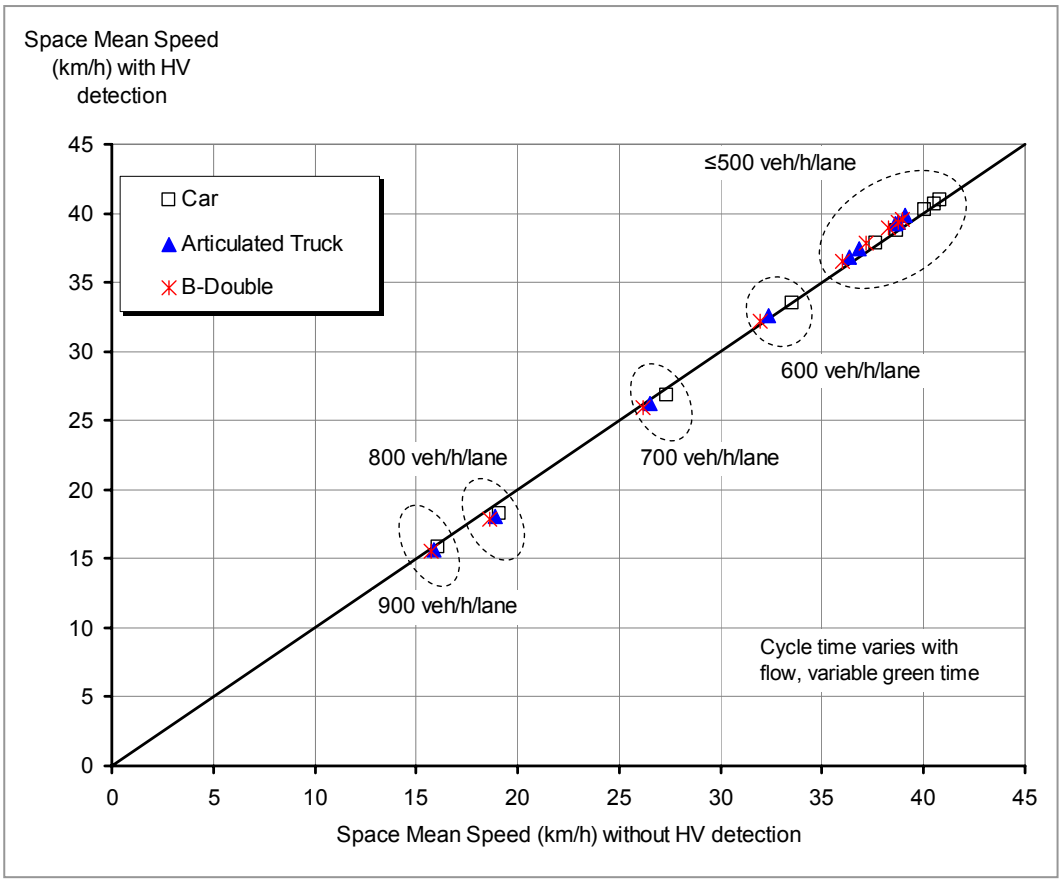


**Figure 10.30 – Speeds of different vehicle types with and without heavy vehicle detection**

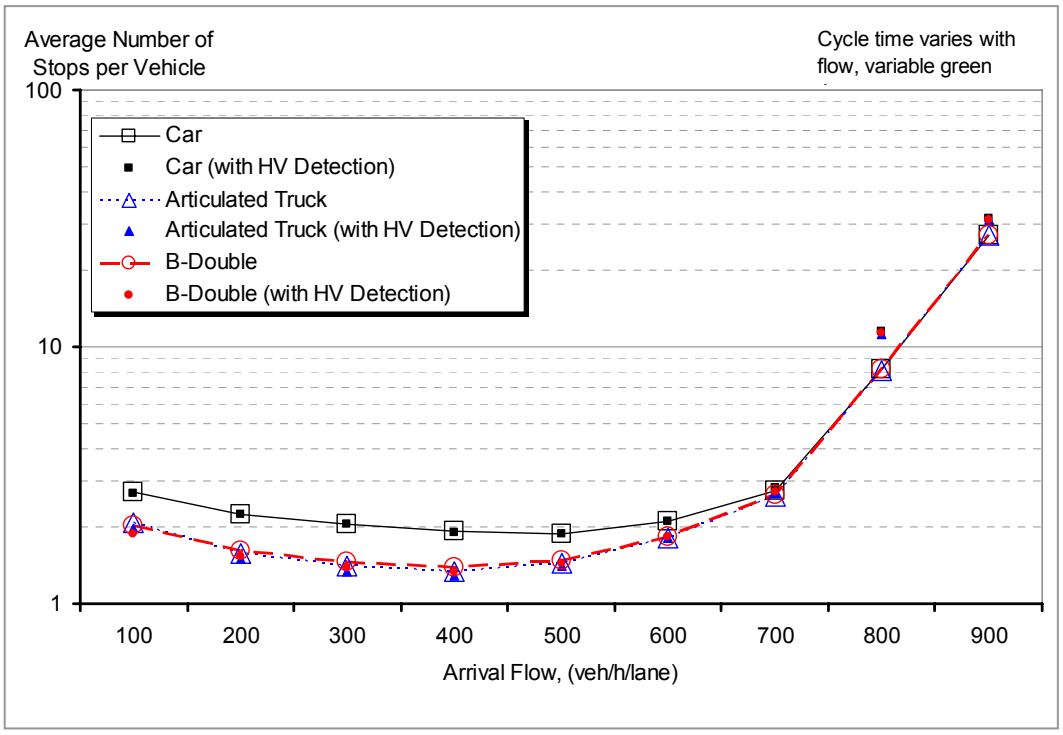


**Figure 10.31 – Effect of heavy vehicle detection on stops per vehicle for various vehicle types at different arrival flows**

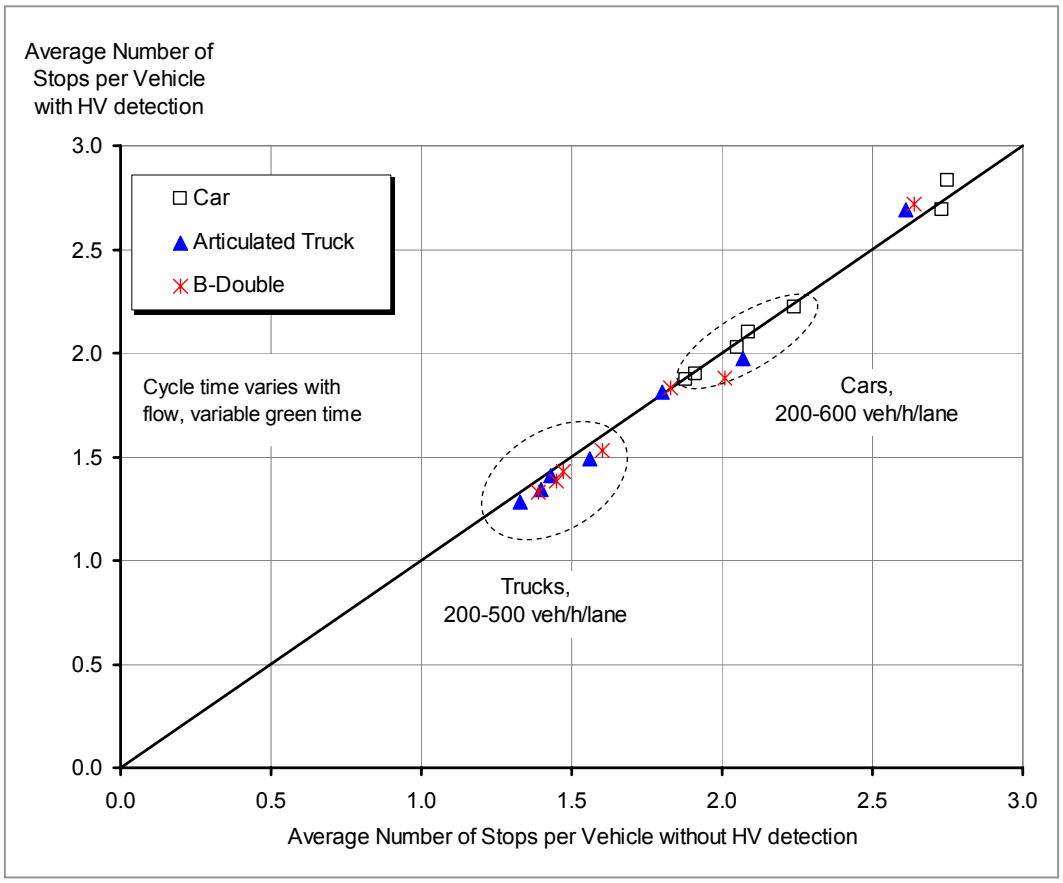


**Figure 10.32 – Number of stops per vehicle with and without heavy vehicle detection for various vehicle types**

### 10.6.6 Effect of heavy vehicle detection on the opposing traffic

Traffic on opposing approaches to the intersections on the corridor is not modelled explicitly in **CorMod**. However, since any time 'borrowed' from opposing movements to permit the passage of a heavy vehicle on the corridor is returned to the opposing movement in the next cycle, the net green time displayed to the opposing movements should be unchanged.

This can be checked by examining the ratio of green time to cycle time for the corridor through-movement at each of the intersections. Figure 10.33 shows this ratio of *G* / *C* for various arrival flow rates. Hollow symbols represent conditions without HV detection, and solid symbols represent conditions with heavy vehicle detection enabled.

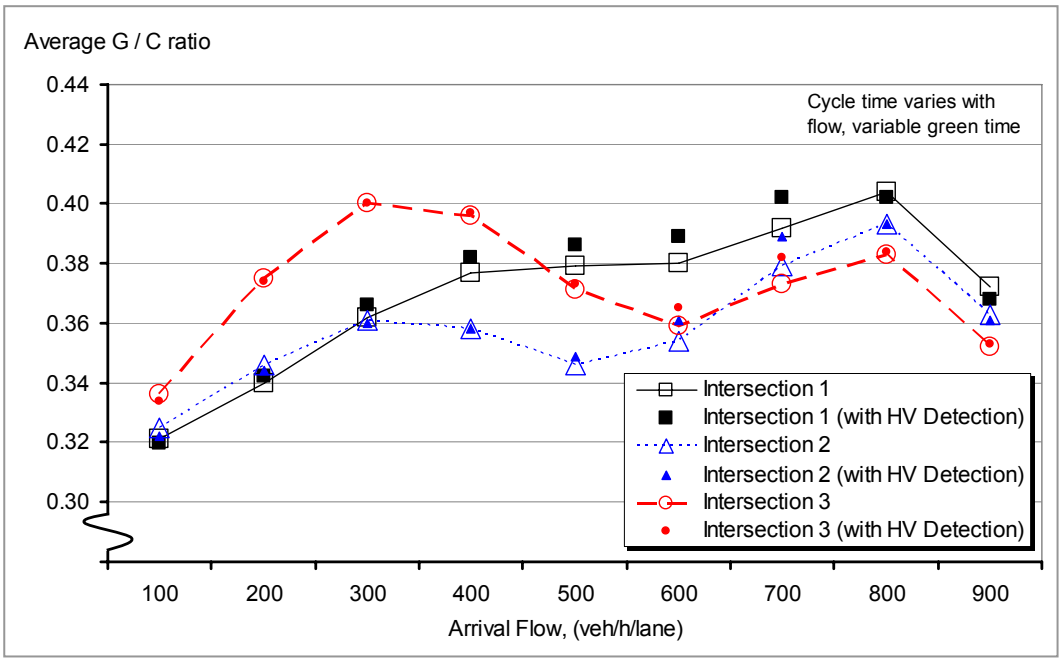


**Figure 10.33 – Average *G* / *C* ratio with and without heavy vehicle detection**

Noting the range of *G* / *C* in Figure 10.33, there is little difference in the average green time ratio when heavy vehicle detection is enabled. A slight increase in *G* / *C* (<2.5%) occurred at medium flow conditions. Ideally, the average *G* / *C* would remain constant (as described above); however, in a vehicle-actuated system such as this, the length of green time is determined from the volume of traffic arriving in each cycle, and thus would vary between scenarios.

The proportion of green time available for opposing movements would also remain relatively constant (a slight decrease during medium flows). However, if the opposing traffic itself is relying on precise timing of a separate corridor, this shift in a single cycle may affect progression of the opposing traffic.

### 10.6.7 Heavy vehicle detection conclusions

As reported earlier, other sources found benefits in using heavy vehicle detection to reduce the stop rates of heavy vehicles at isolated, rural intersections. This current investigation indicates that only modest gains in travel times and stop rates are achievable when applied to an urban arterial traffic corridor in low-to-medium flow conditions. This hypothetical corridor consists of three closely-spaced intersections, in which the timing of the signalised intersections (particularly the progression design speed as covered earlier in this chapter) has a strong influence on the speeds and stop rates of vehicles on the corridor. Extending the green time to permit a heavy vehicle to progress (and delaying the start of the next green time) will act to reduce the benefits in having a closely synchronised set of intersections. The slight reduction in $G$ / $C$ available for opposing movements would also reduce the benefits offered by heavy vehicle detection.

In off-peak conditions, heavy vehicle detection may offer advantages in reducing excessive stopping of heavy vehicles (and the associated noise at night time); however, its use does not appear to be warranted during peak and daytime inter-peak periods.

## 10.7 Quantifying the Benefits of each Scenario

The simulations of the freight policy and traffic management scenarios presented in this chapter have predicted travel times, stop rates and other performance measures for a range of vehicle types. It is useful to aggregate these measures into a single value to give a more readily understood interpretation of the effectiveness of each scenario.

Published valuations of travel times for a range of different vehicle classes were used from the Austroads Guide to Project Evaluation (Austroads 2005, Section 3.6). The travel time valuations shown in Table 10.6 were based on statistics current in June 2002, separately estimating values for vehicle occupants and for the freight being carried.

**Table 10.6 – Estimated values of occupant and freight travel time values**

*Source: Austroads (2005, Table 2.8) – Urban values only*

| | *Occupant travel time* | | *Freight travel time* |
|---|---|---|---|
| *Vehicle Type* | *Occupancy rate (persons/vehicle)* | *Value per occupant (person-hour)* | *Value per vehicle-hour* |
| **Cars** | | | |
| Private | 1.7 | $10.74 | -n/a- |
| Business | 1.3 | $34.35 | -n/a- |
| **Rigid trucks** | | | |
| Light commercial | 1.3 | $21.05 | $1.13 |
| Medium | 1.2 | $21.35 | $3.06 |
| Heavy | 1.0 | $21.80 | $10.48 |
| **Articulated trucks** | | | |
| 4 Axle | 1.0 | $22.09 | $22.56 |
| 5 Axle | 1.0 | $22.39 | $28.78 |
| 6 Axle | 1.0 | $22.39 | $31.03 |
| **Combination vehicles** | | | |
| B-double | 1.0 | $22.39 | $44.91 |

In order to match the five vehicle types used in this study, several of the vehicle types in this table had to be combined. Passenger cars were considered to comprise an equal proportion of business and private use vehicles. A greater proportion of private use is usually assumed, however the simulations in this study seek mainly to model the period during the day between the morning and afternoon peaks, when there is a higher proportion of both heavy vehicles and passenger cars being used for business purposes.

From the proportions recorded by the traffic counter / classifiers used in this study, rigid trucks were assumed to comprise 73% 2-axle trucks and 27% 3-or-more axle trucks; and articulated trucks were assumed to comprise 10% 4-axle, 9% 5-axle and 91% 6-axle vehicles. Table 10.8 presents the aggregated travel time valuations (combining both occupant and freight values) for the five vehicle classes used in the simulation in this chapter.

**Table 10.7 – Aggregated values of urban travel time**

| *Vehicle Type* | *Aggregated travel time value (per vehicle-hour)* |
|---|---|
| Car | $31.46 |
| 4WD/LCV | $28.50 |
| Rigid truck | $29.63 |
| Articulated truck | $52.34 |
| B-double | $67.30 |

Table 10.8 presents the total value of travel time per year under each scenario, and the savings in the value of travel time compared to the baseline scenario. These values are calculated based on an inter-peak analysis period of 6 hours per day and 250 working days per year.

The corridor consisting only of cars indicated the greatest saving in value of travel time. However, it should be realised that this scenario does not have any freight travel time costs. The freight that would have been using this corridor would have been diverted to an alternative route – incurring greater travel time costs for the freight itself and for other users of the alternative route.

**Table 10.8 – Estimated value of travel time savings under each scenario**

| *Scenario* | *Total travel time value per year* | *Savings compared to baseline scenario* | *Proportion of baseline scenario* |
|---|---|---|---|
| Baseline | $ 5.29 M | - | - |
| All Cars * | $ 4.23 M | $ 962 K | 18.2% |
| No B-doubles | $ 5.41 M | - $ 127 K | -2.4% |
| More B-doubles | $ 5.09 M | $ 218 K | 4.1% |
| Some B-triples | $ 5.17 M | $ 114 K | 2.2% |
| Trucks only use lane 1 | $ 5.07 M | $ 220 K | 4.2% |
| Trucks only use lanes 1&2 | $ 5.09 M | $ 193 K | 3.6% |
| Big trucks only use lane 1, small trucks use lanes 1 & 2 | $ 5.05 M | $ 237 K | 4.5% |
| Heavy vehicle detection ** | $ 5.28 M | $ 2 K | 0.04% |

Notes: * *Does not realise the cost of moving freight to an alternative corridor*

** *Does not account for adverse impacts on conflicting movements*

The freight vehicle mode split scenario that offers the greatest savings in the value of travel time is a greater use of B-doubles. Elimination of B-doubles would increase the travel time costs over the baseline scenario.

The greatest savings in the value of travel time, whilst still carrying the same volume of freight, occurs in restricting the different vehicle types to the greatest extent possible, placing all large trucks in one lane, allowing small trucks to use either of two truck lanes, and prohibiting trucks from one of the lanes. Al-Kaisy and Jung (2004) also found this lane utilisation strategy to offer the greatest savings in a study of congested freeway conditions.

Heavy vehicle detection offers minimal savings in the value of travel time; however, the reduction on the number of stops for heavy vehicles would have savings in vehicle and pavement maintenance. These are less easy to quantify.

Additional benefits would be likely to occur in terms of reduced stop rates, and secondary measures such as wear & tear, fuel emissions. However, quantifying these benefits is beyond the scope of this thesis.

## 10.8 Summary and Conclusions of this Chapter

This chapter has described the results of simulations of a hypothetical traffic corridor under various freight policy and traffic management scenarios.

The continuing growth in urban freight volumes was predicted to lead to continuing decreases in average speeds and increases in stop rates across all vehicle types.

Various strategies were developed for lessening these adverse effects of increased urban road freight; these are outlined below.

### 10.8.1 Freight policies

Considering the corridor in isolation, the greatest reduction in travel times and stop rates occurred by removing heavy vehicles. This has to be balanced against the increased time and costs in moving freight on an alternative route, and the resulting increased congestion on that route.

Encouraging a greater use of more freight-efficient vehicles had benefits in reducing the number of vehicles required to carry an existing volume of freight on the corridor. However, if the performance of those alternative freight vehicle types is substantially below that of the vehicles they are replacing, then an overall degradation in corridor performance may result.

### 10.8.2 Lane utilisation

The greatest savings in travel costs and the greatest reduction on stop rates occurred by segregating the various vehicle types to the greatest degree possible. A scenario in which large trucks were restricted to one lane, medium trucks to that lane and another, and permitting cars the exclusive use of a third lane gave the greatest travel time cost savings of all scenarios carrying freight on the corridor. Implementation and enforcement of such a strategy would be challenging.

### 10.8.3 Signal coordination

All vehicle types had their average speeds maximised at the same progression design speed (PDS) of 35 km/h. The minimum number of stops for trucks occurred at a PDS of 40 km/h and for cars at a PDS of 45 km/h. An optimum PDS of 40 km/h gave a low stop rate and high average speed for all vehicle types.

### 10.8.4 Heavy vehicle detection

Assuming the same behaviour when confronted with a signal changing from green, heavy vehicles were found to be more likely to arrive at the front of a queue at an intersection. Unfortunately, this is the position where they have the greatest effect on increase start loss and reducing saturation flow when the queue discharges.

Heavy vehicle detection was seen to be a means of facilitating the progress of heavy vehicles along the corridor, being more effective at low-to-medium arrival volumes. At higher volumes, it can lead to a reduction in the bandwidth offered to traffic passing between coordinated signals.

### 10.8.5 General

The scenarios presented in this chapter were conducted using a simple hypothetical corridor without any grade and having uniformly spaced signalised intersections. The next chapter applies these scenarios to a more realistic corridor, using grades and intersection spacings taken from an existing corridor.

# CHAPTER 11 APPLICATION OF THE MODEL TO A REAL URBAN CORRIDOR

## 11.1 Introduction

This chapter describes the application of the corridor-level traffic model to a section of an existing urban traffic corridor that carries a high proportion of freight vehicles amongst a large volume of traffic.

The chapter is intended to demonstrate the applicability of the model to investigations of alternative scenarios (described in the previous chapter) on an existing traffic corridor.

## 11.2 Method

A model was created that had the same road profile and intersection spacings as the eastern end of the Brisbane Urban Corridor, between Logan Road and Gateway Motorway. Only the eastbound traffic was considered, however a simple model of the westbound traffic could be created by inverting the profile and intersection spacings.

The same freight policy and traffic management scenarios were examined as in the previous chapter, including

- Freight mode split
- Lane allocation
- Optimisation of progression design speed
- Heavy vehicle detection and green time extension

The corridor model was created using information obtained from the GPS units used in the chase car surveys, as reported in Chapter 6. The GPS unit contained an inbuilt barometric altimeter, which is claimed by the manufacturer to be more accurate in determining elevations than using the distances to overhead GPS satellites.

The elevation profiles recorded during the 63 eastbound trips over the corridor were averaged, giving the mean profile shown in Figure 11.1. There are five intersections in the corridor being modelled, indicated by vertical dashed lines with the names of the cross roads. The two unnamed vertical dashed lines to the left of the corridor represent intersections outside the corridor section being modelled. **CorMod** requires a piecewise-linear elevation profile, with the road consisting of sections of constant gradient, not necessarily having uniform length. The peaks and troughs of the measured profile were used to estimate the piecewise-linear elevation profile. An alternate method would have been to use uniform length sections, interpolating the elevations at the section end points. This alternative was not used since it had the potential to underestimate gradients if a peak or trough was missed. The locations of the intersections along the corridor were also determined from the GPS units. Waypoints were set at the intersections' eastbound stop-lines, and their coordinates used to determine the elevations and intersection locations.

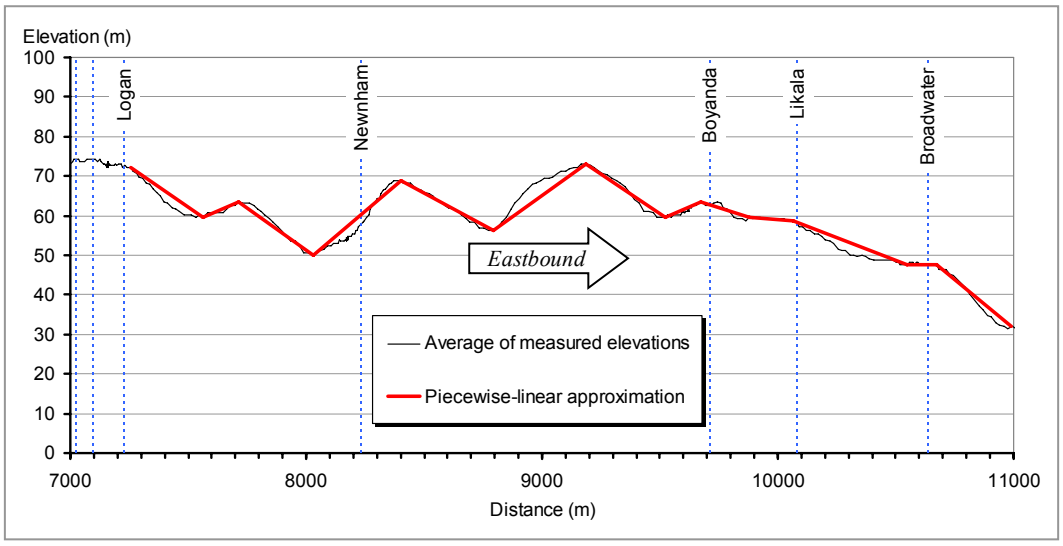


**Figure 11.1 – Measured and approximated elevations and intersection locations**

Figure 11.2 shows an extract of the **CorMod** input file used to set the grades and intersection spacing for this model. A total of 14 road sections were used, each having a specified starting chainage and elevation. The gradient on the section is determined by dividing the difference in elevation between the start of the next section and the start of the current section by the length of the current section. If not specified, the speed limit on each section is taken from the previous section.

```
[intersection1]
Location=8235          ; location of signal stop-line, metres
CycleTime=90           ; cycle time, [same for downstream interxns]
MaxGreen=0.667         ; max green time, in secs or proportion of cycle time
ProgressionSpeed=40    ; speed at which signals are coordinated to, in km/h

[intersection2]        ; takes default parameters from upstream intersection
Location=9711

[intersection3]
Location=10084

[intersection4]
Location=10640

[section1]
Start=7250             ; section start (finishes when next section starts), m
SpeedLimit=60          ; speed limit, km/h
Elevation=72.2         ; elevation at section start, metres
                       ;     used to calculate grade on previous section
[section2]
Start=7564
Elevation=59.7

[section3]
Start=7712
Elevation=63.6

[section4]
Start=8029
Elevation=50

[section5]
Start=8400
Elevation=68.9

[section6]
Start=8793
Elevation=56.4

[section7]
Start=9185
Elevation=73.2

[section8]
Start=9521
Elevation=59.7

[section9]
Start=9671
Elevation=63.6

[section10]
Start=9877
Elevation=59.7

[section11]
Start=10064
Elevation=58.8

[section12]
Start=10549
Elevation=47.7

[section13]
Start=10672
Elevation=47.7

[section14]
Start=10992
Elevation=31.9
```

**Figure 11.2 – Extract of corridor model input file**

## 11.3 Results

A typical **CorModW** trajectory diagram for the corridor is shown in Figure 11.3. It appears similar to those presented in previously chapters, apart from the uneven intersection spacing.

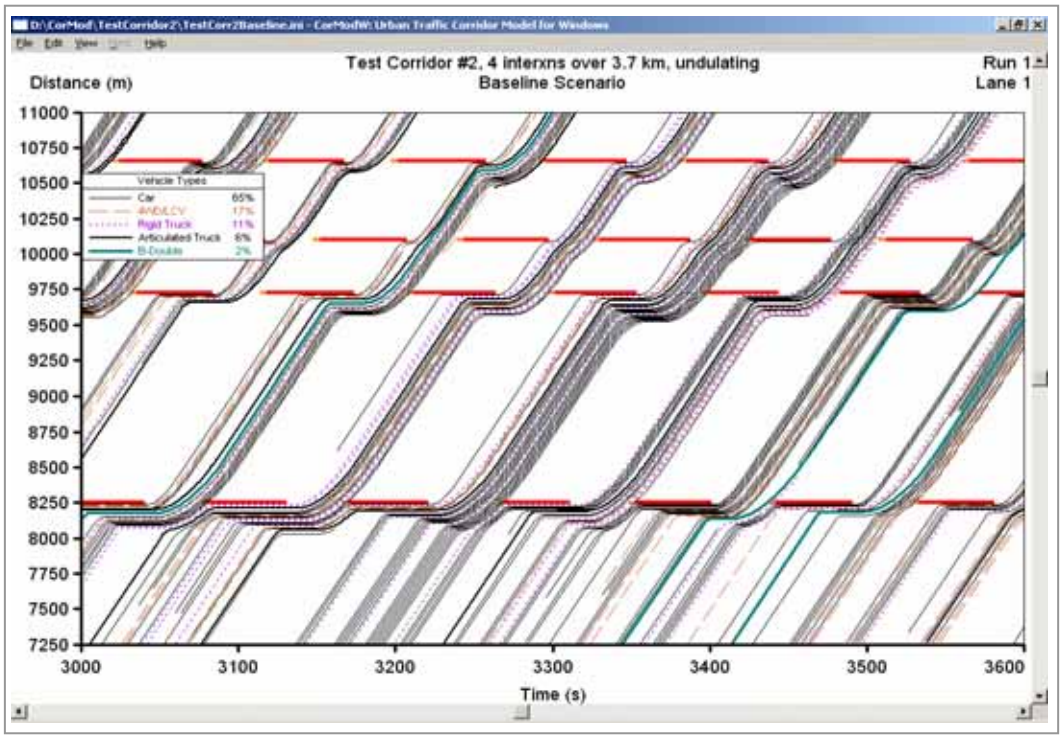


**Figure 11.3 – Typical trajectory diagram for the urban corridor**

The first intersection (at 8250m) is on a grade of +5%, compared to the other three intersections on slight negative gradients of -1.9%, -2.3% and -3.0%. This effect of grade on heavy vehicles is evident in the trajectory diagrams, with both articulated trucks and B-doubles taking longer to accelerate to the free-flow speed when departing from intersection 1 compared to the other intersections. The large headways in front of them are occasionally filled by light vehicles changing into the lane in front of the heavy vehicle. These are indicated by trajectories appearing on the diagram as they disappear from the trajectory diagram of another lane; for example, two vehicles change lanes in front of a B-double as it leaves intersection 1 at a time of 3450 seconds.

The same scenarios as used previously were applied to this corridor, with 1000 repeat runs being undertaken for each scenario.

### 11.3.1 Increasing arrival flows

The volume of traffic being 'fed' into the corridor was varied from 100 vehicles per hour per lane to 900 vehicles per hour per lane. Cycle times at each of the intersections were increased from 40 seconds through to 120 seconds, as described in the previous chapter.

Figure 11.4 shows the reduction in space mean speeds of all vehicle types as the arrival flow was increased. This figure is similar to that presented in Figure 9.4 (flat corridor, 3 evenly-spaced intersections, same speed limit of 60 km/h), however, the speeds are slightly higher at low arrival flows and lower at high arrival flows.

The greater difference between speeds of the different vehicle types at low flow conditions was attributed to the +5% grade at the first intersection. The reduction in the acceleration capability with grade is greater for heavy vehicles than for light vehicles, and vehicles are more likely to have to stop at this first intersection because their arrival pattern is random, rather than the platooned arrivals at the downstream intersections (see Figure 11.3).

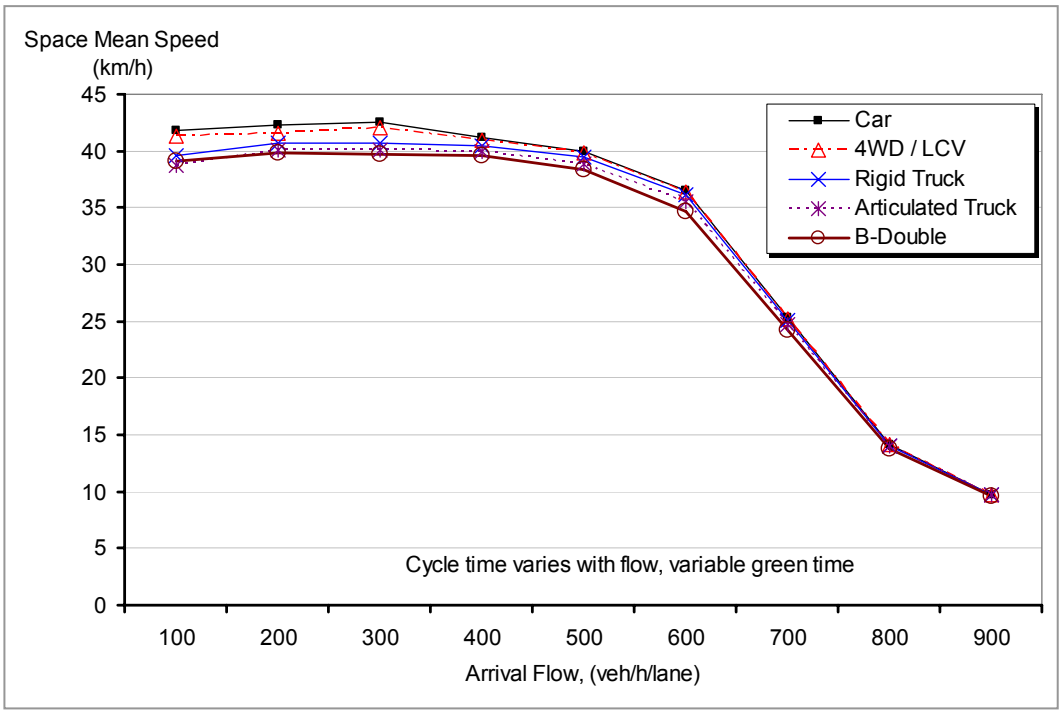


**Figure 11.4 – Reduction in speed as flow increases**

Figure 11.5 shows the increasing number of stops with increasing arrival flows. There is less difference between stop rates of the different vehicles than was shown earlier in Figure 9.5. This was attributed to the propensity for light vehicles to change lanes in front of heavy vehicles on this corridor. There were not so many large headways in front of heavy vehicles, so the probability of them having to come to a complete stop when approaching the back of queue at an intersection would be much closer to that of light vehicles.

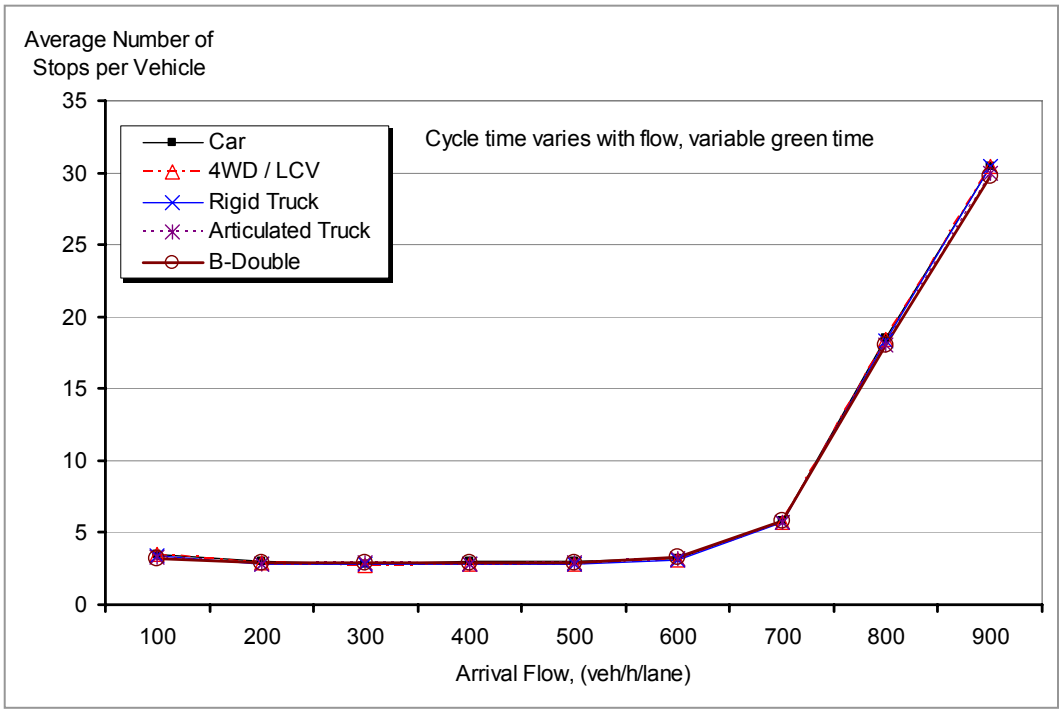


**Figure 11.5 – Increase in number of stops as flow increases**

### 11.3.2 Freight vehicle mode choice scenarios

Five freight vehicle mode choice scenarios were examined for this corridor:

- All cars
- Baseline corridor
- No B-doubles
- Increased B-doubles
- Some B-triples

The proportions of each vehicle type and arrival flows were the same as used in the previous chapter (Table 10.3).

Figure 11.6 shows the space mean speed of each vehicle type under each scenario. As shown earlier in Figure 10.4, speeds were highest without any heavy vehicles on the corridor, and lowest when B-triples were introduced. There was little difference between the baseline scenario and those that varied the number of B-doubles. This was attributed to the poorer performance of individual B-doubles on grades (particularly at intersection 1) acting to decrease speeds, whilst having fewer freight vehicles on the corridor acting to increase speeds. B-triples caused an even greater disruption to this corridor than that described in the previous chapter; this was attributed to their poorer gradeability (15%, versus 19% for a B-double) greatly increasing their acceleration delay when departing from the +5% grade at intersection 1.

As mentioned earlier, the network-wide effects of relocating freight traffic must be considered in the first scenario; and the performance of the B-triple in urban traffic was not measurable, and had to be estimated.

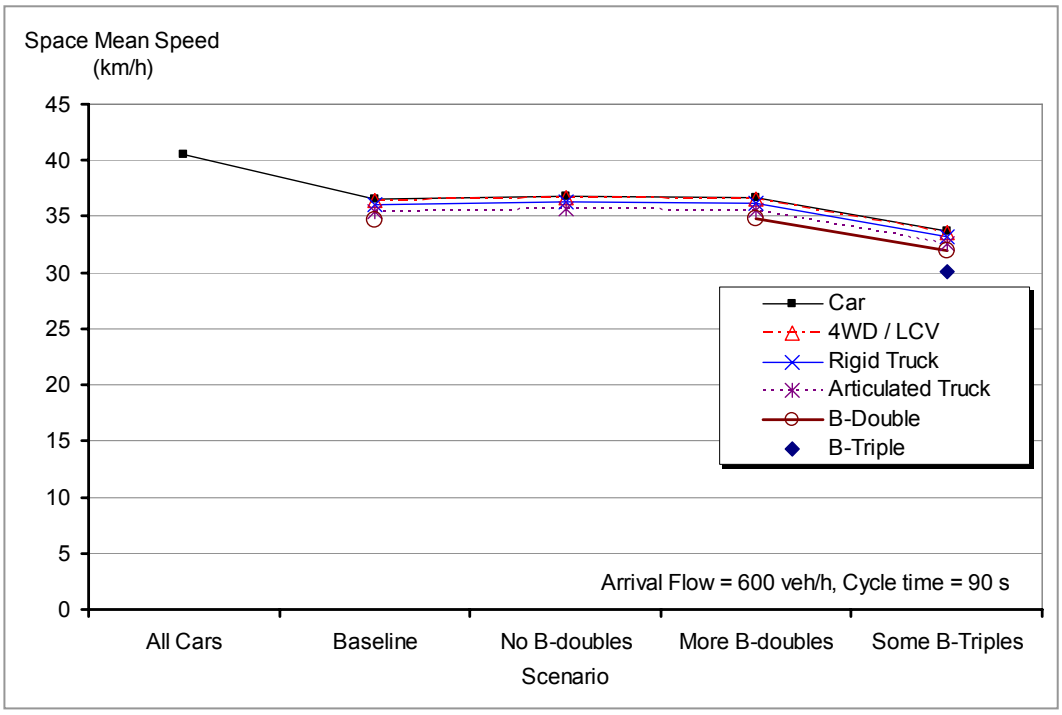


**Figure 11.6 – Variation in space mean speed with freight scenario**

Figure 11.7 shows the number of stops for each vehicle type. Stops were generally higher on this corridor than for that shown in Figure 10.5, having four intersections compared to three intersections used previously. There was little difference between the B-double scenarios, for the reasons described above. The introduction of B-triples greatly increased the number of stops, primarily attributed to the problems departing the grade at intersection 1.

Further, there is less difference between the stop rates of the different vehicle types than that found using the previous corridor. As mentioned in the previous subsection, this was attributed to cars changing lanes in front of heavy vehicles leading to them being more likely to come to a complete stop at an intersection.

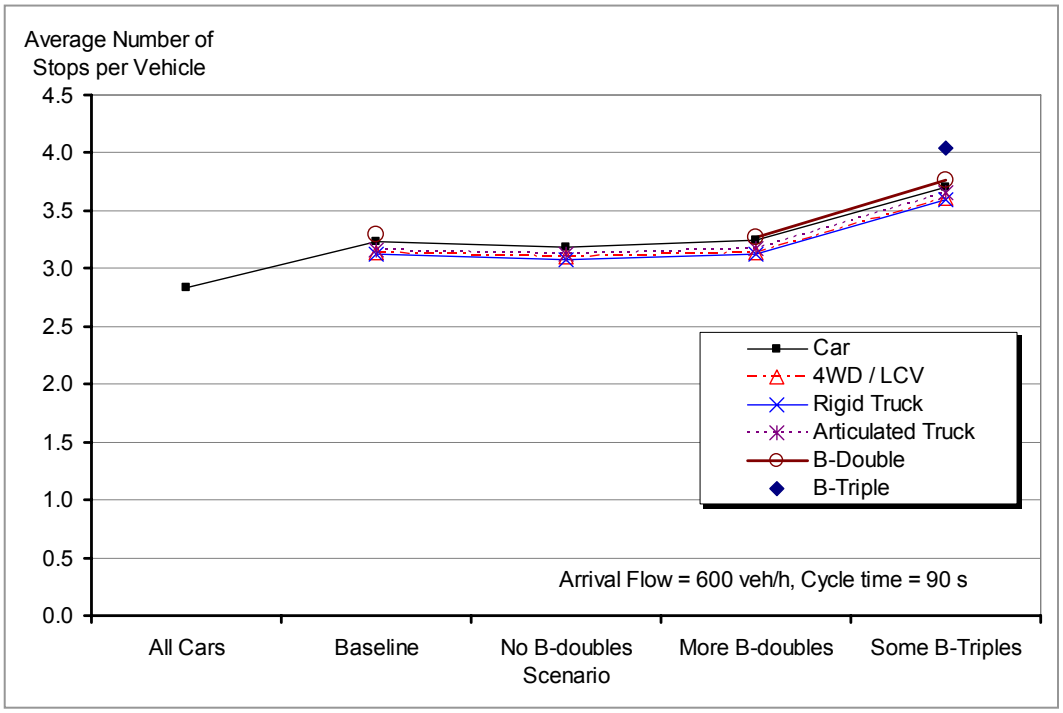


**Figure 11.7 – Variation in number of stops with freight scenario**

### 11.3.3 Lane utilisation scenarios

The same lane utilisation scenarios as were used in the previous chapter (and in Al-Kaisy and Jung 2004) were applied to this corridor:

**Baseline** All vehicle types are permitted to use any of the three lanes

**All trucks use lane 1** All rigid trucks, articulated trucks and B-doubles must use lane 1. Cars and 4WDs/LCVs may use any lane

**All trucks use lanes 1 and 2** All rigid trucks, articulated trucks and B-doubles must use lanes 1 or 2. Cars, 4WDs and LCVs may use any lane.

**Large trucks in lane 1, small trucks in lanes 1 and 2** All articulated trucks and B-doubles must use lane 1. Rigid trucks must use lane 1 or lane 2. Cars may use any lane, but lane 3 is for their exclusive use.

Figure 11.8 shows the space mean speeds of each vehicle type under each of these scenarios, derived from 1000 simulations of each scenario. Figure 11.9 shows the number of stops by each vehicle type under these scenarios.

Results are very similar to those shown in the previous chapter (Figure 10.9 and Figure 10.10, respectively). Restricting all trucks to the one lane leads to an over utilisation of that lane, with spare capacity existing in the two car-only lanes. Additionally, the vehicle-actuated signals at each of the intersections would have their green times extended to the maximum permitted in an attempt to manage the heavy demand of trucks; this would be at the expense of the green time available for opposing traffic movements.

The most beneficial lane utilisation appears to be to segregate the different vehicle types to the greatest degree possible, as was found in the previous chapter.

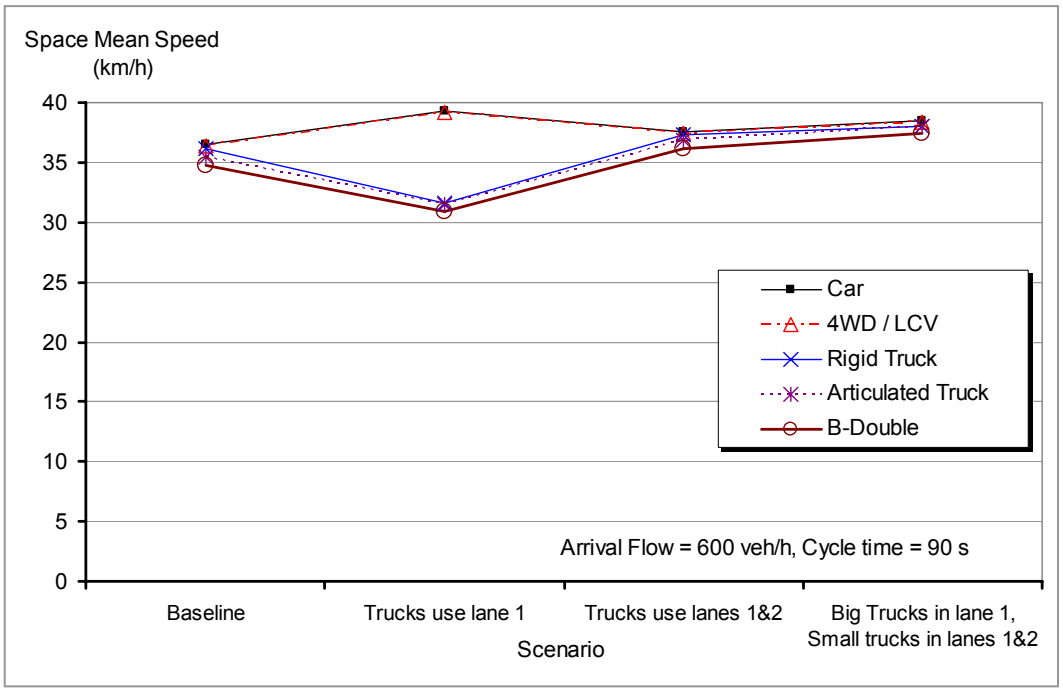


**Figure 11.8 – Variation in space mean speed with lane utilisation scenario**

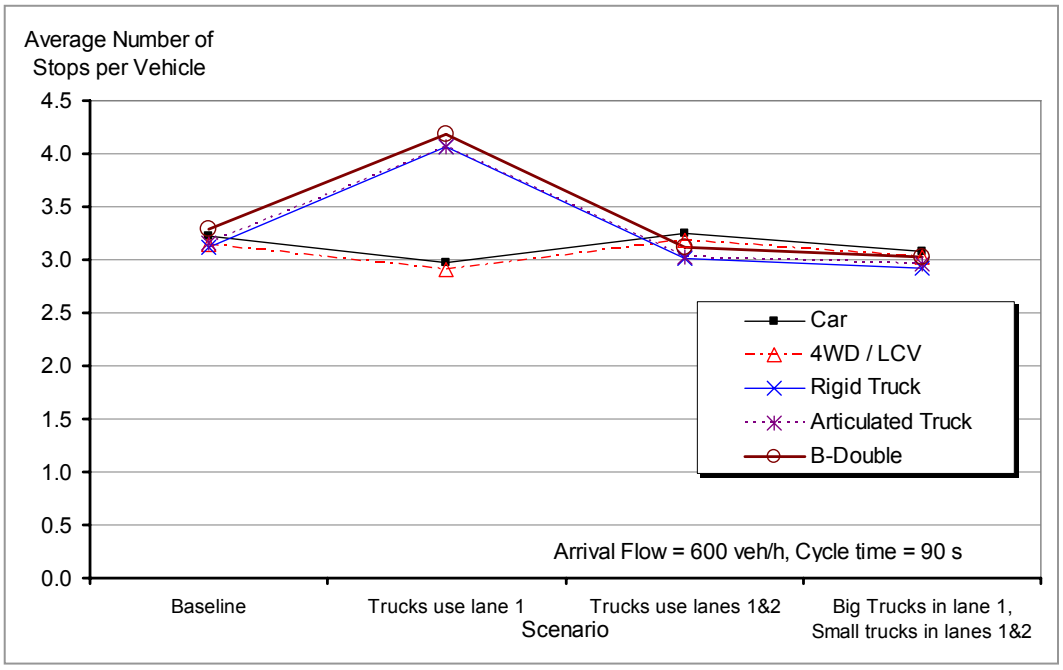


**Figure 11.9 – Variation in number of stops with lane utilisation scenario**

### 11.3.4 Optimal signalised corridor progression design speed

Unlike the corridor described in the previous chapter, the varying grades and intersection spacings on the current corridor were more representative of typical conditions, and a useful test of whether progression of different vehicle types along a corridor would still be able to be maximised by specifying offsets between the signalised intersections on the corridor.

To test this, the progression design speed (PDS) was varied from 20 km/h through to 70 km/h, with 1000 simulations being conducted at each PDS value.

Figure 11.10 shows the space mean speeds of the different vehicle types as the PDS was varied, and Figure 11.11 shows the number of stops per vehicle as the PDS was varied. These may be compared to Figure 10.17 and Figure 10.18, respectively, for the corridor examined in the previous chapter.

PDS values at and above the speed limit of 60 km/h were intentionally included to show the poor progression that results from a PDS close to or above the speed limit. Since vehicles are unable to pass through in the designed bandwidth they must wait until the next cycle, being subjected to an effective progression speed that is much lower than either the PDS or the speed limit. For example, a PDS of 72 km/h (20 m/s) between two intersections spaced 500 metres apart having a common cycle time of 90 seconds would have an effective progression speed of 500 / (90+500/20) = 4.34 m/s, or 15.6 km/h.

The optimum PDS in terms of providing maximum speeds on the corridor for all vehicle types was a speed of 40 km/h (90 seconds offset per kilometre between intersections). The minimum number of stops for all vehicle types was achieved at a PDS of 45 km/h (80 seconds offset per kilometre).

Although these optimum PDS values are the same as those for the previous corridor, there was more variation in both the speeds and the number of stops as PDS was varied compared to those found previously.

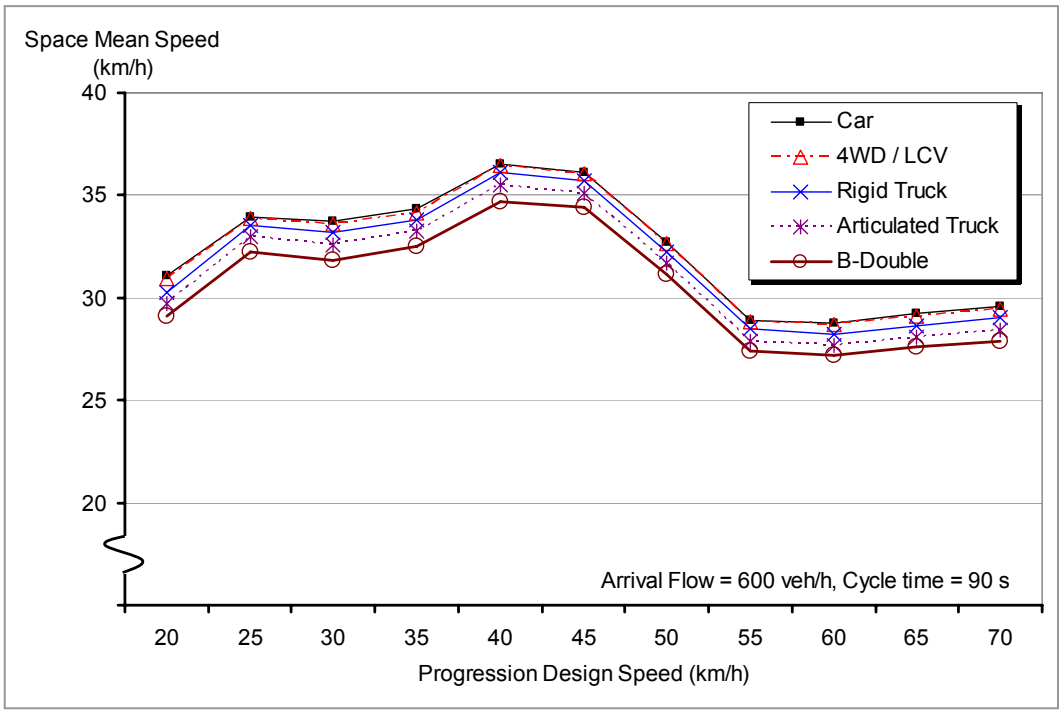


**Figure 11.10 – Variation in space mean speed with progression design speed**

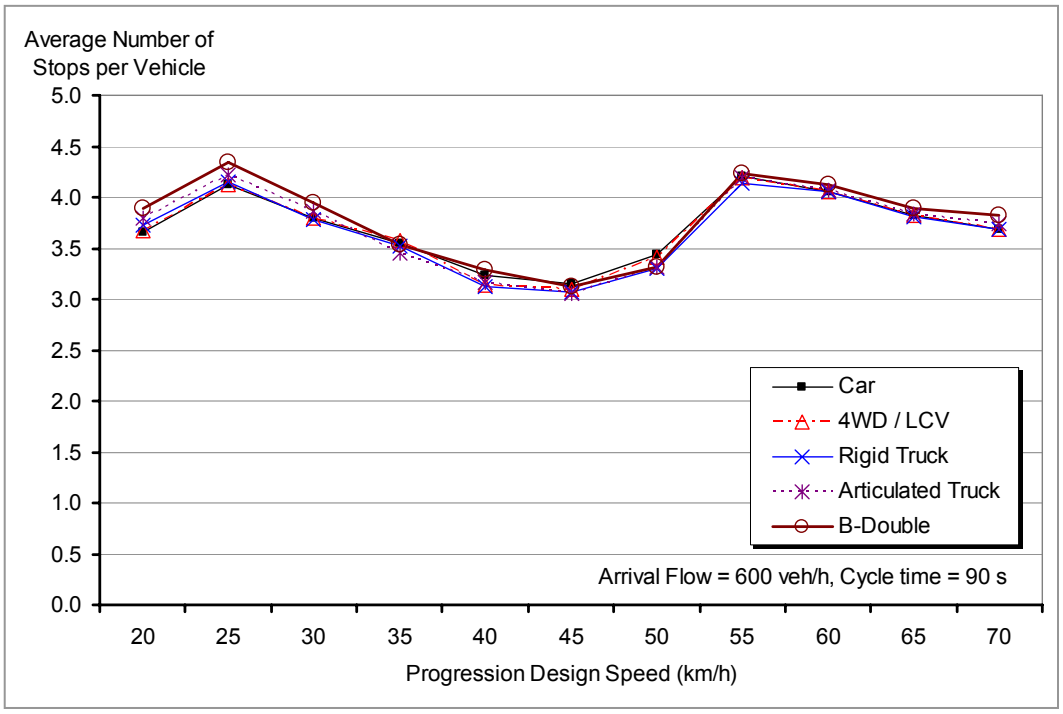


**Figure 11.11 – Variation in number of stops with progression design speed**

Having non-uniform intersection spacings and different grades on the sections between consecutive intersections, the average speeds taken by vehicles between intersections would not be the same. It would then be expected that different PDS values would optimise progression between different pairs of consecutive intersections. For example, if there were a positive gradient between two intersections, vehicles would take a longer time to travel between them, and would benefit from a lower PDS value. This would be particularly so for heavy vehicles.

This explains the greater variability in both speeds and stops as PDS was varied. Unlike for the previous corridor, progression through different sections of the current corridor would be maximised at different PDS values.

Unlike previously, the same PDS value was found to give the minimum number of stops for heavy and light vehicles on this corridor. As mentioned earlier in this chapter, the number of stops of heavy vehicles was closer to those of light vehicles, due to their larger headways being filled in by lane changing vehicles.

### 11.3.5 Heavy vehicle detection

An identical heavy vehicle detection and green time extension algorithm to that described in the previous chapter was applied to the current corridor.

Figure 11.12 shows the space mean speeds of different vehicle types both with and without heavy vehicle detection, at different arrival flows. It can be compared to Figure 10.30 for the speeds on the previous corridor.

Figure 11.13 shows the number of stops with and without heavy vehicle detection for arrival flows below 700 veh/h/lane (those above 700 veh/h/lane would have been a long distance off the scale).

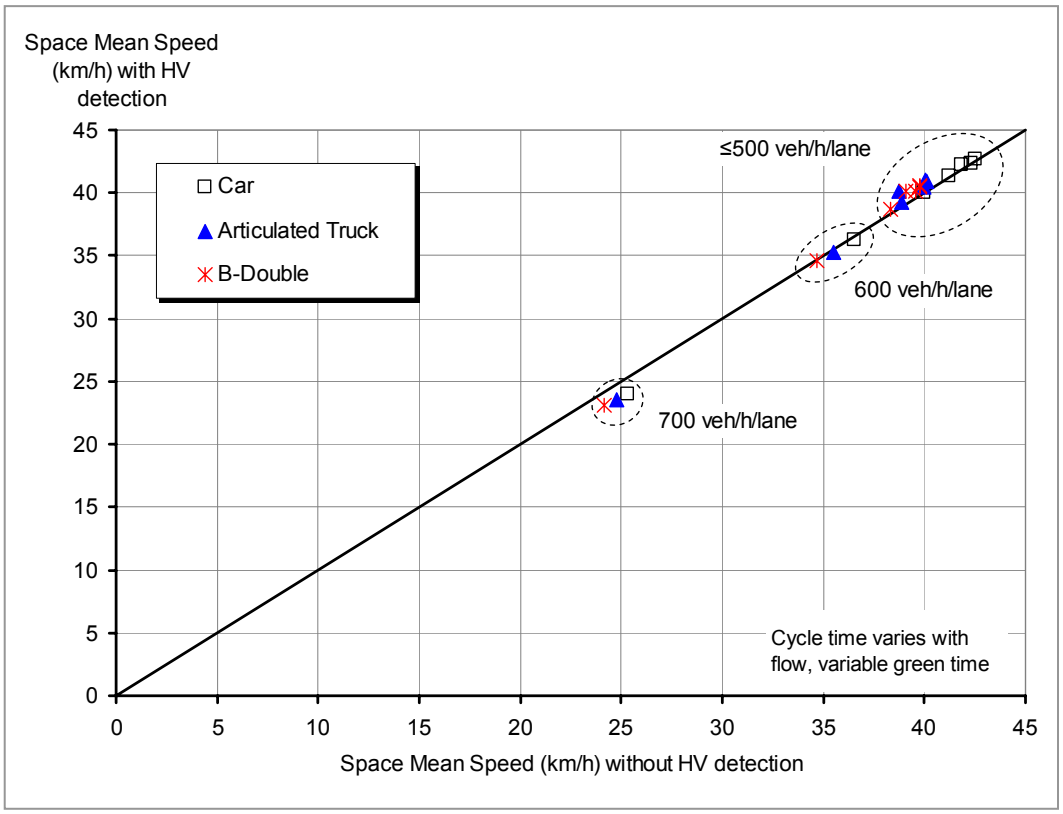


**Figure 11.12 – Speeds at various flows with and without HV Detection**

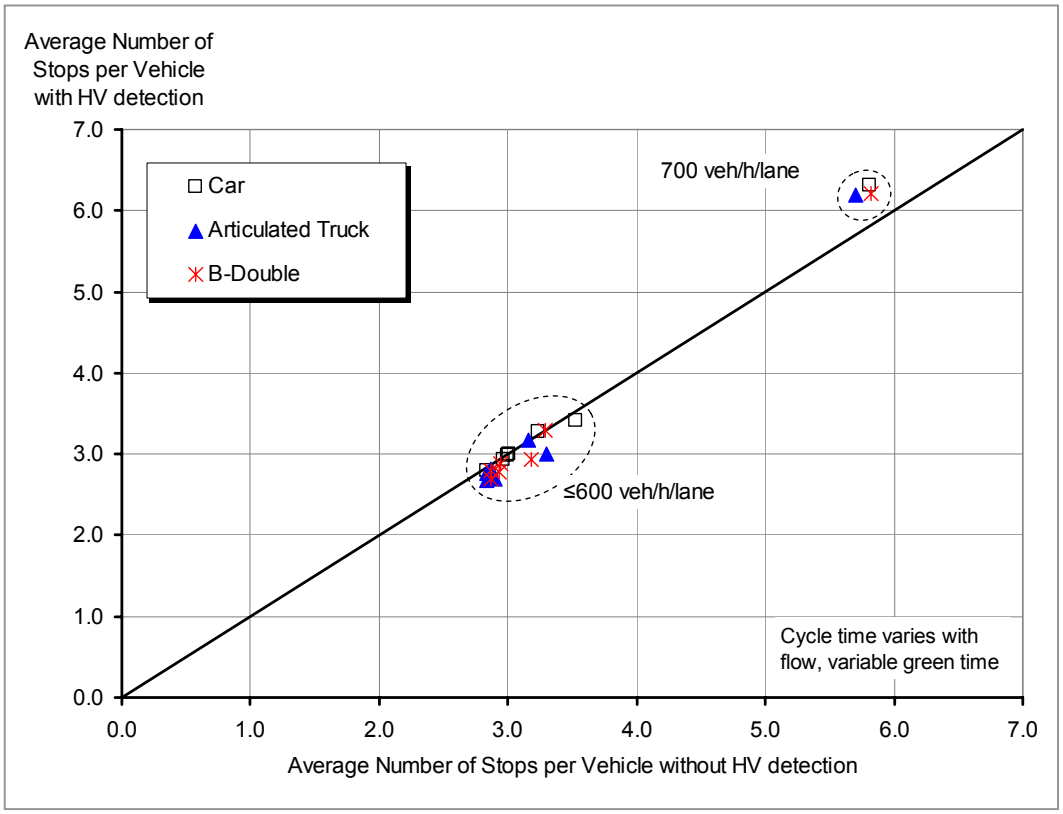


**Figure 11.13 – Number of stops at various flows with and without heavy vehicle detection**

As found previously, heavy vehicle detection offers a slight benefit in increasing speeds and reducing stop rates of all vehicle types at low-to-medium flow rates. At higher flow rates, it often serves to disrupt progression along a corridor with linked traffic signals, with the increased stop rate at downstream intersections negating many of the benefits provided by the initial green time extension.

## 11.4 Statistical Significance of the Simulation Results

The simulations conducted in this and the preceding two chapters comprise a large number of repetitions of the same scenario, differing only in the random numbers used to initialise the models. The results that have been reported represent the means of these multiple runs. Standard deviations were calculated by the CorMod program at the same time as the means in order to enable statistically meaningful comparisons of the results to be made.

It was found that, due to the very large number of vehicles involved (1000 repetitions of a one-hour simulation of a flow of 600 veh/h across 3 lanes results in 1.8 million vehicles), even very small differences become statistically significant.

For example, in the baseline scenario of this urban corridor section, travel times were found to be 364.4 ± 48.1 seconds for cars (n = 1166172) and 383.8 ± 52.8 seconds for B-doubles (n = 26949). A two-sample t-test of the difference in travel times gives a t-statistic of 59.74, whereas the critical t-value for the 5% level of significance is 1.96.

Similarly, the number of stops by cars in the baseline scenario was 3.23 ± 1.07 and for B-doubles was 3.29 ± 0.94. A two sample t-test of the difference in the number of stops results in t = 10.32, once again being a statistically significant difference. Were a lesser number of repetitions made, this small difference in number of stops would not be likely to be statistically significant.

## 11.5 Summary and Conclusions of this Chapter

This chapter demonstrates the applicability of the model to an existing corridor. The general findings are similar to those of the previous two chapters that used a simpler corridor.

The undulating grades on the corridor reported in this chapter were found to have led to larger headways developing in front of heavy vehicles (particularly at the first intersection with a grade of +5%). This, in turn, resulted in a greater propensity for light vehicles changing lanes in front of the heavy vehicles, as shown in the trajectory diagram (Figure 11.3). Heavy vehicles that would otherwise have come to a partial stop would subsequently need to come to a complete stop.

The same findings from the previous chapter in terms of freight vehicle mode split and lane utilisation were found to apply to this corridor. The scenario that carried the same freight volume on an increased number of B-doubles was found to offer slight increases in corridor performance, as did segregation of different vehicle types into specific lanes.

Optimum progression design speeds were found to be similar for both heavy and light vehicles, although there was some evidence that having PDS (and the offsets between signals) varying with grade may result in an even more optimal solution.

This chapter has shown that the urban traffic corridor model developed in this project is equally applicable to a real existing corridor as to a hypothetical corridor. There are considerable opportunities to enhance the model further, such as inclusion of traffic opposing, entering and exiting the corridor – these will be mentioned further in the next chapter, which concludes the Thesis.

# CHAPTER 12 CONCLUSIONS AND RECOMMENDATIONS

This research was conducted with the aim of developing an improved representation of large freight vehicles (LFVs), such as B-doubles, in urban traffic corridor operations. This chapter presents the main conclusions of the study in relation to the aims and objectives presented in Chapter 1, and in terms of how they may be of use to researchers and practitioners in managing our urban freight corridors. The scope of the project was also defined at the start of the thesis, and in the course of the project, several areas of investigation were identified that were considered beyond that scope; those opportunities for further related research are also outlined later in this chapter.

## 12.1 Main Conclusions of this Study

The project objectives defined in Chapter 1 are repeated below, together with a concise description of the work undertaken towards those objectives in each of the chapters of this thesis. Note that the chapter numbering is not strictly sequential, since the objectives were worked towards concurrently through the project.

### 12.1.1 Improve the understanding of the interaction of LFVs within urban arterial traffic corridors

Three chapters of this thesis reviewed existing studies into LFVs, traffic models, and their interactions. The synthesis of this information in the one place helps to clarify the understanding of work done to date and opportunities to further this understanding.

**Chapter 2:** LFVs were found to comprise an ever-increasing proportion of the vehicles on Australia's urban and rural roads. This has partially been in recognition that a more diverse range of vehicle types is required to deal with the increasing freight volumes being carried. Despite this, the use by traffic practitioners of heavy vehicle sizes and other characteristics that predate their introduction remains common. Passenger Car Equivalence values were found to vary with queue position as well as with vehicle type, indicating the potential for

benefits using technologies that reduced the likelihood of LFVs stopping at the front of queue at a signalised intersection. A range of measures for reducing traffic impacts of LFVs were identified, some of which were investigated in this project.

**Chapter 3:** A review of signalised intersection traffic models was conducted, noting their handling of non-standard vehicles. The Australian, United States and Canadian guides for determining intersection capacity and delay all use a similar heavy vehicle factor to reduce the saturation flow rate upon queue discharge. Acknowledging the deficiencies of constant PCE models, the review concluded that a microsimulation-level analysis was required to characterise LFVs in urban traffic accurately.

**Chapter 4:** Various component models suitable for use within microsimulation frameworks were reviewed. A vehicle acceleration model that decreased linearly with increasing speed was found to be most appropriate, with readily interpretable parameters and being formulated independently of the elapsed time. In addition to the lower acceleration rates correctly attributable to LFVs, their greater reaction time when starting from rest must also be considered. A car following model that was formulated in terms of the required acceleration to maintain a safe following distance was identified as being suitable for use in the this project.

**Chapter 6:** In-service characterisation of the behaviour of different vehicle types (including LFVs) was measured from a GPS-equipped chase car. This method had not previously been used to collect a large sample of acceleration profile data efficiently and accurately, and was able to be validated by comparing trajectories of the lead and chase vehicle. Previous testing of heavy vehicle acceleration performance had been in controlled conditions, with the driver aware of the existence and purpose of the experiment. This data set and methodology should prove to be valuable in setting performance requirements, both for heavy vehicles accessing urban roads and for road-related technologies (such as signalised intersection and railway level crossing timing). Traffic volume and headway data was also collected, enabling a better characterisation of the proportions and

headways distributions of the different vehicle types on the corridor than had previously existed.

**Chapter 8:** Lane changing behind LFVs was also investigated, modelling a driver's lane changing decision when approaching the back of queue at a signalised intersection based on the expected time taken to reach free speed after passing through the intersection in each candidate lane. A long queue consisting only of passenger cars may be more attractive than a short queue including a B-double.

**Chapter 10:** Heavy vehicle detection and green time extension was initially seen as an effective means of achieving this. However, in closely coordinated corridors such as those modelled in this study, the breakdown in natural progression at downstream intersections due to the green time extension acted against gains made at the first intersection.

**Chapter 11:** Behaviour of light vehicles around LFVs was also examined – with the work reported in the previous chapter finding that lane changing in front of LFVs contributes to a greater probability of their having to stop, resulting in increased stops and delays for all traffic.

### 12.1.2 Define a methodology to quantify the traffic-related effects of LFVs upon urban arterial traffic corridor performance.

**Chapter 5:** Acknowledgement of the differences in acceleration capability and length of LFVs compared to general access vehicles was seen as the key to quantifying their traffic-related effects. A methodology was developed that incorporated an accurate representation of the longitudinal characteristics of different vehicle types in a basic traffic microsimulation environment. Previous microsimulation software generally had not modelled vehicle characteristics to the same level of accuracy. A spreadsheet implementation of that methodology was developed, proving to be useful but inefficient for simulations involving many vehicles and intersections.

### 12.1.3 Implement that methodology as a practical application

**Chapter 7:** The input parameters for the model were calibrated using the data collected in this project. A procedure was devised for estimating the typical in-service acceleration characteristics of particular vehicle types from GPS data recorded from a chase car following a sample of vehicles. Headway distributions for each vehicle type were estimated from automatic traffic counter data.

**Chapter 8:** A corridor-level traffic model was developed to use the above methodology of modelling vehicles in detail within a microsimulation environment. A C++ traffic microsimulation program was developed from first principles to achieve this, proving to be a robust and efficient means of examining simple traffic corridor performance with multiple vehicle types. The software was always intended to be a research tool, and although it can produce a trajectory diagram of the corridor, it lacks many of the features of commercial microsimulation software.

**Chapter 9:** A parametric study was undertaken to verify the correct operation of the model. A range of model outputs, including travel times and stop rates, were examined as input variables were adjusted. Increasing traffic arrival volumes had the strongest influence on corridor performance. Grade had a strong effect, particularly for heavy vehicles but also for light vehicles behind them. A uniform grade over a road section was found give a better corridor performance than a varying grade with the same start and end elevations, but a steeper middle section.

### 12.1.4 Evaluate the effectiveness of existing and alternative scenarios in minimising the traffic-related impacts of LFVs

**Chapters 10 and 11:** The corridor-level traffic model was used to investigate several freight policy and traffic management scenarios on two corridors – a hypothetical corridor and one based on part of an existing corridor. Increasing traffic volumes were found to adversely affect the travel times and stop rates of all

vehicles. This occurred to the same extent whether that increase was due to an increased number of all vehicles or an increased number of heavy vehicles.

Several freight vehicle mode choice strategies were examined. Elimination of freight from the corridor offered the greatest reduction in travel times and stop rates, however the necessary relocation of freight to an alternative route was not considered in the analysis. Maintaining freight on the corridor, a modest increase in the use of B-doubles was found to reduce the total number of vehicles on the corridor and hence improve travel times and stops. Introduction of B-triples on the corridor also reduced the number of vehicles, but these gains were offset by their assumed inferior performance (more mass but same power as a B-double). It should be noted that B-triple performance in urban traffic could only be estimated from that of smaller vehicles.

Lane utilisation was also evaluated, finding that restricting all trucks to a single lane led to oversaturation of the truck lane and underutilisation of the car lanes. Traffic opposing the corridor would also be disadvantaged due to the shorter green time available to them in trying to cope with the oversaturated truck lane. A policy of restricting large trucks to one lane, smaller trucks to that lane and another, and allowing cars to use any lane was found to offer the greatest benefits to all vehicle types. Implementation and enforcement of such a lane utilisation strategy would be problematic.

Heavy vehicle detection was found to offer some benefits in reducing the stop rates and travel times, particularly in low-to-medium flow conditions. In high flow conditions, the green time extension was found to affect progression at downstream intersections, negating any benefits at the first intersection.

## 12.2 Applications of this Research to the Analysis and Management of Urban Road Freight Corridors

This main contribution of this research has been the development of a methodology to quantify LFVs effects on urban arterial traffic corridor performance. This novel method involves a more detailed characterisation of individual vehicles' longitudinal performance, combined with a Monte-Carlo style method of conducting multiple simulations based on different random number inputs. The model has been calibrated using data collected from a representative urban corridor carrying a large proportion of LFVs, and has been applied to two test corridors in the examination of various strategic policies.

The model has been specifically designed to investigate a single-direction urban corridor without entering, exiting or opposing traffic. This is considered appropriate for investigations of the relative effects of different vehicle types on corridor performance. These limitations must however be considered when comparing model outputs to measurable corridor performance indicators, or when applying the model to other purposes.

The research has also developed a methodology for estimating the in-service acceleration behaviour of different vehicle types during queue discharge from signalised intersections. This methodology involves following a sample of vehicles with a GPS-equipped chase car, enabling a large sample of data to be accurately obtained. Drivers of the lead vehicles are generally unaware that their driving is being monitored, and are unable to be identified in the survey.

Several freight policy and traffic management scenarios were examined in this project, the results of which are summarised in the previous section. These findings may be considered in the management of urban road freight corridors and the vehicles eligible to use them.

Although this project has focussed on the traffic management aspects of large freight vehicles on urban traffic corridors, its findings have many broader potential applications in addressing many common social, community and environmental concerns. Together with the primary measures of speed and stop

rate, secondary measures can be estimated such as fuel consumption, noise and gaseous emissions, crash rates, pavement wear and vehicle operating costs. These may then be used to provide indicators of changes in tertiary measures including urban amenity and quality-of-life, which are less easy to quantify.

The costs and savings of various scenarios that were estimated at the end of chapter 10 may be extended to include costs associated with the secondary and even tertiary measures. Austroads (2005) provides information and typical parameter values that are of use in project evaluation applications.

Reduction of emissions, particularly of carbon dioxide, is becoming a greater concern at various levels. This project has highlighted benefits of various freight policy and traffic management scenarios in reducing stop rates and travel times of journeys, with corresponding savings in emissions.

The cost of implementing heavy vehicle detection at isolated rural signalised intersections had previously been justified solely in terms of reduced pavement maintenance requirements (Middleton *et al.* 1997; Sunkari *et al.* 2000). This current project has found that it is equally applicable in low-to-medium flow conditions on urban traffic corridors. Pavement maintenance reductions would be expected to be even greater on thin chip-seal pavements that are more susceptible to shear stresses from braking and accelerating heavy vehicles.

The noise associated with heavy vehicle stopping and starting at night time has been reported as of primary concern to residents living on or nearby urban freight routes (Jan Taylor and Associates 2003). Heavy vehicle detection was found to be more effective in reducing the number of stops of heavy vehicles in off-peak conditions than in peak conditions. It thus has potential for decreasing the occurrences of acceleration and braking noise of heavy vehicles at night.

## 12.3 Further Research Opportunities

### 12.3.1 Braking

The different in-service braking characteristics of various vehicle types has not received as much attention in this project as acceleration has, since braking capabilities have a lesser effect on the control delay of vehicles passing through signalised intersections. This research project has defined a methodology for collecting and analysing objective in-service vehicle longitudinal behaviour. That methodology (and the data collected in this project) would be equally applicable to the calculation of in-service braking behaviour as to acceleration behaviour. Associated with this, differences between vehicle types in the dilemma zone when approaching a changing traffic signal also need further investigating.

### 12.3.2 Speeds on downgrades

The vehicle acceleration model used in this project assumes that acceleration decreases linearly with increasing speed and grade, up until the posted speed limit is reached. Heavy vehicles (in particular when laden) do not travel down steep grades at speeds from which they are unable to stop. The model used in this project does not consider those, and is thus likely to underestimate the traffic-related effects of heavy vehicles on steep down grades. A more realistic representation would be to calculate the maximum safe speed at which the vehicle could descend the grade, and limit it to that speed.

### 12.3.3 External costs

There is opportunity to calculate additional cost measures associated with traffic on an urban corridor. Fuel consumption and emissions can be calculated for each vehicle using an instantaneous power model (for example Akçelik and Besley 2003) as the simulation proceeds, and accumulated for each vehicle type at the end of the simulation. Additional costs, such as vehicle maintenance and pavement deterioration would be expected to have a component depending on the number of stops of each vehicle type.

### 12.3.4 Vehicle classification

An improved vehicle classification algorithm has been developed, as described in Appendix A. This dramatically reduced the number of unclassifiable vehicles compared to the default algorithm. Opportunities exists to develop a bi-directional traffic version of this algorithm, and to incorporate it into existing commercial traffic counter software.

### 12.3.5 Headways

A number of different headway distributions have been developed in this project, based on vehicle data collected at one location on an urban arterial traffic corridor. There is an opportunity to validate this with data collected at other sites on the corridor and elsewhere. Additionally, the effects of using different headway distributions can be examined in further detail.

### 12.3.6 Chase car survey method

Having developed a method for collecting and analysing GPS data from a chase car survey, there is an opportunity to use this equipment and method for further travel time and vehicle performance studies at QUT. The equipment is considered to be safe, is not distracting to the driver, and has already been used successfully in other applications (for example Bunker *et al.* 2005).

It would be useful to conduct follow-up surveys on the test corridor to determine changes in travel times and stop rates that may be attributable to altered traffic volumes and route selection by heavy vehicles that have occurred in the intervening period.

### 12.3.7 Model enhancements

The existing corridor model only considers unidirectional traffic that does not enter or leave the corridor other than at its two ends. With the emphasis of the project on effects of LFVs, **traffic opposing and crossing** the corridor had not been considered directly, (cycle time had empirically been increased with flow to account for this indirectly). If the software developed in this project is to be used

for other applications, these need to be included as a minimum. Any general purpose investigation of progression design speed needs to consider traffic heading in both directions (the investigations reported in Chapter 10 were not considered general purpose as they were looking for differences in PDS between vehicle types). Inclusion of bi-directional traffic would enable testing of TTM Consulting's (1987) proposal to "link signals on the basis of counter-peak travel times when congestion in the peak direction precludes linking".

Traffic **entering and leaving** the corridor would be expected to cause greater disruption to heavy vehicles than light vehicles, due to their need to regain lost momentum. It may also have an effect on the lane utilisation strategies mentioned in Chapters 10 and 11, since truck drivers anecdotally tend to travel in the centre lane of a three-lane carriageway to avoid turning traffic.

**Platoon dispersal** is widely used in microsimulation (and many macrosimulation) traffic models. The model developed in this project does not include this, having all vehicles accelerate up to the speed limit and remain exactly at that speed at a constant headway to the vehicle in front, until having to stop if required at the next intersection. A degree of platoon dispersion will be introduced by specifying a range of driver types and a distribution of parameters within each vehicle type. Introduction of platoon dispersion would be expected to increase the benefits of heavy vehicle detection, as the green time extension would not have as much of an effect on arrivals at downstream intersections.

**Lane merging and diverging** had also not been considered, since this was seen in Section 9.6 to only indirectly influence LFV impacts on traffic flow.

### 12.3.8 Model implementation

There is an opportunity for some of the specific features of the corridor-level traffic model to be incorporated into other existing microsimulation software. These features include, but are not limited to:

- The detailed acceleration model, having a vehicle's maximum acceleration dependent on speed and grade (including the abovementioned restrictions on downgrades)
- The novel lane change decision model, based on comparing expected queue discharge times in alternative lanes when approaching the back of queue at a signalised intersection.

### 12.3.9 Validation

There remains a need for overall validation of the multi-vehicle corridor-level traffic simulation model developed in this project. The model has been calibrated using traffic and vehicle data collected on an urban arterial traffic corridor, as reported in Chapter 7, and its operation verified under typical test cases in Chapter 8. Validation of the outputs of the model against an independent source is an important step that would be required if it were to gain wider acceptance. This validation may be conducted by comparing results with an existing validated microsimulation model, or preferably by comparison to results collected on another urban traffic corridor that had not been used for calibration of the model.

# APPENDIX A DEVELOPMENT OF THE VEHICLE CLASSIFICATION ALGORITHM

## A.1 Classifying Vehicles from Axle Detections

The automatic vehicle counter / classifier used in this project detects vehicles by using two rubber hoses placed across the road perpendicular to the direction of travel. As a vehicle axle passes over a hose, a pulse of air is sent along the hose to an air-switch. This air switch closes an electric circuit, the precise time of which is stored in the counter's internal memory. Each axle should be detected twice, once at each detector – this enables the vehicle's speed to be estimated and allows for some redundancy if detections are missed. If a hose is not perpendicular to the vehicle's direction of travel, or the vehicle's axle is misaligned, two pulses may be recorded in quick succession. At the completion of the traffic survey, the axle detection times are downloaded to a laptop computer as a text file.

Vehicle classification involves matching the axle detection events for individual vehicles; and estimating the speed and class of each vehicle from these events (Austroads 2006). The process is illustrated in Figure A1.1. The known and constant distance between the two detectors is divided by the time between the first detections at each detector, giving an estimate of the speed of the vehicle. This speed is then multiplied by the time between consecutive axle detections to give the spacing between axles. This continues until a large spacing is reached (typically a spacing greater than 10 metres), indicating the start of a new vehicle.

The number of axles on the vehicle, number of axle groups (groups of axles spaced closely together), and spacing between axles are used to determine the Austroads '94 classification of the vehicle, as presented in Figure 2.4.

## A.2 Deficiencies in the Existing Vehicle Classification Program

The software that was provided with the vehicle counter / classifier automatically handles the classification of vehicles; producing a text file containing the time, class and speed of each vehicle that could be classified. Two problems were encountered with using the existing classification software:

1) The text output only resolves the times at which vehicles pass the leading detector to one-second resolution, despite the fact that the axle detections are reported to sub-microsecond resolution. The vehicle passage times were needed at a greater resolution in order to obtain a more accurate characterisation of the headway distributions.

2) A number of incorrectly classified vehicles and axles records could not be assembled into classifiable vehicles. A total of 307,487 axle detections were recorded across the two lanes of traffic. The original classification program assembled these into 66,432 classifiable vehicles and 1,433 unclassifiable groups of axles (2.1%). Further, despite road trains not being permitted on the test corridor, a number of vehicles were classified as either Austroads class 11 or class 12.

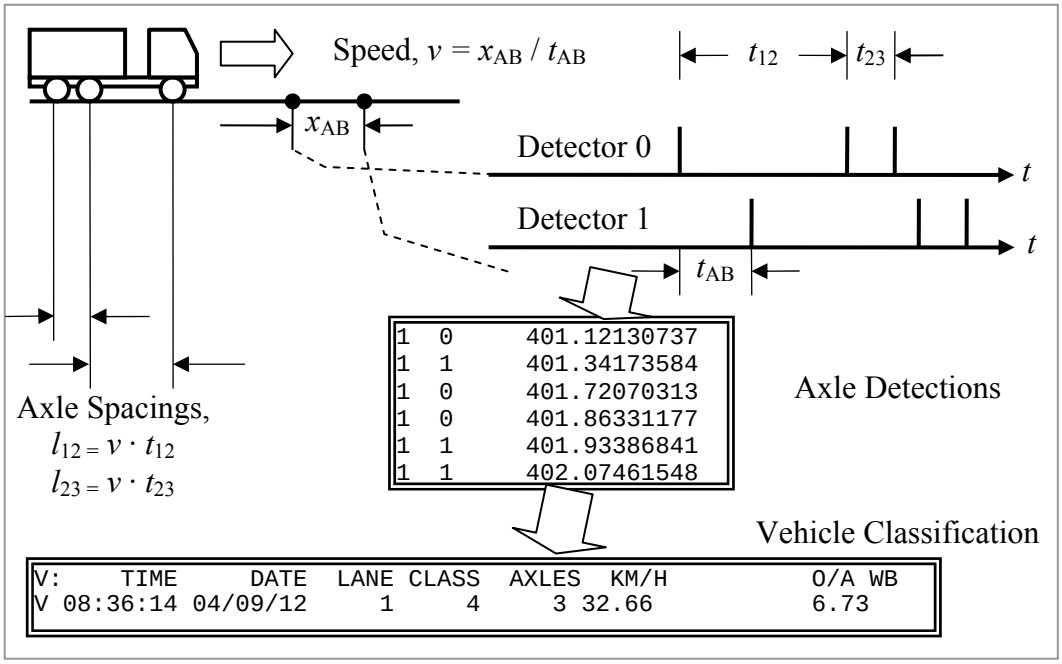


**Figure A1.1 – Basic principle of vehicle classification from axle detections**

An examination of the axle detection patterns corresponding to some of these misclassifications showed that the following events occurred relatively frequently, the method used to handle the problem is also mentioned:

- "Bounce" on detectors, with two closely-spaced detections occurring in quick succession from the left and right tyres on the axle. One of the detections is disregarded.

- The detection of the first axle on the first detector was missing. A valid vehicle record was constructed from the remaining axles.
- Cars closely following other vehicles, being considered a continuation of the lead vehicle. In many cases, these could be split into two classifiable vehicle records.
- Cars were being closely followed by other vehicles, once again being considered part of the one vehicle. In many cases, these could be split into two classifiable vehicle records.
- Vehicles travelling slowly over the detectors were misclassified or unclassifiable. A search was conducted for closer-timed detections that would lead to a faster vehicle.
- General-access B-doubles, having a widespread tandem axle group on the second trailer, were being misclassified as Austroads class 11 (Double Road train) vehicles. The trailing widespread tandem axle group on these vehicles was explicitly searched for, and these vehicles were handled as separate cases.

## A.3 Development of a New Vehicle Classification Program

Not having access to the source code for the original vehicle classification program, a new program was created to replicate its function. **Vehwrite** is a command-line program, written in the C programming language, taking the name of the raw axle detection file as input, and producing a classified vehicle listing file as output (which is typically redirected to a file). The output file format was kept similar to that used in the original classification program, except for increasing the resolution of the vehicle crossing times to one-millisecond instead of one-second, and adding a column for the headway to the previous vehicle.

The six cases considered above were explicitly searched for, reconstructing and splitting vehicles prior to determining their correct classification and printing them to the output file.

Several parameters were adjusted to minimise the number of misclassifications. The parameters used in the program are presented in Table A1.1.

**Table A1.1 – Model parameters used to minimise misclassifications**

| *Parameter* | *Value* | *Comment* |
|---|---|---|
| `MinSpeed` | 5.0 km/h | Don't even attempt to assemble a vehicle which would be travelling below this speed |
| `SlowSpeed` | 40.0 km/h | Consider using possible alternative axle detections pairs that would give a higher speed |
| `MaxSpac` | 10.0 m | Maximum spacing between axles in the same vehicle – start a new vehicle if the spacing greater than this, |
| `MinSpac` | 0.7 m | Axles cannot be closer than this – ignore detections closer than this, which are probably due to 'bounce' in the circuit |
| `MaxGrpSpac` | 2.1 m | Maximum spacing for axles within a group – if spacing is greater than this, start a new axle group |
| `MaxCarWB` | 3.2 m | Maximum wheelbase for a car, determines whether a vehicle is class 1 or class 3 |
| `MinFollowSpac` | 5.0 m | Minimum following spacing (rear axle to front axle), used to split possible closely following vehicles |

The classification program **Vehwrite** is designed to handle unidirectional traffic. Classifier performance is often poorer where bi-directional traffic is being monitored and particularly when higher traffic volumes create problems of co-incidence of vehicles crossing the detectors. Although not required in the current project, an opportunity exists to develop a bi-directional vehicle classification version of this program.

## A.4 Results of the New Vehicle Classification Program

Figure A1.2 and Figure A1.3 show samples of the original and new vehicle classification program outputs. As an example, the original program could not classify a number of axle records occurring at time 10:13:11, whereas the new program classifies these into a short vehicle (car) being closely followed by a short vehicle towing. The output format of the new program was altered to give a greater time resolution; as well as including the number of axle groups, the

headway from the front of the previous vehicle and a simple diagram of the axle spacings for vehicles with more than two axles.

```
V:    TIME     DATE  LANE CLASS  AXLES  KM/H          O/A WB
V 10:11:51 04/09/12     1     1     2 71.32           2.80
V 10:13:08 04/09/12     1     1     2 91.34           2.81
V 10:13:09 04/09/12     1     1     2 79.01           2.51
V 10:13:11 04/09/12     1    13      72.460122
V 10:13:12 04/09/12     1     1     2 71.84           2.60
V 10:13:13 04/09/12     1     1     2 70.30           2.91
V 10:13:18 04/09/12     1     2     4 65.96           7.51
V 10:13:19 04/09/12     1     1     2 67.08           2.78
V 10:13:20 04/09/12     1     1     2 66.35           2.69
V 10:13:21 04/09/12     1     1     2 62.96           2.48
V 10:13:24 04/09/12     1     8     5 64.29          14.95
V 10:13:27 04/09/12     1     2     3 62.83           5.77
V 10:13:31 04/09/12     1     1     2 74.45           2.55
V 10:13:35 04/09/12     1     1     2 86.33           2.80
V 10:13:37 04/09/12     1     1     2 78.41           2.62
V 10:14:32 04/09/12     1     2     4 88.76           8.03
```

**Figure A1.2 – Extract from the original vehicle classification program output**

```
___DATE___ ____TIME___ LA CL AXGP KM/H  H/WAY  OAWB
2004/09/12 10:11:51.397 1  1 0202 71.32 1.713  2.80
2004/09/12 10:13:07.833 1  1 0202 91.34 76.44  2.81
2004/09/12 10:13:09.153 1  1 0202 79.01 1.320  2.51
2004/09/12 10:13:10.316 1  1 0202 72.46 1.163  2.42
2004/09/12 10:13:10.819 1  2 0303 72.42 0.503  5.97 o o  o
2004/09/12 10:13:12.029 1  1 0202 71.84 1.210  2.60
2004/09/12 10:13:13.576 1  1 0202 70.30 1.546  2.91
2004/09/12 10:13:17.685 1  2 0403 65.96 4.109  7.51 o o  oo
2004/09/12 10:13:18.798 1  1 0202 67.08 1.113  2.78
2004/09/12 10:13:19.940 1  1 0202 66.35 1.142  2.69
2004/09/12 10:13:21.526 1  1 0202 62.96 1.585  2.48
2004/09/12 10:13:24.225 1  8 0503 64.29 2.700 14.95 o oo       oo
2004/09/12 10:13:27.530 1  2 0303 62.83 3.305  5.77 o o o
2004/09/12 10:13:30.943 1  1 0202 74.45 3.413  2.55
2004/09/12 10:13:34.606 1  1 0202 86.33 3.663  2.80
2004/09/12 10:13:36.836 1  1 0202 78.41 2.230  2.62
2004/09/12 10:14:32.487 1  2 0403 88.76 55.65  8.03 o o  oo
```

**Figure A1.3 – Corresponding extract from the new classification program output**

## A.5 Effectiveness of the New Vehicle Classification Program

The effectiveness of the original and new programs was compared using a data set of 307 487 axle detections recorded in two lanes in a 96-hour survey period. Table A1.2 shows the results of the comparison. Combining results from two lanes, the original program classified 97.84% of detections into 66 432 valid vehicles, whereas the new program classified 99.38% of detections into 67 031 valid

vehicles. This increased classification rate was attributed mainly to a number of 4-axle vehicles (classes 5 and 7) being split into two short vehicles. There is also a noticeable decrease in the proportion of unclassifiable vehicles from 2.11% to 0.10%.

**Table A1.2 – Classification rates, combining data from both lanes**

| *Vehicle Classification* | | *Original Program* | | *New Program* | |
|---|---|---|---|---|---|
| 1 | Short vehicle | 57 452 | 84.66% | 57 438 | 85.61% |
| 2 | Short vehicle towing | 698 | 1.03% | 754 | 1.12% |
| 3 | 2-axle truck or bus | 3 429 | 5.05% | 3 743 | 5.58% |
| 4 | 3-axle rigid truck or bus | 1 003 | 1.48% | 1 180 | 1.76% |
| 5 | 4+-axle rigid truck | 257 | 0.38% | 165 | 0.25% |
| 6 | 3-axle articulated truck | 138 | 0.20% | 88 | 0.13% |
| 7 | 4-axle articulated truck | 335 | 0.49% | 204 | 0.30% |
| 8 | 5-axle articulated truck | 351 | 0.52% | 273 | 0.41% |
| 9 | 6-axle articulated truck | 1 890 | 2.78% | 2 386 | 3.56% |
| 10 | B-double | 822 | 1.21% | 791 | 1.18% |
| 11 | Double Road train | 54 | 0.08% | 9 | 0.01% |
| 12 | Triple Road train | 3 | 0.00% | 0 | 0.00% |
| **Total classifiable** | | **66 432** | **97.89%** | **67 031** | **99.90%** |
| 13 | Unclassifiable | 1 433 | 2.11% | 65 | 0.10% |
| **Total vehicle records** | | **67 865** | **100.00%** | **67 096** | **100.00%** |
| *Classifiable axle detections* | | *300 842* | *97.84%* | *305 584* | *99.38%* |

The new program classified a greater number of class 9 vehicles, many of which had previously been merged with leading or following vehicles. Given that the data set was taken from an urban traffic corridor, no road trains (class 11 or 12 vehicles) would have been expected in the data. The few remaining class 11 vehicles were found to have an axle spacing pattern matching that of a prime mover towing a dolly at the front of a low-loader platform having a quad axle group on the rear. The large spacing between axles 2 and 3 of the quad axle group caused these vehicles to be classified as having five, rather than four, axle groups.

# LIST OF REFERENCES


ABS (1999-2006) *Survey of motor vehicle use*. Cat. No. 9208.0, Australian Bureau of Statistics, Canberra, ACT.

ABS (2006) *Sales of new motor vehicles*. Cat. No. 9314.0.55.001, Australian Bureau of Statistics, Canberra, ACT.

Akcelik and Associates (2006) *SIDRA Intersection user guide*. Akcelik and Associates Ltd, Melbourne.

Akçelik, R. (1981) *Traffic signals: Capacity and timing analysis*. Research Report ARR 123, Australian Road Research Board, Vermont South, Victoria.

Akçelik, R. (1995) *Traffic signals: Capacity and timing analysis*. Research Report ARR 123 (Sixth Reprint), ARRB Transport Research, Vermont South, Victoria.

Akçelik, R. (2006) Speed-flow and bunching models for uninterrupted flow. *5th International Symposium on Highway Capacity and Quality of Service*, Yokohama, Japan.

Akçelik, R. and Besley, M. (2002) Queue discharge flow and speed models for signalised intersections. In *15th International Symposium on Transportation and Traffic Theory*, ed Taylor, M. A. P., pp. 99-118. Pergamon, Amsterdam.

Akçelik, R. and Besley, M. (2003) Operating cost, fuel consumption, and emission models in aaSIDRA and aaMotion. *25th Conference of Australian Institutes of Transport Research (CAITR 2003)*, University of South Australia, Adelaide.

Akçelik, R., Besley, M. and Roper, R. (1999) *Fundamental relationships for traffic flows at signalised intersections*. Research Report ARR 340, ARRB Transport Research Ltd, Vermont South, Victoria.

Akçelik, R. and Biggs, D. C. (1987) Acceleration profile models for vehicles in road traffic. *Transportation Science*, 21(1), 36-54.

Al-Kaisy, A. F., Hall, F. L. and Reisman, E. S. (2002) Developing passenger car equivalents for heavy vehicles on freeways during queue discharge flow. *Transportation Research Part A: Policy and Practice*, 36(8), 725-742.

Al-Kaisy, A. F. and Jung, Y. (2004) Examining the effect of heavy vehicles on traffic flow during congestion. *Road & Transport Research*, 14(4), 3-14.

Al-Kaisy, A. F., Jung, Y. and Rakha, H. (2005) Developing passenger car equivalency factors for heavy vehicles during congestion. *Journal of Transportation Engineering*, 131(7), 514-523.

Australia (1999) *Australian Vehicle Standards Rules*. Commonwealth of Australia, Canberra, ACT.

Austroads (1995) *Design vehicles and turning path templates*. Austroads Publication AP-34/95, Austroads, Sydney, NSW.

Austroads (1997) *Rural Road Design*. Austroads Publication AP-1/89, Austroads, Sydney, NSW.

Austroads (2000) *Guidelines for multi-combination vehicle route access assessment*. AP-R173/00, Austroads, Sydney, NSW.

Austroads (2002) *Geometric design for trucks - when, where and how?* AP-R211/02, Austroads, Sydney, NSW.

Austroads (2003) *Guide to traffic engineering practice: Part 7 - Traffic signals*. AP-11.7:03, Austroads, Sydney, NSW.

Austroads (2004) *Guide to traffic engineering practice: Part 3 - Traffic studies*. AP-11.3:04, Austroads, Sydney, NSW.

Austroads (2005) *Guide to project evaluation - Part 4: Project evaluation data*. AGPE04/05, Austroads, Sydney.

Austroads (2006) *Automatic Vehicle Classification by Vehicle Length*. AP-T60/06, Austroads, Sydney.

Benekohal, R. F. and Zhao, W. (2000) Delay-based passenger car equivalents for trucks at signalized intersections. *Transportation Research Part A: Policy and Practice*, 34(6), 437-457.

Bester, C. J. (2000) Truck speed profiles. *Transportation Research Record*, 1701, 111-115.

Bham, G. H. and Benekohal, R. F. (2002) Development, evaluation, and comparison of acceleration models. *81st TRB Annual Meeting*, Washington, DC, United States.

Bonneson, J. A. (1992) Modeling queued driver behavior at signalized junctions. *Transportation Research Record*, 1365, 99-107.

Bonneson, J. A. and Messer, C. J. (1998) Phase capacity characteristics for signalized interchange and intersection approaches. *Transportation Research Record*, 1646, 96-105.

Bosch (2004) *Automotive handbook*. Society of Automotive Engineers, Warrendale, PA, United States.

Bourrel, E. and Lesort, J.-B. (2003) Mixing micro and macro representations of traffic flow: Hybrid model based on LWR theory. *Transportation Research Record*, 1852, 193-200.

Brackstone, M. and McDonald, M. (1999) Car-following: A historical review. *Transportation Research Part F: Traffic Psychology and Behaviour*, 2(4), 181-196.

Branston, D. and van Zuylen, H. (1978) The estimation of saturation flow, effective green time and passenger car equivalents at traffic signals by multiple linear regression. *Transportation Research*, 12(1), 47-53.

Briggs, T. (1977) Time headways on crossing the stop-line after queueing at traffic lights. *Traffic Engineering & Control*, 18(5), 264-265.

Brown, G. E. and Ogden, K. W. (1988) The effect of vehicle category on traffic signal design: A re-examination of through car equivalents. *14th Australian Road Research Board Conference*, Canberra, ACT, pp. 27-37.

Bruce, B. and Morrall, J. F. (2000) Long combination vehicle operating characteristics in urban areas. *6th International Symposium on Heavy Vehicle Weights and Dimensions*, Saskatoon, Saskatchewan, Canada, pp. 239-249.

Bruzsa, L. and Hurnall, J. (1998) Initial results of the B-triple trial in Queensland. *5th International Symposium on Heavy Vehicle Weights and Dimensions*, Maroochydore, Queensland, pp. 279-302.

BTRE (2002) *Greenhouse Gas Emissions from Transport: Australian Trends to 2020*. Report 107, Bureau of Transport and Regional Economics, Canberra, ACT.

BTRE (2006) *Freight measurement and modelling in Australia*. Report 112, Bureau of Transport and Regional Economics, Canberra, ACT.

Bunker, J. M. and Haldane, M. J. (2003) Establishing multi-combination vehicle trajectories under acceleration from rest. *Road & Transport Research*, 12(3), 3-15.

Bunker, J. M., McKellar, C., Bauer, J. and Wikman, J. (2005) High Occupancy Vehicle Lanes Work: Analysis of Waterworks and Lutwyche Roads, Brisbane. *AITPM National Conference*, Brisbane, pp. 229-244.

Bunker, J. M. and Troutbeck, R. J. (2003) Prediction of minor stream delays at a limited priority freeway merge. *Transportation Research Part B: Methodological*, 37(8), 719-735.

Campbell, J. F. (1995) Using small trucks to circumvent large truck restrictions: Impacts on truck emissions and performance measures. *Transportation Research Part A: Policy and Practice*, 29(6), 445-458.

Chandler, R. E., Herman, R. and Montroll, E. W. (1958) Traffic dynamics: Studies in car following. *Operations Research*, 6(2), 165-184.

Cohen, S. L. (2002a) Application of car-following systems in microscopic time-scan simulation models. *Transportation Research Record*, 1802, 239-247.

Cohen, S. L. (2002b) Application of car-following systems to queue discharge problem at signalized intersections. *Transportation Research Record*, 1802, 205-213.

Cowan, R. J. (1975) Useful headway models. *Transportation Research*, 9(3), 371-375.

Cuddon, A. P. and Ogden, K. W. (1992) The effect of heavy vehicles on saturation flows at signalised intersections. *16th Australian Road Research Board conference*, Perth, Western Australia, pp. 1-18.

Daganzo, C. F. (1994) The cell-transmission model: A dynamic representation of highway traffic consistent with the hydrodynamic theory. *Transportation Research Part B: Methodological*, 28(4), 269-287.

Daganzo, C. F. (1997) *Fundamentals of transportation and traffic operations*. Pergamon.

Di Cristoforo, R., Hood, C. and Sweatman, P. F. (2004) *Acceleration and deceleration testing of combination vehicles*. Report to Main Roads Western Australia, Document Number RUS-04-1075-01-05, Roaduser Systems, Sunshine, Victoria.

Dion, F., Rakha, H. and Kang, Y.-S. (2004) Comparison of delay estimates at under-saturated and over-saturated pre-timed signalized intersections. *Transportation Research Part B: Methodological*, 38(2), 99-122.

Elefteriadou, L., Torbic, D. and Webster, N. (1997) Development of passenger car equivalents for freeways, two-lane highways, and arterials. *Transportation Research Record*, 1572, 51-58.

Evans, L. and Rothery, R. W. (1981) Influence of vehicle size and performance on intersection saturation flow. In *Proc., 8th International Symposium on Transportation and Traffic Theory*, pp. 193-222. University of Toronto Press, Toronto, Ontario.

Fitch, J. W. (1993) *Motor truck engineering handbook*. Society of Automotive Engineers, Warrendale, PA, United States.

Forkenbrock, D. J. and Hanley, P. F. (2003) Fatal crash involvement by multiple-trailer trucks. *Transportation Research Part A: Policy and Practice*, 37, 419-433.

Fox, K., Chen, H., Montgomery, F., Smith, M. and Jones, S. (1998). *Selected vehicle priority in the UTMC environment: Literature review*, from http:// www.its.leeds.ac.uk/projects/spruce/utmc1rev.pdf

Gazis, D. C., Herman, R. and Rothery, R. W. (1961) Non-linear follow-the-leader models of traffic flow. *Operations Research*, 9(4), 545-567.

Gipps, P. G. (1981) A behavioural car-following model for computer simulation. *Transportation Research Part B: Methodological*, 15(2), 105-111.

Gipps, P. G. (1986) A model for the structure of lane-changing decisions. *Transportation Research Part B: Methodological*, 20(5), 403-414.

Haldane, M. J. and Bunker, J. M. (2002) Examining the impact of large freight vehicles on signalised intersection operation. *AITPM National Conference*, Perth, Western Australia, pp. 255-268.

Hassall, K. (2002) Urban truck accidents in Australia, fatalities and serious injuries: 1990 to 1999. *National Heavy Vehicle Safety Seminar*, Melbourne, Vic, pp. 149-160.

Herman, R., Lam, T. and Rothery, R. W. (1971) The starting characteristics of automobile platoons. *5th International Symposium on the Theory of Traffic Flow and Transportation*, pp. 1-17.

Jan Taylor and Associates (2003) *Brisbane Urban Corridor planning study*. Community Consultation Report, Jan Taylor and Associates, Brisbane, Queensland.

Kimber, R. M., McDonald, M. and Hounsell, N. B. (1985) Passenger car units in saturation flows: Concept, definition, derivation. *Transportation Research Part B: Methodological*, 19(1), 39-61.

Kulakowski, B. T. (2003) Performance-based standards - The time has come. *International Seminar on Performance-based standards - Moving from theory to practice*, Melbourne, Vic.

Laval, J. A. and Daganzo, C. F. (2003) *A hybrid model of traffic flow: Impacts of roadway geometry on capacity*. Department of Civil and Environmental Engineering, Transportation Group, University of California, Berkeley.

Lechner, G. and Naunheimer, H. (1999) *Automotive Transmissions - Fundamentals, Selection, Design and Application*. Springer-Verlag, Berlin.

Lighthill, M. H. and Whitham, G. B. (1955) On kinematic waves: I Flow movement in long rivers. II A theory of traffic flow on long crowded roads. *Proceedings of the Royal Society, Series A*, 229, 281-345.

Long, G. (2000) Acceleration characteristics of starting vehicles. *Transportation Research Record*, 1737, 58-70.

Long, G. (2002) Intervehicle spacings and queue characteristics. *Transportation Research Record*, 1796, 86-96.

Maddock, J. (1988) *A history of road trains in the Northern Territory (1934-1988)*. Kangaroo Press, Kenthurst, NSW.

Main Roads (2006) *Road planning and design manual*. Queensland Department of Main Roads, Brisbane.

McLean, J. R. (1989) *Two-lane highway traffic operations - Theory and practice*. Gordon and Breach, New York, United States.

McTrans (1990-2002). *TRANSYT-7F - Traffic network study tool, version 7 Federal*, from http://mctrans.ce.ufl.edu/featured/TRANSYT-7F/

Messer, C. J. and Bonneson, J. A. (1998) *Capacity analysis of interchange ramp terminals: Final report, Project 3-47*. NCHRP Web Document 12, Transportation Research Board, National Research Council, Washington, DC, United States.

Messer, C. J. and Fambro, D. B. (1977) Effects of signal phasing and length of left-turn bay on capacity. *Transportation Research Record*, 644, 95-101.

Middleton, D. R., Jasek, D. L., Charara, H. A. and Morris, D. (1997) *Evaluation of innovative methods to reduce stops to trucks at isolated signalized intersections*. TTI Research Report 2972-S, Texas Transportation Institute, College Station, Texas, United States.

Miller, A. J. (1963) Settings for fixed-cycle traffic signals. *Operations Research Quarterly*, 14(4), 373-386.

Miller, A. J. (1968a) *Australian road capacity guide - Signalized intersections*. Bulletin No. 4, Australian Road Research Board.

Miller, A. J. (1968b) *The capacity of signalized intersections in Australia*. Bulletin No. 3, Australian Road Research Board.

Molina, C. J. (1987) Development of passenger car equivalents for large trucks at signalized intersections. *ITE Journal*, 57(11), 33-37.

NAASRA (1985) *Review of road vehicle limits for vehicles using Australian roads*. National Association of Australian State Road Authorities, Sydney.

NAASRA (1988) *Guide to traffic engineering practice: Part 3 - Traffic studies*. National Association of Australian State Road Authorities, Sydney.

Newell, G. F. (2002) A simplified car-following theory: a lower order model. *Transportation Research Part B: Methodological*, 36(3), 195-205.

Niittymäki, J. and Pursula, M. (1997) Saturation flows at signal-group-controlled traffic signals. *Transportation Research Record*, 1572, 24-32.

NRTC (2003a) *PBS safety standards for heavy vehicles*. Discussion Paper, National Road Transport Commission, Melbourne.

NRTC (2003b) *PBS infrastructure protection standards for heavy vehicles*. Discussion Paper, National Road Transport Commission, Melbourne.

Ogden, K. W. (1991) Truck movement and access in urban areas. *Journal of Transportation Engineering*, 117(1), 71-90.

Ogden, K. W. (1999) Planning and designing for trucks. In *Traffic engineering and management*, eds Ogden, K. W. and Taylor, S. Y., pp. 387-411. Institute of Transport Studies, Department of Civil Engineering, Monash University, Melbourne, Australia.

Pearson, R. A., Ogden, K. W., Sweatman, P. F. and Jarvis, J. R. (1990) *A study of the practicality of allowing double bottom road trains into metropolitan Perth*. Final Report, R A Peason and Associates, Melbourne, Victoria.

Peters, R. (2002) Managing road train access in a large city - Perth, Western Australia. *7th International Symposium on Heavy Vehicle Weights and Dimensions*, Delft, The Netherlands.

Peters, R. J. (1993) *Review of Austroads vehicle classification system*. Project RUM 3.D.8, Austroads, Sydney, NSW.

Powell, J. L. (1998) Field measurement of signalized intersection delay for 1997 update of the "Highway Capacity Manual". *Transportation Research Record*, 1646, 79-86.

Press, W. H., Teukolsky, S. A., Vetterling, W. T. and Flannery, B. P. (1992) *Numerical recipes in C - The art of scientific computing*. Cambridge University Press.

Rakha, H. and Ding, Y. (2003) Impact of stops on vehicle fuel consumption and emissions. *Journal of Transportation Engineering*, 129(1), 23-32.

Rakha, H. and Lucic, I. (2002) Variable power vehicle dynamics model for estimating truck accelerations. *Journal of Transportation Engineering*, 128(5), 412-419.

Ramsay, E. D. (1998) Interaction of multi-combination vehicles with the urban traffic environment. *5th International Symposium on Heavy Vehicle Weights and Dimensions*, Maroochydore, Queensland, pp. 151-167.

Richards, P. I. (1956) Shockwaves on the highway. *Operations Research*, 4(1), 42-51.

Robertson, D. I. (1969) *TRANSYT: a traffic network study tool*. Laboratory Report 253, Transport and Road Research Laboratory, Crowthorne, Berkshire, United Kingdom.

Rothery, R. W. (1997) Car following models. In *Traffic flow theory - A state-of-the-art report*, eds Gartner, N., Messer, C. J., and Rathi, A. K., pp. 4.1-4.42. Oak Ridge National Laboratory, Oak Ridge, Tennessee, United States.

Smith, G. L. (1970) *Commercial vehicle performance and fuel economy*. Special Publication SP-355, Society of Automotive Engineers, Warrendale, PA, United States.

Society of Automotive Engineers (1996) *Commercial truck and bus SAE recommended procedure for vehicle performance prediction and charting*. Surface Vehicle Recommended Practice J2188, Society of Automotive Engineers, Warrendale, PA, United States.

Standards Australia (1996) *Manual of uniform traffic control devices - Traffic signals*. Australian Standard AS 1742.14, Sydney, NSW.

Sullivan, D. P. and Troutbeck, R. J. (1994) The use of Cowan's M3 headway distribution for modelling urban traffic flow. *Traffic Engineering + Control*, 35(7/8), 445-450.

Sunkari, S. R., Charara, H. A. and Urbanik, T. (2000) *Reducing truck stops at high-speed isolated traffic signals*. Project Report 1439-8, Texas Transportation Institute, Texas A&M University, College Station, Texas, United States.

Sweatman, P. F. and Ogden, K. W. (1995) Urban truck crashes - What really happens. *4th International Symposium on Heavy Vehicle Weights and Dimensions*, Ann Arbor, Michigan, United States, pp. 537-541.

Tanner, J. C. (1962) A theoretical analysis of delays at an uncontrolled intersection. *Biometrika*, 49, 163-170.

Teply, S., Allingham, D. I., Richardson, D. B. and Stephenson, B. W. (1995) *Canadian capacity guide for signalized intersections*. Institute of Transportation Engineers, District 7 - Canada.

Teply, S. and Jones, A. M. (1991) Saturation flow: Do we speak the same language? *Transportation Research Record*, 1320, 144-153.

Transportation Research Board (2000) *Highway Capacity Manual*. National Research Council, Washington, DC, United States.

Troutbeck, R. J. (1997) A review on the process to estimate the Cowan M3 headway distribution parameters. *Traffic Engineering + Control*, 38(11), 600-603.

Troutbeck, R. J. and Brilon, W. (1997) Unsignalised Intersection Theory. In *Traffic flow theory - A state of the art report*, eds Gartner, N., Messer, C. J., and Rathi, A. K., Oak Ridge, TN, United States.

TTM Consulting (1987) *Traffic management strategies for freight*. Prepared for the Road Traffic Authority, Melbourne, Victoria.

Vandebona, U. and Rossi, B. (2006) Bus rapid transit corridors in Sydney for a sustainabIe transport system: benefits of advance detectors. *Road & Transport Research*, 15(1), 54-59.

Webster, F. V. (1958) *Traffic signal settings*. Road Research Laboratory Technical Paper No. 39, Department of Scientific and Industrial Research, Road Research Laboratory, London, United Kingdom.

Webster, F. V. and Cobbe, B. M. (1966) *Traffic signals*. Road Research Laboratory Technical Paper No. 56, Road Research Laboratory, Ministry of Transport, London, United Kingdom.

West, J. E. and Thurgood, G. S. (1995) Developing passenger-car equivalents for left-turning trucks at compressed diamond interchanges. *Transportation Research Record*, 1484, 90-97.

Yurysta, T. H. and Michael, H. L. (1976) Effect of commercial vehicles on delay at intersections. *Transportation Research Record*, 601, 59-65.